

NASA Conference Publication 2481

Fifteenth NASTRAN[®] Users' Colloquium

Proceedings of a colloquium held in
Kansas City, Missouri
May 4-8, 1987

NASA
National Aeronautics
and Space Administration

Scientific and Technical
Information Office

1987

FOREWORD

NASTRAN® (NASA STRUCTURAL ANALYSIS) is a large, comprehensive, nonproprietary, general purpose finite element computer code for structural analysis which was developed under NASA sponsorship and became available to the public in late 1970. It can be obtained through COSMIC® (Computer Software Management and Information Center), Athens, Georgia, and is widely used by NASA, other government agencies, and industry.

NASA currently provides continuing maintenance of NASTRAN through COSMIC. Because of the widespread interest in NASTRAN, and finite element methods in general, the Fifteenth NASTRAN Users' Colloquium was organized and held at the Americana Hotel, Kansas City, Missouri on May 4-8, 1987. (Papers from previous colloquia held in 1971, 1972, 1973, 1975, 1976, 1977, 1978, 1979, 1980, 1982, 1983, 1984, 1985 and 1986 are published in NASA Technical Memorandums X-2378, X-2637, X-2893, X-3278, X-3428, and NASA Conference Publications 2018, 2062, 2131, 2151, 2249, 2284, 2328, 2373 and 2419.) The Fifteenth Colloquium provides some comprehensive general papers on the application of finite element methods in engineering, comparisons with other approaches, unique applications, pre- and post-processing or auxiliary programs, and new methods of analysis with NASTRAN.

Individuals actively engaged in the use of finite elements or NASTRAN were invited to prepare papers for presentation at the Colloquium. These papers are included in this volume. No editorial review was provided by NASA or COSMIC; however, detailed instructions were provided each author to achieve reasonably consistent paper format and content. The opinions and data presented are the sole responsibility of the authors and their respective organizations.

NASTRAN® and COSMIC® are registered trademarks of the National Aeronautics and Space Administration.

PRECEDING PAGE BLANK NOT FILMTM

CONTENTS

	Page
FOREWORD	111
1. ADDITION OF THE AUTOSPC FEATURE TO NASTRAN	1
by P. R. Pamidi (RPK Corporation) and Horace Q. Turner (Unisys Corporation)	
2. IBM JCL MADE EASY BY MEANS OF ISPF DIALOG APPLICATION	36
by Charles E. Cooper (Magnavox Electronic Systems Company)	
3. A NEW APPROACH TO FINITE ELEMENT MODELING, ANALYSIS AND POST-PROCESSING	56
by Gil White (Intergraph Corporation)	
4. THE APPLICATION OF NASCAD AS A NASTRAN PRE- AND POST-PROCESSOR . .	59
by Alan N. Peltzmann (University of Maryland)	
5. EXPERIENCES RUNNING NASTRAN ON THE MICROVAX II COMPUTER	72
Thomas G. Butler (Butler Analyses) and Reginald S. Mitchell (Goddard Space Flight Center)	
6. CHECKPOINT AND RESTART PROCEDURES FOR SINGLE AND MULTI-STAGE STRUCTURAL MODEL ANALYSIS IN NASTRAN/COSMIC ON A CDC 176.	88
by George H. Camp and Dennis J. Fallon (David Taylor Naval Ship Research & Development Center)	
7. INTERACTIVE PLOTTING OF NASTRAN DATA ON MICROCOMPUTERS	98
by Robert L. Norton (Jet Propulsion Laboratory)	
8. COMPUTER ANIMATION OF MODAL AND TRANSIENT VIBRATIONS	111
by Robert R. Lipman (David Taylor Naval Ship Research & Development Center)	
9. BUBBLE VECTOR IN AUTOMATIC MERGING	118
by P. R. Pamidi (RPK Corporation) and Thomas G. Butler (Butler Analyses)	
10. MASS MODELING FOR BARS	136
by Thomas G. Butler (Butler Analyses)	

11.	THE USE OF NASTRAN IN THE DESIGN OF WIND TUNNEL RESEARCH AIRCRAFT	166
	by Michael Cooper (Dynamic Engineering, Inc.)	
12.	APPLICATION OF NASTRAN/COSMIC IN THE ANALYSIS OF SHIP STRUCTURES TO UNDERWATER EXPLOSION SHOCK	184
	by D. J. Fallon, F. A. Costanzo, R. T. Handleton, G. C. Camp and D. C. Smith (David Taylor Naval Ship Research & Development Center)	
13.	CALCULATION OF FORCES ON MAGNETIZED BODIES USING COSMIC NASTRAN	207
	by T. J. Sheerer (Texas Instruments)	
14.	BUCKLING ANALYSIS OF THE QUADRIPOD STRUCTURE FOR THE NASA 70-METER ANTENNA	214
	by Chian T. Chian (Jet Propulsion Laboratory)	
15.	THEORETICAL ANALYSIS OF HVAC DUCT HANGER SYSTEMS	222
	by R. D. Miller (NKF Engineering)	
16.	COUPLED NASTRAN/BOUNDARY ELEMENT FORMULATION FOR ACOUSTIC SCATTERING	250
	by Gordon C. Everstine and Francis M. Henderson (David Taylor Naval Ship Research & Development Center) and Luise S. Schuetz (Naval Research Laboratory)	
17.	NASTRAN APPLICATION FOR THE PREDICTION OF AIRCRAFT INTERIOR NOISE	266
	by Francesco Marulo (University of Naples) and Todd B. Beyer (NASA Langley Research Center)	
18.	A STRUCTURAL ANALYSIS OF AN OCEAN GOING PATROL BOAT SUBJECTED TO PLANING LOADS	286
	by James H. Clark, Robert Lafreniere, Robert Stoodt and John Wiedenheft (Naval Underwater Systems Center)	

ADDITION OF THE AUTOSPC FEATURE TO NASTRAN

by

P. R. Pamidi
RPK Corporation
Columbia, Maryland

and

Horace Q. Turner
Unisys Corporation
Huntsville, Alabama

SUMMARY

A new capability called the AUTOSPC feature has been incorporated in the April 1987 release of NASTRAN. It gives the user the option of automatically applying single-point constraints for the purpose of removing potential grid (and scalar) point singularities that have not been otherwise already constrained out. This paper gives details of the implementation of this feature and describes its usage, illustrating it with an example problem.

INTRODUCTION

In pre-April 1987 releases of NASTRAN, a table data block called GPST (Grid Point Singularity Table) was generated by the EMA (Element Matrix Assembler) module in all Rigid Formats. This table contains data on potential grid (and scalar) point singularities and was based on an examination of the stiffness matrix assembled by the EMA module. Based on the constraints specified by the user, as processed by the GP4 (Geometry Processor - Phase 4) module, this GPST table was subsequently examined by the GPSP (Grid Point Singularity Processor) module in order to identify those singularities that have been removed by the application of single-point or multipoint constraints. Any singularities not so removed were identified for the user's information because of potential problems that might be caused in the subsequent decomposition process.

In pre-April 1987 releases of NASTRAN, there was also a supplementary functional module called GPSPC (Constrain Stiffness Matrix Singularities). While not a part of any of the Rigid Formats, this module was designed to replace the GPSP module and to do not only what GPSP was doing, but, in addition, to automatically constrain singularities not otherwise constrained. However, this GPSPC module has had serious flaws both in design and implementation and has never worked properly as advertised in the NASTRAN User's Manual.

In order to resolve the above problem and have an effective means of automatically constraining singularities, the AUTOSPC feature has been introduced in the April 1987 release of NASTRAN. Details of its implementation and usage are given below, along with an illustrative example problem.

IMPLEMENTATION OF THE CAPABILITY

For the sake of efficiency and user convenience, the AUTOSPC feature was incorporated into NASTRAN by modifying and expanding the code in the existing GP4 module. This is the most logical and elegant way of doing this as this module processes all constraint data. There is no reason for a separate module to handle the new feature.

The following points summarize the important details of the implementation of the capability.

1. Deletion of old modules

The GPSP and GPSPC modules existing heretofore in NASTRAN were deleted from the code.

2. Addition of a new module

The GPST data block that has until now been generated by the EMA module has been based on the stiffness matrix assembled by the EMA module and has not included the contributions of general elements. This has now been corrected by postponing the computation of the GPST data block until after the contributions of the general elements have been added to the stiffness matrix assembled by the EMA module and by basing the computation of GPST on this total stiffness matrix. In order to perform this efficiently, a new module called GPSTGEN (GPST GENERation) was developed and incorporated into NASTRAN. This new module generates the GPST data block using the same method as was used earlier by the EMA module.

3. Changes to the EMA module

As a result of the above, the EMA module was considerably simplified by the deletion of the code associated with the generation of the GPST data block. Also, as a result, the number of output data blocks generated by the EMA module was reduced from 2 to 1.

4. Changes to the GP4 module

Significant changes were made to the GP4 module. These changes are described below.

- a. The GP4 module was modified to process the GPST data block generated by the new GPSTGEN module. A new subroutine called GP4SP was added to the GP4 module for this purpose. If the AUTOSPC feature is not turned on (the default), the GP4 module processes the GPST data block in the same way as was done earlier by the old GPS module. However, if the user has turned on the AUTOSPC feature, then the GP4 module additionally applies single-point constraints to remove potential grid (and scalar) point singularities as per the scheme outlined later under the usage of the feature.
- b. As a result of the above change, the number of output data blocks for the GP4 module was increased from four to five. The fifth output data block is suitable for processing by the OFP

(Output File Processor) module and contains information about potential singularities that have not been removed.

- c. In order to enhance user convenience, a new set, called the SAUTO-set, was added to the displacement sets already existing and recognized in NASTRAN. This new displacement set consists of those degrees of freedom that have been constrained by the GP4 module by the automatic application of single-point constraints when the AUTOSPC feature has been turned on. This new set is a subset of the s-set (single-point constraints). Until now, the s-set comprised two subsets, namely, the sg-set (permanent constraints) and the sb-set (boundary constraints). Under the new scheme, the s-set may also include the SAUTO-set. The printouts generated by DIAGs 21 and 22 in the GP4 module have been expanded to display the degrees of freedom belonging to this new SAUTO-set. (The SAUTO-set in DIAG 21 output is referred to as the AUTO SPC displacement set in DIAG 22 output.) These expanded printouts will be of great help to users.
- d. In addition, when automatic single-point constraints are applied as above, SPC1 cards are generated and printed out (and, on option, also punched out), indicating the degrees of freedom that have been automatically constrained. This is explained further later under the usage of the feature.
- e. Additional messages were introduced into the GP4 module to inform the user of the automatic application of single-point constraints when the AUTOSPC feature is turned on.

5. Resolution of a software problem

While the new capability was being developed, it was discovered that the GPST table was never generated in the HEAT approach, except in an extremely rare situation. This was traced to a software problem in the EMA module. This problem was resolved when the new GPSTGEN module was developed.

6. Changes to the Rigid Format Data Base

As a result of the work described above, all of the Rigid Formats in the Rigid Format Data Base were revamped as follows:

- * The new GPSTGEN module was incorporated.
- * The old GPSP module was deleted.
- * The EMA and GP4 module DMAP statements were modified as per the changes outlined above.
- * Other miscellaneous changes called for by the above modifications were made.

Also, all of the COSMIC-supplied DMAP ALTER packages were appropriately modified in line with the above changes.

USAGE OF THE AUTOSPC FEATURE

The AUTOSPC feature is exercised by the use of an integer DMAP parameter called AUTOSPC, normally specified via a PARAM bulk data card. It is available in all Rigid Formats. The default value of 0 for this parameter causes the new feature to be not used, thereby not changing the status quo. The new feature is exercised by specifying a non-zero value for this parameter. Acceptable values are 1, 2, -1 and -2. (Unacceptable values cause the singularity processing to be skipped.) The meanings of the various values for this parameter are described below.

AUTOSPC = 0

The AUTOSPC feature is not used.

AUTOSPC = 1

All singularities that are not already:

- (a) removed via single-point constraints, or
- (b) removed via multipoint constraints, or
- (c) specified on SUPORT cards,

are removed by the automatic application of single-point constraints.

A set of SPC1 cards is generated and printed out for the user's information and convenience, indicating the singularities that have been automatically removed as above. These SPC1 cards have the same SPC set ID as the current subcase (or a SPC set ID of 1 if the current subcase has no SPC set).

AUTOSPC = 2

There are two possible cases.

Case 1 There are no omitted degrees of freedom in the current subcase.

This case is handled in the same way as the AUTOSPC = 1 case.

SPC1 cards are generated and printed out as in the AUTOSPC = 1 case.

Case 2 There are are omitted degrees of freedom in the current subcase.

This case is handled in the same way as the AUTOSPC = 1 case, but with one important difference as explained below.

All singularities that are not already:

- (a) removed via single-point constraints, or
- (b) removed via multipoint constraints, or
- (c) specified on SUPORT cards, or

are removed by the automatic application of single-point constraints, but only if the singularity is part of the o-set (omitted set).

SPC1 cards are generated and printed out as in the AUTOSPC = 1 case.

AUTOSPC = -1

This case is handled in the same way as the AUTOSPC = 1 case, except that the SPC1 cards generated are punched out as well as being printed out.

AUTOSPC = -2

This case is handled in the same way as the AUTOSPC = 2 case, except that the SPC1 cards generated are punched out as well as being printed out.

AUTOSPC < -2 or > 2

These illegal values cause singularity processing to be skipped in the GP4 module.

As can be seen from the above discussion, when there are no omitted degrees of freedom in a subcase, the use of AUTOSPC = '1' and AUTOSPC = '2' both work the same way, by removing all potential singularities that are not already part of the s-set (single-point constraints), m-set (multipoint constraints) or r-set (degrees of freedom specified on SUPORT cards). However, if there are omitted degrees of freedom in a subcase, then AUTOSPC = '2' will cause that singularity to be removed only if it is part of the o-set, while AUTOSPC = '1' will cause it to be removed even if it is not part of the o-set. This distinction is of relevance and interest in dynamic analyses, where the omit feature is frequently used to reduce the size of the analysis set. The user thus has a choice in the usage of the AUTOSPC feature in such situations.

COMMENTS ON THE USAGE OF THE AUTOSPC FEATURE

In pre-April 1987 releases of NASTRAN, the user has been required to explicitly remove singularities in many common situations. These include such cases as the constraining of grid point rotations in solid elements, the constraining of grid point rotations normal to the plate in plate elements and the constraining of specific grid point components in axisymmetric elements. A GRDSET card has been normally used to explicitly specify such constraints. The AUTOSPC feature now provides an alternative means of handling such situations in a convenient and elegant manner. This is illustrated in the example problem discussed below.

EXAMPLE PROBLEM

In order to demonstrate the usage of the AUTOSPC feature, NASTRAN Demonstration Problem No. D01-07-1A was selected. This problem performs static analysis of a spherical shell using toroidal ring elements (see the NASTRAN Demonstration Problem Manual for details). Among other data cards, this problem employs a GRDSET bulk data card to constrain grid point displacements tangential to the shell surface.

The standard demo was first run by commenting out the GRDSET card in the data deck, thereby introducing singularities into the problem. (In addition, in order to reduce the amount of output, the output request was limited to the displacement output.) The results of this run are shown in Appendix 1. As can be seen, the run terminated due to the singularities introduced into the problem.

The above data was then augmented by adding a PARAM bulk data card with AUTOSPC = 1 specified on it. The results of this run are shown in Appendix 2. As can be seen, this run ran successfully to completion, giving results that match those of the standard demo problem.

The above runs also illustrate some of the new user messages, as well as the expanded output resulting from the use of DIAGs 21 and 22. (Both of the runs were made on a post-April 1986 release of NASTRAN, containing the AUTOSPC feature discussed in this paper.)

CONCLUSIONS

A new capability called the AUTOSPC feature has been incorporated in the April 1987 release of NASTRAN. It gives the user the option of automatically applying single-point constraints for the purpose of removing potential grid (and scalar) point singularities that have not been otherwise already constrained out. This paper has presented the details of the implementation and usage of this new feature, illustrating it with an example problem.

APPENDIX 1

**NASTRAN Demonstration Problem No. D01-07-1A
Modified to Have Singularities**

NASTRAN EXECUTIVE CONTROL DECK ECHO

ID DO1071A.NASTRAN
DIAG 21.22
APP DISPLACEMENT
SOL 1.1
TIME 5
CEND

SPHERICAL SHELL WITH TOROIDAL RING ELEMENT
 NASTRAN DEMO D01-07-1A MODIFIED TO HAVE SINGULARITIES

EXTERNAL PRESSURE LOADING

CASE CONTROL DECK ECHO

CARD
 COUNT

1 TITLE = SPHERICAL SHELL WITH TOROIDAL RING ELEMENT
 2 SUBTITLE = NASTRAN DEMO D01-07-1A MODIFIED TO HAVE SINGULARITIES
 3 LABEL = EXTERNAL PRESSURE LOADING
 4 ECHO = BOTH
 5 SPC = 1
 6 LOAD = 1
 7 OUTPUT
 8 DISP = ALL
 9 BEGIN BULK

1	2	3	4	5	6	7	8	9	10
CTORG 1	1	1			0	2.0			
CTORG 2	1	2	3		2.0	4.0			
CTORG 3	1	3	4		4.0	6.0			
CTORG 4	1	4	5		6.0	8.0			
CTORG 5	1	5	6		8.0	10.0			
CTORG 6	1	6	7		10.0	18.0			
CTORG 7	1	7	8		18.0	20.0			
CTORG 8	1	8	9		20.0	25.0			
CTORG 9	1	9	10		25.0	27.0			
CTORG 10	1	10	11		27.0	29.0			
CTORG 11	1	11	12		29.0	31.0			
CTORG 12	1	12	13		31.0	33.0			
CTORG 13	1	13	14		33.0	38.0			
FORCE 1	2	0	1.0		0	0	-8.85889		
FORCE 1	2	0	1.0		-2.16381	0	-61.9635		
FORCE 1	3	0	1.0		-8.64421	0	-123.818		
FORCE 1	4	0	1.0		-19.4083	0	-184.639		
FORCE 1	5	0	1.0		-34.4038	0	-244.795		
FORCE 1	6	0	1.0		-101.688	0	-576.596		
FORCE 1	7	0	1.0		-287.393	0	-1109.89		
FORCE 1	8	0	1.0		-519.308	0	-1426.78		
FORCE 1	9	0	1.0		-537.248	0	-1153.13		
FORCE 1	10	0	1.0		-366.120	0	-718.958		
FORCE 1	11	0	1.0		-417.584	0	-753.352		
FORCE 1	12	0	1.0		-471.266	0	-784.318		
FORCE 1	13	0	1.0		-536.891	0	-811.340		
SGRDET							2		
GRID 1	0	0	0		90.00				
GRID 2	0	3.141	0		89.9451				
GRID 3	0	6.284	0		89.7804				
GRID 4	0	9.4277	0		89.5068				
GRID 5	0	12.5253	0		89.1243				
GRID 6	0	15.6285	0		88.6329				
GRID 7	0	23.2938	0		86.9337				
GRID 8	0	30.7818	0		84.9721				
GRID 9	0	38.0358	0		81.5679				
GRID 10	0	40.8591	0		80.1908				
GRID 11	0	43.6329	0		78.7158				
GRID 12	0	46.3536	0		77.1453				
GRID 13	0	49.0176	0		75.4803				
GRID 14	0	51.6222	0		73.7235				
GMAT 1	3.066		1.667						

SPHERICAL SHELL WITH TOROIDAL RING ELEMENT
 NASTRAN DEMO D01-07-1A MODIFIED TO HAVE SINGULARITIES
 EXTERNAL PRESSURE LOADING

FEBRUARY 6, 1987 RELEASE APR. 1986 PAGE 4

	1	2	3	4	5	6	7	8	9	10
MOMENT	1	2	3	4	5	6	7	8	9	10
MOMENT	1	3	0	0	1.0	14.83917.0	14.83917.0	-10.1998		
MOMENT	1	4	0	0	1.0	14.79298.0	14.79298.0	-20.3822		
MOMENT	1	5	0	0	1.0	14.73849.0	14.73849.0	-30.5275		
MOMENT	1	6	0	0	1.0	14.73710.0	14.73710.0	-40.6554		
MOMENT	1	7	0	0	1.0	629.8624.0	629.8624.0	-903.492		
MOMENT	1	8	0	0	1.0	223.9160.0	223.9160.0	-1180.88		
MOMENT	1	9	0	0	1.0	217.7740.0	217.7740.0	-1860.45		
MOMENT	1	10	0	0	1.0	-1125.59.0	-1125.59.0	-950.370		
MOMENT	1	11	0	0	1.0	13.35776.0	13.35776.0	-132.642		
MOMENT	1	12	0	0	1.0	12.01803.0	12.01803.0	-141.715		
MOMENT	1	13	0	0	1.0	12.64240.0	12.64240.0	-150.533		
PTORORG	1	12	3.0	3.0	3.0	12.29669.0	12.29669.0	-159.082		
SPC	1	1	14	14	14	14	134	0		
ENDDATA	1	1								

TOTAL COUNT= 57

SPHERICAL SHELL WITH TOROIDAL RING ELEMENT
 NASTRAN DEMO DOI-07-1A MODIFIED TO HAVE SINGULARITIES
 EXTERNAL PRESSURE LOADING

FEBRUARY 6, 1987 RELEASE APR. 1986 PAGE 8

CARD COUNT	1	2	3	4	5	6	7	8	9	10
1-	CTORDRG 1	1	1	1	1	1	1	1	1	1
2-	CTORDRG 2	1	2	3	2.0	2.0	2.0	2.0	2.0	2.0
3-	CTORDRG 3	1	3	4	4.0	4.0	4.0	4.0	4.0	4.0
4-	CTORDRG 4	1	4	5	6.0	6.0	6.0	6.0	6.0	6.0
5-	CTORDRG 5	1	5	6	8.0	8.0	8.0	8.0	8.0	8.0
6-	CTORDRG 6	1	6	7	10.0	10.0	10.0	10.0	10.0	10.0
7-	CTORDRG 7	1	7	8	15.0	15.0	15.0	15.0	15.0	15.0
8-	CTORDRG 8	1	8	9	20.0	20.0	20.0	20.0	20.0	20.0
9-	CTORDRG 9	1	9	10	25.0	25.0	25.0	25.0	25.0	25.0
10-	CTORDRG 10	1	10	11	27.0	27.0	27.0	27.0	27.0	27.0
11-	CTORDRG 11	1	11	12	29.0	29.0	29.0	29.0	29.0	29.0
12-	CTORDRG 12	1	12	13	31.0	31.0	31.0	31.0	31.0	31.0
13-	CTORDRG 13	1	13	14	33.0	33.0	33.0	33.0	33.0	33.0
14-	FORCE 1	1	0	0	0	0	0	0	0	0
15-	FORCE 1	2	0	0	0	0	0	0	0	0
16-	FORCE 1	3	0	0	0	0	0	0	0	0
17-	FORCE 1	4	0	0	0	0	0	0	0	0
18-	FORCE 1	5	0	0	0	0	0	0	0	0
19-	FORCE 1	6	0	0	0	0	0	0	0	0
20-	FORCE 1	7	0	0	0	0	0	0	0	0
21-	FORCE 1	8	0	0	0	0	0	0	0	0
22-	FORCE 1	9	0	0	0	0	0	0	0	0
23-	FORCE 1	10	0	0	0	0	0	0	0	0
24-	FORCE 1	11	0	0	0	0	0	0	0	0
25-	FORCE 1	12	0	0	0	0	0	0	0	0
26-	FORCE 1	13	0	0	0	0	0	0	0	0
27-	GRID 1	0	0	0	0	0	0	0	0	0
28-	GRID 2	0	0	0	0	0	0	0	0	0
29-	GRID 3	0	0	0	0	0	0	0	0	0
30-	GRID 4	0	0	0	0	0	0	0	0	0
31-	GRID 5	0	0	0	0	0	0	0	0	0
32-	GRID 6	0	0	0	0	0	0	0	0	0
33-	GRID 7	0	0	0	0	0	0	0	0	0
34-	GRID 8	0	0	0	0	0	0	0	0	0
35-	GRID 9	0	0	0	0	0	0	0	0	0
36-	GRID 10	0	0	0	0	0	0	0	0	0
37-	GRID 11	0	0	0	0	0	0	0	0	0
38-	GRID 12	0	0	0	0	0	0	0	0	0
39-	GRID 13	0	0	0	0	0	0	0	0	0
40-	GRID 14	0	0	0	0	0	0	0	0	0
41-	MAT 1	12	3.066	51.6222	1.667	73.7235	12.5 E-6.0	10.1996	CHAT11	
42-	MOMENT	1	2	0	1.0	14.83917.0				

SPHERICAL SHELL WITH TOROIDAL RING ELEMENT
 NASTRAN DEMO D01-07-1A MODIFIED TO HAVE SINGULARITIES
 EXTERNAL PRESSURE LOADING

FEBRUARY 6, 1987 RELEASE APR. 1986 PAGE 6

CARD COUNT	1	2	3	4	5	6	7	8	9	10
43-	MOMENT	1	3	0	1.0	14.78298.0	-20.3822			
44-	MOMENT	1	4	0	1.0	14.73848.0	-30.5275			
45-	MOMENT	1	5	0	1.0	14.73710.0	-40.6584			
46-	MOMENT	1	6	0	1.0	628.9824.0	-503.482			
47-	MOMENT	1	7	0	1.0	223.9160.0	-1180.88			
48-	MOMENT	1	8	0	1.0	217.7740.0	-1540.45			
49-	MOMENT	1	9	0	1.0	-1125.58.0	-850.370			
50-	MOMENT	1	10	0	1.0	13.35776.0	-132.642			
51-	MOMENT	1	11	0	1.0	13.01903.0	-141.715			
52-	MOMENT	1	12	0	1.0	12.64240.0	-150.533			
53-	MOMENT	1	13	0	1.0	12.29668.0	-159.082			
54-	PTORORG	1	12	3.0	3.0					
55-	SPC	1	1	14	.0	14	134	.0		
	ENDDATA									

*** USER INFORMATION MESSAGE - GRID-POINT RESEQUENCING PROCESSOR BANDIT IS NOT USED DUE TO SMALL PROBLEM SIZE

NO ERRORS FOUND - EXECUTE NASTRAN PROGRAM

*** USER INFORMATION MESSAGE, TURN DIAG 38 ON FOR ADDITIONAL ELEMENT PROCESSING INFORMATION

SPHERICAL SHELL WITH TOROIDAL RING ELEMENT
NASTRAN DEMO D01-07-1A MODIFIED TO HAVE SINGULARITIES

EXTERNAL PRESSURE LOADING

*** USER INFORMATION MESSAGE 2118, SUBROUTINE GP4PRT - DIAG 21 SET-DOF VS. DISP SETS FOLLOWS.

INT	DOF	EXT	GP	DOF	SAUTO	SB	SG	L	A	F	N	G	R	O	S	M
1	1	1	1	1	1	1	1	1	1	1	1	1	1	1	1	1
2	2	1	2	2	2	2	2	2	2	2	2	2	2	2	2	2
3	3	1	3	3	3	3	3	3	3	3	3	3	3	3	3	3
4	4	1	4	4	4	4	4	4	4	4	4	4	4	4	4	4
5	5	1	5	5	5	5	5	5	5	5	5	5	5	5	5	5
6	6	1	6	6	6	6	6	6	6	6	6	6	6	6	6	6
7	7	2	1	7	7	7	7	7	7	7	7	7	7	7	7	7
8	8	2	2	8	8	8	8	8	8	8	8	8	8	8	8	8
9	9	2	3	9	9	9	9	9	9	9	9	9	9	9	9	9
10	10	2	4	10	10	10	10	10	10	10	10	10	10	10	10	10
11	11	2	5	11	11	11	11	11	11	11	11	11	11	11	11	11
12	12	2	6	12	12	12	12	12	12	12	12	12	12	12	12	12
13	13	3	1	13	13	13	13	13	13	13	13	13	13	13	13	13
14	14	3	2	14	14	14	14	14	14	14	14	14	14	14	14	14
15	15	3	3	15	15	15	15	15	15	15	15	15	15	15	15	15
16	16	3	4	16	16	16	16	16	16	16	16	16	16	16	16	16
17	17	3	5	17	17	17	17	17	17	17	17	17	17	17	17	17
18	18	3	6	18	18	18	18	18	18	18	18	18	18	18	18	18
19	19	4	1	19	19	19	19	19	19	19	19	19	19	19	19	19
20	20	4	2	20	20	20	20	20	20	20	20	20	20	20	20	20
21	21	4	3	21	21	21	21	21	21	21	21	21	21	21	21	21
22	22	4	4	22	22	22	22	22	22	22	22	22	22	22	22	22
23	23	4	5	23	23	23	23	23	23	23	23	23	23	23	23	23
24	24	4	6	24	24	24	24	24	24	24	24	24	24	24	24	24
25	25	5	1	25	25	25	25	25	25	25	25	25	25	25	25	25
26	26	5	2	26	26	26	26	26	26	26	26	26	26	26	26	26
27	27	5	3	27	27	27	27	27	27	27	27	27	27	27	27	27
28	28	5	4	28	28	28	28	28	28	28	28	28	28	28	28	28
29	29	5	5	29	29	29	29	29	29	29	29	29	29	29	29	29
30	30	5	6	30	30	30	30	30	30	30	30	30	30	30	30	30
31	31	6	1	31	31	31	31	31	31	31	31	31	31	31	31	31
32	32	6	2	32	32	32	32	32	32	32	32	32	32	32	32	32
33	33	6	3	33	33	33	33	33	33	33	33	33	33	33	33	33
34	34	6	4	34	34	34	34	34	34	34	34	34	34	34	34	34
35	35	6	5	35	35	35	35	35	35	35	35	35	35	35	35	35
36	36	6	6	36	36	36	36	36	36	36	36	36	36	36	36	36
37	37	7	1	37	37	37	37	37	37	37	37	37	37	37	37	37
38	38	7	2	38	38	38	38	38	38	38	38	38	38	38	38	38
39	39	7	3	39	39	39	39	39	39	39	39	39	39	39	39	39
40	40	7	4	40	40	40	40	40	40	40	40	40	40	40	40	40
41	41	7	5	41	41	41	41	41	41	41	41	41	41	41	41	41

SPHERICAL SHELL WITH TOROIDAL RING ELEMENT
 NASTRAN DEMO D01-07-1A MODIFIED TO HAVE SINGULARITIES
 EXTERNAL PRESSURE LOADING

FEBRUARY 6, 1987 RELEASE APR. 1986 PAGE 8

INT DOF	EXT GP	DOF	SAUTO	SB	SG	L	A	F	N	G	R	O	S	M
42	7 - 6					40	40	40	42	42				
43	8 - 1					41	41	41	43	43				
44	8 - 2					42	42	42	44	44				
45	8 - 3					43	43	43	45	45				
46	8 - 4					44	44	44	46	46				
47	8 - 5					45	45	45	47	47				
48	8 - 6					46	46	46	48	48				
49	9 - 1					47	47	47	49	49				
50	9 - 2					48	48	48	50	50				
51	9 - 3					49	49	49	51	51				
52	9 - 4					50	50	50	52	52				
53	9 - 5					51	51	51	53	53				
54	9 - 6					52	52	52	54	54				
55	10 - 1					53	53	53	55	55				
56	10 - 2					54	54	54	56	56				
57	10 - 3					55	55	55	57	57				
58	10 - 4					56	56	56	58	58				
59	10 - 5					57	57	57	59	59				
60	10 - 6					58	58	58	60	60				
61	11 - 1					59	59	59	61	61				
62	11 - 2					60	60	60	62	62				
63	11 - 3					61	61	61	63	63				
64	11 - 4					62	62	62	64	64				
65	11 - 5					63	63	63	65	65				
66	11 - 6					64	64	64	66	66				
67	12 - 1					65	65	65	67	67				
68	12 - 2					66	66	66	68	68				
69	12 - 3					67	67	67	69	69				
70	12 - 4					68	68	68	70	70				
71	12 - 5					69	69	69	71	71				
72	12 - 6					70	70	70	72	72				
73	13 - 1					71	71	71	73	73				
74	13 - 2					72	72	72	74	74				
75	13 - 3					73	73	73	75	75				
76	13 - 4					74	74	74	76	76				
77	13 - 5					75	75	75	77	77				
78	13 - 6					76	76	76	78	78				
79	14 - 1					77	77	77	79	79			3	
80	14 - 2					77	77	77	80	80			4	
81	14 - 3					78	78	78	81	81			5	
82	14 - 4					79	79	79	82	82				
83	14 - 5					79	79	79	83	83				
84	14 - 6					79	79	79	84	84				
--- COLUMN TOTALS ---										84	0	0	5	0

SPHERICAL SHELL WITH TOROIDAL RING ELEMENT
 NASTRAN DEMO D01-07-1A MODIFIED TO HAVE SINGULARITIES
 EXTERNAL PRESSURE LOADING

FEBRUARY 6, 1987 RELEASE APR. 1986 PAGE 9

*** USER INFORMATION MESSAGE 2119, SUBROUTINE GP4PR1 - DIAG 22 SET DISP SETS VS. DOF FOLLOWS.

		SPC DISPLACEMENT SET									
I=	-1-	-2-	-3-	-4-	-5-	-6-	-7-	-8-	-9-	-10-	
	1-1	1-4	14-1	14-3	14-4						

SPHERICAL SHELL WITH TOROIDAL RING ELEMENT
MASTER TWO DOI-07-1A MODIFIED TO HAVE SINGULARITIES

FEBRUARY 6, 1987 RELEASE APR. 1986 PAGE 10

EXTERNAL PRESSURE LOADING

ANALYSIS DISPLACEMENT SET										
	-1-	-2-	-3-	-4-	-5-	-6-	-7-	-8-	-9-	-10-
1-	1-2	1-3	1-5	1-6	2-1	2-2	2-3	2-4	2-5	2-6
11-	3-1	3-2	3-3	3-4	3-5	3-6	4-1	4-2	4-3	4-4
21-	4-1	4-6	5-1	5-2	5-3	5-4	5-5	5-6	6-1	6-2
31-	6-3	6-4	6-5	6-6	7-1	7-2	7-3	7-4	7-5	7-6
41-	8-1	8-2	8-3	8-4	8-5	8-6	8-1	8-2	9-3	9-4
51-	9-5	9-6	10-1	10-2	10-3	10-4	10-5	10-6	11-1	11-2
61-	11-3	11-4	11-5	11-6	12-1	12-2	12-3	12-4	12-5	12-6
71-	13-1	13-2	13-3	13-4	13-5	13-6	14-1	14-2	14-3	14-4

SPHERICAL SHELL WITH TOROIDAL RING ELEMENT
 NASTRAN DEND D01-Q7-1A MODIFIED TO HAVE SINGULARITIES

EXTERNAL PRESSURE LOADING

		BODY SPC DISPLACEMENT SET									
		-1-	-2-	-3-	-4-	-5-	-6-	-7-	-8-	-9-	-10-
1=	1-1	1-4	14-1	14-3	14-4						

*** USER WARNING MESSAGE 3017

ONE OR MORE POTENTIAL SINGULARITIES HAVE NOT BEEN REMOVED BY SINGLE OR MULTI-POINT CONSTRAINTS.

SPHERICAL SHELL WITH TOROIDAL RING ELEMENT
 NASTRAN DEMO D01-07-1A MODIFIED TO HAVE SINGULARITIES

FEBRUARY 6, 1987 RELEASE APR. 1986 PAGE 12

EXTERNAL PRESSURE LOADING

POINT ID.	TYPE	SINGULARITY ORDER	GRID POINT	SINGULARITY LIST OF COORDINATE COMBINATIONS THAT WILL REMOVE SINGULARITY WEAKER COMBINATION	SPC 1 MPC O	WEAKEST COMBINATION
1	G	1	2	2		
2	G	1	2	2		
3	G	1	2	2		
4	G	1	2	2		
5	G	1	2	2		
6	G	1	2	2		
7	G	1	2	2		
8	G	1	2	2		
9	G	1	2	2		
10	G	1	2	2		
11	G	1	2	2		
12	G	1	2	2		
13	G	1	2	2		
14	G	1	2	2		

SPHERICAL SHELL WITH TOROIDAL RING ELEMENT
 NASTRAN DEMO D01-07-1A MODIFIED TO HAVE SINGULARITIES
 EXTERNAL PRESSURE LOADING

ABORTED BECAUSE THE FOLLOWING COLUMNS ARE SINGULAR--
 66 72 77

*** USER FATAL MESSAGE 3097. SYMMETRIC DECOMPOSITION OF DATA BLOCK KLL
 1 6 12 18 24 30 36 42 48 54 60

*** USER FATAL MESSAGE 3005 IN SUBROUTINE FACTOR
 ATTEMPT TO OPERATE ON THE SINGULAR MATRIX KLL
 FATAL ERROR

APPENDIX 2

Modified NASTRAN Demonstration Problem No. D01-07-1A
of Appendix 1 Run With AUTOSPC = 1

NASTRAN EXECUTIVE CONTROL DECK ECHO

ID DO1071A.NASTRAN
DIAG 21.22
APP DISPLACEMENT
SOL 1.1
TIME 5
CEND

SPHERICAL SHELL WITH TOROIDAL RING ELEMENT
 MODIFIED NASTRAN DEMO DO1-07-1A WITH AUTOSPC = 1
 EXTERNAL PRESSURE LOADING

FEBRUARY 6, 1987 RELEASE APR. 1986 PAGE 2

CARD COUNT	CASE	CONTROL	DECK	ECHO
1	TITLE = SPHERICAL SHELL WITH TOROIDAL RING ELEMENT			
2	SUBTITLE = MODIFIED NASTRAN DEMO DO1-07-1A WITH AUTOSPC = 1			
3	LABEL = EXTERNAL PRESSURE LOADING			
4	ECHO = BOTH			
5	SPC = 1			
6	LOAD = 1			
7	OUTPUT			
8	DISP = ALL			
9	BEGIN BULK			

SPHERICAL SHELL WITH TOROIDAL RING ELEMENT
 MODIFIED NASTRAN DEMO D01-07-1A WITH AUTOSPC = 1
 EXTERNAL PRESSURE LOADING

FEBRUARY 6, 1987 RELEASE APR. 1986 PAGE 3

INPUT BULK DATA DECK ECHO												
1	2	3	4	5	6	7	8	9	10			
CTORDG 1	1	1	1	1	0	2.0						
CTORDG 2	1	2	2	3	2.0	4.0						
CTORDG 3	1	3	3	4	4.0	6.0						
CTORDG 4	1	4	4	5	6.0	8.0						
CTORDG 5	1	5	5	6	8.0	10.0						
CTORDG 6	1	6	6	7	10.0	15.0						
CTORDG 7	1	7	7	8	15.0	20.0						
CTORDG 8	1	8	8	9	20.0	25.0						
CTORDG 9	1	9	9	10	25.0	27.0						
CTORDG 10	1	10	10	11	27.0	28.0						
CTORDG 11	1	11	11	12	28.0	31.0						
CTORDG 12	1	12	12	13	31.0	33.0						
CTORDG 13	1	13	13	14	33.0	35.0						
FORCE 1	1	0	0	1.0	0	0						
FORCE 1	2	0	0	1.0	-2.16381	0						
FORCE 1	3	0	0	1.0	-5.64421	0						
FORCE 1	4	0	0	1.0	-19.4063	0						
FORCE 1	5	0	0	1.0	-34.4036	0						
FORCE 1	6	0	0	1.0	-101.668	0						
FORCE 1	7	0	0	1.0	-287.383	0						
FORCE 1	8	0	0	1.0	-519.309	0						
FORCE 1	9	0	0	1.0	-537.246	0						
FORCE 1	10	0	0	1.0	-368.120	0						
FORCE 1	11	0	0	1.0	-417.584	0						
FORCE 1	12	0	0	1.0	-471.266	0						
FORCE 1	13	0	0	1.0	-526.891	0						
SGRDSET	1	0	0	0	90.00	0						
GRID 1	0	0	0	0	89.9451	0						
GRID 2	0	0	0	0	89.7804	0						
GRID 3	0	0	0	0	89.5068	0						
GRID 4	0	0	0	0	89.1243	0						
GRID 5	0	0	0	0	88.6329	0						
GRID 6	0	0	0	0	86.9337	0						
GRID 7	0	0	0	0	84.5721	0						
GRID 8	0	0	0	0	81.5679	0						
GRID 9	0	0	0	0	80.1909	0						
GRID 10	0	0	0	0	78.7158	0						
GRID 11	0	0	0	0	77.1453	0						
GRID 12	0	0	0	0	75.4803	0						
GRID 13	0	0	0	0	73.7235	0						
GRID 14	0	0	0	0	73.7235	0						
MAT 1	12	3.0E6										

CHART 11

12.5 E-6.0

.1667

SPHERICAL SHELL WITH TOROIDAL RING ELEMENT
MODIFIED NASTRAN DEMO D01-07-1A WITH AUTOSPC = 1

EXTERNAL PRESSURE LOADING

FEBRUARY 6, 1987 RELEASE APR. 1986 PAGE 4

INPUT BULK DATA DECK ECHO										
1	2	3	4	5	6	7	8	9	10	
MOMENT	1	2	0	1.0	14.83917.0					
MOMENT	1	3	0	1.0	14.79298.0					-10.1998
MOMENT	1	4	0	1.0	14.73848.0					-20.3822
MOMENT	1	5	0	1.0	14.73710.0					-30.5275
MOMENT	1	6	0	1.0	628.9624.0					-40.6554
MOMENT	1	7	0	1.0	223.9160.0					-503.492
MOMENT	1	8	0	1.0	217.7740.0					-1180.88
MOMENT	1	9	0	1.0	-1125.59.0					-1560.45
MOMENT	1	10	0	1.0	13.35776.0					-850.370
MOMENT	1	11	0	1.0	13.01903.0					-132.642
MOMENT	1	12	0	1.0	12.64240.0					-141.715
MOMENT	1	13	0	1.0	12.29669.0					-150.533
-FF -		PARAM, AUTOSPC, 1								-159.092
PARAM	AUTOSPC	1								
PTORORG	1	12	3.0	3.0	14	134				.0
SPC	1	1	14	.0						
ENDDATA										

TOTAL COUNT= 58

SPHERICAL SHELL WITH TOROIDAL RING ELEMENT
 MODIFIED NASTRAN DEMO D01-07-1A WITH AUTOSPC = 1
 EXTERNAL PRESSURE LOADING

FEBRUARY 6, 1987 RELEASE APR. 1986 PAGE 5

CARD COUNT	1	2	3	4	5	6	7	8	9	10
1- CTORRG 1	1	1	1	1	1	1	1	1	1	1
2- CTORRG 2	1	1	1	1	1	1	1	1	1	1
3- CTORRG 3	1	1	1	1	1	1	1	1	1	1
4- CTORRG 4	1	1	1	1	1	1	1	1	1	1
5- CTORRG 5	1	1	1	1	1	1	1	1	1	1
6- CTORRG 6	1	1	1	1	1	1	1	1	1	1
7- CTORRG 7	1	1	1	1	1	1	1	1	1	1
8- CTORRG 8	1	1	1	1	1	1	1	1	1	1
9- CTORRG 9	1	1	1	1	1	1	1	1	1	1
10- CTORRG 10	1	1	1	1	1	1	1	1	1	1
11- CTORRG 11	1	1	1	1	1	1	1	1	1	1
12- CTORRG 12	1	1	1	1	1	1	1	1	1	1
13- CTORRG 13	1	1	1	1	1	1	1	1	1	1
14- FORCE 1	1	1	1	1	1	1	1	1	1	1
15- FORCE 1	1	1	1	1	1	1	1	1	1	1
16- FORCE 1	1	1	1	1	1	1	1	1	1	1
17- FORCE 1	1	1	1	1	1	1	1	1	1	1
18- FORCE 1	1	1	1	1	1	1	1	1	1	1
19- FORCE 1	1	1	1	1	1	1	1	1	1	1
20- FORCE 1	1	1	1	1	1	1	1	1	1	1
21- FORCE 1	1	1	1	1	1	1	1	1	1	1
22- FORCE 1	1	1	1	1	1	1	1	1	1	1
23- FORCE 1	1	1	1	1	1	1	1	1	1	1
24- FORCE 1	1	1	1	1	1	1	1	1	1	1
25- FORCE 1	1	1	1	1	1	1	1	1	1	1
26- FORCE 1	1	1	1	1	1	1	1	1	1	1
27- GRID 1	1	1	1	1	1	1	1	1	1	1
28- GRID 2	1	1	1	1	1	1	1	1	1	1
29- GRID 3	1	1	1	1	1	1	1	1	1	1
30- GRID 4	1	1	1	1	1	1	1	1	1	1
31- GRID 5	1	1	1	1	1	1	1	1	1	1
32- GRID 6	1	1	1	1	1	1	1	1	1	1
33- GRID 7	1	1	1	1	1	1	1	1	1	1
34- GRID 8	1	1	1	1	1	1	1	1	1	1
35- GRID 9	1	1	1	1	1	1	1	1	1	1
36- GRID 10	1	1	1	1	1	1	1	1	1	1
37- GRID 11	1	1	1	1	1	1	1	1	1	1
38- GRID 12	1	1	1	1	1	1	1	1	1	1
39- GRID 13	1	1	1	1	1	1	1	1	1	1
40- GRID 14	1	1	1	1	1	1	1	1	1	1
41- MAT 1	1	1	1	1	1	1	1	1	1	1
42- MOMENT 1	1	1	1	1	1	1	1	1	1	1

-8.85885
 -61.9635
 -123.618
 -184.639
 -244.795
 -576.586
 -1109.89
 -1426.78
 -1153.13
 -718.955
 -753.352
 -784.318
 -811.340

CMAT11

12.5 E-6 O
 14.83917 O
 -10.1998

SPHERICAL SHELL WITH TOROIDAL RING ELEMENT
MODIFIED NASTRAN DEMO D01-07-1A WITH AUTOSPC = 1

EXTERNAL PRESSURE LOADING

CARD COUNT	1	2	3	4	5	6	7	8	9	10
43-	MOMENT	1	3	0	1.0	14.79298.0	-20.3822			
44-	MOMENT	1	4	0	1.0	14.73848.0	-30.5375			
45-	MOMENT	1	5	0	1.0	14.73710.0	-40.6554			
46-	MOMENT	1	6	0	1.0	629.9624.0	-503.492			
47-	MOMENT	1	7	0	1.0	223.9160.0	-1180.98			
48-	MOMENT	1	8	0	1.0	217.7740.0	-1560.45			
49-	MOMENT	1	9	0	1.0	-1125.58.0	-950.370			
50-	MOMENT	1	10	0	1.0	13.35776.0	-132.642			
51-	MOMENT	1	11	0	1.0	13.01903.0	-141.715			
52-	MOMENT	1	12	0	1.0	12.64240.0	-150.533			
53-	MOMENT	1	13	0	1.0	12.28669.0	-159.092			
54-	PARAM	AUTOSPC	1							
55-	PTORDRG	1	12	3.0	3.0					
56-	SPC	1	1	14	.0	14	134	.0		
	ENDDATA									

*** USER INFORMATION MESSAGE - GRID-POINT RESEQUENCING PROCESSOR BANDIT IS NOT USED DUE TO SMALL PROBLEM SIZE

***NO ERRORS FOUND - EXECUTE NASTRAN PROGRAM**

*** USER INFORMATION MESSAGE, TURN DIAG 38 ON FOR ADDITIONAL ELEMENT PROCESSING INFORMATION

*** USER INFORMATION MESSAGE 2435, AT USER'S REQUEST, ALL POTENTIAL SINGULARITIES HAVE BEEN REMOVED BY THE APPLICATION OF SINGLE POINT CONSTRAINTS. REFER TO PRINTOUT OF AUTOMATICALLY GENERATED SPC1 CARDS FOR DETAILS.

SPHERICAL SHELL WITH TOROIDAL RING ELEMENT
 MODIFIED NAISTRAN DEMO DO1-07-1A WITH AUTOSPC - 1
 EXTERNAL PRESSURE LOADING

FEBRUARY 6, 1987 RELEASE APR. 1986 PAGE 7

CARD COUNT	AUTOMATICALLY GENERATED SPC1 CARDS									
	1	2	3	4	5	6	7	8	9	10
1-										
2-	SPC1	1	2	1	2	3	4	5	6	
3-	SPC1	1	2	7	8	9	10	11	12	
	SPC1	1	2	13	14					

SPHERICAL SHELL WITH TOROIDAL RING ELEMENT
MODIFIED NASTRAN DEED DO1-07-1A WITH AUTOSPC = 1

FEBRUARY 6, 1987 RELEASE APR. 1986 PAGE 8

EXTERNAL PRESSURE LOADING

*** USER INFORMATION MESSAGE 2118, SUBROUTINE GP4PRT - DIAG 21 SET-DOF VS. DISP SETS FOLLOWS.

INT	DOF	EXT	GP	DOF	SAUTO	SB	SG	L	A	F	N	G	R	O	S	M
1	1	1	1	1	1	1		1			1	1			1	
2	1	2	1	1	1			2			2	2			2	
3	1	3	1	1	1			3		1	3	3			3	
4	1	4	1	1	1			4			4	4				
5	1	5	1	1	1			5		2	5	5				
6	1	6	1	1	1			6		3	6	6				
7	2	1	2	1	1			7		4	7	7			4	
8	2	2	2	1	1			8			8	8				
9	2	3	2	1	1			9		5	9	9				
10	2	4	2	1	1			10		6	10	10				
11	2	5	2	1	1			11		7	11	11				
12	2	6	2	1	1			12		8	12	12				
13	3	1	3	1	1			13		9	13	13			5	
14	3	2	3	1	1			14			14	14				
15	3	3	3	1	1			15	10	10	15	15				
16	3	4	3	1	1			16	11	11	16	16				
17	3	5	3	1	1			17	12	12	17	17				
18	3	6	3	1	1			18	13	13	18	18				
19	4	1	4	1	1			19	14	14	19	19			6	
20	4	2	4	1	1			20	15	15	20	20				
21	4	3	4	1	1			21	16	16	21	21				
22	4	4	4	1	1			22	17	17	22	22				
23	4	5	4	1	1			23	18	18	23	23				
24	4	6	4	1	1			24	19	19	24	24				
25	5	1	5	1	1			25	20	20	25	25			7	
26	5	2	5	1	1			26	21	21	26	26				
27	5	3	5	1	1			27	22	22	27	27				
28	5	4	5	1	1			28	23	23	28	28				
29	5	5	5	1	1			29	24	24	29	29				
30	6	1	6	1	1			30	25	25	30	30			8	
31	6	2	6	1	1			31	26	26	31	31				
32	6	3	6	1	1			32	27	27	32	32				
33	6	4	6	1	1			33	28	28	33	33				
34	6	5	6	1	1			34	29	29	34	34				
35	6	6	6	1	1			35	30	30	35	35				
36	7	1	7	1	1			36	31	31	36	36				
37	7	2	7	1	1			37	32	32	37	37			9	
38	7	3	7	1	1			38	33	33	38	38				
39	7	4	7	1	1			39	34	34	39	39				
40	7	5	7	1	1			40	35	35	40	40				
41	7	6	7	1	1			41	36	36	41	41				

EXTERNAL PRESSURE LOADING

INT	DOF	EXT	OP.	DOF	SAUTO	SB	SG	L	A	F	N	G	R	O	S	M
42	7	-	6					33	33	33	42	42				
43	8	-	1					34	34	34	43	43				
44	8	-	2		8									10		
45	8	-	3					35	35	35	45	45				
46	8	-	4					36	36	36	46	46				
47	8	-	5					37	37	37	47	47				
48	8	-	6					38	38	38	48	48				
49	9	-	1		9			39	39	39	49	49				
50	9	-	2								50	50		11		
51	9	-	3					40	40	40	51	51				
52	9	-	4					41	41	41	52	52				
53	9	-	5					42	42	42	53	53				
54	9	-	6					43	43	43	54	54				
55	10	-	1					44	44	44	55	55				
56	10	-	2		10									12		
57	10	-	3					45	45	45	57	57				
58	10	-	4					46	46	46	58	58				
59	10	-	5					47	47	47	59	59				
60	10	-	6					48	48	48	60	60				
61	11	-	1					49	49	49	61	61				
62	11	-	2		11						62	62		13		
63	11	-	3					50	50	50	63	63				
64	11	-	4					51	51	51	64	64				
65	11	-	5					52	52	52	65	65				
66	11	-	6					53	53	53	66	66				
67	12	-	1					54	54	54	67	67				
68	12	-	2		12						68	68		14		
69	12	-	3					55	55	55	69	69				
70	12	-	4					56	56	56	70	70				
71	12	-	5					57	57	57	71	71				
72	12	-	6					58	58	58	72	72				
73	13	-	1					59	59	59	73	73				
74	13	-	2		13						74	74		15		
75	13	-	3					60	60	60	75	75				
76	13	-	4					61	61	61	76	76				
77	13	-	5					62	62	62	77	77				
78	13	-	6					63	63	63	78	78				
79	14	-	1			3					79	79		16		
80	14	-	2		14						80	80		17		
81	14	-	3			4					81	81		18		
82	14	-	4			5					82	82		19		
83	14	-	5					64	64	64						
84	14	-	6					65	65	65						
--- COLUMN TOTALS ---																
					14	5	0	65	65	65	84	84	0	0	19	0

SPHERICAL SHELL WITH TOROIDAL RING ELEMENT
MODIFIED NASTRAN DEMO D01-07-1A WITH AUTOSPC = 1

EXTERNAL PRESSURE LOADING

*** USER INFORMATION MESSAGE 2119, SUBROUTINE QP4PRT - DIAG 22 SET DISP SETS VS. DOF FOLLOWS.

SPC DISPLACEMENT SET									
	-1-	-2-	-3-	-4-	-5-	-6-	-7-	-8-	-10-
1=	1-1	1-2	1-4	2-2	3-2	4-2	5-2	6-2	7-2
11=	8-2	10-2	11-2	12-2	13-2	14-1	14-2	14-3	14-4
									8-2

SPHERICAL SHELL WITH TOROIDAL RING ELEMENT
MODIFIED NASTRAN DEMO D01-07-1A WITH AUTOSPC = 1

FEBRUARY 6, 1987 RELEASE APR. 1986 PAGE 11

EXTERNAL PRESSURE LOADING

	ANALYSIS DISPLACEMENT SET									
	-1-	-2-	-3-	-4-	-5-	-6-	-7-	-8-	-9-	-10-
1=	1-3	1-5	1-6	2-1	2-3	2-4	2-5	2-6	3-1	3-3
11=	3-4	3-5	3-6	4-1	4-3	4-4	4-5	4-6	5-1	5-3
21=	5-4	5-5	5-6	6-1	6-3	6-4	6-5	6-6	7-1	7-3
31=	7-4	7-5	7-6	8-1	8-3	8-4	8-5	8-6	9-1	9-3
41=	9-4	9-5	9-6	10-1	10-3	10-4	10-5	10-6	11-1	11-3
51=	11-4	11-5	11-6	12-1	12-3	12-4	12-5	12-6	13-1	13-3
61=	13-4	13-5	13-6	14-1	14-3	14-4	14-5	14-6		

SPHERICAL SHELL WITH TOROIDAL RING ELEMENT
MODIFIED NASTRAN DEMO D01-07-1A WITH AUTOSPC = 1

EXTERNAL PRESSURE LOADING

		BODY SPC DISPLACEMENT SET									
I=		-1-	-2-	-3-	-4-	-5-	-6-	-7-	-8-	-9-	-10-
		1-1	1-4	14-1	14-3	14-4					

SPHERICAL SHELL WITH TOROIDAL RING ELEMENT
MODIFIED NASTRAN DEMO D01-07-1A WITH AUTOSPC = 1
EXTERNAL PRESSURE LOADING

FEBRUARY 6, 1987 RELEASE APR. 1988 PAGE 13

AUTO SPC DISPLACEMENT SET

-1-	-2-	-3-	-4-	-5-	-6-	-7-	-8-	-9-	-10-
1-	2-2	3-2	4-2	5-2	6-2	7-2	8-2	9-2	10-2
11-	11-2	13-2	14-2						

***USER INFORMATION MESSAGE 3023--PARAMETERS FOR REAL
TIME ESTIMATE = 1
C AVG = 7
C MAX = 10
ADDITIONAL CORE--242866

SYMMETRIC DECOMPOSITION OF DATA BLOCK KLL
PC AVG = 0
PC MAX = 0
PC GROUPS = 0
SPILL GROUPS = 0

(N = 65)
S AVG = 1
PREFACE LOOPS = 1

*** USER INFORMATION MESSAGE 3035

FOR SURFACE NUMBER 1, EPSILON SUB E = 7.9516343E-14

SPHERICAL SHELL WITH TOROIDAL RING ELEMENT
 MODIFIED NASTRAN DEMO D01-07-1A WITH AUTOSPC = 1
 EXTERNAL PRESSURE LOADING

FEBRUARY 6, 1987 RELEASE APR. 1986 PAGE 14

DISPLACEMENT VECTOR

POINT ID.	TYPE	T1	T2	T3	R1	R2	R3
1	G	0.0	0.0	-5.466944E-04	0.0	1.683363E-06	2.264283E-07
2	G	-1.379353E-05	0.0	-5.465159E-04	9.711448E-09	1.683092E-06	-2.154376E-08
3	G	-2.758300E-05	0.0	-5.460828E-04	-4.874045E-08	1.682892E-06	4.688149E-08
4	G	-4.132202E-05	0.0	-5.448287E-04	-2.865820E-07	1.676808E-06	1.172040E-07
5	G	-5.488748E-05	0.0	-5.421350E-04	-8.169632E-07	1.656754E-06	2.187808E-07
6	G	-6.804022E-05	0.0	-5.369829E-04	-1.700009E-06	1.611340E-06	3.477465E-07
7	G	-9.602270E-05	0.0	-5.048501E-04	-5.882594E-06	1.304370E-06	7.566084E-07
8	G	-1.071690E-04	0.0	-4.272170E-04	-1.345247E-05	4.936754E-07	1.104621E-06
9	G	-8.639758E-05	0.0	-2.89577E-04	-2.183137E-05	-1.014970E-06	8.644736E-07
10	G	-6.754948E-05	0.0	-2.194551E-04	-2.388998E-05	-1.778489E-06	3.991782E-07
11	G	-4.435892E-05	0.0	-1.472862E-04	-2.398923E-05	-2.568128E-06	-3.909324E-07
12	G	-2.046372E-05	0.0	-7.944898E-05	-2.101134E-05	-3.285147E-06	-1.983341E-06
13	G	-2.309794E-06	0.0	-2.593311E-05	-1.352425E-05	-3.788745E-06	-3.284960E-06
14	G	0.0	0.0	0.0	0.0	-3.883259E-06	-5.282908E-06

IBM JCL MADE EASY BY MEANS OF ISPF DIALOG APPLICATION

Charles E. Cooper
Magnavox Electronic Systems Company

SUMMARY

An interactive CRT terminal application has been developed, which automatically generates the JCL (Job Control Language) and submits NASTRAN batch jobs at an IBM mainframe installation. The relevant parameters for each NASTRAN batch job are stored in a table. Once a table entry is defined, the corresponding NASTRAN batch job may be submitted as often as desired with a minimum of keystrokes. For most users, there is no need for any knowledge of JCL.

INTRODUCTION

Users of the IBM version of COSMIC NASTRAN sometimes complain about the IBM system's burdensome JCL. Part of the aggravation arises from the fact that the rules change from time to time. Changes are necessitated by operating system upgrades, accounting procedure modifications, and even new releases of COSMIC NASTRAN. The hapless occasional NASTRAN user becomes frustrated when he finds that the JCL he used a few months ago no longer works. These problems can be virtually eliminated by use of an IBM program product, the Dialog Management Services of ISPF (Interactive System Productivity Facility).

At our installation, NASTRAN users access the IBM mainframe by means of TSO (Time Sharing Option) terminals. NASTRAN input data is prepared by use of the ISPF text editor PDF (Program Development Facility) on the IBM host and Supertab, a finite element modeling tool by Structural Dynamics Research Corporation (SDRC) running on a DEC VAX computer. On the IBM system, NASTRAN input data may be stored on disk either as an ordinary sequential data set or under the aegis of PANVALET, a data management system by Pansophic Systems, Incorporated. Thus, while the TSO dialog application described in this paper is specific for our installation, it could serve as an illustration for developers of similar applications at other IBM installations.

As implemented at Magnavox, the NASTRAN dialog utilizes full-screen selection, data entry, and help panels in a format familiar to PDF users. At the beginning of the dialog session, the user is presented with a selection menu that provides methods for creating or modifying a table entry as well as submitting a NASTRAN batch job based on an existing table entry. A new table entry may be defined parameter by parameter through a series of data entry panels, or may be copied automatically from an existing table entry and then modified. An online tutorial is also provided, the appropriate sections of which may be accessed by means of the HELP command from any panel.

DESIGN CONSIDERATIONS

Of primary concern was that the dialog should not itself become a burden to the frequent user. Therefore, it was deemed necessary to retain all user entries relating to the definition of JCL related parameters. A single table was chosen to store the run parameters as opposed to a private "user profile" for each user, since it seemed desirable to be able to share NASTRAN batch job descriptions among the several users. A possible drawback to this approach is that only one user can access the table at a time. However, since the typical session is very brief, conflicts at our installation are very rare.

Another consideration was that the user interface should be as consistent as possible with that of PDF and other familiar ISPF utilities. With this in mind, the main menu items were arranged such that the more frequently used options appear at the top of the list. Conventional use was made of the message display capability for reporting errors in the user's input or confirmation of user requested actions.

Several programming language options including the TSO command language (CLIST) were available. The author chose to implement the bulk of the application in VS FORTRAN (IBM's FORTRAN 77) for its convenience and efficiency. (The FORTRAN code consists mainly of calls to the ISPF Dialog Management Facility routines.) A TSO CLIST is used to allocate the needed libraries and initiate the dialog function.

Finally, the application was designed to fully support all known usage of COSMIC NASTRAN at our installation, including the READFILE and CHECKPOINT/RESTART capabilities. If the need develops, the capability of storing the generated JCL as a data set for further user modification could easily be added.

USING THE NASTRAN DIALOG

Creating a New Table Entry

At the TSO READY prompt, the user enters the command "NASTRAN". After a brief wait for the file allocations, the main selection panel or menu, Figure 1, is displayed. On the first run for a NASTRAN model, the user will either select the "C" option to copy the run parameters from a similar job, or the "A" option to enter the parameters from scratch. In either case, the run-name selection panel, Figure 2, is displayed next.

The run-name panel has two data entry fields, the first of which is a 40-character run description field. For a new entry, the description should be entered at this time to aid in future identification of the NASTRAN model. The second input field is the run name, the name by which a table entry is identified to the system. If this field is left blank, on pressing the <ENTER> key, a table display panel, Figure 3, will appear next.

The run-name table display panel provides a scrollable list of all the current table entries. On this panel, the user may "select" a unique name for his new entry on the command line and proceed immediately to the next data entry panel, or merely press the <ENTER> key to return to the name entry panel. Once an acceptable name for the new entry is provided, the name entry panel will be redisplayed with the prompt for the name of the entry to be copied, if the COPY option had been selected on the main menu. Otherwise, the remaining data entry panels, Figures 4-9, will be displayed in turn.

Default values (sometimes blanks) are provided for all the remaining input fields. In the case of the COPY option, of course the values will be those of the copied entry. The user need only scan through the data entry panels making changes as needed. When the last panel is completed, or at any time the user enters the END command (normally by means of a PF key), the main menu is redisplayed.

Submitting a NASTRAN Batch Job

Once a table entry has been defined, the corresponding batch job may be submitted to the computer by selecting the SUBMIT option from the main menu. When the run-name selection panel is displayed, it will already contain the name of the last entry accessed by that user. A press of the <ENTER> key is all that is needed to then submit that job. If a different job is to be submitted, the user may enter the appropriate run name, or select it from the table display panel.

Reviewing or Modifying a Table Entry

The REVIEW option on the main menu provides for the selection of a table entry in the usual way and the display of all the data entry panels in order. Changes may be made to any of the data values displayed except for the run name itself and the description.

Deleting One or More Table Entries

If it should become necessary to reduce the number of table entries for space considerations, or if any of the entries are no longer useful, deletions may be accomplished by selecting the DELETE option on the main menu. The same run-name selection and table display panels are used for this option, but a couple of differences may be noted. First, the selection character is the letter D instead of the letter S for the table display panel. The second difference is that multiple names may be selected on the table display panel. Upon pressing the <ENTER> key, the main menu is redisplayed with a message indicating the number of entries deleted. As an additional safety feature, the user may enter the CANCEL command at this point to "undo" the deletions.

Using the Tutorial and HELP Screens

The tutorial panels for this application also serve as the HELP screens.

Shown in Figures 10 through 29, these panels may be accessed by selecting the TUTORIAL option from the main menu, or by entering the HELP command on any data entry or selection panel. From any of the tutorial panels, the user may request help on how to use the tutorial by entering the HELP command. At this point, the standard ISPF tutorial on "How to Use Tutorials" is provided, which shows the user how to navigate the hierarchical structure of tutorials.

MAINTENANCE EXPERIENCE

As of this writing, the dialog application described herein has been in use for about 17 months. So far, no difficulties attributable to the dialog itself have been reported. Maintenance has been minimal. The few changes required related mainly to the installation of the April, 1986, Release of COSMIC NASTRAN.

CONCLUSION

IBM System 370 JCL is indeed a language, as its name implies. While it may be easy enough for the systems programmer who uses it regularly, most engineers would rather not be bothered by JCL. The NASTRAN dialog application described in this paper has proved quite successful at our installation, and no doubt equally successful NASTRAN ISPF dialogs could be implemented at other IBM mainframe installations.

REFERENCES

1. MVS/Extended Architecture JCL Reference, GC28-1352. IBM, 1985.
2. Interactive System Productivity Facility (ISPF) Dialog Management Services, SC34-2088. IBM, 1985.
3. OS/VS2 TSO Command Language Reference, GC28-648. IBM, 1978.

```

----- NASTRAN BATCH JOB STREAM PROCESSOR -----
OPTION  ===>

S  SUBMIT      - Submit a NASTRAN batch job
R  REVIEW      - Review/Update a NASTRAN job profile
C  COPY        - Copy an existing NASTRAN job profile
A  ADD         - Create a NASTRAN job profile
D  DELETE      - Delete a NASTRAN job profile
T  TUTORIAL    - Display information about this application
X  EXIT        - Terminate ISPF using list/log defaults

USERID  - D528CEC
TIME    - 13:03
TERMINAL - 3278
PF KEYS - 24

NOTE: For assistance, call CHARLIE COOPER, X-5109.

Press ENTER to continue.
Enter END or RETURN command to terminate application.
Enter CANCEL command to abandon updates and terminate application.

```

Figure 1 Main Menu

```

----- NASTRAN -- RUN-NAME SELECTION -----
COMMAND  ===>
ADD NAME

DESCRIPTION OF THIS NASTRAN RUN:

DESCRIPTION  ===>                                (Any characters)

ENTER RUN-NAME OR LEAVE BLANK TO DISPLAY CURRENT LIST:

RUN-NAME    ===>                                (Up to 8 alphanumeric characters, the
                                                first of which must be alpha.)

Press ENTER to continue.
Enter END command to return to main menu.
Enter RETURN command to exit ISPF.

```

Figure 2 Run-Name Selection Panel

```

----- NASTRAN -- RUN-NAME SELECTION -----
COMMAND ===> ADD NAME SCROLL ===> PAGE

Enter S to left of selected name or S runname on command line.

Run-name  Userid  Created  Accessed  Description.....
D01011A   D528CEC  11/12/85  1/13/87  Demo Problem D01011A
D01011B   D528CEC  11/12/85  11/12/85  Demo, RESTART with load change.
D01011C   D528CEC  11/12/85  7/21/86  Demo, RESTART with rigid format switch.
D01061A   D528CEC  6/02/86  7/30/86  Demo Problem D01-06-1A
D04011A   D528CEC  8/26/86  8/26/86  Demo 4-1-1, Differential Stiffness Anal.
S800      D632ARS  12/08/85  10/03/86  S800 air blast analysis
S800ISO   D632ARS  1/04/86  10/03/86  S800 analysis with isolators
S800VAX   D632ARS  1/11/86  1/11/86  S800 model to SUPERTAB
***** BOTTOM OF DATA *****

```

Figure 3 Run-Name Scrollable List

```

----- NASTRAN -- JCL JOB STATEMENT -----
COMMAND ===>

JOBNAME SUFFIX  ===> N      (Any alphanumeric character)
PROCESS NUMBER  ===> DESIGN (Departmental process number, 1-6 alphanumerics)
CHARGE NUMBER   ===> 1102   (Valid J.O. #, 1100 series #, or Dept. #)
USER INFO       ===> NASTRAN (Up to 20 characters)
JOB CLASS       ===> A      (1,A,B,I,Y, corresponding with maximum CPU time:
                             2 sec, 1 min, 5 min, 30 min, >30 min, resp.)
MSGCLASS        ===> 0      (Output class: A=print, 0=hold, Z=discard)
PRINT DEST      ===> VAX10A (TESTCTR, VAX10A, MAHWAH, etc.)
NOTIFY          ===>        (Leave blank to omit; or enter TSO userid.)

Press ENTER to continue.
Enter END command to return to main menu.
Enter RETURN command to terminate application.

```

Figure 4 JCL JOB Statement Panel


```

----- NASTRAN -- JCL PROC OPTIONS -----
COMMAND ===>

*****
** NOTE: For most runs, the NASTRAN PROC **
** defaults are adequate. Therefore, these **
** fields should normally be left blank. **
*****

REGION (K)      ===>      (REGION size in K-bytes, 2500 to 9999)
RELEASE YEAR    ===>      (NASTRAN Release year, 86 or 85)

WORKING DISK STORAGE ALLOCATION:
      ALLOC UNITS  PRIMARY ALLOC  SECONDARY ALLOC
PRIMARY FILES  ===>      ===>      ===>
SECONDARY FILES ===>      ===>      ===>
TERTIARY FILES ===>      ===>      ===>

Press ENTER to continue.
Enter END command to return to main menu.
Enter RETURN command to terminate application.

```

Figure 5 JCL PROC Options Panel

```

----- NASTRAN -- INPUT DATA SOURCE -----
COMMAND ===>

MAIN INPUT DATA SET:  (Enter one of the following:)
  PANVALET MEMBER  ===>      (COMMON.PANVALET.STORAGE member)
  DEMO PROBLEM     ===>      (ENGR.NASTRAN.DEMO member)
  OTHER DATA SET* ===>

READFILE DATA SETS:  (Enter following fields as required:)
      DDNAME          DATA SET NAME*
  ===>              ===>
  ===>              ===>
  ===>              ===>
  ===>              ===>
  ===>              ===>
  ===>              ===>
  ===>              ===>

* Enter fully qualified data set name(s) without quotes.

Press ENTER to continue.
Enter END command to return to main menu.
Enter RETURN command to terminate application.

```

Figure 6 Input Data Source Panel


```

----- NASTRAN -- PLOT OPTIONS -----
COMMAND --->

PLOT OPTION      ---> N      (N=No plot, V=Versatec, C=Calcomp)

VERSATEC PLOTTERS:
  PLOT DESTINATION ---> PLOT10A (PLOT10A, PLOT3B, etc.)

CALCOMP 1012 PLOTTER:
  PLOT FILE NAME  --->      (1-8 alphanumerics, first must be alpha.)
  PAPER TYPE      ---> F10   (Paper type: F00, F01, F10)
  PEN NUMBER      ---> 1     (Pen number: 1, 2, 3, or 4)
  INK COLOR       ---> BLACK (Color: BLACK, RED, BLUE, GREEN)
  ROTATE OPTION   ---> NO    (YES/NO)

Press ENTER to continue.
Enter END command to return to main menu.
Enter RETURN command to terminate application.

```

Figure 7 Plotter Options Panel

```

----- NASTRAN -- CHECKPOINT/RESTART -----
COMMAND --->

CHECKPOINT      ---> NO      (YES/NO)
RESTART         ---> NO      (YES/NO)

CHECKPOINT DATA SETS:
  DICTIONARY     --->      (Output CP-dictionary, final DSNAME qualifier*)
  BULKDATA       --->      (NPTP output final DSNAME qualifier*)

RESTART DATA SETS:
  DICTIONARY     --->      (Input CP-dictionary, final DSNAME qualifier*)
  BULKDATA       --->      (OPTP input final DSNAME qualifier*)

* Enter HELP command for rules regarding Checkpoint/Restart final DSNAME
  qualifiers.

Press ENTER to continue.
Enter END command to return to main menu.
Enter RETURN command to terminate application.

```

Figure 8 Checkpoint/Restart Panel

```

----- NASTRAN -- DATALOADER OUTPUT -----
COMMAND --->                                (For SUPERTAB)

INCLUDE DATALOADER STEP ---> NO             (YES/NO)
VAX CHARGE NUMBER       ---> 1102           Charge number for VAX batch job.
VAX FILE NAME           ---> SY1:USERID[SUPERTAB.UNIV
                                   (Complete VAX file name for
                                   Dataloader output file.)

Press ENTER to continue.
Enter END command to return to main menu.
Enter RETURN command to terminate application.

```

Figure 9 SUPERTAB Dataloader Panel

```

TUTORIAL ----- NASTRAN BATCH JOB STREAM PROCESSOR ----- TUTORIAL
OPTION --->

----- INTRODUCTION -----

This Dialog Application maintains a table of NASTRAN run
parameters which at the user's option may be used to submit
NASTRAN batch jobs to the IBM mainframe system. Each table
entry is given a name by the user who creates it, and the
name of the last entry accessed by a user is retained in the
user's application profile. Thus, when it is desired to
resubmit a NASTRAN job after making input modifications, only
a few keystrokes are required.

----- TUTORIAL CONTENTS -----

This tutorial consists of two main sections which may be
viewed sequentially, or selected by entering the corresponding
one letter code in the OPTION field on line 2.

      S Main selection menu.      D Data entry panels.

```

Figure 10 Tutorial Introduction

TUTORIAL ----- NASTRAN BATCH JOB STREAM PROCESSOR ----- TUTORIAL
OPTION --->

----- MAIN SELECTION MENU -----

The options provided on the main menu allow you to create, modify, or submit a NASTRAN batch job. The parameters for tailoring the Job Control Language (JCL) are all stored in a table which is permanently maintained. Therefore, once a set of parameters is defined, they need not be reentered for subsequent runs. However, you may create a temporary entry, or make temporary updates to a permanent table entry by simply entering the CANCEL command before exiting the application.

Each of the menu options will be presented in order, or may be selected by entering the one letter code in the OPTION field on line 2:

- | | |
|---------------------------|---------------------------------|
| A ADD a new table entry. | S SUBMIT a NASTRAN batch job. |
| C COPY an existing entry. | T TUTORIAL on this application. |
| D DELETE a table entry. | X EXIT to TSO READY. |
| R REVIEW/UPDATE an entry. | |

Figure 11 Tutorial for Main Menu

TUTORIAL ----- NASTRAN BATCH JOB STREAM PROCESSOR ----- TUTORIAL
OPTION --->

----- A - ADD OPTION -----

This option allows the creation of a NASTRAN job profile table entry completely from scratch. Upon selection of this option, a sequence of data entry panels will be presented covering all the available parameter options for this application. Default values are provided for most parameters; so you will need only to revise the ones which are inappropriate. Upon completion, or entry of the END command, the main selection menu will be redisplayed.

An alternate method for creating a new NASTRAN job profile table entry is provided via option C (COPY).

Figure 12 Tutorial for ADD Option

TUTORIAL ----- NASTRAN BATCH JOB STREAM PROCESSOR ----- TUTORIAL
OPTION ==>

----- C - COPY OPTION -----

This option allows the creation of a NASTRAN job profile table entry by copying an existing entry and then making necessary modifications. Upon selection of this option you are first asked to supply the name of the new entry, and in a subsequent panel, the name of the entry to be copied. In both cases, you will have the option of viewing the list of current entries; first to assure the selection of a unique name for the new entry, and next to choose an available entry to copy.

After the new entry has been thus created, a sequence of data entry panels will be presented covering all the available parameter options for this application. You may then proceed to make the desired changes. Upon completion, or entry of the END command, the main selection menu will be redisplayed.

Figure 13 Tutorial for COPY Option

TUTORIAL ----- NASTRAN BATCH JOB STREAM PROCESSOR ----- TUTORIAL
OPTION ==>

----- D - DELETE OPTION -----

When a NASTRAN job profile table entry is no longer needed, either for submitting NASTRAN runs or for use as an example for future COPYING, it may be deleted by means of the DELETE option. Upon selection of a current entry name, that entry will be deleted from the table and the main selection panel will be redisplayed. Multiple entries may be deleted by entering a D in the selection field on the name list display panel opposite each name to be deleted.

Should you change your mind after deleting an entry (or entries), but before terminating the dialog, simply enter the CANCEL command. (Note, however, that CANCEL abandons all table updating activity for the session in which it is used.)

Figure 14 Tutorial for DELETE Option

TUTORIAL ----- NASTRAN BATCH JOB STREAM PROCESSOR ----- TUTORIAL
OPTION --->

----- R - REVIEW/UPDATE OPTION -----

This option allows you to examine, and if desired, to modify any or all the available parameter options for an existing table entry. Upon completion, or entry of the END command, the main selection menu will be redisplayed.

Figure 15 Tutorial for REVIEW/UPDATE Option

TUTORIAL ----- NASTRAN BATCH JOB STREAM PROCESSOR ----- TUTORIAL
OPTION --->

----- S - SUBMIT OPTION -----

Once a NASTRAN job profile table entry contains all the desired parameter settings, the SUBMIT option enables the submission of the corresponding NASTRAN batch job. Upon selection of the desired NASTRAN job profile table entry, the job will be submitted to the internal reader and the main selection menu will be redisplayed.

Note that the CANCEL command of this dialog has no effect on a job once it is submitted. However, you may use the TSO cancel command with the appropriate job name (your TSO userid with the designated one-character suffix).

Figure 16 Tutorial for SUBMIT Option


```

TUTORIAL ----- NASTRAN BATCH JOB STREAM PROCESSOR ----- TUTORIAL
OPTION --->

      ----- T - TUTORIAL OPTION -----

This series of HELP panels follows the standard ISPF pattern for
tutorials. For more information on the use of this tutorial, enter
the HELP command.

```

Figure 17 Tutorial for TUTORIAL Option

```

TUTORIAL ----- NASTRAN BATCH JOB STREAM PROCESSOR ----- TUTORIAL
OPTION --->

      ----- X - EXIT OPTION -----

Entry of the X option is identical to entering the END command from the
primary selection menu. Any table updates made during the dialog session
will be written to disk and you will be returned to TSO READY mode, or to
the alternate dialog if you are in split screen mode.

The CANCEL command has the same effect except that table updates will be
abandoned.

```

Figure 18 Tutorial for EXIT Option

TUTORIAL ----- NASTRAN BATCH JOB STREAM PROCESSOR ----- TUTORIAL
OPTION --->

----- DATA ENTRY PANELS -----

All the parameters required to tailor a NASTRAN batch job stream are collected through a series of data entry panels. The user may exit this series of input panels at any time by entering one of the following commands (or pressing a corresponding PF key) in the COMMAND field:

END - Return to main menu.
RETURN - Exit to TSO READY (or alternate dialog).
CANCEL - Same as RETURN except that table updates are abandoned.

Each of the data entry panels will be presented in order, or may be selected by entering the one letter code in the OPTION field on line 2:

R	Run-name selection.	I	NASTRAN Input data source.
L	List Table entries.	P	Plotter options.
J	JCL JOB statement data.	C	Checkpoint/Restart options.
N	NASTRAN JCL proc options.	S	SUPERTAB dataloader option.

Figure 19 Tutorial -- Introduction to Data Entry Panels

TUTORIAL ----- NASTRAN -- RUN-NAME ----- TUTORIAL
OPTION --->

This panel is used in several contexts as indicated by the subtitle shown on line 3. The two input fields are explained as follows:

RUN-NAME - After the first use of this dialog by a user, this field will usually contain the last accessed run-name by that user. If it is cleared to blanks prior to pressing the ENTER key, the list of entries currently in the table will be displayed on the next panel. Otherwise, the table display panel will be skipped. Note: when selecting the run-name for a new entry, the DESCRIPTION field should be filled in even if the RUN-NAME field is left blank.

DESCRIPTION - This field is significant only in the process of creating a new table entry. (It may be updated for existing table entries by a series of COPY and DELETE operations.) Lower case letters are retained for this field; so the shift key should be used where upper case letters are desired.

Figure 20 Tutorial for Run-Name Selection Panel

TUTORIAL ----- NASTRAN -- RUN-NAME LIST ----- TUTORIAL
OPTION --->

The RUN-NAME LIST panel is displayed only if the run-name is not supplied on the RUN-NAME SELECTION panel. The run-name of any existing table entry may be selected from the scrollable list by keying the letter S to the left of the run-name field in the same manner that PDS or PANVALET members may be selected in PDF EDIT or BROWSE.

Also, as in PDF EDIT or BROWSE, a run-name (either new or existing) may be selected by keying S runname in the COMMAND field where "runname" is any acceptable name.

If neither method of selecting a run-name on this panel is used, the RUN-NAME SELECTION panel will be redisplayed upon entry of the END command. The RETURN command will cause the main selection panel to be redisplayed.

Figure 21 Tutorial for Scrollable Run-Name List

TUTORIAL ----- NASTRAN -- JOB STATEMENT ----- TUTORIAL
OPTION --->

All the input fields on this panel relate to the IBM JCL JOB statement. Since the rules for these items are subject to change by DP Technical Resources, only minimal verification is provided by this dialog. Each field is treated separately below:

JOBNAME SUFFIX - A single character (alphanumeric or national) which is appended to your TSO userid to form the JCL JOB name.

PROCESS NUMBER - The first field of the accounting information in accordance with your departments practice. (It is often used to indicate the department number for which the run is made.)

CHARGE NUMBER - The second accounting information field. It must be a valid Job Order number, department number, or other valid charge number.

(more)

Figure 22 Tutorial for JOB Statement Panel

TUTORIAL ----- NASTRAM -- JOB STATEMENT (Page 2) ----- TUTORIAL
OPTION --->

- | | |
|-------------------|---|
| USER INFO | - This 20-character field is usually for the submitter's name. DO NOT use quotes; they are provided by the dialog function. Other special characters are okay, including leading and imbedded blanks. |
| JOB CLASS | - The appropriate JOB class character in accordance with DP Operations rules. |
| MSGCLASS | - The MSGCLASS serves not only for JCL and JES2 messages, it also covers the NASTRAM printouts. DON'T use class Z unless you want to eliminate ALL printout! |
| PRINT DEST | - Enter the appropriate print destination ID to direct the printout to a convenient printer. |
| NOTIFY | - Enter your TSO userid if you wish to be notified of your NASTRAM job's status at your TSO terminal. |

Figure 23 Tutorial for JOB Statement Panel (Continued)

TUTORIAL ----- NASTRAM -- JCL PROC OPTIONS ----- TUTORIAL
OPTION --->

For very large models, it may be necessary to increase the amount of main storage and/or disk storage allocations. Since indiscriminate increases in these parameters could have a negative impact on total system performance, it is recommended that they be used with caution.

The only parameter on this panel not related to size is the RELEASE YEAR. Normally, only the current release and the most recent past release of NASTRAM will be available for use.

If you have a need to code any field on this panel, please notify CHARLIE COOPER, X-5109.

Figure 24 Tutorial for JCL PROC Options Panel

TUTORIAL ----- NASTRAN -- INPUT SOURCE(S) ----- TUTORIAL
OPTION ==>

MAIN INPUT DATA SET:

The NASTRAN input "deck" from the NASTRAN "card" to the ENDDATA "card" may be a member of COMMON.PANVALET.STORAGE or a sequential disk data set. If the NASTRAN deck is a member of a Partitioned Data Set (PDS), the member name must also be included. The NASTRAN Demo Problem PDS is included as a special case of the sequential data sets for which only the member name need be given. The three fields for identifying the source of the main NASTRAN input deck are mutually exclusive, ie. only one of the three fields may be coded. If the input is neither a PANVALET member or a DEMO problem, the fully qualified DSNNAME, including member name in parentheses if a PDS member, must be coded in the OTHER DATA SET field.

(more)

Figure 25 Tutorial for Input Sources Panel

TUTORIAL ----- NASTRAN -- INPUT SOURCE(S) (part 2) ----- TUTORIAL
OPTION ==>

READFILE DATA SETS:

The NASTRAN READFILE facility lets you include data into the NASTRAN deck from other sequential disk files. For data sets not already defined in the NASTRAN cataloged JCL procedure, the DDNAME and DATA SET NAME fields must be supplied in order to identify the disk file to be read. In the case of PDS members, the member name must be coded as a part of the DATA SET NAME as shown in the following example:

```
In NASTRAN deck:  READFILE MYDATA
DDNAME:          MYDATA
DATA SET NAME:    D52BCEC.TSO.FORT(MYNBR)
```

Note that the DDNAME's must be unique and different from any DDNAME in the NASTRAN cataloged JCL procedure, such as RFDATA, NPTP, OPTP, ALTERS, DISP1DL, DISP3DL, etc.

Figure 26 Tutorial for Input Sources Panel (Continued)

TUTORIAL ----- NASTRAN -- PLOT OPTIONS ----- TUTORIAL
 OPTION ==>

The PLOT OPTION entry is the only required parameter on this panel. If N (No plot) is selected, all other input fields will be ignored. The other two options (V and C) indicate the type of plotter to be used (Versatec or Calcomp 1012). Parameters for both supported types may be supplied, but only the ones corresponding to the selected type will be used.

VERSATEC PLOTTERS:

The PLOT DESTINATION is the destination ID as assigned by Technical Resources for the particular Versatec plotter you wish to use.

CALCOMP 1012 PLOTTER:

- PLOT FILE NAME - Final DSNAME qualifier for the plot output.
- PAPER TYPE - F00=plain,short; F01=grid,short; F10=plain,long.
- PEN NUMBER - Always use 1 (one); others not yet supported.
- INK COLOR - Indicate desired color; BLACK, RED, BLUE, GREEN.
- ROTATE OPTION - Enter YES if you want 90 degree rotation.

Notes: PLOT FILE NAME must be unique with respect to currently active Calcomp 1012 plot file data sets. PAPER TYPE will normally be F10 for structure plots.

Figure 27 Tutorial for Plotter Options Panel

TUTORIAL ----- NASTRAN -- CHECKPOINT/RESTART ----- TUTORIAL
 OPTION ==>

The CHECKPOINT/RESTART input panel provides for the required JCL overrides to support runs involving the NASTRAN checkpoint and/or restart facilities. The related data set names will have your userid as the leading (high level) qualifier. Thus, from TSO READY, you may check on their existence merely by keying the LISTCAT command.

A data set name (DSNAME) qualifier consists of from 1 to 8 alphanumeric characters, the first of which must be alphabetic. In a run involving both checkpoint and restart, the respective DICTIONARY and BULKDATA final DSNAME qualifiers must differ.

The restart DICTIONARY and BULKDATA data set names must match the respective checkpoint DICTIONARY and BULKDATA data set names of a previous run. Therefore, if you wish to restart a NASTRAN run checkpointed by another user, you must first rename or copy the checkpoint DICTIONARY and BULKDATA data sets with your own TSO userid as the leading qualifier.

Figure 28 Tutorial for CHECKPOINT/RESTART Panel

42573-787

TUTORIAL ----- NASTRAN -- DATALOADER OUTPUT ----- TUTORIAL
OPTION --->

If the DATALOADER step is included in the NASTRAN run, a batch job will be submitted to the VAX A computer to create the SUPERTAB universal file. (The NASTRAN data deck must, of course, include the necessary DMAP ALTERS to produce the OUTPUT2 data for DDNAME FT18F001.)

If YES is coded on the option line, then a valid VAX charge number and an appropriate file name must be supplied in the designated fields. Please consult the cognizant VAX support personnel for current rules.

Figure 29 Tutorial for SUPERTAB Dataloader Panel

A NEW APPROACH TO FINITE ELEMENT MODELING, ANALYSIS AND POST-PROCESSING

By: Gil White, Intergraph Corporation

ABSTRACT

Today's structural engineer is confronted with a host of CAD/CAE systems that offer solutions to the problems of finite element model construction, analysis and results interpretation. The history of computer-aided design and analysis has followed a path that provided for the quickest method for automating specific functions. This evolution has created islands of automation. Various attempts have been made to link segregated databases and form cohesive systems. Some attempts have proven successful but their efficiency is limited. Recent developments in both hardware and software have opened the door to systems of fundamental new design. The industry is now seeing the development of fully standalone workstation platforms that provide new and exciting opportunities for the COSMIC NASTRAN user.

INTRODUCTION

Increased computer computational power combined with advances in the field of finite element analysis have revolutionized structural engineering. Today, this revolution is continuing and displays itself in the form of full integration between mechanical design and various types of engineering analysis. Systems displaying full functionality between design and analysis are becoming the standard for companies of all sizes as CAE becomes increasingly more cost effective. These systems offer a significant cost improvement by reducing the turnaround time for product development and verification. In many cases, the need for prototype development is omitted from the design process completely.

The ideal finite element modeling system would be a system of multi-functionality that meets the needs of different users. Such a system would have a database that serves as a foundation for geometric design as well as engineering analysis. The COSMIC NASTRAN user is now confronted with more alternatives in the selection of pre- and post-processors as well as methods for full system integration.

A NEW APPROACH TO FINITE ELEMENT MODELING, ANALYSIS AND POST-PROCESSING

The benefits of full integration between CAD and CAE are nowhere more obvious than in the area of finite element analysis. By linking the design and analysis process, the COSMIC NASTRAN user can improve accuracy and reduce modeling time. The cost benefits of such integrated software are multiplied when these functions can be performed on a standalone workstation. The major expense in the area of finite element analysis is incurred during model construction; modeling time is greatly reduced when the analyst uses the geometric design as a basis for the FE model. This concept, known as geometry-based mesh generation, represents the new generation of finite element modeling systems. In addition, integrated design and analysis produces cost savings with respect to trouble shooting, elimination of modeling errors and increased accuracy.

Historically, the COSMIC NASTRAN user has constructed models by one of two methods. He either input all components (nodes, elements and materials) by single entry operations, or he used some type of automated mesh generation process. These methods for inputting information required the engineer to address segments of the model independently; they also required that this data be reformatted if the part geometry changed. Both of these limitations increase FEA cost. Therefore, the ideal modeling system would be one that automated these functions by fully integrating design and analysis.

Post-processing and results interpretation are also expedited through graphic and analysis links. Visual inspection of the analysis results provides the quickest method for evaluating the model. This quality of CAE has long been recognized as one of the strong points in its application to the field of finite element analysis. The ideal post-processing environment would not only provide graphic and conventional methods for reviewing output, but would also offer a data management system. Such a data management system would allow the user to manipulate analysis results, to create new output, as well as providing re-analysis capability.

INTERGRAPH addresses the needs of the COSMIC NASTRAN user with a new workstation-based finite element modeling system called I/FEM. This product was developed using object-oriented programming which provides the foundation for true integration between design and engineering analysis. Object-oriented programming methods were chosen over more conventional procedure style programming because it permits code to be reused thus greatly reducing the time dedicated to programming. Also, object-oriented programming allows addition of new data types without modifying existing code.

The I/FEM modeler has the ability to construct all components of the finite element model. Model construction actually begins during the design session when geometry is enhanced with FEA attributes. This "intelligent" geometry greatly accelerates the analysis process. Fully automatic meshing gives fast, accurate and efficient model construction. The user can optimize the mesh with respect to predefined criteria. The system can automatically remesh when required. Loads and boundary conditions may be defined prior to meshing and later edited, or placed at any time after the mesh has been created; the load and boundary condition criteria are assigned to the geometry as opposed to the mesh. The I/FEM modeler constructs the vast majority of input data for the COSMIC NASTRAN user.

The I/FEM solver employs the finite element method in the solution of several classes of applied mechanics and field problems. I/FEM offers basic analysis capabilities that can be expanded by adding other analysis modules. The solver is described as an out-of-core solver which limits model size to the amount of local disk storage only. The I/FEM post-processor offers both graphic and nongraphic methods for reviewing any of the results that are output from the local solver or any third-party solvers including COSMIC NASTRAN. I/FEM offers the ability to do reanalysis within the postprocessing environment. The system will automatically determine if a new decomposition is required and if so will instruct the solver accordingly. Also, within this environment one will be able to perform arithmetic and algebraic operations on any of the output data. New data sets may be created to enhance COSMIC NASTRAN results interpretation. The user-friendly interface of the I/FEM post-processor is seen in the way COSMIC NASTRAN analysis results are reviewed. All naming schemes and nomenclature are transferred from COSMIC NASTRAN to the I/FEM environment without any change. This gives the COSMIC NASTRAN user the feeling of working in one software package.

I/FEM takes an innovative approach to interfacing COSMIC NASTRAN and I/FEM. The ideal data transfer procedure is one which passes all information to a "neutral" file. From this neutral file, routines may be written to access data in a variety of ways. In recognition of the fact that an "open" architecture is essential to a complete system, I/FEM will maintain such a "neutral" file translator. For selected third-party solvers, such as COSMIC NASTRAN, Intergraph will also provide the interface from the neutral file to the third-party solver, thereby completing the interface between I/FEM and COSMIC NASTRAN. This method also provides a reliable way to securely archive models.

CONCLUSIONS

Recent advances in both hardware and software have opened the door to a new generation of finite element modeling systems. INTERGRAPH CORP has combined an innovative programming concept with a standalone workstation hardware platform to produce a new standard in finite element modeling. This system offers the COSMIC NASTRAN user full integration between design and analysis. I/FEM not only addresses the needs of the COSMIC NASTRAN user of today, it also provides for continued evolution of the COSMIC NASTRAN product.

**THE APPLICATION OF NASCAD AS A NASTRAN
PRE- AND POST-PROCESSOR***

**Alan N. Peltzman
University of Maryland**

INTRODUCTION

NASCAD (NASA Computer Aided Design) is a 3-D computer aided design (CAD) package that was developed under NASA auspices. In 1985, this powerful, low-cost software package was released to COSMIC and became public-domain.

NASCAD is part of the overall Computer Integrated Manufacturing (CIM) package called NEXUS/NASCAD. NEXUS stands for NASA Engineering eXtensible Unified Software. Part of the motivation for developing NASCAD was to create a CAD system which would interconnect with other CAD/CAM related software. This network of connections is what makes NASCAD such an effective engineering tool.

Lloyd Purves, the creator and guiding force behind NASCAD, made sure that the software could be incorporated into a general CIM framework. He anticipated the relational needs of design analysis and manufacturing. Thus, NASCAD was written to hook into other software packages and standards such as APT, IGES, & NASTRAN. To have NASCAD become an "island of automation" would be an anathema. NASCAD is intended not just to be a drafting or design package but to be an intimate part of the overall CIM process. More to the point of this conference, NASCAD is especially attractive as a pre- and post-processor for NASTRAN.

*Funding for this report made possible by Texas Instruments Corporation

NASCAD AS A NASTRAN PRE-PROCESSOR

Let us see how NASCAD can be used as a NASTRAN pre-processor by creating a hypothetical scenario involving a 1) designer and 2) NASTRAN analyst (fig. 1). For purposes of illustration we are ignoring the possibility that the designer and the analyst are the same person. In our scenario, a designer has created and refined a geometric model using NASCAD. The NASCAD computer file is given to an analyst. It is understood that the analyst will not alter the design ingredients but will use the design data base primarily as source material. The analyst's task will be to generate a finite element mesh that faithfully represents the properties of the design. The analyst loads the design data file into NASCAD and goes about the task of creating a finite element model. NASCAD's wealth of geometric modules and algorithms enables the user to fashion a mesh to suit the level of detail that he needs. With NASCAD, the analyst can zoom in on a certain area of the model and select only the geometry that interests him. Another special feature is a series of storage bins or buffers called levels. These "levels" (also known as layers) can be employed to partition the model by function, geometry, or any criterion the analyst finds appropriate. Some of the more useful groupings for finite element applications are element type, material properties, loading, and constraints. In figures 2-5, levels are used to group data by element type.

Once an area of the design has been selected for modeling, gridpoints are defined and elements are added to that mesh. The analyst can interactively attach such properties as mass and load constraints to the elements. NASCAD supports lines, polygons, polyhedra, and advanced surfaces such as bicubic splines. NASCAD's macro language allows the user to create super-commands that will speed the generation of meshes. T.G. Butler of Butler Analyses has created a set of macro's to facilitate the creation of NASCAD meshes (fig. 6).

As a visual check, the analyst can display his model from any view (including perspective). Hidden line processing (fig. 7), color, and shading can also be added to enhance the effect. On the basis of these visual checks, the analyst can interactively modify and refine the mesh (as well as change properties). Once the analytic model has been satisfactorily defined, the user can store it off as a NASCAD file for future use.

After completing the NASCAD analytic file, the analyst then invokes "C2N", the NASCAD to NASTRAN translator. C2N converts the NASCAD analytic model into a NASTRAN input data deck (NID). It transforms NASCAD mesh points into NASTRAN grid points. C2N converts the NASCAD finite elements into NASTRAN connection cards (CBAR, CTRETA, etc.). C2N can also be instructed to create property cards for specific groups of elements.

At this point, the analyst leaves NEXUS/NASCAD and enters the NASTRAN domain.

Once in the NASTRAN domain, the analyst uses a text editor to modify the NID file, adding executive control, case control, and output management statements. The analyst does not have to specify plotting control information because NASCAD can be used to produce very effective plots. The analyst runs NASTRAN which will produce modal analysis, vibration analysis, stress analysis, and deformation analysis at the user's discretion.

NASCAD AS A NASTRAN POST-PROCESSOR

After the NASTRAN run is completed, the analyst will undoubtedly want to display the results. Once again, NASCAD can be used to great benefit. The NASTRAN to NASCAD translator (N2C) will convert the NASTRAN data to NASCAD data. Displacements (fig. 8) and stresses are successfully brought over as NASCAD data. The analyst can display the deformed and undeformed model as well as create stress contour displays using NASCAD's color capabilities. In both post-process and pre-process phases the user will probably want to create plots of his data. The advantage that NASCAD has over NASTRAN is that with NASTRAN the analyst has to anticipate the orientation needed for a structure in order to display pertinent features. He must convert his mental image into specific plot commands prior to his analysis run. Usually he does a lot of guessing. If he guesses wrong, he is compelled to rerun his job with a new set of guesses. But with NASCAD the analyst need not do any anticipating. He can display the results and reorient different views until a pertinent feature is shown to best advantage. The analyst can then plot that designated view.

In addition to obtaining a best view, NASCAD offers the analyst the ability to edit and highlight his display to focus the reader's attention on essentials of the analysis. He can add boxes, arrows, colors, and text to make the drawing more informative. NASCAD will allow plots of single or multiple views (fig. 9) and support electrostatic plotters, dot matrix printers, and pen plotters. NEXUS also has a pre-plotting capability that allows the user to simulate his plot on a terminal before committing himself to paper (or vellum).

Using NASCAD as a post-processor, the analyst can zoom in on trouble spots and pinpoint where anomalies are occurring. If an analyst's results reveal design defects, NASCAD can assist the analyst with changes in his finite element model. The analyst can also refine the mesh by calling up and changing the stored analytic NASCAD model. NASCAD facilitates the analysis cycle by allowing the user to readily display and alter his analytic model. This allows more NASTRAN runs and greater product refinement.

CONCLUDING REMARKS

The NASCAD graphics package provides an effective way to interactively create, view, and refine analytic data models. NASCAD's macro language, combined with its powerful 3-D geometric data base allows the user important flexibility and speed in constructing his model. This flexibility has the added benefit of enabling the user to keep pace with any new NASTRAN developments. NASCAD allows models to be conveniently viewed and plotted to best advantage in both pre- and post-process phases of development, providing useful visual feedback to the analysis process. NASCAD, used as a graphics complement to NASTRAN, can play a valuable role in the process of finite element modeling. Like NASTRAN, NASCAD is available in the public domain and is distributed, complete with source code, translators, and plotting packages, through COSMIC.

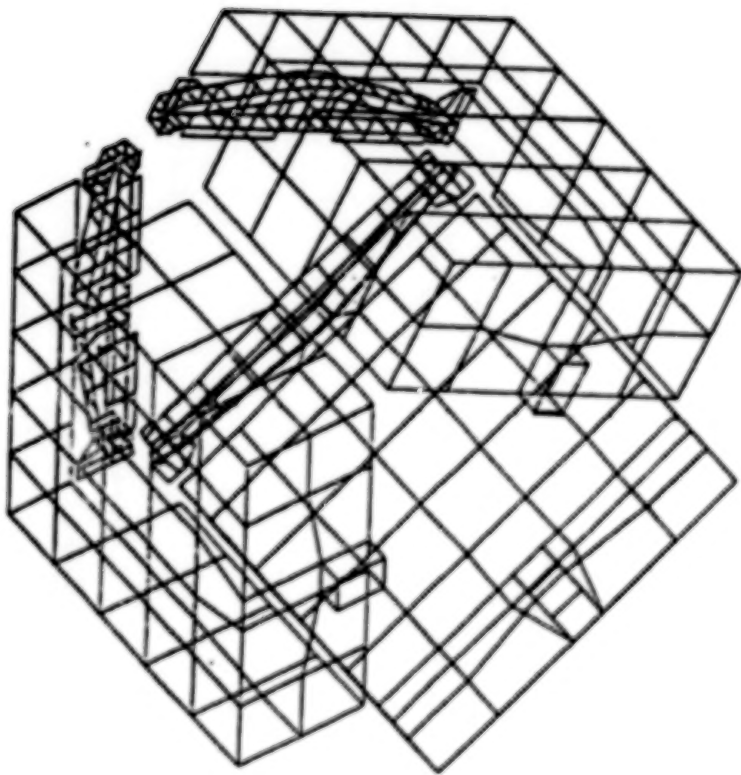


Figure 2. Isometric view of multission satellite (MMS) -
quadrilateral elements only



Figure 3. Isometric view of MMS - triangular elements only

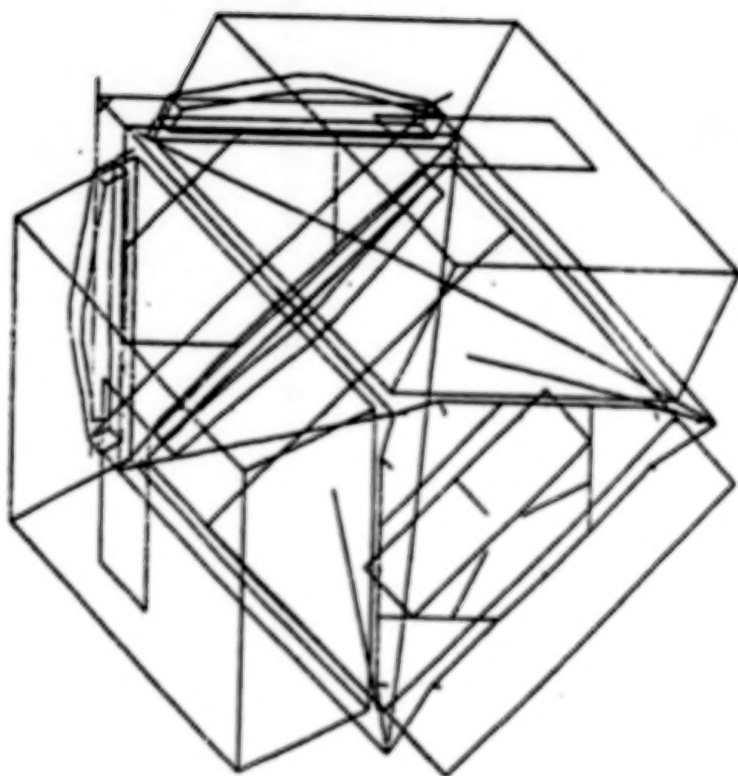


Figure 4. Isometric view of MMS - bar elements only



Figure 5. Isometric view of MMS - rigid elements only

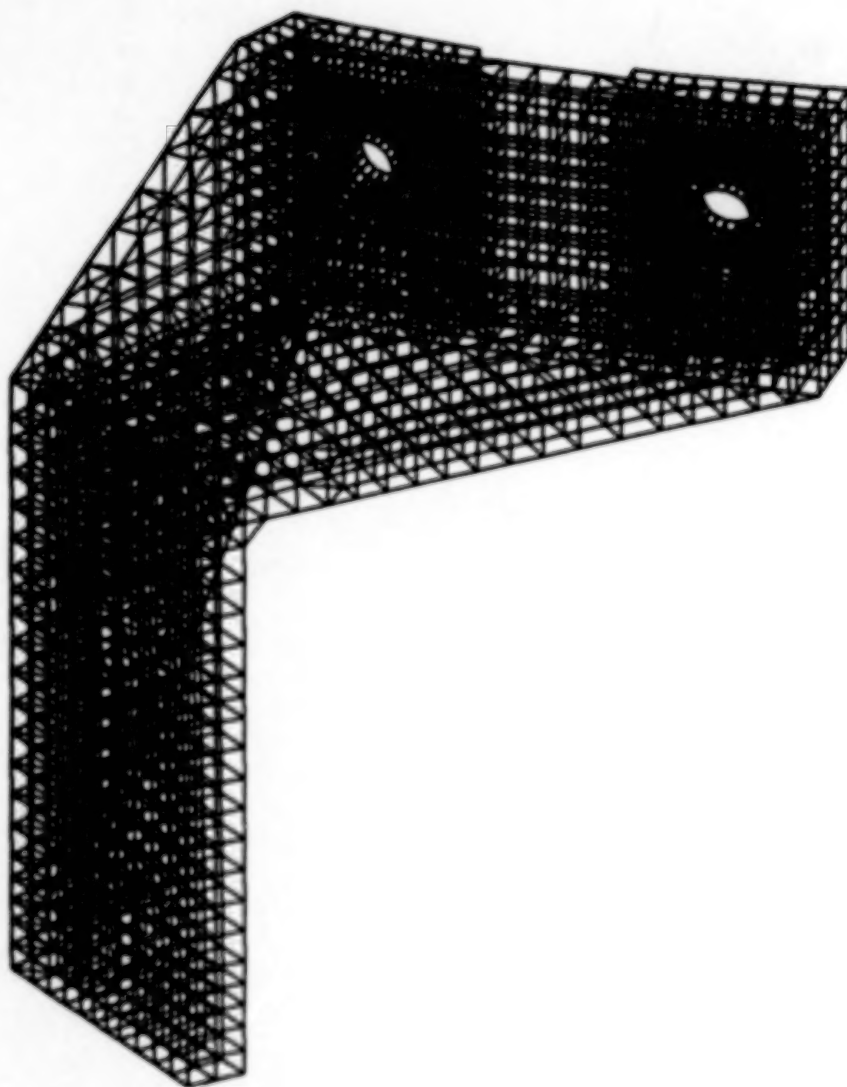


Figure 6. Butler Analyses bracket model.
NASCAD macro's enabled the construction of this
complex model.

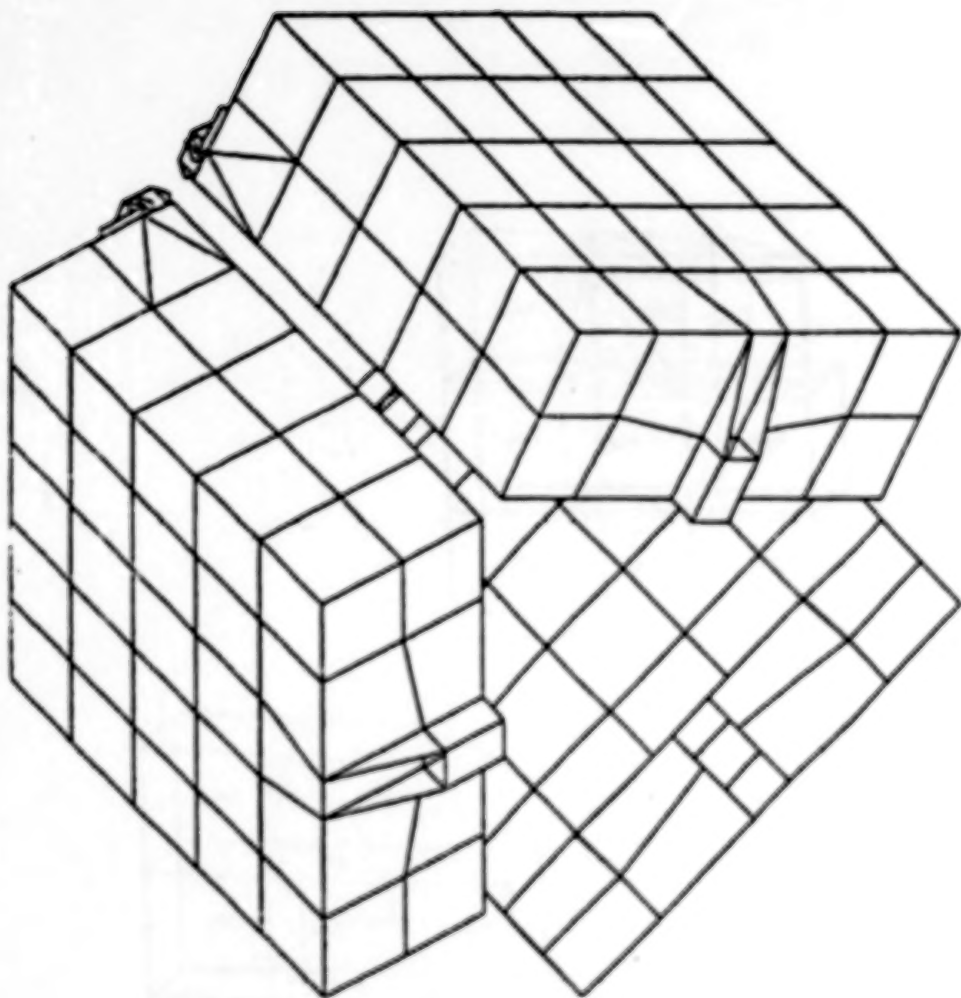


Figure 7. Hidden line drawing of multi-mission satellite

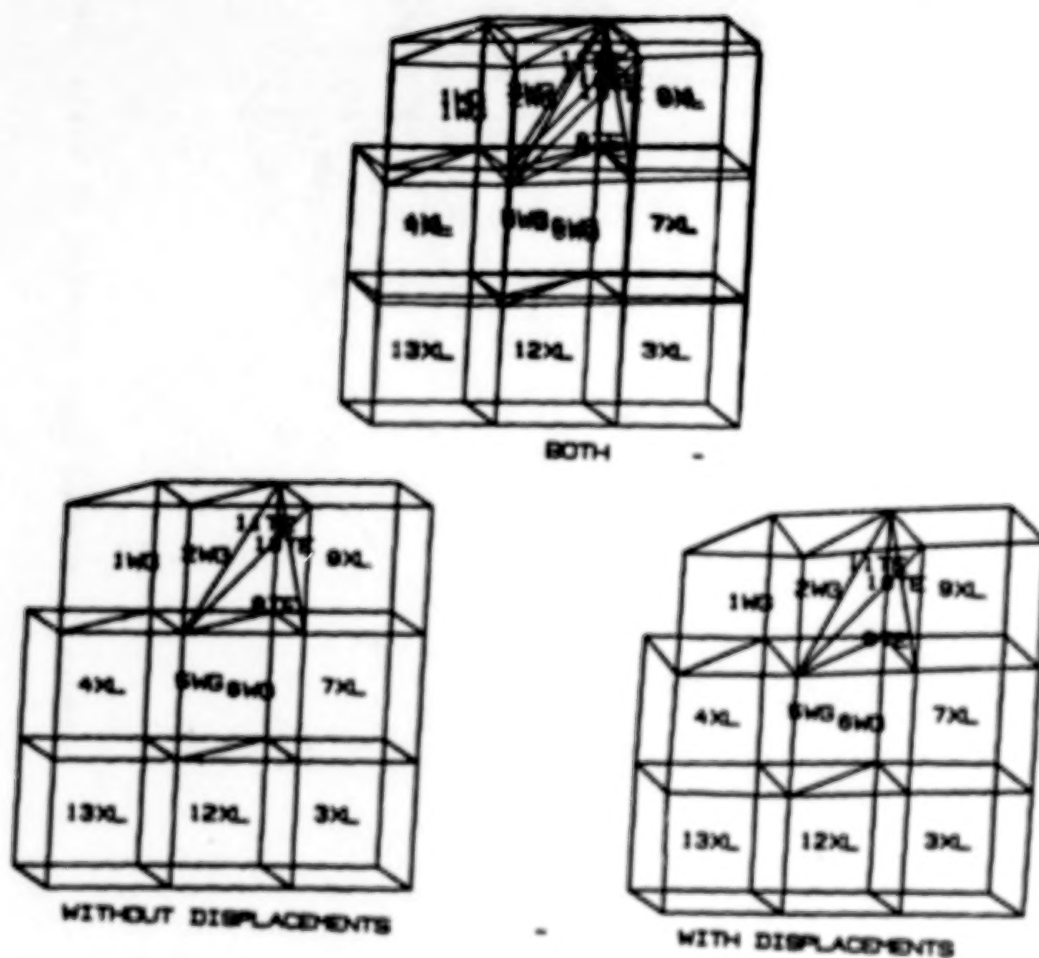


Figure 8. Display of test model with and without displacements

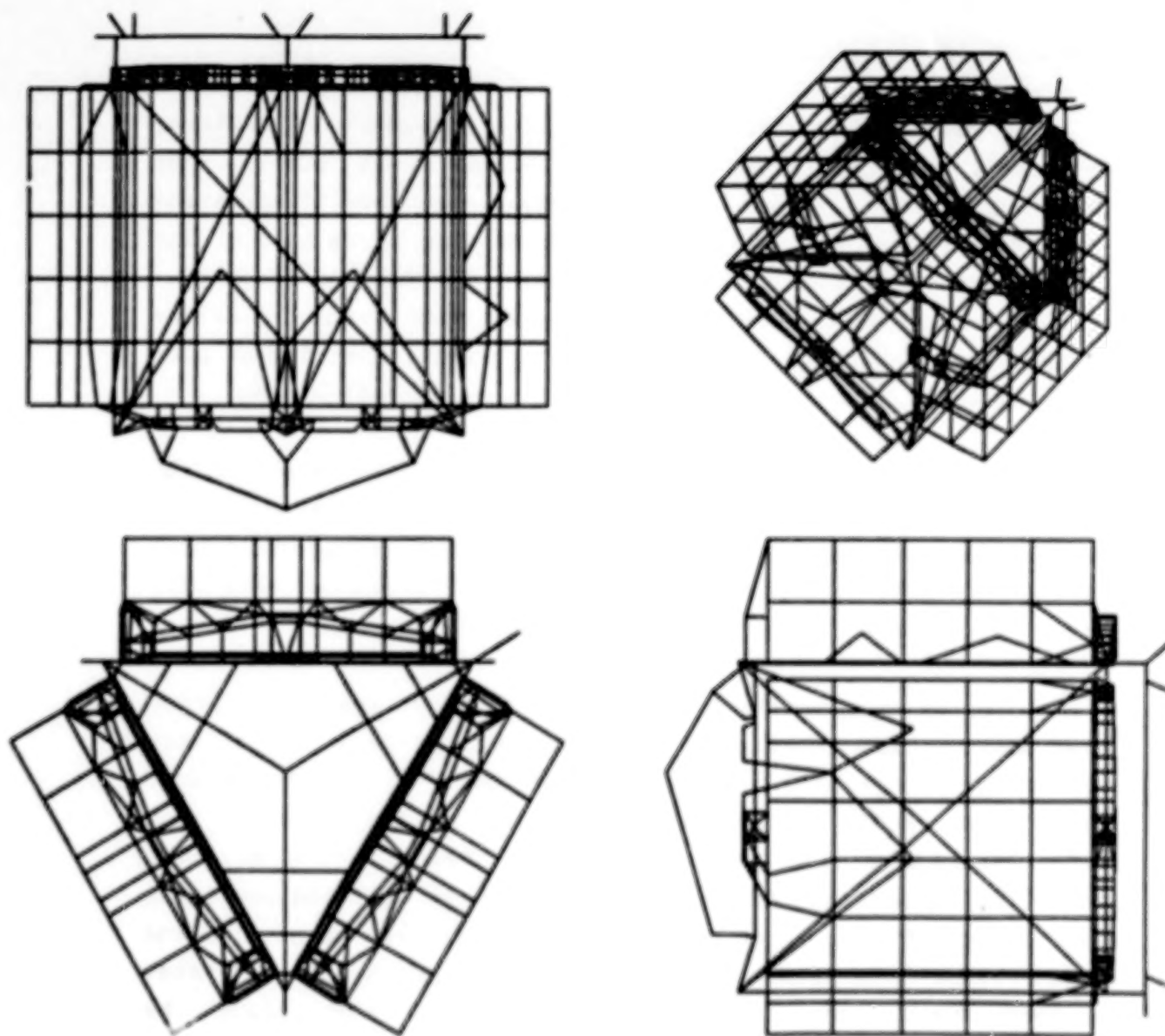


Figure 9. Multiple views of multi-mission satellite

EXPERIENCES RUNNING NASTRAN ON THE MICROVAX II COMPUTER

Thomas G. Butler and Reginald S. Mitchell
BUTLER ANALYSES GODDARD SPACE FLIGHT CENTER

INTRODUCTION

The engineering analyst operates in an entirely new environment today compared to the days when NASTRAN went public. No individual could afford to own a computer capable of operating NASTRAN in 1972. And rarely did an engineering group have a computer dedicated solely to its purposes. Any NASTRAN-sized computer generally had a staff of people associated with its various requirements. It would have a systems staff, a utilities programming staff, a maintenance section and an operating crew.

The engineering analyst would generally interface with the operating staff (dispatcher) and submit his job to be processed by the operations group. This same operations group would collect his output, input, plots, and tapes and assemble them for him by job in his "output-box" or his courier station.

Later on when remote batch terminals (card read and print stations) became available, the user would by-pass part of this interface by inserting his job directly into the input queue. Operations people still manipulated and processed most of the output as before. With the improvement in remote terminals and with the extension of job control language, the analyst could take charge of this input and monitor the progress of his job and even change its status with respect to other traffic (delete, postpone, wait, control sequence). Generally, even though he knew that he had that access, he sought the tutelage of a systems programmer to set up a series of commands for him so that a job would proceed according to his wishes. Any demands on resources

were certainly routed through a systems programmer; i.e. extra memory beyond user quota, or extra disk space at a certain stage of his job, or routing storage to tape, transferring files between jobs, etc.

In essence, then, even though the analyst had access to commands to control the routing of his job, he generally opted for the easy way out by placing his dependency on the systems programmer. A fair number of analysts struggled along without help and lapsed into unenlightened ruts which were a combination of hints from others who operated similar jobs, reaction to scoldings from dispatch personnel, and occasional discussions with systems programmers. But in any such exchanges there must be good communication. The analyst must project his objectives in sufficiently jargon-free phrases that the systems programmer can grasp the requirements to provide a scheme of commands to allow resources in a timely fashion and obtain approvals for the temporary hoarding of storage or priorities or post-processing. One aspect of systems programming that was almost opaque to the analyst was (and still is) the tailoring of main memory, secondary storage, limits on system management facilities, allocation of utilities, assigning of queues, and assigning of priorities to a given software package. A program such as NASTRAN has needs such as few other programs. NASTRAN jobs can run sluggishly or efficiently depending on how well the systems programmer matches the allocations of computer resources to the program's resident memory requirements, scratch disk space requirements, and I/O requirements.

Interpretations of diagnostics to find out what mistakes the analyst made in his data were the tasks attended to by a computer's support staff. And in case an error was too elusive, the problem could be rerun with a core dump and any anomalous step could be pinpointed. Such is the help obtainable from the support staff.

Thanks to competition amongst computer manufacturers, two trends worked to the advantage of the analyst---system commands

became friendlier and editing languages improved greatly. With a little digging an analyst could prepare problem data more easily and could also have more confidence in simpler job control tasks. But he tended to reach a plateau of only simple skills and still depended on the computer staff for considerable support.

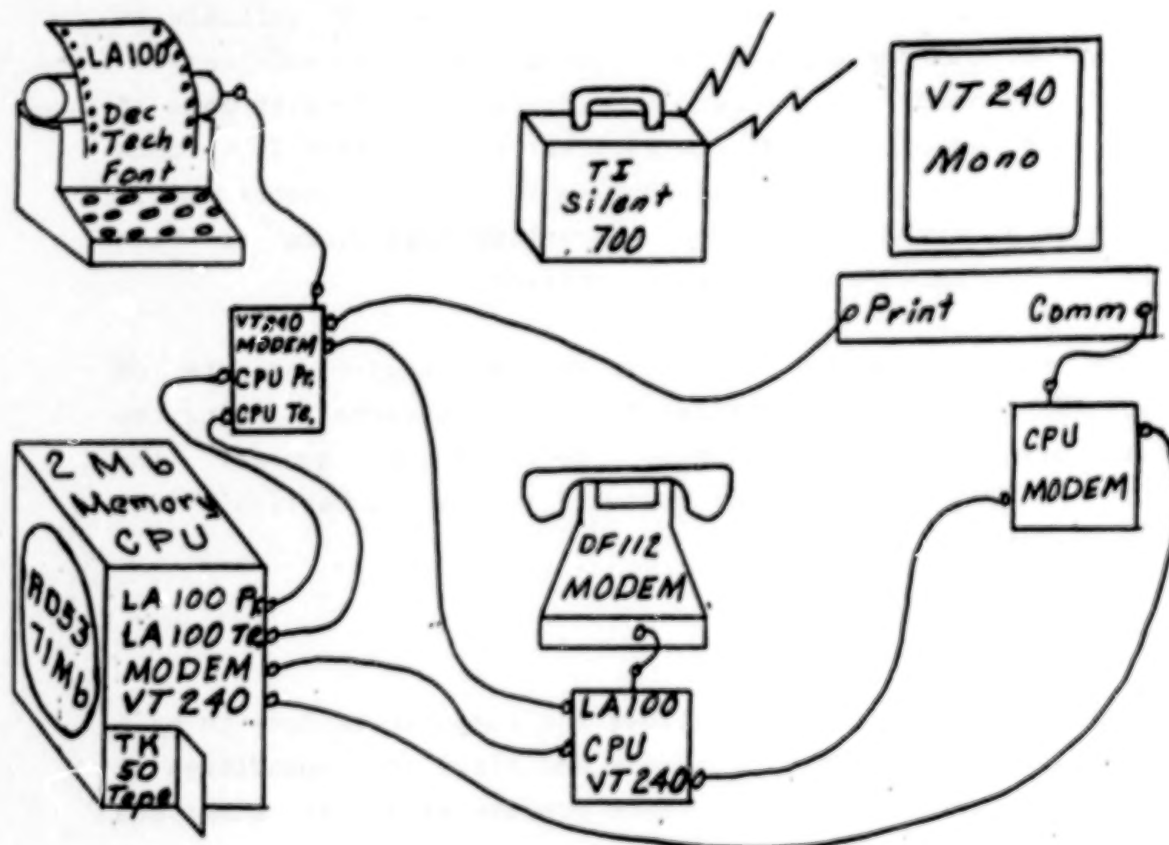
The next change of his computer environment came with the popularity of mini-computers. But the word mini implies less, so the budgets that usually went with the purchase of mini-computers were less than those for main-frames. This meant less staff--and sometimes no staff at all. Systems programmers who were assigned to a mini-computer would be available on prime-time shifts only and had so many other duties that they could give only limited help to analysts. This is a kind of good news--bad news story in which the engineers had their own computer, but were too ignorant in computerese to take advantage of it. A small cadre' buckled down and became computer wizards, but most engineers remained awestruck by the computer.

Then the unbelievable happened. Micro computers were marketed with such power that they could operate NASTRAN. Their cost was under \$50,000! Now it became economical and logical for an individual engineer to have his own unshared computer that could be linked to any other installation for which he had traffic. Good News and Bad News. He has his own computer BUT he has to be his own staff. When he gets a message for instance that max pages has been exceeded, he instinctively seeks help from a systems programmer. But then is me. Change hats and answer your own questions. Whoops! That's where we are today. Some of us got ourselves into this fix voluntarily and others became involuntary victims of this computer tyranny. The rest of the paper will be devoted to a description of the computer staff burdens that an individual analyst/owner of a MicroVAX II has to assume when he wants to use it to run NASTRAN. The topics will be divided according to the logic of getting NASTRAN to operate on a new MicroVAX installation.

DECIDING ON THE HARDWARE

Many of the system configuration decisions depend on the hardware that the system is to manage and the applications programs which operate with it. The MicroVAX II hardware that I installed is as follows: 2 Megabytes of main memory, RD53 71-Megabyte Winchester Disk Drive, TK50 Drive for magnetic tape cartridges, VT240 Monochrome Terminal with Bit Mapping and port to printer, LA100 Typewriter Terminal/Printer with DEC Tech Math Font, DF112 Modem for 300 and 1200 baud transmissions, TI Silent 700 Typewriter Terminal for telephone access, Black Boxes for switching channels between components, Q-BUS backplane for expandable main memory and disk space, VMS Level 4.2 Operating System (No FORTRAN).

The configuration is shown in a diagrammatic sketch showing how the black boxes provide for various interconnections.



The modus that I intended for NASTRAN was: (a) to prepare the bulk data for analytical jobs and debug them well so that they can be reliable for submission to a remote main-frame; (b) to use NASCAD as a pre and post processor to help prepare input data and to massage the output from remote main-frames for final reports; (c) to make pilot runs to prove out solution strategies before enabling them on big jobs; and (d) to compose DMAP code for special applications and debug them thoroughly before incorporating them into an application run.

I chose not to subscribe to either a software or a hardware maintenance license, because the cost was prohibitive for a single user. Unfortunately, it would have paid off if I had, because my office had an air-conditioning failure which caused the computer to cook. Without a maintenance contract, the MicroVAX owner is treated by DEC like a second class citizen. It takes a long time to thread through their bureaucracy to pin point the right group to engage for service. With trouble one first has to establish whether the problem is software or hardware. Even after service is engaged, the non-maintenance-contract customer is shifted to lowest priority with days of waiting. It was a rude shock to be treated so shabbily. Once service was rendered, it was excellent. But to someone who is not systems oriented, it becomes a harrowing experience to have an emergency without a maintenance contract.

The systems approach to getting NASTRAN ready to operate on a MicroVAX-II will be discussed in this sequence: sizing the system; preparing the system disk; defining user quotas; installing NASTRAN; monitoring hardware errors; establishing day to day operations.

SIZING THE SYSTEM

The VMS operating system allows the computer manager to parcel all available memory (both main and disk) into quantities of storage that can be assigned to each process as it is submitted.

to the system. The name given to this parcel is "page" when referring to main memory and "block" when referring to disk space. A page on the VAX is a measure equal to 512 bytes. A disk block turns out to be the same size - 512 bytes. The system doles out memory to processes in units of pages. It seems logical to provide for the case in which the only traffic on the computer would be the largest program in the library. If the largest is NASTRAN, which needs 16,000 pages of memory for it to reside all at once in the computer, it would be most desirable to be able to give it a parcel of 16,000 pages. Since the MicroVAX does not come with that much real memory, we must take advantage of VAX's virtual (make believe) memory capability. Virtual memory means that only a portion of a program needs to reside in the real hardware memory at any given time (this portion is called the "working set"). The rest of the program and its data at any given moment reside on disk in the image (EXE) file and the system PAGEFILE, respectively.

The first task facing the new owner is deciding how much virtual (make believe) memory to have. This number must be chosen with some care because if it is too small, large program images will not run at all. On the other hand, making the virtual size too big wastes system resources. One can find out how much virtual space NASTRAN needs by consulting the LINK map that is part of the delivery package from COSMIC. To determine how many virtual pages are needed by NASTRAN, examine each LINK map (there are 15 for COSMIC NASTRAN) and note the largest value of virtual space (the figure is near the end of each map). The current value is around 8 megabytes. Since each page is one-half kilo-byte, this converts to about 16,000 virtual pages. NASTRAN and NASCAD need about the same amount of virtual pages to operate, so I chose a value of 16,000 for my Virtual Page Count (abbreviated VIRTUALPAGECNT). VMS also allows the computer manager to regulate how main memory is divided up amongst the traffic of processes it serves. A user-supplied system parameter defines the maximum parcel of main memory to be assigned to a given process at any time. This parameter is given the name Working Set Maximum (abbreviated WSMAX). Since the subject

machine has a 2 megabyte memory (4,096 pages of 512 bytes each), the decision then is to pick a fraction of 4096 pages as the maximum that any process will be allowed. First of all it would be a good idea to see if DEC supplied everything as you ordered it, memory-wise. There is a Digital Command Language (DCL) command that will report on this fact. Key in the command SHOW MEMORY. The response will be a display of a table of values. It confirms that there are 4096 total pages of physical memory available. The last line reports the number of physical pages occupied by the system. The table shows that my VMS 4.2 is occupying 1350 pages. Subtracting 1350 from 4096 gives 2746 pages that are available to processes. An example display of the SHOW MEMORY report is shown below.

System Memory Resources on _____				
Physical Memory Usage (pages):	Total	Free	In Use	Modified
Main Memory (2.00Mb)	4096	1945	2102	49
Slot Usage (slots):	Total	Free	Resident	Swapped
Process Entry Slots	12	6	6	0
Balance Set Slots	10	6	4	0
Fixed-Size Pool Areas (packets):	Total	Free	In Use	Size
Small Packet (SRP) List	117	24	93	96
I/O Request Packet (IRP) List	73	17	56	208
Large Packet (LRP) List	10	2	8	656
Dynamic Memory Usage (bytes):	Total	Free	In Use	Largest
Nonpaged Dynamic Memory	299520	197312	102208	193248
Paged Dynamic Memory	81920	24368	57552	23552
Paging File Usage (pages):		Free	In Use	Total
DISK\$MICROVMS:[SYS0.SYSEXEL]SWAPFILE.SYS		3040	1056	4096
DISK\$MICROVMS:[SYS0.SYSEXEL]SWAPFILE1.SYS;1		3448	0	3448
DISK\$MICROVMS:[SYS0.SYSEXEL]PAGEFILE.SYS		13788	212	14000
DISK\$MICROVMS:[SYS0.SYSEXEL]PAGEFILE1.SYS;1		2192	0	2192

Of the physical pages in use, 1350 pages are permanently allocated to VMS.

Even though I am the sole user I may have more than one process running at once on my VAX. I can have a NASTRAN job running in batch. I can be preparing another job with NASTRAN interactively. Another job could be printing. Then I could telephone the modem with the Silent 700 terminal to interrogate the progress of the queues. If the maximum parcel of main memory is fixed at 2,000 pages of main memory, the system will be able to handle the traffic with this upper limit for any one. If the machine is busy, the actual working set for a given process may be smaller than WSMAX, but it may never be larger. So now the plan is to set VIRTUALPAGECNT to 16000 and to set WSMAX to 2000. How does one go about setting these values on the system? Log on as SYSTEM. Set the Default Directory to SYS\$SYSTEM. At the s prompt send the DCL command RUN SYSGEN. The screen will now display a new prompt SYSGEN>. Issue the command SHOW/MAJOR and the response will be a new table giving values to parameters. If they need to be changed, issue the command SET VIRTUALPAGECNT 16000 and SET WSMAX 2000. Issue another SHOW/MAJOR to confirm that the parameters are correct. Then type EXIT. When the s prompt is shown it will be necessary to issue the command @SHUTDOWN after which you should reboot the system by pressing the "Restart" button on the face of the CPU cabinet. During the rebooting, the system resets the values of parameters including the ones just prescribed. Check SYSGEN again to see that the parameters do have the new values. Now it is time for the next step.

PREPARING THE SYSTEM DISK

Parameters to be set in this section will govern the disk space to support the machine's memory. Three quantities will be set. The character of their names is that of files, because the system views these logically as files. Their names are PAGEFILE.SYS, SWAPFILE.SYS, and DUMPFIL.SYS. The reason that these files need to be created is that VMS is a virtual system. This means that only a fraction of a given IMAGE (program) is in main memory at any given time. What fraction is operating depends on the traffic in main memory, subject to the limit imposed

by WSMAX. If several programs are running and all are small, then they might all fit into main memory simultaneously, but if several large programs try to gain their allowable maximum, the system limits each to less main memory and completes their complement of virtual memory by calling for disk space from the file PAGEFILE.SYS. Ultimately the system will vacate low priority jobs from main memory and roll them entirely out to disk into a space called SWAPFILE.SYS. One more disk file is set aside for use by the system called DUMPFIL.SYS. Its purpose is to take over when an abort threatens and save everything that is in random access memory (main memory) and transfer it to the less volatile magnetic memory (disk). Here is the strategy for setting the size of these 3 files. Take a census of all the things that will be in permanent storage on disk and subtract that total from the rating of the disk. The quantity used to measure magnetic storage (disk, tape, and floppies) is the block. One block of disk space is set to 512 bytes (the same as a page), so we will use the block and page interchangeably in computing our disk space needs. The way to inquire of the system as to the sizes of these various disk files is to log onto the account with the directory in question and issue the DCL command DIR/SIZE=ALL. This will report on each file and give a total for all. NASTRAN occupies 16,000 blocks. The system files in the directory SYS\$SYSTEM occupy 14,674 blocks before any assignment is given to these three job management files. The system files in the directory SYS\$LIBRARY is 10,160 blocks. The system files for doing housekeeping of files on disk (directory DUA0:[0,0]) occupy 3,639 blocks. Other major programs like NASCAD and the WordMARC word processor occupy 8,900 blocks and 8,600 blocks respectively. This amounts to a burden of 60,672 blocks. Subtracting this from 138,000 blocks leaves 77,268 blocks. A rule of thumb for a MicroVAX sizing of PAGEFILE.SYS is to set it slightly larger than VIRTUALPAGECNT; e.g. 16,200 blocks. The rule of thumb for sizing SWAPFILE.SYS is to set it equal to half of PAGEFILE.SYS; e.g. 7,500 blocks. The rule for sizing DUMPFIL.SYS is to set it equal to the number of real pages in main memory plus 4; i.e. $4096 + 4 = 4100$ blocks. Check to see that the total assignment

is within the remaining capacity of the disk; i.e. 27,800 vs. 77,268. There is a 49,460 block margin.

Now that we have figured out what size to make these files, the next step is to actually invoke this plan. Log onto the system account and set the default directory (SET DEF) to SYS\$UPDATE. Execute the system utility by issuing the command @SWAPFILES. Immediately the display gives a directory/size report on the subject files and reports on the available disk space. The utility prompts for the assignments first for the paging file, then for the dump file, and then for the swap file. After finishing, reboot the system as was explained in SIZING MAIN MEMORY above, in order to enforce these values into the system. All of this should take place before NASTRAN or other programs are loaded. Once the disk becomes cluttered with files, it becomes harder to find the solid block of room required for the PAGEFILE.SYS.

DEFINING USER QUOTAS

User resource quotas now need to be set in order to dictate how much of these computer resources will be allowed to a user at any one time. The resources that become important for a NASTRAN user are as follows. A limit is set on the maximum number of files that may be open at any one time (abbreviation FILLM). NASTRAN associates a large number of files with an execution so a satisfactory number would be 60. A limit is set on the amount of the PAGEFILE.SYS file that a user may have at any one time (abbreviation PGFL quota). To accomodate NASTRAN the user should get 10,000 pages. A limit is set on the maximum number of bytes the user can have involved in buffered I/O operations (abbreviation BYTLM). This should fall in the range from 8,000 to 12,000.

The way to implement these decisions is to log onto the SYSTEM account and set the default directory to SYS\$SYSTEM. Next issue the command RUN AUTHORIZE. A new prompt, AUTH>, will appear on the screen. If the user account already exists, use the commands:

MODIFY/FILLM=60/PGFLQUOTA=10000/BYTLM=12000 useraccount

and

EXIT.

In order to put these parameters into effect the user logs off then back on again.

There is a related task that must be attended to. There must be a Job Queue set up for running NASTRAN as a batch background job. This is done in two steps. First the queue is defined, then it is started. In order to define the queue, certain decisions have to be made with respect to how the manager wants it to operate for the NASTRAN users. These considerations are: How many jobs may be operating simultaneously? (abbreviation JOB_LIMIT). For a MicroVAX it is wise to limit this to one at a time. What type of queue shall it be? It has already been decided this will be a batch queue (abbreviation BATCH). What priority will the background job be given? (abbreviation BASE_PRIORITY). In order to give good turn-around to interactive users, the priority for batch jobs should be a low value like 2. What is the limit on the amount of main memory that can be assigned to a job in this queue? (abbreviation WSEXTENT). The system cannot give more than the value of WSMAX, but because consideration for NASTRAN was the prime factor in setting the value of WSMAX, WSEXTENT should be made equal to WSMAX. What protection should be assigned to jobs running this queue? (abbreviation PROTECTION). Other users should be able to find out what traffic there is on the computer so that they can adjust their activities accordingly, so set the protection to allow the World to Read. There is no need to set a time limit on the queue unless a host of users descends on your private world. To enable the queue definition, log into the SYSTEM account and set the default to SYS\$MANAGER. Send the DCL command

INITIALIZE/QUEUE/BATCH/BASE_PRIORITY=2/JOB_LIMIT=1/WSEXTENT=2000-
/PROT=(W;R) SYS\$BATCH.

The other part of this task is to arrange for this queue to be available every time the user submits a job, which is tantamount to saying that it should be started every time that the system is booted. Incorporate the startup arrangement in the command procedure called SYSTARTUP.COM, by editing the file with the EDT editor. There is a system manager utility that has to be enabled before any queue starting command will be honored. Therefore this preceding command must be entered into the .COM file before doing the editing; \$START/QUEUE/MANAGER. Next insert the command \$START/QUEUE SYS\$BATCH. Save the file and reboot the system so that this queue will go into effect. NASTRAN's new computer home is now ready for it to move into.

INSTALLING NASTRAN

The computer environment for NASTRAN is now set. NASTRAN can be loaded into any account and any directory you may choose. It is advisable to give such a big program its own directory. The protection of this directory should be prescribed so as to allow access to the NASTRAN executable from other user accounts in other directories. In order to establish a NASTRAN directory, log into the SYSTEM and set the default to SYS\$MANAGER. Issue the command

```
CREATE/DIRECTORY DUA0:[NASTRAN]-  
/OWNER_UIC=[XXXX.YYY]/PROTECTION=(S:RWED,O:RWED,G:RE,W:RE)
```

Now log onto the new NASTRAN account and load the cartridge containing NASTRAN into the TK50 tape drive and read all files from the tape into the NASTRAN directory. Included in this delivery are two prototype command procedures named NASTRAN.COM and NASTRANF.COM. There is a line in both of these procedures that needs to have variable parameters specified. It starts out \$DVC_DIR:=. Whatever follows the equal sign should be deleted and the directory as defined above in the CREATE statement should be entered, but enclosed in double quotes; i.e. "DUA0:[NASTRAN]".

At last, NASTRAN is ready to run!!

MONITORING HARDWARE ERRORS

The spectre of having a computer disaster which would disable everything is something that can be minimized. All that is necessary is to use the maintenance tools that DEC has provided with your MicroVAX VMS system. There is a utility procedure called STABACKIT.COM (Standalone BACKUP) which is nicely organized with prompts to generate a stand-alone BACKUP program tape (stand-alone means that the VMS system is bypassed while using the program). The program tape must be made before the need for it arises - sort of like filling the fire barrels before the fire starts. If your computer crashes and you can't communicate with the VMS system, this tape can be mounted and booted and a crutch set of system BACKUP utility commands can be issued from the keyboard. This Stand-alone BACKUP program can process the set of BACKUP save tape files to re-establish the system on disk. This works if there weren't any physical damage to either the tape drive or the disk drive.

The Stand-alone BACKUP program tape is generated by logging into the system and setting the default directory to SYS\$UPDATE. The MicroVAX is more limited than other VAX machines, so temporary space assignments must first be arranged to ensure that the utility will have room to operate. Reset the default directory to SYS\$MANAGER and issue the command RUN SYSGEN. The following parameter values need to be set.

NPAGEDYN 60000

NPAGEVIR 400000

PAGEDYN 190000.

Reboot as before.

Start the procedure by typing GSTABACKIT.COM. From there on it is a matter of obeying or answering the prompts. After the stand alone backup tape has been generated, go back to SYSGEN and revert the parameters to their initial values.

Files on the disk should be backed up periodically. They can be full backups of everything on the disk, or they can be

incremental backups of just the new items since the last catalogue. There are certain parameters that are recommended for inclusion in the BACKUP command. They are:

/RECORD -- this writes an entry in the directory header of every file to say when it was last backed up. When incremental backups are made this date is consulted along with the dates logged for last modification in deciding whether a new backup is needed.

/LOG -- this displays the activity of writing the backup tape; diagnostics of anomalies are displayed on line.

/OUTPUT=filename -- this creates a file on the disk of the tape contents with any diagnostics; this is useful for storing with the tape for reference.

/BUFFER=5 -- this is peculiar to the MicroVAX; it sets the I/O buffers for efficient running of backup.

/REWIND -- this ensures that the tape is at the beginning.

/IMAGE -- this is used if a complete backup is desired.

/SINCE=BACKUP -- this is used if an incremental backup is being run.

The VAX has an internal sensing of hardware misbehavior as part of its design. The VMS operating system provides utilities to record errors as they happen and later display them upon command. A record is kept of what device, what operation, and when the anomaly occurred. The utility that manages this service is called ERRFMT. It is well to ensure that this utility is enabled. If the command SHOW SYSTEM is issued from any account, it produces a display of system activities. If the utility ERRFMT is shown to be active, then it is enabled. If not, then steps should be taken to put it into operation. The first place to check if it is not operational is in SYSTARTUP.COM. It might be that the prototype COM file had the RUN ERRFMT statement commented out with an exclamation mark.

The user can get a gross report on the total number of errors that have been found for each device by issuing the command SHOW ERROR. More detail can be obtained by logging into SYSTEM and setting the default directory to SYS\$ERRORLOG where a number

of files pertaining to errors are kept. The most relevant file is called ERRLOG.SYS. This is a binary file and is difficult for the uninitiated to read. However, this file can get crowded, making it a chore to filter out the most recent information from the chaff. A routine maintenance step should be to periodically rename the existing file from ERRORLOG.SYS to ERRORLOG.OLD. The error files can be read with another VMS utility called ANALYZE. Issue the DCL command ANALYZE/ERROR_LOG and it gives a complete report. DEC repair men are trained to read these reports and they are extremely valuable to them in case of an emergency. With a little trouble the computer manager can get the gist of what is going wrong at least to the extent that he might sense when it is time to call in a repair man.

OPERATION POLICIES

A certain number of does and don'ts are good ideas to observe. So long as the ambient temperature is acceptable, it is best to leave the MicroVAX running even when there is no traffic on it. The reason to apply this policy is to avoid the most damaging stress that the computer chips see--thermal cycling stress. Shut down when the computer is to be vacated for protracted periods or when ambient conditions are critical.

The Winchester disc is a delicate piece of machinery. Avoid jarring it or moving the CPU case where it is installed.

Install a thermal power cut-off switch which senses a temperature threshold and interrupts power to the computer when that threshold is exceeded.

Install a recording max-min room air temperature thermometer which can provide you with legal data of how well the air conditioning system was maintained prior to a catastrophe, so that compensation can be claimed.

Install a surge and spike protector in the power supply line to catch power anomalies. This is especially useful if your area

power lines are above ground. A lightning strike or car knocking down a power pole could damage your VAX in milli-seconds.

Read the error log periodically. Read the ACCOUNTING.DAT file periodically to check on foreign usage.

Keep a set of BACKUP tapes distant from the computer site, so that a magnetic record is available in case of fire damage or other major disaster. If several sets of BACKUP tapes are kept, it is a simple matter to cycle old tapes back to the computer and new sets to the off-site storage location. Remember, new VAXes are available from DEC in a matter of days, but your data base might take months or even years to replace.

Join DECUS (DEC User Society) for a useful exchange of information with other VAX and MicroVAX users. Every VAX owner may join at no charge. There is a large amount of exchange software available at little or no charge through DECUS.

CONCLUSION

The MicroVAX operates NASTRAN so well that the only detectable difference in its operation compared to an 11/780 VAX is in the execution time. Execution immediately upon submission considerably offsets the slower running time. On the modest installation that was described here an individual engineer has all of the tools that he needs to do an excellent job of analysis. There is room to install NASTRAN, NISCAD, WordMARC and many handy utilities and still leave space for files of results. All of these tools, both hardware and software, have great capability at affordable prices. It is possible to expand main memory to about 10 Megabytes and to expand connected disk space to over 500 Megabytes. Running large NASTRAN jobs is possible. The biggest difficulty for most analysts of having a "private NASTRAN computer" is having to wear so many hats. This paper has tried to reduce the uneasiness one feels with the unfamiliar by suggesting guidelines for some of the essentials that the engineer/analyst/systems type must deal with.

Checkpoint and Restart Procedures for Single and Multi-stage
Structural Model Analysis in NASTRAN/COSMIC on a CDC 176

George H. Camp and Dennis J. Fallon
David Taylor Naval Ship Research and Development Center

Summary

The Underwater Explosions Research Division (UERD) of David Taylor Naval Ship Research and Development Center (DTNSRDC) makes extensive use of NASTRAN/COSMIC on a CDC 176 to evaluate the structural response of ship structures subjected to underwater explosion shock loadings in the time domain. As relatively new users, UERD research engineers have encountered many problems on various levels during the analysis process and have found it necessary to utilize the checkpoint/restart feature of NASTRAN/COSMIC. As the USER'S Manual is vague on the subject of checkpoints/restarts, a set of working procedures were developed for the implementation of the checkpoint/restart feature in the transient analysis (Rigid Format # 9) of single stage structural models and multi-stage substructure models. These working procedures are the subject of this paper. Examples are illustrated in the Appendix to highlight these procedures for a CDC 176 computer.

Introduction

NASTRAN/COSMIC was designed to run large problems usually requiring lengthy execution times and/or large memory allocations. User errors are common. Operator, hardware, or system failures resulting in the abnormal termination of a problem are not entirely uncommon, even with the best of computer systems. Due to machine and code dependent parameters, the termination of a run because of exceeded time and/or memory allocations is quite possible.

To prevent costly loss of information generated immediately prior to the point of termination and/or to allow added flexibility as well as efficiency in the solution process, the user is encouraged to utilize the checkpoint/restart feature available in NASTRAN/COSMIC.

The checkpoint/restart feature of NASTRAN/COSMIC was designed to allow the user to checkpoint a NASTRAN run and later restart it by executing only those modules needed for completion of the solution. The restart deck submitted to NASTRAN may include corrections to erroneous or omitted data in the original checkpoint run, additional data entries, or may simply consist of the original data deck in cases where the program terminated abnormally due to a system failure. Unfortunately, the NASTRAN User's Manual is not entirely clear on the procedures for checkpointing and restarting problems, particularly those for

multi-stage substructure model analysis. Hence, a few points in the procedure are worthy of discussion.

Checkpoint Procedure

The checkpoint/restart feature is applicable to the analysis of single stage structural models as well as multi-stage substructure models, and the procedure for checkpointing the problems is identical.

Outlined in Example 1 of the Appendix is a listing of the job and executive control decks for a single stage model and a multi-stage substructure model analysis problem. These examples are accompanied by a brief explanation of the additional and pertinent commands necessary for the execution of the checkpoint procedure on a CDC 176 computer.

The user may find it difficult to predict the memory and time requirements of large problems without some knowledge developed through experience. There are methods available which are somewhat dependable for the estimation of these parameters [1]. However, these methods can not guarantee the successful completion of the job, nor, in some cases, are these procedures easily implemented. If the problem warrants it, the time and memory limits may be set at the maximum values [2], but doing so has the trade-off of changing the priority of the job. This will be accompanied by a delay in the execution of the problem. In many instances at the DTNSRDC computer facility it is wise to schedule blocktime [2] for the solution of large problems, thus reducing the cost of execution. However, the job is still dependent on the system whose failures are not easily controlled or anticipated.

In the case of substructure modeling, the user has the option of checkpointing a Phase One run for subsequent Phase Three restarts. It is UERD's experience that in most cases this is neither economical nor advantageous. The disadvantage is that it requires more computer time to execute the checkpointed Phase One run, more cost due to storing the large new problem tape (NPTP) and requires more computer time due to increased I/O in the Phase Three run.

Restart Procedure

Assuming the checkpointed solution run terminated abnormally due to one of the afore mentioned conditions, and both the "NPTP" and "PUN" files were created and successfully stored, recovery of the job consists of a few simple modifications to the original input deck and resubmitting it for execution. The modifications consist of: 1) attaching the "NPTP", 2) merging the restart dictionary into the executive control deck, 3) making any corrections to the case control or bulk data decks and 4) including an "ALTER" if the problem is a substructure model analysis.

Outlined in Examples 2 and 3 of the Appendix are listings of the job and executive control decks required for the unmodified restart (no changes) of single stage structural model and multi-stage substructure model analysis problems. Each of these examples are followed by a brief description of the additional and pertinent commands.

If the termination is due to error(s) in the case control or bulk data, the effective changes should be included in the restart run. For case control errors, the correction is included or replaces the erroneous command. If errors in the bulk data exist, only the corrections need to be included and the rest of the bulk data deck is omitted. Adjustments to time and memory limits may be required depending on their values in the checkpointed run and the point at which the job terminated in the solution sequence. The point of termination is determined by examining the dayfile messages or by inspecting the checkpointed DMAP sequence list which appears in the PUN file or restart dictionary (the last sequence reentered is the point of termination).

For most large problems in which time or memory allocations were insufficient, the program may terminate in the dynamic loop. For substructure analysis problems which terminate within the dynamic loop, restarting the problem requires the addition of an ALTER statement which enters the DMAP sequence immediately after the last sequence checkpointed (see Example 3, statement 20). The purpose of this ALTER is to regenerate substructure control deck information required for recovery of the solution vector which is not checkpointed by NASTRAN/COSMIC. This problem occurs at executive decision making levels in the solution process and can only be remedied by the inclusion of an ALTER statement at this time. Future code changes may correct this problem.

Concluding Remarks

This paper illustrates working procedures for application of the checkpoint/restart feature to the transient analysis using NASTRAN/COSMIC. The importance of the substructure modeling technique has grown in proportion to the growth in complexity of problems UERD research engineers are tasked to solve. Just as the complexity of problems increases, so does the need for flexible and efficient solution techniques. The checkpoint/restart feature of NASTRAN/COSMIC was designed to accomplish this objective. Following the procedures illustrated in this paper will aid new users to become more proficient in the use of this powerful tool.

APPENDIX

Example # 1 : Checkpointing of direct transient analysis of single stage or multi-stage structural models.

```
1.  CS^^,CM260000,T50,P3.
2.  CHARGE,CS^^,XXXXXXXXXX.
3.  LIMIT,7777.
4.  REQUEST,OUT,*PF.
5.  REQUEST,NPTP,*PF.
6.  REQUEST,PUN,*PF.
7.  MSACCES,^^^^.
8.  ATTACH,NASTRAN.
9.  BEGIN,NASTRAN,NASTRAN,260000,,OUT,PUN.
10. EXIT,U.
11. CATALOG,OUT,OUTPUT,ID=CS^^.
12. CATALOG,NPTP,ID=CS^^.
13. CATALOG,PUN,RESTDICTNRY,ID=CS^^.
14. EOR
15. NASTRAN TITLEOPT=-2,SYSTEM(71)=1,FILES=NPTP ??
16. ID FOREMAST,ANALYSIS
17. APP DISP
18. SOL 9,0
19. TIME 50
20. DIAG 8,14,22
21. CHPNT YES
22. CEND
23. TITLE .....
    *
    *
    ETC.
```

***Note: CASE CONTROL AND BULK DATA DECKS AS USUAL.**

Description of Commands

1. The central memory "CM260000" and total job time "T50" resources allocated here may be the cause of an abnormal termination and may need to be adjusted for the restart run depending on the size of the problem and how much of the solution was completed [2]. Close inspection of the dayfile and output messages may show the reason(s) and point of termination. When the job aborts due to exceeding the CPU time limit, the system will allow time to catalog and unload files, so the "NPTP" and "PUN" files will be available for restart.

3. The amount of mass storage which may be used at one time is specified via the "LIMIT" card [2]. If the mass storage is inadequate the job will terminate. Again, the need to increase this parameter will be determined by the size of the problem and how much of the solution was completed prior to termination.

5.,6. To catalog these files, which are essential to restart the problem, they must be requested as permanent files. The "NPTP" (new problem tape) is the file that contains the information generated prior to termination needed to complete the solution. The "PUN" (punch output file) is a file containing the checkpoint dictionary (a complete listing of all DNAP sequences that were executed and checkpointed). The checkpoint dictionary must be edited to remove all "EOR" messages that appear, then merged in the executive control deck of the restart run. The creation of these files is mandatory.

9. The files "OUT" and "PUN" should appear as parameters in this statement for definition and creation.

12.,13. The files "NPTP" and "PUN" must be catalogued for retrieval.

15. Among the parameters utilized, the user is urged to set "SYSTEM(71)" to "1", which will suppress some of the information routed to the dayfile. This information is, however, printed in the output file. This reduces the chance of the program terminating due to exceeding the dayfile message limit but still provide the information which may be useful in tracking other errors. The "NPTP" must be specified as an executive file via "FILES=NPTP" on the NASTRAN card.

16. The problem ID should be specified as per instructions in the User's Manual for the checkpoint run [3]. This is due to the format requirements of the restart card in the checkpoint dictionary. Incorrect format will cause difficulty in the restart process.

19. This command specifies the maximum time allotted to NASTRAN for problem execution. If the amount specified is inadequate the job will terminate, producing fatal error messages in the output. The user will then be required to submit a restart deck to recover the job. The time may need to be increased upon restart depending on the point of termination. The time required for NASTRAN execution is less than the total job time required.

21. This command initiates the checkpoint process. It is mandatory for checkpointing the problem [3].

Example # 2 : Unmodified restart of direct transient analysis of single stage structural model

```

1.  CS^^,CM260000,T500,P3.
2.  CHARGE,CS^^,XXXXXXXXXX.
3.  LIMIT,7777.
4.  REQUEST,OUT,*PF.
5.  NSACCES,XXXXX.
6.  ATTACH,NASTRAN.
7.  ATTACH,OPTP,NPTP,ID=CS^^.
8.  BEGIN,NASTRAN,NASTRAN,260000,,OUT.
9.  EXIT,U.
10. CATALOG,OUT,OUTPUT,ID=CS^^.
11. EOR
12. NASTRAN TITLEOPT=-2,SYSTEM(71)=1,FILES=OPTP
13. ID A1234567,B7654321
14. APP DISP
15. SOL 9,0
16. TIME 50
17. DIAG 8,14,22
18. RESTART A1234567,B7654321 , 9/17/86, 48570,
    1,  XVPS      ,  FLAGS = 0,  REEL = 1,  FILE = 5
    2,  REENTER AT DMAP SEQUENCE NUMBER 6
    3,  GPL       ,  FLAGS = 0,  REEL = 1,  FILE = 6
    4,  EQEXIN    ,  FLAGS = 0,  REEL = 1,  FILE = 7
    5,  GPD       ,  FLAGS = 0,  REEL = 1,  FILE = 8
    6,  CSTM      ,  FLAGS = 0,  REEL = 1,  FILE = 9
    7,  BGPDT     ,  FLAGS = 0,  REEL = 1,  FILE = 10
    8,  SIL       ,  FLAGS = 0,  REEL = 1,  FILE = 11
    9,  XVPS      ,  FLAGS = 0,  REEL = 1,  FILE = 12
   10, REENTER AT DMAP SEQUENCE NUMBER 7
   11, BGPDT     ,  FLAGS = 0,  REEL = 1,  FILE = 13
      .
      .
      .
   203, TOL      ,  FLAGS = 0,  REEL = 1,  FILE = 85
   204, XVPS     ,  FLAGS = 0,  REEL = 1,  FILE = 86
   205, REENTER AT DMAP SEQUENCE NUMBER 125
   206, PDT      ,  FLAGS = 0,  REEL = 1,  FILE = 87
   207, XVPS     ,  FLAGS = 0,  REEL = 1,  FILE = 88
$  END OF CHECKPOINT DICTIONARY
19. CEND
20. TITLE = .....
    *
    *
    ETC.

```

*Note: IF NO EFFECTIVE CHANGES, CASE CONTROL DECK IDENTICAL TO CHECKPOINT RUN AND BULK DATA DECK OMITTED.

Description of Commands

1. This particular problem is the restart of the checkpointed previous example. The problem aborted because the time allocated (T50) was not sufficient for completion of the run. Although the checkpoint dictionary indicates that the program was almost completed (the last sequence reentered was 125), the time limit was extended to "T500" for restart. This amount would have been sufficient for the run to be completed in the checkpoint phase.

3. This command remains unchanged.

7. The "NPTP" is made available to NASTRAN via this statement, and must be renamed as the "OPTP" (old problem tape). This command is mandatory for restarting the problem since the NPTP/OPTP contains the information required by NASTRAN to continue the solution sequence.

12. As previously mentioned, "SYSTEM(71)" is set to "1" and the "OPTP" is specified as an executive file.

16. The NASTRAN execution time, "TIME 50", is deemed adequate and remains unchanged.

18. This is a partial listing of the checkpoint/restart dictionary which is contained in the PUN file. The first card shown is the restart card [3]. This card identifies the problem as a restarted job. The first entry is the ID of the checkpointed problem. This entry is compared to the NPTP/OPTP to verify that it corresponds to the problem being restarted. The cards which follow indicate the DMAP modules which were executed and checkpointed. As can be seen from this deck, the last successfully completed and checkpointed sequence was DMAP module 124. Number 125 was reentered, but checkpointing was not completed. Therefore, sequence number 125 is the point at which NASTRAN will pick up the solution process. This complete file is mandatory.

Note: The case control deck is required for restarting the job, but the bulk data deck may be omitted if there are no changes. Also, a restart run may be checkpointed as any other problem which is eligible for checkpointing, but the user should weigh the benefits of doing so to keep computer costs minimal.

Example # 3 : Unmodified restart of direct transient analysis of multi-stage substructure model

```

1.  CS^^,CM377700,T400,P3.
2.  CHARGE,CS^^,XXXXXXXXXX.
3.  LIMIT,10000.
4.  REQUEST,OUT,*PF.
5.  NSACCES,XXXXX.
6.  NSFETCH,OTPT,ID=CS^^.
7.  ATTACH,NASTRAN.
8.  ATTACH,SOFA,ID=CS^^.
9.  BEGIN,NASTRAN,NASTRAN,377700,,OUT,PUN.
10. EXIT,U.
11. CATALOG,OUT,TESTOUT,ID=CS^^.
12. EXTEND,SOFA.
13. EOR
14. NASTRAN TITLEOPT=-2,SYSTEM(71)=1,FILES=OTPT
15. ID APTMODEL,ANALYSIS
16. APP DISP,SUBS
17. SOL 9,0
18. TIME 150
19. RESTART APTMODEL,ANALYSIS , 8/21/86, 76863,
    1,  XVPS      ,  FLAGS = 0,  REEL = 1,  FILE = 6
    2,  REENTER AT DMAP SEQUENCE NUMBER 6
    3,  GPL       ,  FLAGS = 0,  REEL = 1,  FILE = 7
    4,  EQEXIN   ,  FLAGS = 0,  REEL = 1,  FILE = 8
    5,  GPDIT    ,  FLAGS = 0,  REEL = 1,  FILE = 9
    6,  BGPDT    ,  FLAGS = 0,  REEL = 1,  FILE = 10
    7,  SIL      ,  FLAGS = 0,  REEL = 1,  FILE = 11
    8,  GE3S     ,  FLAGS = 0,  REEL = 1,  FILE = 12
    9,  GE4S     ,  FLAGS = 0,  REEL = 1,  FILE = 13
   10,  DYN      ,  FLAGS = 0,  REEL = 1,  FILE = 14
   11,  XVP3     ,  FLAGS = 0,  REEL = 1,  FILE = 15
   12,  REENTER AT DMAP SEQUENCE NUMBER 5
   13,  XVPS     ,  FLAGS = 0,  REEL = 1,  FILE = 16
      .
      .
      .
  203,  REENTER AT DMAP SEQUENCE NUMBER 125
  204,  PDT      ,  FLAGS = 0,  REEL = 1,  FILE = 75
  205,  XVPS     ,  FLAGS = 0,  REEL = 1,  FILE = 76
  206,  REENTER AT DMAP SEQUENCE NUMBER 126
  207,  UDVT     ,  FLAGS = 0,  REEL = 1,  FILE = 77
  208,  XVPS     ,  FLAGS = 0,  REEL = 1,  FILE = 78
$ END OF CHECKPOINT DICTIONARY
20. ALTER 126 $
21. SGEN CASECC, GEOM3, GEOM4, DYNAMICS/CASESS, CASEI,
    DUMA1, DUMA2, DUMA3, DUMA4, DUMA5, DUMA6, DUMA7,
    DUMA8/1/*TOTAL*/DUM1/DUMN $
22. ENDALTER
23. DIAG 8,14,22

```

ETC.

TO CHECKPOINT RUN AND BULK DATA DECK OMITTED.

Description of Commands

1. This particular problem required the maximum amount of core memory available "CM377700" [2]. The time allotted here was reduced from the original value specified because of the point at which the program terminated. The solution vector was completed but never recorded in the "SOF" (substructure operational file), therefore, the restart was performed to simply retrieve the solution from the NPTP/OTTP and store it in the "SOF" for use in Phase Three. This procedure required a considerable amount of memory, but not much time.

3. The original problem did not allocate ample mass storage (LIMIT 7777.) which was the cause of the program termination. The limit was extended to the maximum for the restart [2].

6. Due to the size of the NPTP/OPTP, it was placed in mass storage by the checkpoint run. This command retrieves the OPTP from mass storage for restart.

19. This is a partial listing of the checkpoint dictionary for this problem (again found in the PUN file). This list indicates that the last DMAP module checkpointed was sequence number 125. Therefore, the first module flagged for execution in the restart phase is number 126 and the ALTER occurs at this point.

20.-22. This ALTER regenerates information necessary for recovery of the solution vector. SGEN is a structurally oriented functional module producing data blocks as required for the solve operation [4]. NASTRAN does not checkpoint some of the output data blocks from this module which are necessary to the solution process. Therefore, the user must regenerate these data blocks (CASESS and CASEI) for restarting the problem. The remaining output data blocks and parameters need not be regenerated and are given dummy labels. These cards are mandatory for restart of substructure analysis problems.

References

- 1.) Everstine, G. C., and Hurwitz, M. M., "Nastran Theory and Application Course Supplement". David Taylor Naval Ship Research and Development Center, Bethesda, Md., Report DTNSRDC/CNLD-81-05, Feb. 1981.
- 2.) Sommer, D. V., "Computer Center Introductory Reference Manual for CDC Cyber". David Taylor Naval Ship Research and Development Center, Bethesda, Md., Report DTNSRDC/CNLD-84-09, May 1984.
- 3.) "The Nastran User's Manual", COSMIC, Athens, Ga., NASA SP-222, Dec. 1980.
- 4.) "Nastran Programmer's Manual", COSMIC, Athens, Ga., NASA SP-223, Dec. 1979.

INTERACTIVE PLOTTING OF NASTRAN DATA ON MICROCOMPUTERS

Robert L. Norton

**Applied Technologies Section
Jet Propulsion Laboratory
California Institute of Technology
Pasadena, California 91109 USA**

Summary

A microcomputer based program has been developed to aid in the development of NASTRAN models. The program reads in the complete NASTRAN data deck, produces a diagnostic print file, and then allows the user to view the model in an interactive mode. The program runs on a wide variety of hardware by making use of the Virtual Device Interface.

Introduction

When NASTRAN was introduced the most powerful computers available were required to run it. To even process the bulk data deck required a substantial computer. In the years since there has been enormous progress in computer hardware, providing substantial computing power for the desktop. While it is not yet possible to run NASTRAN on a personal computer it is now possible to do a significant amount of model development on a personal computer.

In addition to the great strides in computer hardware development, computer software has developed to the point that the phrase "user friendly" has become a cliché. Computer users now longer feel that they have to put up with obscure error messages and difficult interfaces with the computer. Instead they demand an interactive computing environment that allows for simple, intuitive commands.

In many facilities users now rely heavily on personal computers for word processing, spreadsheet manipulation, data preparation, and terminal emulation. Users in these facilities often make use of spreadsheet programs for bulk data preparation and data reduction of the NASTRAN output. In this way the central computer workload is reduced somewhat, and many users prefer the local control allowed by personal computers.

This paper presents research results carried out in part at the Jet Propulsion Laboratory, California Institute of Technology, under contract with the National Aeronautics and Space Administration (NASA).

This program consists of two major modules. The first module is used to process the entire NASTRAN deck and produce the files required for plotting. This module is essentially run in a batch mode, with little user interaction. The files produced consist of the location of grid points in the basic system and a file with the element information. The second module is the interactive graphics module. This second module reads the two files produced by the first module and provides a highly interactive environment for the user. As the plots are created they can also be sent to the hard copy device.

NASTRAN Reader

The NASTRAN deck must contain the BEGIN BULK card and the ENDDATA card (or its permutations ENDDATA and END DATA). The executive and case control sections are optional, although the TITLE card information will be used if it is present. At this point the program will work with line elements (CBAR, CONROD and CROD) and the three or four node plate or membrane elements (CQDMEM, CQDMEM1, CQDMEM2, CQDPLT, CQUAD1, CQUAD2, CSHEAR, CTRBSC, CTRIA1, CTRIA2, CTRMEM, and CTRPLT). Solid elements could be added, but the complexity of typical solid element models is probably more than the typical user would care to endure on a personal computer.

The model geometry can be described with the usual coordinate system definition cards and the printed output will give a listing of all grid locations in the basic coordinate system. The free field input capability of NASTRAN is also supported.

The user must first create the NASTRAN data deck with a text editor, word processor, spreadsheet, or other convenient means. After the data deck has been prepared the NASTRAN reader is run and asks the user for the file name, with an assumed extension of DAT. The user enters the base file name, and the output is sent to file.PRT, file.ELE, and file.NOD. The printed output contains the grid point information in the basic coordinate system and element information. The other two files are used as input to the NASTRAN Plotter program.

NASTRAN Plotter

After the NASTRAN data has been read and the output files have been created the user may then run the second module to interactively plot the NASTRAN model. The user interface is modeled after some widely used microcomputer programs, providing a menu at the top of the screen. Just below the menu is an information line, giving a very brief description of the action that will be taken if the currently highlighted selection is made. The cursor keys are used to move across the menu structure, with the selection made by pressing the down arrow key. Alternately the selection may be made by typing the capitalised letter of the command (usually the initial letter). The user can move to the main level in the menu structure by pressing the up arrow key or the escape key.

The main menu consists of three items: View selections, Scene selections, and Display options. The View selections allow the user to specify the mapping of the model axes onto the screen axes, rotate around the model or screen axes, translate on the screen, zoom

in a portion of the current display, clip the model fore and aft, and to reset the defaults. The Scene selections allow the user to display selected element types, specify hidden line elimination, shrink the elements, and to specify perspective plotting. The Display options allow the user to have the node and/or element labels shown on the plot and allow the user to add text at a user specified location on the screen.

In addition to the command line at the top of the screen, certain other commands are entered by using the first four of the function keys. F1 provides a context sensitive help screen, F2 exits the program, F3 plots the model using the current selections, and F4 makes a hard copy plot using the current selections.

The hidden line algorithm incorporates the Hedgley hidden line code (1). The Hedgley code processes only polygons, so the line elements are omitted if the hidden line option is selected.

Program Performance

Five typical NASTRAN models were used for Figures 1-6. These models were taken from some ongoing work and are typical of the range of model complexity suitable for this program. The characteristics of these models are tabulated in Table 1. The models range from 30 to 1216 nodes and from 30 to 1299 elements. The time required for the NASTRAN reader and for a screen image to be drawn are shown in Table 2. Also shown in Table 2 are the times for a popular commercial program to perform similar tasks on the same NASTRAN data decks. The commercial program was run on a VAX-11/780 with a typical afternoon workload. The microcomputer times are based on a 6 MHz IBM AT.

In reviewing Table 2 certain trends are evident. The relative performance of the microcomputer program vs. the commercial program on the VAX depends on the model size. The smallest deck is processed by the NASTRAN reader on the microcomputer faster than by the commercial program on the VAX. As the models get more complex the commercial program gets faster relative to the microcomputer. For moderate size problems this microcomputer program is adequately fast.

The microcomputer based program is consistently faster than the VAX based commercial program in screen drawing times when using the 1200 baud dial-up lines. Even when comparing the microcomputer performance with the VAX using a 9600 baud connection the times are generally comparable.

Examples

Figures 1 through 8 show examples of various program options with the sample NASTRAN decks listed in Table 1. Figure 1 shows a truss model plotted with moderate perspective. Figures 2 and 3 show a plate model with no perspective, first with node numbers, and then with the element numbers. Figure 4 shows the same model with the hidden lines removed. Figure 5 shows a plate model which used a cylindrical coordinate system for the grid point generation. Figures 6 and 7 show the same model, first with

element shrink enabled, and then with the hidden lines removed. Figure 8 is the most complex model and is shown with moderate perspective. The illustrations in this paper are reduced from their normal size to fit the manuscript requirements. Normally the plots take 8×9.8 inches on a 8.5×11 inch paper.

Programming Environment

Both modules of this program were written in FORTRAN. There are several popular FORTRAN compilers available for microcomputers now; this program was developed with Microsoft FORTRAN, version 3.31. The program should work with the other popular compilers as well.

A major problem area for developers of microcomputer programs that use a graphics interface is trying to address the wide variety of hardware available. There are three primary display devices available and a multitude of printers and plotters for the hard copy device. To address this problem, IBM has released a Virtual Device Interface system which allows the programmer to use a virtual screen to develop the graphics and let low level drivers convert the virtual screen to the specific hardware that the user has implemented. In addition to the drivers available from IBM the company that developed the VDI for IBM, Graphic Software Systems of Beaverton, Oregon, has released drivers for non-IBM hardware, such as the popular laser printer used to create the plots in this paper with 150 dots/in resolution.

Program Limitations

The NASTRAN reader program has a current limit of about 5000 nodes, and about 15,000 elements of any given type. The patience of the user would place a much lower limit on the practical size. The NASTRAN plotter program has a current limit of about 5000 nodes and an unlimited number of elements. The Hedgley algorithm has a limit of about 275 elements with the current memory allocation.

References

1. "A General Solution to the Hidden-Line Problem," David R. Hedgley, Jr., NASA Reference Publication 1085, 1982. Also available from COSMIC as M86-10038.

Table 1
Model Characteristics

Number	No. grids	No. elements	No. cards
1	30	82	199
2	46	30	117
3	104	148	122
4	1216	1299	2192

Table 2
Model Performance (times in seconds)

Model	Hidden Line?	Microcomputer		VAX	
		Bulk Data Reader	Screen Plot	Bulk Data Reader	Screen Plot 1200/9600 baud
1	no	42	2.8	97	14.6/2.7
2	no	26	3.0	50	12.5/2.8
	yes		14.2		14.2/7.2
3	no	91	7.6	54	27.9/4.5
	yes		86.7		27.8/21.6
4	no	826	35.9	245	162.4/24.1

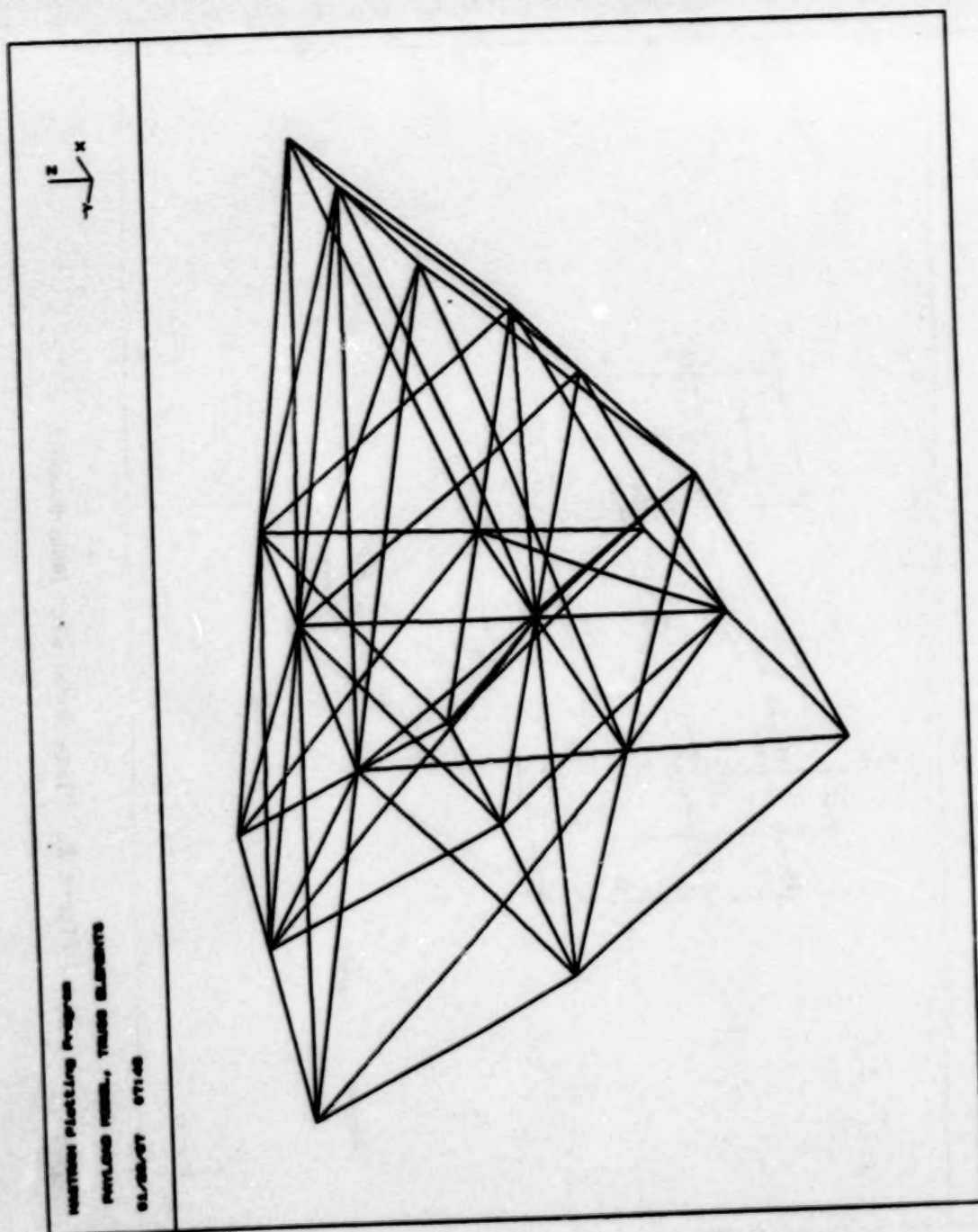


Figure 1. Truss Model with Perspective

HANDBOOK Plotting Program
 PLYWOOD MODEL, PLATE ELEMENTS
 01/05/77 07140

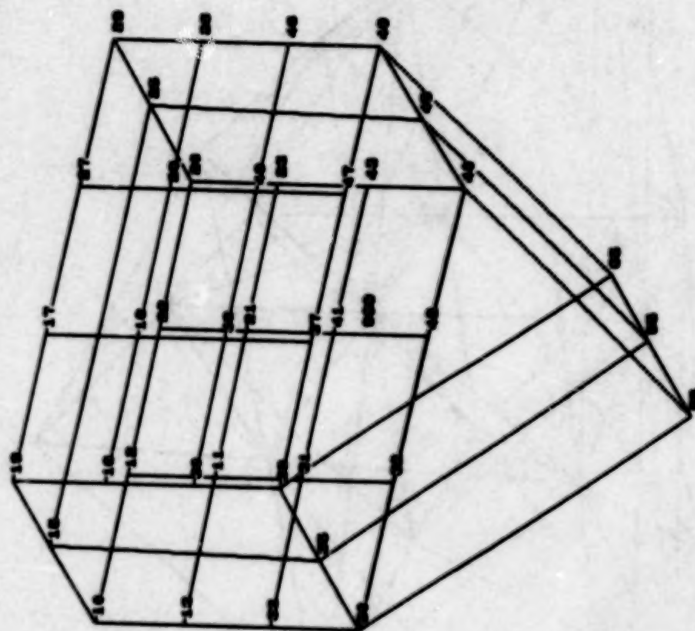


Figure 2. Plate Model with Node Numbers

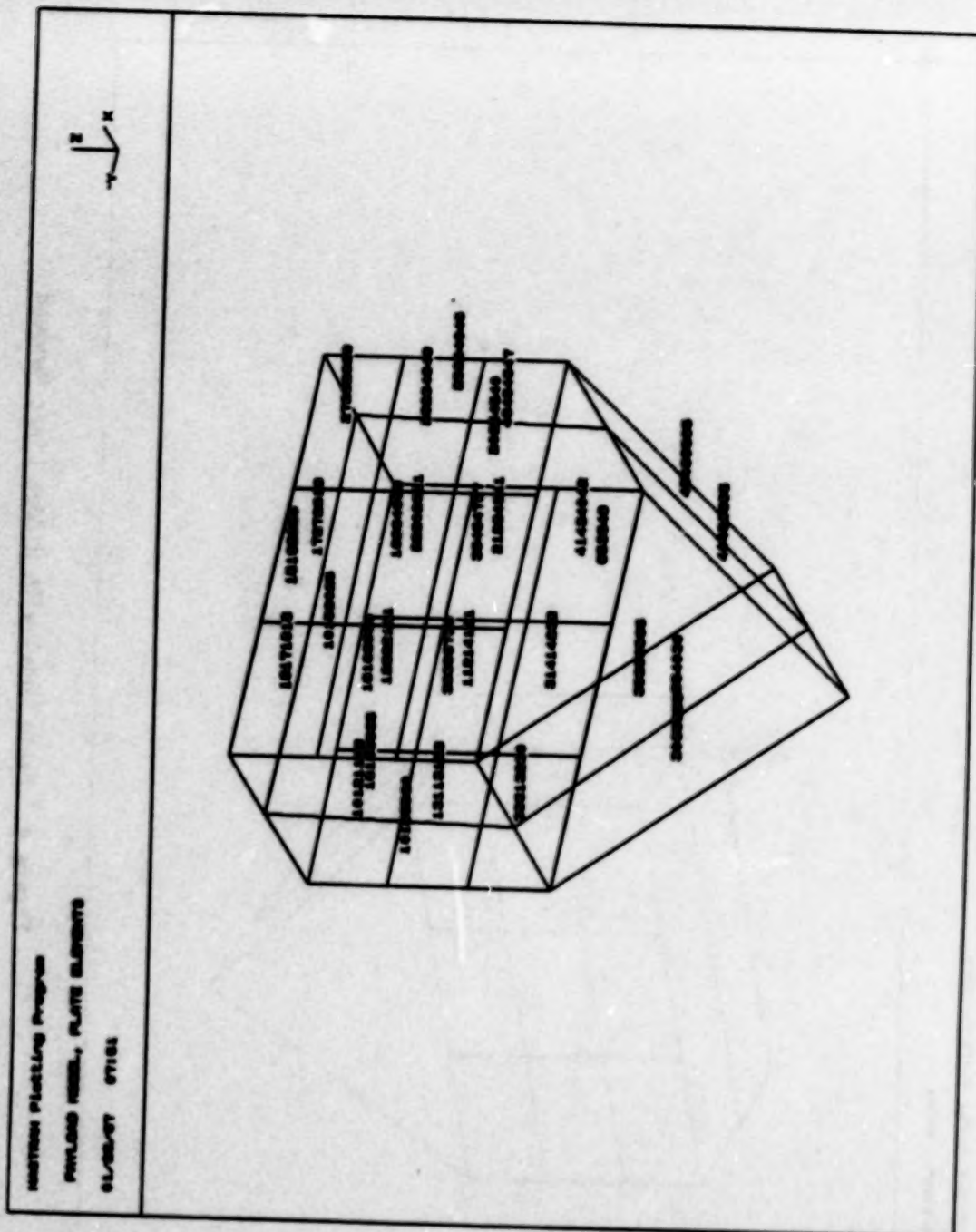


Figure 3. Plate Model with Element Numbers

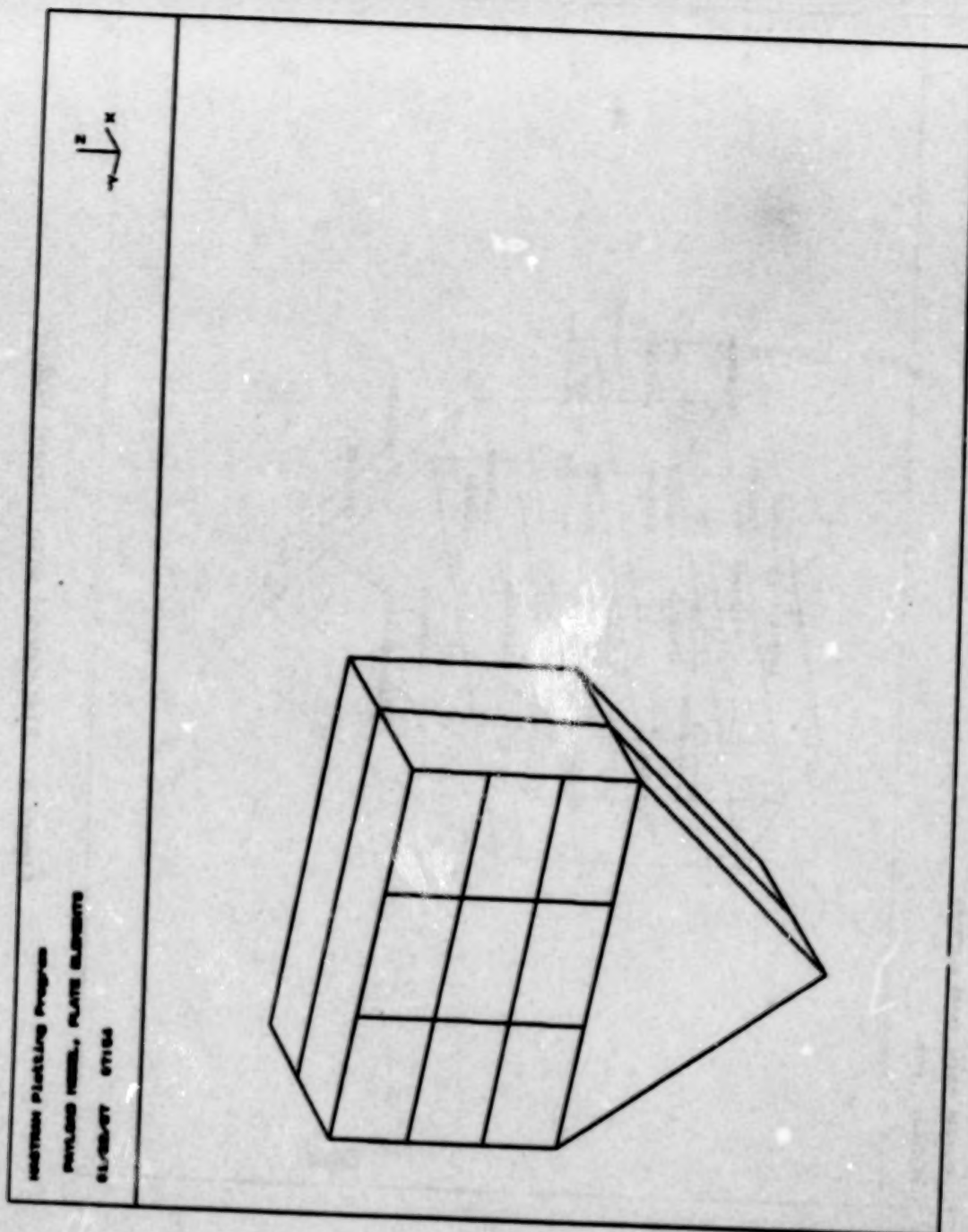


Figure 4. Plate Model with Hidden Lines Removed

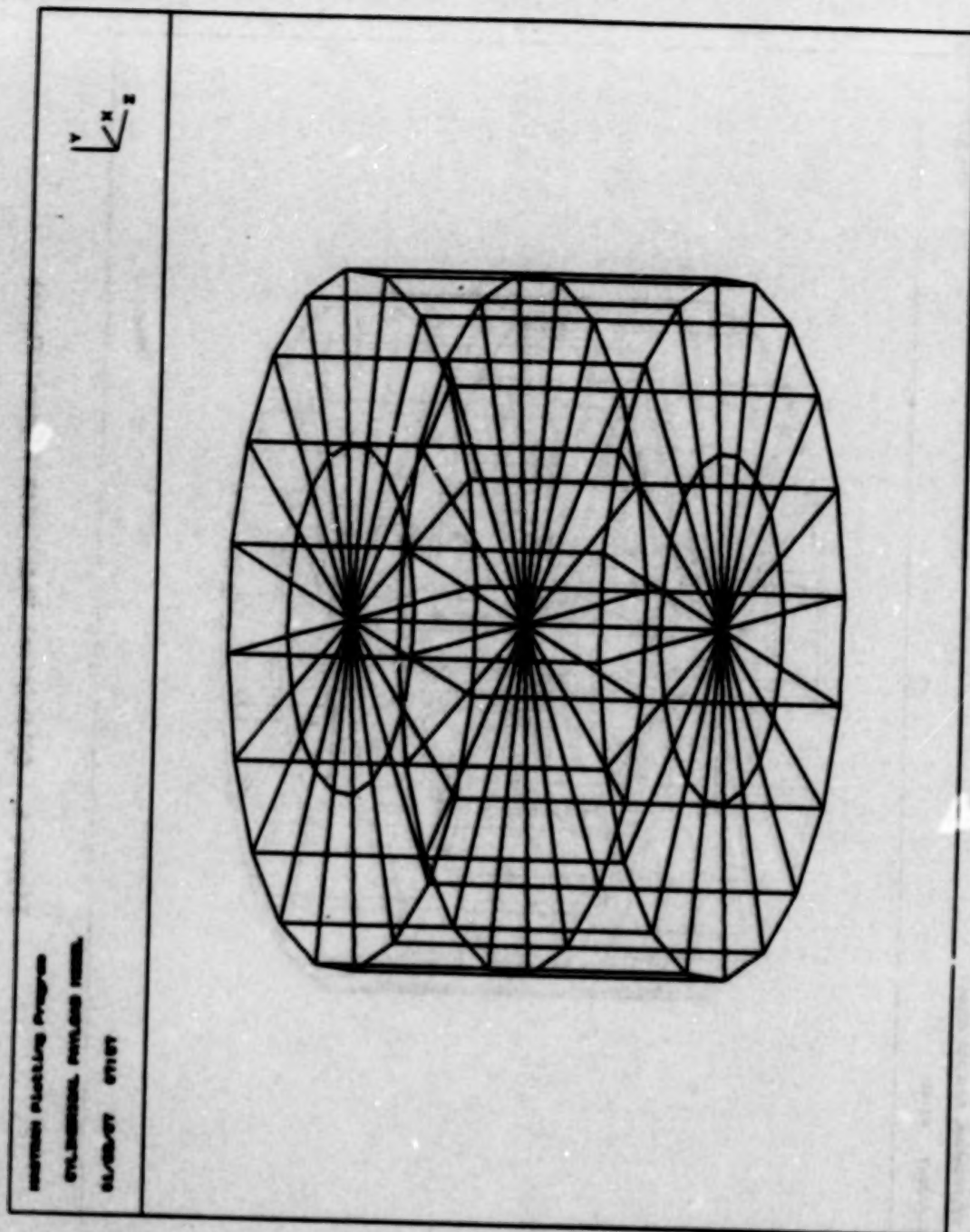


Figure 5. Cylindrical Model

NORTON PLOTTING PROGRAM
 CYLINDRICAL SHELLS MODEL
 01/02/87 07100

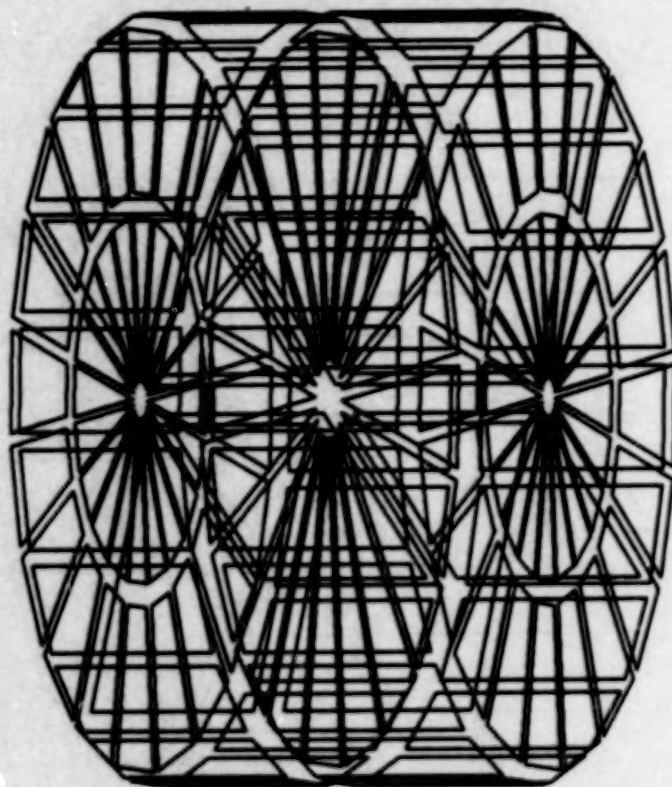


Figure 6. Cylindrical Model with Element Shrink

NUMERICAL PLOTTING PROGRAM
CYLINDRICAL, POLYLINE MODE
01/08/87 0001

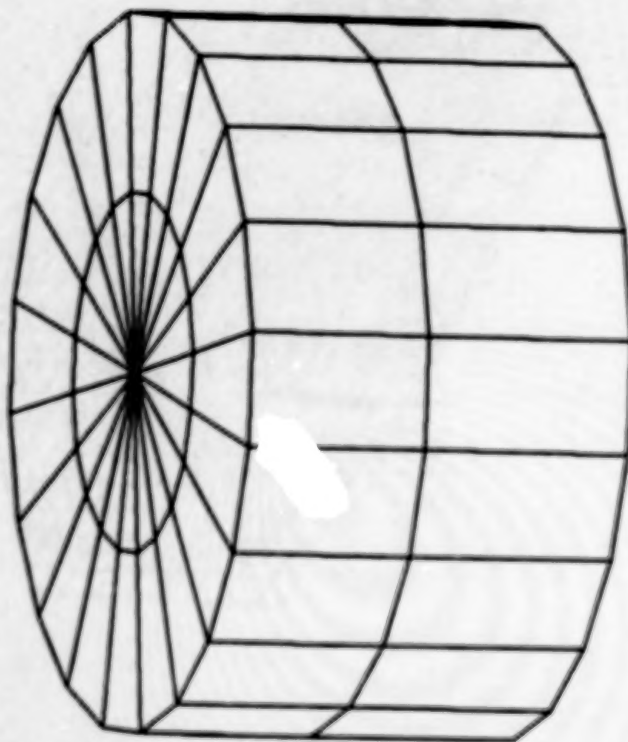


Figure 7. Cylindrical Model with Hidden Lines Removed

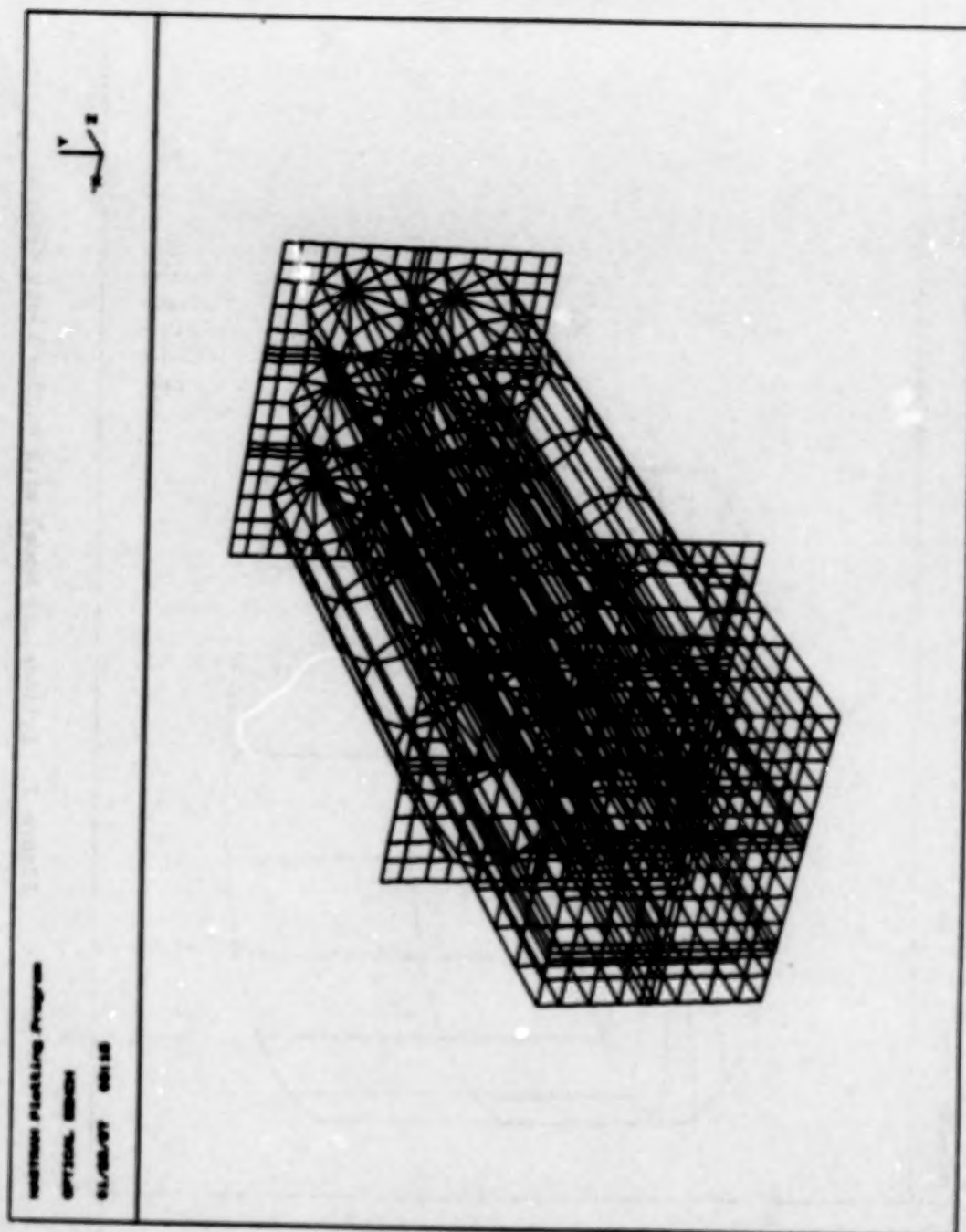


Figure 8. Optical Bench with Perspective

COMPUTER ANIMATION OF MODAL AND TRANSIENT VIBRATIONS

Robert R. Lipman

David W. Taylor Naval Ship Research and Development Center
Numerical Structural Mechanics Branch (Code 1844)
Bethesda, Maryland 20884-5000

SUMMARY

An interactive computer graphics postprocessor is described that is capable of generating input to animate modal and transient vibrations of finite element models on an interactive graphics system. The results from NASTRAN can be postprocessed such that a three-dimensional (3-D) wire-frame picture, in perspective, of the finite element mesh is drawn on the graphics display. Modal vibrations of any mode shape or transient motions over any range of time steps can be animated. The finite element mesh can be color-coded by any component of displacement. Viewing parameters and the rate of vibration of the finite element model can be interactively updated while the structure is vibrating.

INTRODUCTION

As the computational power of computers has increased, the size of finite element models that an engineer can analyze in a reasonable amount of time has also increased. Finite element models that are analyzed overnight on an average computer can now be analyzed routinely in under an hour on a supercomputer. However, an engineer is still faced with the task of assimilating and drawing meaningful conclusions from large amounts of output generated by the finite element analysis programs. Output from these programs is presented as almost endless values of stress, strain, and displacement associated with nodes and/or elements. The interpretation of the finite element results is made even more difficult when real and imaginary values are considered. Structural deformations or color contours of nodal results for various mode shapes or time steps can be plotted in addition to graphs of the response of a finite element node versus time or frequency. However, the engineer is still depending on static plots to understand the dynamic behavior of a structure.

A postprocessing computer program, CANDI (Color Animation of Nastran Displacements) for NASTRAN finite element analysis results has been developed. CANDI generates input for an interactive graphics system so that modal and transient vibrations of finite element models can be animated. Providing the capability to animate finite element results has greatly improved the engineer's ability to interpret dynamic results that were previously viewed with static plots.

Unfortunately, the black and white reproduction of this paper cannot show the color animation that is generated by the hardware and software to be described. The reader will have to use his imagination.

HARDWARE

The hardware that is used to display the animation of finite element analysis results is an Evans & Sutherland PS-330 interactive graphics system (ref. 1). The PS-330 has the ability to process a large number of vectors, as would be dictated by complex finite element meshes, and to perform real-time 3-D interactive transformation of those vectors. The user can manipulate the PS-330 graphics display

by means of a display data structure, a function network, and various input devices. The display data structure represents the finite element mesh and transformations applied to the mesh for scaling, rotation, translation, and other viewing purposes.

The function network represents a user-programmable system for describing the processing of interactive input and output local to the PS-330. The function network determines the effect of input from interactive devices on the display data structure (in the form of a finite element mesh). The user interacts with the function network through programmable interactive control dials and function keys. The display processor refreshes the screen image in real-time by traversing the display data structure which the function network is potentially modifying.

The graphics display consists of a 16-inch color vector refresh display. Finite element meshes are displayed in color or with depth-cueing. Depth-cueing enhances the illusion of depth and three dimensions by drawing vectors lighter the "farther away" they are from the viewer. Also, to enhance the illusion of three dimensions, perspective viewing of the finite element mesh is used.

FUNCTION NETWORKS

Function networks on the PS-330 are an example of data flow programming (ref. 2). An operator of a data flow program is known as a function instance. The PS-330 has a predefined set of over 100 function instances such as add, multiply, and rotate. Each function has a fixed number of inputs and outputs with predefined meanings. Data flow programming is accomplished by creating function instances and connecting inputs and outputs of the function instances to create the desired effect.

Function networks are data driven. A function becomes active only when data arrive at its inputs to be processed. Once a function has executed its task, it becomes dormant again until another set of input arrives. The entire function network is dormant until activity occurs at the interactive device to which it is connected.

Figure 1 shows a small part of the function network used in the animation of finite element model

```

WS_ROT := F:OMUL;
WS_MULX := F:MULO;
WS_XROT := F:XROTATE;
SEND 'X-ROT' TO <1>DLABEL1;
CONNECT DIALS<1>:<1>WS_MULX;
SEND 100 TO <2>WS_MULX;
CONNECT WS_MULX<1>:<1>WS_XROT;
CONNECT WS_XROT<1>:<2>WS_ROT;
CONNECT WS_XROT<1>:<1>WS_ROT;
CONNECT WS_ROT<1>:WORLD_ROT;

```

Fig. 1. Rotation function network

vibrations. This part of the function network sets up a control dial to control the X rotation of the finite element model on the display screen. Figure 2 shows a schematic of that function network. The first three lines, of the rotation function network, instance (refer to) some of the PS-330 functions. The fourth line sends a label to the LED lights on Control Dial 1. The fifth line connects the output of the control dial to the first input of one of the function instances. The sixth line sends a constant value of 100 to the second input of the same function instance. The remaining four lines connect the inputs

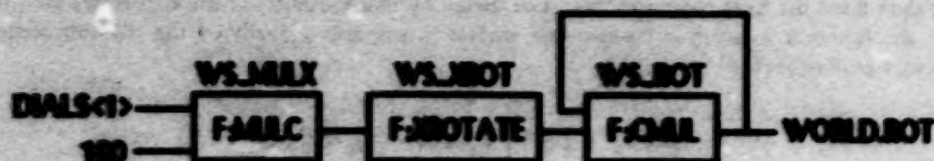


Fig. 2. Schematic of rotation function network

and outputs of the function instances in the correct manner. When the user rotates Control Dial 1, the end result is that the finite element model on the display screen will rotate about the screen's X axis.

To animate model or transient vibrations of finite element models, a function network must be loaded into the PS-230. The basic function network used with CANDI sets up: (1) the control dials to do rotations and translations of the finite element model about the X, Y, and Z axes, and (2) function keys or control dials to both control the rate of vibration and cycle through the animation sequence. For transient vibrations, the animation sequence consists of deformed shapes of the finite element model over a range of time steps. For modal vibrations, the animation sequence consists of a sinusoidal variation of the deformation of the finite element model.

In addition to controlling the function of the control dials and function keys, the function network also contains the geometry of the finite element model that is to be animated. The geometry is written in a vector list function. The vector list contains the necessary XYZ coordinate information to draw the finite element mesh. A coordinate value in the vector list will be computed from the undeformed XYZ coordinates of the finite element model plus the product of displacement of that coordinate and a scale factor. An example of a vector list is shown in figure 3.

```

BEAM := VEC COLOR ITEM
P 1.000, 0.000, 0.000 H=130.
L 1.500, 0.500, 0.000 H=130.
L 2.000, 0.000, 0.000 H=130.
L 2.500, 0.000, 0.000 H=130.
L 3.000, 0.000, 0.000 H=130.
L 3.500, 0.000, 0.000 H=130.
L 4.000, 0.000, 0.000 H=130.
L 4.500, 0.000, 0.000 H=130.
L 5.000, 0.000, 0.000 H=130.;
  
```

Fig. 3. Example vector list

The first line of the vector list establishes a name for the vector list function instance. The remaining lines give the XYZ coordinates of the finite element mesh. The "P" means move to that coordinate. The "L" means draw to that coordinate. Associated with each coordinate is a color, "H=", which is specified by a value between zero and 360. The colors blue, magenta, red, yellow, green, and cyan have values of 0, 60, 120, 180, 240, and 300, respectively. If a line has the same color specified at the beginning and end, the entire line will be drawn with that single color. If the beginning and end of a line have different color values, then the color of the line will change between the beginning and end of the line. The finite element mesh can be color-coded by assigning a color value to each XYZ coordinate according to a nodal value of displacement.

Rather than have the host computer calculate the sinusoidal variation of the deformations for modal vibrations, the function network computes the animation sequence locally on the PS-330 according to the following equation (ref. 3):

$$F_i = V_o + DSF [V_{re} \sin \theta_i - V_{im} \cos \theta_i]$$

where F_i is one frame in the animation sequence, V_o is the undeformed vector list, V_{re} is the real deformation vector list, V_{im} is the imaginary deformation vector list, DSF is the deformation scale factor, and θ_i is the angle for F_i . Usually a value of i between 12 and 16 is an acceptable number of frames for smooth animation.

POSTPROCESSING OF NASTRAN RESULTS

The program CANDI can postprocess results from several different NASTRAN analyses: static, eigenvalues, direct frequency response, direct transient response, and modal frequency response. (A static analysis is handled in CANDI as a transient analysis with only one time step.) The NASTRAN analysis must generate a file that CANDI will postprocess. To write out that file, DMAP ALTER statements must be included in the NASTRAN executive control deck. Figure 4 shows an example of the

```
ALTER $ $ Apr 88 Version
OUTPUT CASEOC,BGPD T,ECT,LAMA,PPHIG $
ENDALTER $
```

Fig. 4. NASTRAN ALTER statements

ALTER statements required for an eigenvalue analysis. The data blocks that are written by these ALTER statements contain the following information: CASEOC - case control information, BGPD T - XYZ nodal coordinates, ECT - element connectivity, LAMA - eigenvalues, and PPHIG - eigenvectors. There are similar ALTER statements to write the appropriate data blocks for the other types of analyses.

The data block that contains nodal displacements, for example PPHIG, is only generated when plotting is requested in the NASTRAN run. Therefore, plotting cards are required in the NASTRAN case control deck. This displacement data block is used rather than other displacement data blocks within NASTRAN, because the displacements are already in a basic XYZ cartesian coordinate system. Displacement in other data blocks would have to be transformed to that system.

CANDI USAGE

CANDI is an interactive program that prompts the user for various inputs and generates undeformed shape and displacement vector lists. All possible responses are listed with each question. A sample interactive session with CANDI is shown in figure 5. The user has many options to control the parts of the finite element model to be written to the vector lists. Elements can be excluded by element type or element identification number. Given a range of XYZ coordinate values, any element not within that range can also be excluded. Elements can be color-coded by element type; for example, plate elements may be green and solid elements cyan. The finite element mesh can also be color-coded

by a nodal value of displacement. A user-modifiable deformation scale factor is computed. This scale factor multiplies the real displacements so that their magnitude will be similar to the dimensions of the finite element model. For a transient analysis, any range of time steps can be written to the displacement vector list. For an eigenvalue or frequency response analysis, any frequency also can be written to the displacement vector list.

DISPLAYING THE ANIMATION

Before the finite element model vibrations can be animated, the function network that sets up the function of the control dials and function keys must be sent from the host computer to the PS-330. The definition of the control dials and function keys for modal vibrations is shown in figure 6 and, for transient vibrations, in figure 7. Once either function network has been transmitted to the PS-330, the undeformed shape and displacement vector lists can be sent to the PS-330 from the host computer. Usually, the user will generate one undeformed shape and multiple displacement vector lists during one interactive session with CANDL. To animate different displacement vector lists, the desired vector list is downloaded to the PS-330. Once the required vector lists reside on the PS-330, the user has complete control over the animation through the use of the control dials and function keys.

REFERENCES

1. "PS-300 User's Manual," Evans & Sutherland Computer Corporation, Salt Lake City, Utah, 1983.
2. McGraw, J.R., "Data Flow Computing - Software Development," in: *IEEE Transactions on Computers*, Vol. C-29, No. 12, December 1980.
3. Ehlers, R., "Modal Vibration Simulation Package," Evans & Sutherland Computer Corporation, Salt Lake City, Utah, 1984.

```

$ candi

CANDI - Color Animation of Nastran Displacements

ENTER FILE NAME OF THE UTI FILE ? fs.uti

COORDINATE LIMITS OF THE STRUCTURE
XMIN=2.39E+02 YMIN= 0.00E+00 ZMIN= 1.03E+03
XMAX= 2.39E+02 YMAX= 2.39E+02 ZMAX= 1.38E+03

DO YOU WANT TO EXCLUDE ELEMENTS BY COORDINATE RANGES (Y/N) ? n

3 ELEMENT TYPES, CURRENTLY RECOGNIZED BY CANDI, WERE FOUND IN THE FEM.
180-CBAR 58-CQUAD2 53-CTRIA2

DO YOU WANT TO EXCLUDE ELEMENTS BY ELEMENT TYPE (Y/N) ? n

DO YOU WANT TO EXCLUDE ELEMENTS BY ELEMENT ID (Y/N) ? n
READING CBAR
READING CQUAD2
READING CTRIA2

DO YOU WANT THE VECTOR LISTS TO BE WRITTEN
1 - COLOR CODED BY ELEMENT TYPE
2 - DEPTH CUED
? 1

ENTER FILE NAME FOR THE UNDEFORMED FEM VECTOR LIST ? fs.und
WRITING VECTOR LIST

DO YOU WANT TO GENERATE ANY DISPLACEMENT VECTOR LISTS (Y/N) ? y

NUMBER OF SUBCASES = 1, SUBCASE IDS = 1
NUMBER OF EIGENVECTORS = 3 (MODE-FREQUENCY)
1-3.65E+01 2-3.83E+01 3-5.00E+01

ENTER A MODE NUMBER ? 2

ENTER FILE NAME FOR THE DISPLACEMENT VECTOR LIST ? fs.m2
ENTER NUMBER OF FRAMES OF ANIMATION ? 16
WRITING VECTOR LIST
MAXIMUM DEFORMATION = 1.1632E+00
DEFORMATION SCALE FACTOR = 2.0553E+01

DO YOU WANT TO WRITE ANOTHER DISPLACEMENT VECTOR LIST (Y/N) ? n
FORTRAN STOP

```

Fig. 5. Sample interactive session of CANDI

CD(1) - X rotation
 CD(2) - Y rotation
 CD(3) - Z rotation
 CD(6) - X translation
 CD(8) - Y translation
 CD(7) - Z translation
 CD(8) - Scale

 FK(1) - Start modal vibration
 FK(2) - Stop modal vibration
 FK(4) - Step through animation sequence
 FK(5) - Slow down rate of vibration
 FK(6) - Speed up rate of vibration
 FK(9) - Reset all rotations and translations
 FK(10) - Toggle on/off undeformed shape
 FK(11) - Toggle on/off coordinate axes
 FK(12) - Calculate animation sequence from the undeformed
 vector list and the displacement vector lists

Fig. 6. Modal vibration control dial and function key definitions

CD(1) - X rotation
 CD(2) - Y rotation
 CD(3) - Z rotation
 CD(4) - Control rate of vibration
 CD(5) - X translation
 CD(6) - Y translation
 CD(7) - Z translation
 CD(8) - Scale

 FK(1) - Start/stop transient vibration
 FK(9) - Reset all rotations and translations
 FK(10) - Toggle on/off undeformed shape
 FK(11) - Toggle on/off coordinate axes

Fig. 7. Transient vibration control dial and function key definitions

BUBBLE VECTOR IN AUTOMATIC MERGING

P. R. PMIDI and T. G. BUTLER
 RPK Corporation BUTLER ANALYSES

SUMMARY

This paper shows that it is within the capability of the DMAP language to build a set of vectors that can grow incrementally to be applied automatically and economically within a DMAP loop that serve to append sub-matrices that are generated within a loop to a core matrix. The method of constructing such vectors is explained. In an appendix are four DMAP packets for applying these techniques in different ways.

PURPOSE

The objective is to build a set of partitioning vectors that will grow incrementally to be applied automatically in a DMAP loop without analyst intervention for the purpose of appending the sub-matrices, formed in the loop, to the product matrix accumulated from preceding passes through the loop; i.e.

$$\begin{bmatrix} 0 & 1 \end{bmatrix}^T$$

$$\begin{bmatrix} 0 & 0 & 1 \end{bmatrix}^T$$

$$\begin{bmatrix} 0 & 0 & 0 & 1 \end{bmatrix}^T$$

$$\begin{matrix} . \\ . \\ . \\ . \end{matrix}$$

$$\begin{bmatrix} 0 & 0 & \dots & 0 & 0 & 1 \end{bmatrix}^T$$

DILEMMA

The DMAP language in EASTRAN does not have a module that will generate vectors of arbitrary size. No matrix mathematical operations will increase the order of a matrix as demonstrated here.

When two matrices are added or subtracted, the order of the result stays the same:

$$\begin{bmatrix} a & b \\ c & d \end{bmatrix}_{2 \times 2} \begin{pmatrix} + \\ - \end{pmatrix} \begin{bmatrix} m & n \\ p & q \end{bmatrix}_{2 \times 2} = \begin{bmatrix} (a \pm m) & (b \pm n) \\ (c \pm p) & (d \pm q) \end{bmatrix}_{2 \times 2}$$

If two matrices are multiplied, the order of the result will not exceed the bounding order of the multiplicands:

$$\begin{bmatrix} a & b \\ c & d \end{bmatrix}_{2 \times 2} \times \begin{bmatrix} m & n \\ p & q \end{bmatrix}_{2 \times 2} = \begin{bmatrix} (am + bp) & (an + bq) \\ (cm + dp) & (cn + dq) \end{bmatrix}_{2 \times 2}$$

If a matrix is squared, the order of the result stays the same:

$$\begin{bmatrix} a & b \\ c & d \end{bmatrix}_{2 \times 2}^2 = \begin{bmatrix} (a^2 + bc) & (ab + bd) \\ (ca + dc) & (cb + d^2) \end{bmatrix}_{2 \times 2}$$

Merging does produce a matrix of expanded order if one has at hand a partitioning vector, of the order desired, to monitor the merging. This is tantamount to saying that you can expand the order of a matrix if you already have one around which is of the size that you want. A scheme is therefore needed which employs a sequence of DMAP utility modules to provide an incrementally expanding partitioning vector. However, no single module available in EASTRAN will continually increase the order of a partitioning vector as desired here. If you let this notion

soak in for a time, then the inspiration percolates to the front of your brain to say "start with something big and extract the object of required order from it." Our ideas at this point are still a long way away from the final algorithm, but this is the seminal idea. After a number of crude tries, the algorithm shown here finally took shape.

NOTATION

A vector is a column matrix : $(V) = \begin{pmatrix} a_1 \\ a_2 \\ a_3 \\ \vdots \\ a_n \end{pmatrix}$

The transpose of a vector is a row matrix:

$$(V)^T = [a_1 \ a_2 \ a_3 \ a_4 \ \dots \]$$

To save space in the text, vectors will be written as transposes of row matrices:

$$\begin{pmatrix} a_1 \\ a_2 \\ a_3 \\ \vdots \\ a_n \end{pmatrix} = [a_1 \ a_2 \ a_3 \ a_4 \ \dots \ a_n]^T$$

INITIAL CONSIDERATIONS

The design of the DMAP ALTER packet will hinge on the range of certain parameters.

1. The size of the core matrix to which sub-matrices are to be appended. (Number of starting columns or rows)
2. The position at which sub-matrices are to be appended; i.e. Pre or Post.
3. The size of the final matrix after all sub-matrices have been appended (Final number of columns or rows).

6. The number of columns or rows in the sub-matrix generated in each pass through the DMAP loop (Increment).

SCHEME FOR APPENDING A SUB-MATRIX IN EACH PASS THROUGH A LOOP

The nub of the idea is to operate with a series of vectors of order larger than that of the matrix to be built in the DMAP loop. The final MONITOR vector, that will be used for the actual merge operation, will be extracted from the SOURCE. The technique which is used in the intermediate operations for managing the incremental growth of the MONITOR vector is where the real interest lies. This will be elaborated in detail, but as an introduction suffice it to say that there are two SOURCE vectors which are companions such that one has the increment at the tip of the vector and the other has the increment at the base of the vector. A BUBBLE vector is created whose length remains invariant, but whose increment moves inward from its starting position in a sea of zeroes. The BUBBLE vector leaves a trail of its previous positions as an accumulation of the increments into a vector called CLUSTER. The overall length of the CLUSTER vector remains invariant as the collection of increments increases. CLUSTER is used to partition the MONITOR from one of the SOURCE vectors.

(SOURCE) ~~CLUSTER~~ (MONITOR)

The steps in managing these vectors follow. For example, in the case of post-appending a single column in each pass, the SOURCE vector would have leading zeroes and a one in the last position, so a logical name would be BAS.

[0000.....0000000.....00000000000.....0001]^T

Use this SOURCE vector as as a replenishable reservoir from which to take slices of increasing length to form the MONITOR vector as the product matrix grows from successive appending loops.

Several examples of these slices follow:

$$\begin{bmatrix} 01 \end{bmatrix}^T$$

Slice taken to create a MONITOR vector to merge a single vector to the right hand side of a core consisting of a single vector, resulting in a product matrix of 2 columns.

$$\begin{bmatrix} 00000001 \end{bmatrix}^T$$

Slice taken to create a MONITOR vector to merge a single vector to the right hand side of a 7-col core matrix, resulting in a product matrix of 8 columns.

$$\begin{bmatrix} 0000000000000001 \end{bmatrix}^T$$

Slice taken to create a MONITOR vector to merge a single vector to the right hand side of a 14-col core matrix, resulting in a product matrix of 15 columns.

The CLUSTER vectors needed to do the slicing from the SOURCE would be of the same order as the SOURCE, but would have a cluster of increments equal to the number of columns in the product matrix after the end of a pass; i.e. the three CLUSTER vectors that would be used to slice the three MONITOR vectors shown above from the SOURCE would be respectively:

$$\begin{bmatrix} 000000.....0000000.....000000000000.....0011 \end{bmatrix}^T$$

$$\begin{bmatrix} 000000.....0000000.....000000000000.....11111111 \end{bmatrix}^T$$

$$\begin{bmatrix} 000000.....0000000.....000000000000.....1111111111111111 \end{bmatrix}^T$$

It is evident from the above three examples that the number of ones in the CLUSTER vector grows by an increment after each pass (in this example the increment is one). The needs of

the algorithm will be met by saving only the latest CLUSTER vector and devising some way of adding another increment in the next interior position. For example, in building the CLUSTER for the pass after the product has grown to order eight, one could add a vector to the "8" CLUSTER vector, which is of the same order as the "8" CLUSTER vector, but has zeroes everywhere except for a one in the 9th-from-the-end interior position.

```

[ 000000.....0000000.....00000000.....0001111111 ]T
      ↓
      ↓
      ↓
      ↓
[ 000000.....0000000.....000000000000.....001000000000 ]T
      ↓
      ↓
      ↓
      ↓
[ 000000.....0000000.....000000000000.....11111111 ]T

```

Well, here is a situation that can be used to evolve pass by pass. It is a matter of moving the "1" in the intermediate matrix to the next-interior-position. All well and good. But how does one do that? In a vulgar analogy, just bite off a zero from the front and spit it onto the end. The tools are already at hand to do just that. The two companion SOURCE vectors are of the right order. There is a "1" on the front of one of the two companions to do the biting off of a zero from the front. The other of the pair has a "1" on the end to do the spitting of a zero onto the end. This intermediate vector is saved from pass to pass. Conceptually the "1" keeps travelling to the interior on successive passes. It is analogous to a bubble moving in a liquid-filled tube; thus the name BUBBLE vector.

Using this scheme, our needs will be met;

1. The MONITOR vector grows by an increment on each pass to do the merging of an increment to the product. The MONITOR is discarded after each pass; and is regenerated on a succeeding pass.
2. The CLUSTER vector augments its cluster of "1's" by an increment on each pass to do its job of slicing off a new MONITOR vector from the SOURCE vector. It is saved in its augmented form after each pass.
3. The BUBBLE vector shifts its set of ones to the interior by an increment on each pass to do its job of adding an increment to the CLUSTER. It is saved after being shifted in each pass.
4. The pair of SOURCE vectors remains unchanged during the whole operation.

REQUIREMENTS

The analyst is to supply simple initial bulk data and should be free of having to intervene in making entries in the DMAP code, once the author has incorporated the BUBBLE scheme into a DMAP loop. It should be easy for the author to use. It should be economical on storage space.

ALGORITHM FOR APPENDING

Now to build an algorithm to meet the stipulated requirements, we will consider these requirements one by one.

Specification: Simple initial bulk data.

The user supplies 2 SOURCE vectors. Because they are sparse, it will take a minimum of 2 cards for each vector for a total minimum of four cards. This is simple. He knows how big "big" is from the nature of the problem that he is analyzing. He knows the size of the sub-matrix to be appended so he can set the vectors' increments.

ORIGINAL PAGE IS
OF POOR QUALITY

Specification: Easy for the author.

To illustrate the ease of concept, examples of the Ith step of a loop (I = 4) will be used to demonstrate how simple it is to shift from pre or post appending or from column or row appending. The operations can be characterized as CROP, SHIFT, SUM, HARVEST, AND APPLY. The first example shows pre-appending of columns and the second example shows post-appending of columns.

Pre-appending

CROP	SHIFT	SUM	HARVEST	APPLY
			TIPMON	(1 0 0 0 0)
(0) (0) (0)	(1) → (0) (0) →	(1) (0) (1)	(1) → (1) (1)	(a) [A B C D]
(0) (0) (0)	(0) (0) (0) →	(1) (0) (1)	(1) → (0) (0)	(b) [E F G H]
(0) (0) (0)	(0) (0) (0) →	(1) (0) (1)	(1) → (0) (0)	(c) [I J K L]
(0) (1) (1)	(0) (0) (0) →	(1) (0) (1)	(1) → (0) (0)	(d) [M N O P]
(0) (0) (0)	(0) (1) (1) →	(0) → (1) → (1)	(1) → (0) (0)	(e) [Q R S T]
(0) (0) (0)	(0) (0) (0) →	(0) (0) (0)	(0) (0) (0)	(f) [U V W X]
(0) (0) (0)	(0) (0) (0) →	(0) (0) (0)	(0) (0) (0)	(g) [Y Z z y]
(0) (0) (0)	(0) (0) (0) →	(0) (0) (0)	(0) (0) (0)	(h) [x w v u]
(1) → (0) (0)	(0) (0) (0) →	(0) (0) (0)	(0) (0) (0)	(i) [t s r q]
PARTN	MERGE	ADD	PARTN	MERGE
Ith Names				
BAS DUMMY	TIP BUBLJ	CLUSI CLUSJ	CLUSJ TIPMON	SUBMTX PRODI
BUBLI	DUMMY	BUBLJ	↓ TIP	= PRODJ
		↓	↓	↓
Prep for Loop		BUBLI	CLUSI	PRODI
SWITCH to				

Post-appending

CROP	SHIFT	SUM	HARVEST	APPLY
			BASHMON	(0 0 0 0 1)
(1) → (0) (0)	(0) (0) (0) →	(0) (0) (0)	(0) (0) (0)	[A B C D] (a)
(0) (0) (0)	(0) (0) (0) →	(0) (0) (0)	(0) (0) (0)	[E F G H] (b)
(0) (0) (0)	(0) (0) (0) →	(0) (0) (0)	(0) (0) (0)	[I J K L] (c)
(0) (0) (0)	(0) (0) (0) →	(0) (0) (0)	(0) (0) (0)	[M N O P] (d)
(0) (0) (0)	(0) (1) (1) →	(0) → (1) → (1)	(1) → (0) (0)	[Q R S T] (e)
(0) (1) (1)	(0) (0) (0) →	(1) (0) (1)	(1) → (0) (0)	[U V W X] (f)
(0) (0) (0)	(0) (0) (0) →	(1) (0) (1)	(1) → (0) (0)	[Y Z z y] (g)
(0) (0) (0)	(0) (0) (0) →	(1) (0) (1)	(1) → (0) (0)	[x w v u] (h)
(0) (0) (0)	(1) → (0) (0) →	(1) (0) (1)	(1) → (1) (1)	[t s r q] (i)
PARTN	MERGE	ADD	PARTN	MERGE
Ith Names				
TIP DUMMY	BAS BUBLJ	CLUSI CLUSJ	CLUSJ BASHMON	PRODI SUBMTX
BUBLI	DUMMY	BUBLJ	↓ BAS	= PRODJ
		↓	↓	↓
Prep for Loop		BUBLI	CLUSI	PRODI
SWITCH to				

Specification: Economical on storage space

The two source vectors will remain in storage for the whole time that the loop is in operation. Their length may be in the thousands, but the vectors are stored in packed form so the storage will consist of the header, the increment of 1's, and the packing index for the position of nonzero entries.

The CLUSTER will be the same length as the SOURCE vectors and will have a cluster of "1's" instead of a small increment of 1's, but the content will be mostly zeroes in packed form; so its storage requirements will be low until its cluster grows to the final size of the PRODUCT matrix at the end of the loop.

The BUBBLE vectors will be the same length as the SOURCE vectors and will have a single non-zero increment like the SOURCE vectors so their storage will be exactly the same as the SOURCE vectors.

The MONITOR vectors will exist for the duration of a merge within a loop. Their brief storage requirements are exactly the same as the SOURCE vectors, because they will differ from the source only in the order number in the header.

ALGORITHM FOR POST APPENDING A MATRIX

Organize a pair of SOURCE vectors of large order; one with leading zeroes before the increment of "1's"; and the other with trailing zeroes after the increment of "1's". Call these respectively BAS and TIP.

BAS $[0 \ 0 \ 0 \ 0 \ 0 \ \dots \ 0 \ 0 \ 0 \ 0 \ 0 \ 0 \ 0 \ 0 \ 0 \ 1 \ 1]^T$
The # of 1's is governed by the sub-matrix order/pass; i.e. increment.

TIP $[1 \ 1 \ 0 \ 0 \ 0 \ 0 \ 0 \ \dots \ 0 \ 0 \ 0 \ 0 \ 0 \ 0 \ 0 \ 0 \ 0]^T$
The # of 1's is governed by the increment/pass.

ORIGINAL PAGE IS
OF POOR QUALITY

Find out the order of the core matrix prior to entering the loop. Use PARAML with operator = TRAILER and RECONO = trailer position # 1 corresponding to the number of columns in the core matrix. Call the parameter value that is returned by the name CORCOL for the number of core columns. But, if the sub-matrix is to be augmented by rows, set RECONO = trailer position #2 corresponding to the number of rows; then call the returned parameter by the name COROW for the number of core rows. The remainder of the explanation for this algorithm will be based upon the logic of post appending columns.

```
PARAML    CORENTX//*TRAILER*/1/CORCOL $  
EQUIV     CORENTX.PRODI/TRUE $
```

Move the bubble to that CORCOL position in unity increments with these preparatory steps.

Set up a small loop to prepare the vectors BUBLI and CLUSI ahead of the main loop. Companion source vectors (SOURCE1) with increments of unity called BAS1 and TIP1 are supplied by the user with DMI cards in the bulk data. Make copies of BAS1 to act as starting configurations for CLUSI and BUBLI for molding into their loop configurations.

```
COPY      BAS1/CLUSI/0 $ For the case of post-appending.  
COPY      BAS1/BUBLI/0 $
```

Set the number of movements of the bubble that are needed to prepare BUBLI.

```
PARAM     //*SUB*/SHIFT/CORCOL/1 $  
  
LABEL     BUBTOP $  
FILE      BUBLI= SAVE/ CLUSI = SAVE/ PRODI = SAVE $
```

Partition off a zero from the starting vector of BUBLI with TIP1.

$$(BUBLI) \leftarrow TIP1, \begin{pmatrix} 0 \\ DUBBY \end{pmatrix}$$

PARTN BUBLI, TIP1/DUBBY.../+7 \$

Merge a zero onto the truncated stub of the BUBBLE vector with BAS1

$$\begin{pmatrix} DUBBY \\ 0 \end{pmatrix} \leftarrow BAS1 \rightarrow (BUBLJ)$$

MERGE DUBBY, , , , BAS1/BUBLJ/+7 \$

The increment is now moved interior-ward in the BUBBLE vector. Combine the shifted BUBBLE vector with the starting vector of CLUSI.

$$(CLUSI) + (BUBLJ) = (CLUSJ)$$

ADD CLUSI,BUBLJ/CLUSJ/ \$

Reset the internal loop names to the starting assignments in order to prepare for the next pass.

SWITCH BUBLJ,BUBLI/ /-1 \$

SWITCH CLUSJ,CLUSI/ /-1 \$

Return to the starting label if the loop count (internally monitored by NASTRAN) is less than the prescribed value of SHIFT.

REPT BUBTOP,SHIFT \$

Now the positions of the ones in both BUBLI and CLUSI matches the size of the CORE matrix.

Set up the loop for post appending an incremental sub-matrix onto the CORE matrix in each pass.

LABEL CORTOP \$

Keep shifting the increment (which can now be different from unity depending on the need of the sub-matrix in the loop) in the BUBBLE vector once per pass (with BAS and TIP instead of BAS1 and TIP1) now that it has been set by the preparatory packet. Start by truncating an increment of leading zeroes.

$$(BUBLI) \leftarrow TIP, \begin{pmatrix} 0 \\ DUMMY \end{pmatrix}$$

PARTN BUBLI, ,TIP/DUMMY,,,/+7 \$

Merge on an increment of trailing zeroes to push the bubble into the interior.

$$\begin{pmatrix} DUMMY \\ 0 \end{pmatrix} \leftarrow BAS \rightarrow (BUBLJ)$$

MERGE DUMMY, , , , ,BAS/BUBLJ/+7 \$

Combine the shifted BUBBLE vector with the CLUSTER vector "CLUSI".

$$(CLUSI) + (BUBLJ) = (CLUSJ)$$

ADD CLUSI,BUBLJ/CLUSJ/ \$

Partition off the MONITOR vector to the size of the PRODUCT matrix being built in this pass.

$$(BAS) \leftarrow CLUSJ, \begin{pmatrix} 0 \\ MWTRI \end{pmatrix}$$

PARTN BAS, ,CLUSJ/,MWTRI, , /+7 \$

The desired merging vector has been produced and is ready to be applied to the job of joining the current sub-matrix to the current PRODUCT matrix.


```

##MOCK FUNCT'L MODULE "MIXOPN" PRODUCES THE SUB-MATRIX "SUBMTX"
MIXOPN DBIN/SUBMTX/ $
## PRODUCT MATRIX "PRODI" IS AVAILABLE FROM A PREVIOUS PASS.

```

```

[PRODI : SUBMTX] ==MTRI [PRODJ]

```

```

MERGE PRODI, ,SUBMTX, ,MTRI, /PRODJ/ +7 $

```

Prepare for the next pass by resetting the matrix names to their initial assignments.

```

SWITCH PRODJ,PRODI/ /-1 $
SWITCH CLUSJ,CLUSI/ /-1 $
SWITCH BUBLJ,BUBLI/ /-1 $

```

Apply a test to see how far the merging has proceeded with respect to the requirements of the matrix operations. Set the value of a threshold to negative when the loop is done so that a conditional jump takes the OSCAR outside the loop.

```

##MOCK FUNCT'L MODULE "TESTOPN" PROVIDES A TEST LOGIC FOR LOOPS.
TESTOPN VARY, , /DBOUT/THRESHLD $
COND OUTSIDE,THRESHLD $

```

Loop back to the top of the main loop so long as the value of THRESHLD remains positive. When it turns negative the conditional jump takes the sequence of operations beyond the loop.

```

REPT CORTOP,## $ ## VALUE IS LARGER THAN THAT
## EXPECTED FOR THRESHOLD
LABEL OUTSIDE $ PRODI IS PASSED OUTSIDE THE LOOP WITH
## SUB-MATRICES FROM ALL LOOPS MERGED ONTO IT

```

This completes the explanation for the algorithm following the example of post-appending any sized sub-matrix by columns. In the appendix, this algorithm is coded for the four permutations of:

1. Post-append by columns.
2. Pre-append by columns.
3. Post append by rows.
4. Pre-append by rows.

CONCLUSION

It has been shown that it is within the capability of the DMAP language to build a set of vectors that can grow incrementally to be applied automatically and economically within a DMAP loop to serve to append sub-matrices that are generated within a loop to a product matrix.

APPENDIX FOR FOUR PATHS OF THE BUBBLE ALGORITHM

\$POST APPEND COLUMNS.

```

PARAML      COREMTX/ /*TRAILER*/ 1 /CORCOL $
COPY        BAS1 /CLUSI/ 0 $
COPY        BAS1 /BUBLI/ 0 $
PARAM       /*SUB*/SHIFT/CORCOL/ 1 $
LABEL       BUBTOP $
FILE        BUBLI = SAVE/ CLUSI = SAVE/ PRODI = SAVE $
PARTN       BUBLI, , TIP1 /DUMMY, , , /+7 $
MERGE       DUMMY, , , , BAS1 /BUBLJ/+7 $
ADD         CLUSI,BUBLJ/CLUSJ/ $
SWITCH      BUBLJ,BUBLI/ /-1 $
SWITCH      CLUSJ,CLUSI/ /-1 $
REPT        BUBTOP,SHIFT $
LABEL       CORTOP $
PARTN       BUBLI, ,TIP /DUMMY, , , /+7 $
MERGE       DUMMY, , , , BAS /BUBLJ/+7 $
ADD         CLUSI,BUBLJ/CLUSJ/ $
PARTN       BAS , ,CLUSJ/ ,MNTRI, , /+7 $
MTXOPN      DBIN/MODE/ $
MERGE       PRODI, ,MODE, ,MNTRI, /PRODJ/+7 $
SWITCH      PRODJ,PRODI/ /-1 $
SWITCH      CLUSJ,CLUSI/ /-1 $
SWITCH      BUBLJ,BUBLI/ /-1 $
TSTOPN      VARY, , /DBOUT/THRESHLD $
COND        OUTSIDE,THRESHLD $
REPT        CORTOP,MNR $
LABEL       OUTSIDE $

```


\$PRE APPEND COLUMNS.

PARAM	CORRECT/ /*TRAILER*/1/CORCOL \$
COPY	TIP1 /CLUSI/ 0 \$
COPY	TIP1 /BUBLI/ 0 \$
PARAM	/*SUB*/SHIFT/CORCOL/ 1 \$
LABEL	BUSTOP \$
FILE	BUBLI = SAVE/ CLUSI = SAVE/ PRODI = SAVE \$
PARTN	BUBLI, , BAS1 /DUMMY, , , /+7 \$
MERGE	DUMMY, , , , TIP1 /BUBLJ/+7 \$
ADD	CLUSI,BUBLJ/CLUSJ/ \$
SWITCH	BUBLJ,BUBLI/ /-1 \$
SWITCH	CLUSJ,CLUSI/ /-1 \$
REPT	BUSTOP,SHIFT \$
LABEL	CORTOP \$
PARTN	BUBLI, ,BAS /DUMMY, , , /+7 \$
MERGE	DUMMY, , , , TIP /BUBLJ/+7 \$
ADD	CLUSI,BUBLJ/CLUSJ/ \$
PARTN	TIP , ,CLUSJ/ ,MWTRI, , /+7 \$
MERGE	DBIN/MODE/ \$
MERGE	PRODI, ,MODE, ,MWTRI, /PRODJ/+7 \$
SWITCH	PRODJ,PRODI/ /-1 \$
SWITCH	CLUSJ,CLUSI/ /-1 \$
SWITCH	BUBLJ,BUBLI/ /-1 \$
TSTOPN	VARY, , /DBOUT/THRESHLD \$
COND	OUTSIDE,THRESHLD \$
REPT	CORTOP,MWR \$
LABEL	OUTSIDE \$

\$POST APPEND ROWS.

PARAML	COREMEX/ /A/ TRAILER/2/ COROW \$
COPY	BAS1 /CLUSI/ 0 \$
COPY	BAS1 /BUBLI/ 0 \$
PARAM	//A/SUBA/SHIFT/COROW/ 1 \$
LABEL	BUSTOP \$
FILE	BUBLI = SAVE/ CLUSI = SAVE/ PRODI = SAVE \$
PARTN	BUBLI, , TIF1 /DUMMY, , , /+7 \$
MERGE	DUMMY, , , , BAS1 /BUBLJ/+7 \$
ADD	CLUSI,BUBLJ/CLUSJ/ \$
SWITCH	BUBLJ,BUBLI/ /-1 \$
SWITCH	CLUSJ,CLUSI/ /-1 \$
REPT	BUSTOP,SHIFT \$
LABEL	CORTOP \$
PARTN	BUBLI, ,TIP /DUMMY, , , /+7 \$
MERGE	DUMMY, , , , BAS /BUBLJ/+7 \$
ADD	CLUSI,BUBLJ/CLUSJ/ \$
PARTN	BAS , ,CLUSJ/ ,MBTRI, , /+7 \$
MTXOPN	DBIN/MODE/ \$
MERGE	PRODI,MODE , , , ,MBTRI /PRODJ/+7 \$
SWITCH	PRODJ,PRODI/ /-1 \$
SWITCH	CLUSJ,CLUSI/ /-1 \$
SWITCH	BUBLJ,BUBLI/ /-1 \$
TSTOPN	VARY, , /DBOUT/THRESHLD \$
COND	OUTSIDE,THRESHLD \$
REPT	CORTOP,MBR \$
LABEL	OUTSIDE \$

\$PRE APPEND ROWS.

PARAM	COROMER/ /A*TRAILER*/2/COROM \$
COPY	TIP1 /CLUSI/ 0 \$
COPY	TIP1 /BUBLI/ 0 \$
PARAM	//A*SUB*/SHIFT/COROM/ 1 \$
LABEL	BUSTOP \$
FILE	BUBLI = SAVE/ CLUSI = SAVE/ PRODI = SAVE \$
PARTN	BUBLI, , BAS1 /DUMMY, , , /+7 \$
MERGE	DUMMY, , , , TIP1 /BUBLJ/+7 \$
ADD	CLUSI,BUBLJ/CLUSJ/ \$
SWITCH	BUBLJ,BUBLI/ /-1 \$
SWITCH	CLUSJ,CLUSI/ /-1 \$
REPT	BUSTOP,SHIFT \$
LABEL	CORTOP \$
PARTN	BUBLI, ,BAS /DUMMY, , , /+7 \$
MERGE	DUMMY, , , , TIP /BUBLJ/+7 \$
ADD	CLUSI,BUBLJ/CLUSJ/ \$
PARTN	TIP , ,CLUSJ/ ,MWTRI, , /+7 \$
MEMOPN	DBIN/MODE/ \$
MERGE	PRODI,MODE, , , ,MWTRI /PRODJ/+7 \$
SWITCH	PRODJ,PRODI/ /-1 \$
SWITCH	CLUSJ,CLUSI/ /-1 \$
SWITCH	BUBLJ,BUBLI/ /-1 \$
TSTOPN	VARY, , /DBOUT/THRESHLD \$
COND	OUTSIDE,THRESHLD \$
REPT	CORTOP,MWER \$
LABEL	OUTSIDE \$

MASS MODELING FOR BARS

by

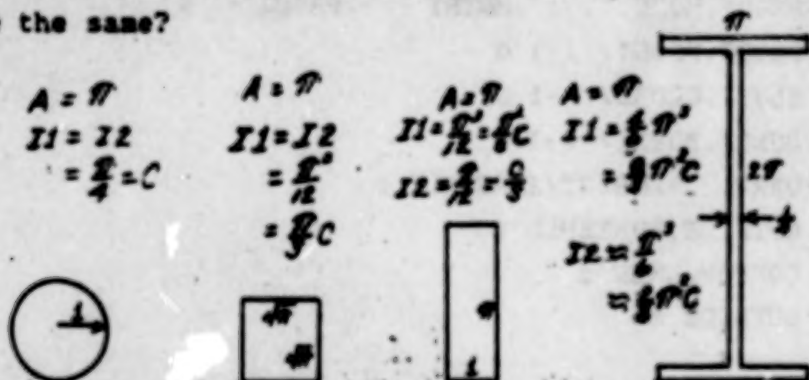
Thomas G. Butler
BUTLER ANALYSES

Summary

Methods of modeling mass for bars are surveyed. A method for extending John Archer's concept of consistent mass beyond just translational inertia effects to rotational inertia effects is included. Results are compared against detailed models. Recommendations are published for various types of modeling situations.

Methods

Would you say that the inertia matrix for beams of these four sections would be the same if the area, material and length for all four were the same?



That is exactly what NASTRAN will give you if you ask for Coupled Mass on the PARAM card. NASTRAN looks at the area, the span and the density and gives you a coupled mass matrix based only on the amount of uniformly distributed mass between grid points. The COUPMASS routine does not concern itself with the sectional data that you include on your PBAR card other than area. It does compute moment-of-inertia terms based on the assumption that inertia effects are the same in plane 1 and plane 2. You may wonder why I bother to engage in such an inquiry. It all came about as I was investigating how to formulate the mass matrix for beams of variable cross-section

when modeled as equivalent prismatical beams. I found that a considerable correction was needed to balance the inertias in the two principal planes after coupled mass formulation. I was inclined to base any such corrections as an extension of the logic which may have already been applied to the uniform bar. When I observed that coupled mass formulation was insensitive to distribution over the section, I thought that it would be worthwhile to try to extend the theory to these additional terms.

That is the truth. Now let's form a judgement. Is this bad? It will be shown below that coupled mass in spite of its insensitivity to differences in section is a definite improvement over the default condition of breaking the total mass into two pieces and lumping it at the two ends without first and second moments. In order to form a basis of judgement, let's look at the various ways to model mass in bar elements. NASTRAN only admits of prismatical BAR elements. That means a constant cross-section over its entire length. So this study will be confined to the modeling of mass for prismatical beams. The criterion for goodness of modeling will be the match that a given model makes with the frequencies of free-free beam modes using Timoshenko (1) as the arbiter for correctness. Free-free modes were chosen, because these modes activate more of the bar mass than other modes. There are essentially two elastic conditions that the user opts for in his modeling of bending--with or without shear stiffness. Because the shear contribution to elastic bending always acts in series with the contribution from curvature, the net effect of including shear stiffness in the bending behavior of a model, is to lower the modal frequencies. In reality, there are 3 elastic conditions; because if the user includes a complement of properties including longitudinal, bending and torsion, but confines his freedoms to only translations, he is depriving his model of some of the rotational contributions to bending, which act in parallel with the transverse translational terms with the net result that the modal frequencies will be lower than those containing a complete set of rotational freedoms. All of the beams that were modeled in this study were done without shear deformation terms in the stiffness matrix. Because of the importance of all of these conditions, the descriptions of the various patterns of modeling

that are to be described, will be identified with both the stiffness and the mass modeling schemes.

Scheme 1. SCALAR MASS

Translational DOF's 3 dof/GP

Stiffness properties A, I1, I2

Non-zero rows & cols of KGG Matrix 1,2,3....7,8,9

Non-zero rows & cols of MGG Matrix 1,2,3....7,8,9



Figure 1

Scheme 1A. SCALAR FINE MESH

Patterns the same as SCALAR except the mesh of GP's is fine.

Scheme 1B. SCALAR 3 CONDENSE

Patterns the same as SCALAR FINE MESH except the fine mesh is condensed to a coarse mesh.

Scheme 1C. SCALAR 5 CONDENSE

Translational & 2 Bending DOF's 5 dof/GP

Stiffness Properties A, I1, I2

Non-zero rows & cols of KGG Matrix 1,2,3...5,6,7,8,9,...,11,12

Non-zero rows & cols of MGG Matrix 1,2,3,.....7,8,9.....

Non-zero rows & cols of MAA Matrix 1,2,3...5,6,7,8,9,...,11,12

Scheme 2. LUMPED MASS

Translational & Rotational DOF's 6 dof/GP

Stiffness Properties A, I1, I2, J

KGG Matrix All rows & cols active

MGG Matrix 6x6 groups/GP. No coupling between GP's

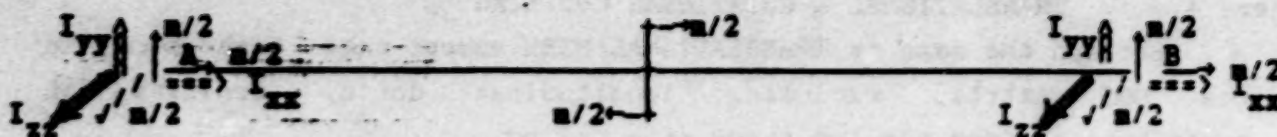


Figure 2

Scheme 2A. LUMPED FINE MESH

Pattern same as LUMPED MASS except the mesh of GP's is fine.

Scheme 2B. LUMPED CONDENSED

Pattern same as LUMPED FINE MESH except MAA matrix develops same coupling between GP's that KAA matrix has.

Scheme 3. TRANSLATIONAL COUPLING

No Torsional DOF's 5 dof/GP

Stiffness Properties A, I1, I2

Non-zero rows & cols of KGG 1,2,3,...5,6,7,8,9,...11,12

Non-zero rows & cols of MGG 1,2,3,...5,6,7,8,9,...11,12

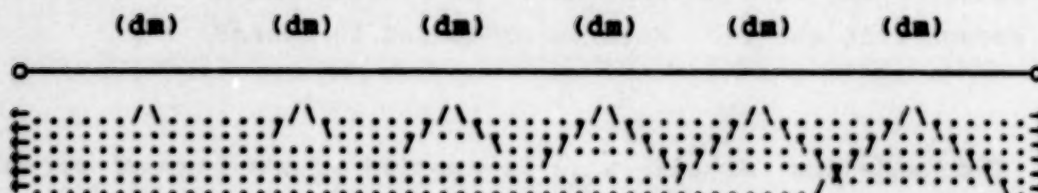


Figure 3

Scheme 3A. TRANSLATIONAL COUPLING FINE MESH

Pattern the same as TRANSLATIONAL COUPLING except the mesh of GP's is fine.

Scheme 3B. TRANSLATIONAL COUPLING CONDENSED

Pattern the same as TRANSLATIONAL FINE MESH except the fine mesh is condensed to a fine mesh.

Scheme 4. TRANSLATIONAL & ROTATIONAL COUPLING

Pattern the same as TRANSLATIONAL MESH except that each term in the MGG matrix, excluding longitudinal dof's, consists of contributions from the two types of coupling.

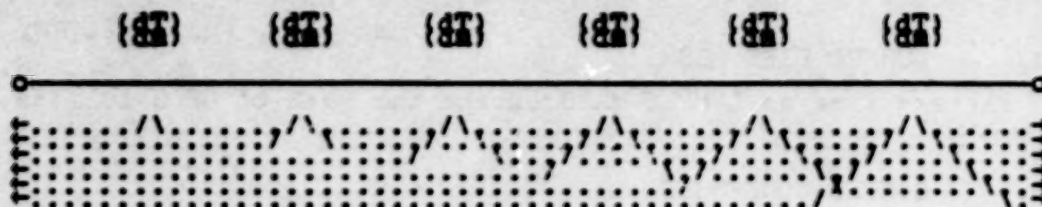


Figure 4

Scheme 4A. TRANSLATIONAL & ROTATIONAL COUPLING FINE MESH

Pattern the same as TRANSLATIONAL & ROTATIONAL COUPLING except that the mesh of GP's is fine.

Scheme 4B. TRANSLATIONAL & ROTATIONAL COUPLING CONDENSED

Pattern the same as TRANSLATIONAL & ROTATIONAL COUPLING FINE MESH except that the fine mesh is condensed to coarse.

The modeling schemes will be applied to one beam of circular cross-section and to another of rectangular cross-section. In order to maintain the results as comparable as possible, the same eigenvalue extraction method was used wherever possible. GIVENS method was used for all runs except two, where INVPWR was substituted when GIVENS had difficulty. The results are shown in tabular form. But before the results are discussed, the subject of coupled mass will be taken up. John Archer (2) made a huge contribution to our field with his consistent mass method of modeling mass in finite elements. He took the arbitrariness out of apportioning of mass into finite elements. He operated on the premise that any particle of mass located between the end points of a span had an influence in dynamics on both connecting points. He very cleverly said that the dynamic deformation in bending can be reasonably approximated by the static deformation in bending, under loading conditions that matched those

used during the determination of the stiffness terms. Thus the phrase consistent seemed appropriate. But the cleverest part of his scheme was his method of vectoring the interior contributions to the connecting points. He appealed to Maxwell's Reciprocity Law in the particular form popularly known in Civil Engineering circles as the Mueller-Breslau principle of influence lines. Graphically, here is how it works. Impose a boundary deformation that is used for the stiffness matrix for example a unit transverse deformation at end B and solve for the deformation at all interior points, while holding displacements at all other connecting degrees of freedom to zero.

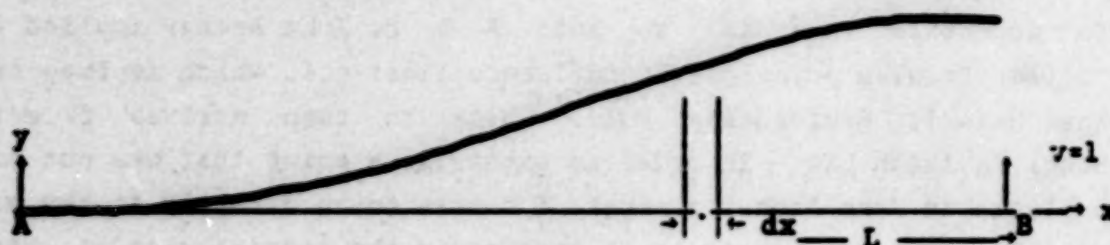


Figure 5

The non-dimensionalized equations for displacement and slope are

$$v(x) = 3 \left(\frac{x}{L}\right)^2 - 2 \left(\frac{x}{L}\right)^3, \quad \theta(x) = \frac{6}{L} \left[\frac{x}{L} - \left(\frac{x}{L}\right)^2 \right].$$

Now assume that $v(x)$ represents the amplitude of the acceleration at any location x along the beam.

$$\ddot{acc}(x) = v(x) \ddot{q}.$$

The increment of mass at x is $(\rho A dx)$. So the approximate increment of force produced by this assumed acceleration is

$$dF = (\rho A dx) v(x) \ddot{q}$$

Because the cross-section is constant, the density can be written as a linear density; i.e.

$$(\rho A) = \lambda.$$

The approximate increment of force at x due to transverse dynamic displacement at end B is

$$\delta F(B) = \lambda v(x) dx \ddot{q}.$$

To apportion $(\lambda v \ddot{q} dx)$ to ends A & B, John Archer applied the Mueller-Breslau principle of influence lines (3), which derives from the Maxwell Reciprocity Rule, which in turn derives from the Betti/Rayleigh Law. In order to emphasize a point that was not made explicit in John Archer's paper, I choose to go directly to the Maxwell Reciprocity Theorem as it applies in the special case of beams under concentrated loads. It says that if a beam is loaded with two different sets of loads and constraints, F_1 and F_2 , and the response to these respective loads are u_1 and u_2 , the work done by the first set of loads acting through the second set of displacements is equal to the work done by the second set of loads acting through the first set of displacements (4).

$$F_1 \times u_2 = F_2 \times u_1.$$

The beam systems to which we will apply this law are as follows. The inertia load δP acting at x on a beam that is clamped at both ends and displaced a unit amount at end B. Label the displacement curve $v(x)$ and the curve of slopes $\theta(x)$.

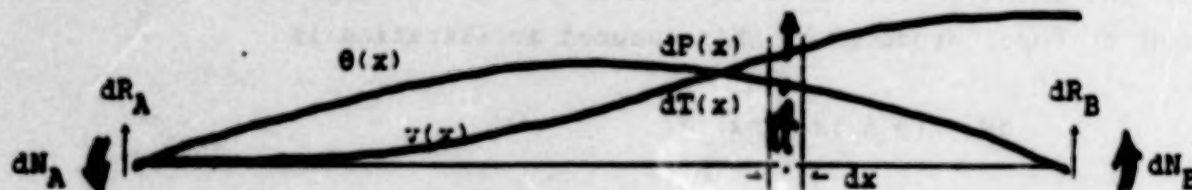


Figure 6

The other condition is for the beam to be displaced a unit amount at end A and all other displacements and rotations are held to zero. Label the displacement curve $\xi(x)$ and the curve of slopes $\phi(x)$.

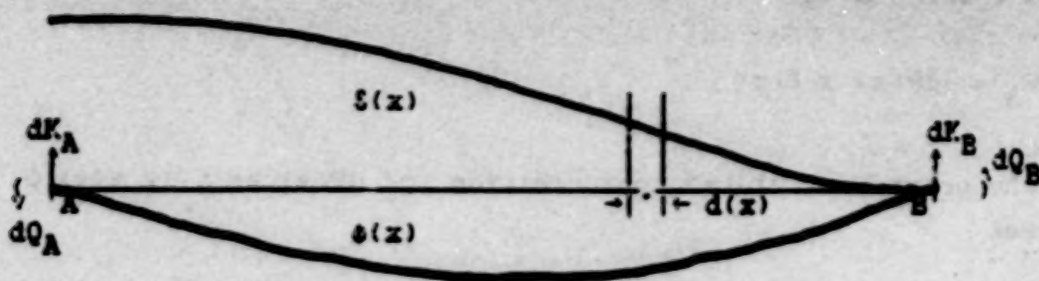


Figure 7

The nondimensionalized displacement and slope are calculated to be

$$\xi(x) = 1 - 3 \left(\frac{x}{L}\right)^2 + 2 \left(\frac{x}{L}\right)^3, \quad \phi(x) = -\frac{6}{L} \left[\frac{x}{L} - \left(\frac{x}{L}\right)^2\right].$$

Apply Maxwell's Law to the free bodies from A to x for this pair

$$\begin{aligned} dR_A \times \xi(0) + dP(x) \times \xi(x) + dN_A \times \phi(0) + dT(x) \times \phi(x) \\ = dK_A \times v(0) + dQ_A \times \theta(0). \end{aligned}$$

Substitute the boundary values

$$dR_A \times 1 + dP(x) \times \xi(x) + 0 + dT(x) \times \phi(x) = 0 + 0$$

This collapses to

$$dR_A = -dP(x) \times \xi(x) - dT(x) \times \phi(x).$$

Here $dT(x)$ is approximated in terms of sectional property I to be

$$dT(x) = (I \, dx) \, \theta(x) \, \ddot{\theta}.$$

Archer specialized the situation by considering the moment of inertia distribution $\int \delta(x) dx$ to be negligible; thus the increment of reaction at end A due to an increment of translational force at intermediate point x is

$$dR_A = -dP(x) x \delta(x)$$

Using the previously stated approximation for $dP(x)$ as $\lambda dx v(x) \ddot{q}$, it becomes

$$dR_A = \lambda v(x) \delta(x) \ddot{q} dx.$$

If dR_A is assumed to be made of an incremental inertia term dM_A being accelerated through coordinate q , the equation can be written as

$$dR_A = dM_A \ddot{q} = \lambda \left[x(x) \delta(x) \right] dx \ddot{q}.$$

The total inertial reaction from incremental contributions over the whole beam is obtained by integrating over the length L .

$$M_A = \lambda \int_0^L v(x) \delta(x) dx.$$

So, for our example case, letting λL equal the total mass m of the beam,

$$M_{A,B} = \lambda \int_0^L \left[1 - 3\left(\frac{x}{L}\right)^2 + 2\left(\frac{x}{L}\right)^3 \right] \left[3\left(\frac{x}{L}\right)^2 - 2\left(\frac{x}{L}\right)^3 \right] dx = 22 \frac{\lambda L^2}{420} = \frac{22L}{420} m.$$

In words, this term represents the amount of mass that couples to the y translational dof at end A due to a dynamic displacement of the y translational dof at end B. This is the pattern of analysis

that is used to develop the bending terms in the 12×12 coupled translational mass matrix. Turning to similar coupling for axial (longitudinal) deformation, the shape functions are modified from pure static deformation. No coupling is provided for torsion, because relationships between 2nd area moments in the KGG matrix and 2nd mass moments in the KGG matrix are highly variable for torsion. The total translational coupled mass for a bar is shown on page 8.2-22 of the Programmer's Manual which for convenience is duplicated below.

$$[M^0] = \frac{m}{420} \begin{bmatrix} 175 & 0 & 0 & 0 & 0 & 0 & 35 & 0 & 0 & 0 & 0 & 0 \\ & 156 & 0 & 0 & 0 & 221 & 0 & 54 & 0 & 0 & 0 & -134 \\ & & 156 & 0 & -221 & 0 & 0 & 0 & 54 & 0 & 134 & 0 \\ & & & 0 & 0 & 0 & 0 & 0 & 0 & 0 & 0 & 0 \\ & & & & 41^2 & 0 & 0 & 0 & -134 & 0 & -31^2 & 0 \\ & & & & & 41^2 & 0 & 134 & 0 & 0 & 0 & -31^2 \\ \hline & & & & & & 175 & 0 & 0 & 0 & 0 & 0 \\ & & & & & & & 156 & 0 & 0 & 0 & -221 \\ & & & & & & & & 156 & 0 & 221 & 0 \\ & & & & & & & & & 0 & 0 & 0 \\ & & & & & & & & & & 41^2 & 0 \\ & & & & & & & & & & & 41^2 \end{bmatrix}$$

SYN

where

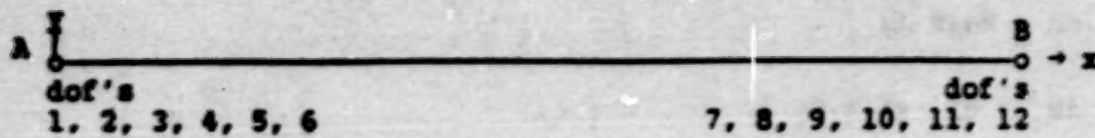
$$m = (\rho A + \mu) l$$

Figure 8

One of the main purposes of this paper is to explore the significance of the moment terms that Archer de-emphasized. I use this word advisedly, because Archer states his general formula in 3 dimensions, but he applies it to only translational inertia in one dimension. The general formula is

$$m_{ij} = \int_{Vol} m(x,y,z) \gamma_i(x,y,z) \gamma_j(x,y,z) d Vol.$$

Note the density "m" is written as varying in 3 dimensions and so are the two shape functions γ_i and γ_j . I was encouraged on the basis of this generality to enquire as to the contributions from distributions of mass over the cross-section. Why bother to investigate these details? Well, I was provoked into this inquiry when I was concentrating on a related topic. I was wrestling with the problem of finding a logical analytical approach to the mass properties of non-prismatical beams when modeling with equivalent bars. I frequently referred to the mass matrix. I was startled by the mass matrix which was generated with the coupled mass option for a bar with a rectangular cross-section. The moments of inertia for bending about both transverse axes were the same. I checked the theoretical manual. The formula there did not discriminate by axis. I checked John Archer's paper and the formula he published matched that in the theoretical manual. I checked the Programmer's Manual for the algorithm actually used for the BAR element. It did not discriminate either. I went back to John Archer's paper and studied it very hard. Non-prismatical beams should be much more sensitive to transverse variations of mass, so I had the incentive to explore Archer's general equation further. But, the translational case brought such startling improvements over the lumping practices of the times of the early 60's that there was no immediate incentive to explore coupled mass properties for terms other than translational. I proceeded in the same spirit that Archer used. The shape function for the slope of the static deformation would be used as the dynamic approximation to the amplitude of the rotational acceleration at a point. This required that the slope functions as well as displacement functions for the solutions of the Bernoulli-Euler beam would both have to be catalogued. They are shown in Figure 9.



$$v_2 = 1 - 3\left(\frac{x}{L}\right)^2 + 2\left(\frac{x}{L}\right)^3$$

$$v_8 = 3\left(\frac{x}{L}\right)^2 - 2\left(\frac{x}{L}\right)^3$$

$$\theta_2 = -\frac{6}{L}\left[\frac{x}{L} - \left(\frac{x}{L}\right)^2\right]$$

$$\theta_8 = \frac{6}{L}\left[\frac{x}{L} - \left(\frac{x}{L}\right)^2\right]$$

$$v_3 = 1 - 3\left(\frac{x}{L}\right)^2 + 2\left(\frac{x}{L}\right)^3$$

$$v_9 = 3\left(\frac{x}{L}\right)^2 - 2\left(\frac{x}{L}\right)^3$$

$$\theta_3 = -\frac{6}{L}\left[\frac{x}{L} - \left(\frac{x}{L}\right)^2\right]$$

$$\theta_9 = \frac{6}{L}\left[\frac{x}{L} - \left(\frac{x}{L}\right)^2\right]$$

$$v_5 = -x + 2\frac{x^2}{L} - \frac{x^3}{L^2}$$

$$v_{11} = \frac{x^2}{L} - \frac{x^3}{L^2}$$

$$\theta_5 = -1 + 4\frac{x}{L} - 3\left(\frac{x}{L}\right)^2$$

$$\theta_{11} = 2\frac{x}{L} - 3\left(\frac{x}{L}\right)^2$$

$$v_6 = x - 2\frac{x^2}{L} + \frac{x^3}{L^2}$$

$$v_{12} = -\frac{x^2}{L} + \frac{x^3}{L^2}$$

$$\theta_6 = 1 - 4\frac{x}{L} + 3\left(\frac{x}{L}\right)^2$$

$$\theta_{12} = -2\frac{x}{L} + 3\left(\frac{x}{L}\right)^2$$

Figure 9

Now we are ready to develop the rotational coupling inertia terms. The contribution to the end reactions due to an incremental moment

can be written according to the Maxwell equation for concentrated loads on a beam as

$$dR_1 = dT_j(x) \times \theta_1(x) \quad \text{where,}$$

$$dT_j = \rho I_j \theta_j \ddot{q} \quad \text{and,}$$

$$dR_1 = dM_{1j} \ddot{q} \quad \text{====>} \quad dM_{1j} \ddot{q} = (\rho I_j \theta_j dx) \theta_1 \ddot{q}.$$

Integrate all increments over the entire length of the beam with the appropriate slope functions taken from the listings in Figure 9, to obtain the expression for rotational coupling inertia at end j due to an acceleration of end i. Density and Sectional area moment are constant over the length. The matrix for all i and j then follows.

$$M_{1j} = \rho I_j \int_0^L \theta_1(x) \theta_j(x) dx.$$

	x_A	y_A	z_A	θ_A	ϕ_A	ψ_A	x_B	y_B	z_B	θ_B	ϕ_B	ψ_B
x_A												
y_A		$\frac{36}{L} I_{yy}$				$3I_{zz}$		$-\frac{36}{L} I_{zz}$				$3I_{zz}$
z_A			$\frac{36}{L} I_{yy}$	$-3I_{yy}$					$-\frac{36}{L} I_{yy}$	$-3I_{yy}$		
θ_A												
ϕ_A			$-3I_{yy}$	$4I_{yy}L$					$3I_{yy}$	$-I_{yy}L$		
ψ_A												
x_B						$4I_{zz}L$		$-3I_{zz}$				$-I_{zz}L$
y_B		$-\frac{36}{L} I_{zz}$				$-3I_{zz}$		$\frac{36}{L} I_{zz}$				$-3I_{zz}$
z_B			$-\frac{36}{L} I_{yy}$	$3I_{yy}$					$\frac{36}{L} I_{yy}$	$3I_{yy}$		
θ_B												
ϕ_B			$-3I_{yy}$	$-I_{yy}L$					$3I_{yy}$	$4I_{yy}L$		
ψ_B						$-I_{zz}L$		$-3I_{zz}$				$4I_{zz}L$

Figure 10

Notice that torsional and axial inertias are not addressed. This is consistent with Bernoulli-Euler theory which assumes no coupling between bending and torsion and between bending and axial. The intention of this development is to augment the mass matrix based on translational distributions; so it would not supplant the COUPMASS operation. It would be added to it. It is interesting to compare the matrix of translational coupling with rotational coupling term by term to gauge their relative importance. Importance will be based on comparing magnitudes of samplings of like terms, by using a rectangular cross-section to reflect the difference in roles about the two axes.

Let the height to breadth ratio $h/b = 3/1$. In order to put corresponding terms in the same dimensions, the various quantities will be written with rectangular factors substituted into the properties: i.e.

$$m = \rho AL = \rho bhL. \quad I_{zz} = \frac{bh^3}{12} \quad I_{yy} = \frac{hb^3}{12}$$

Term 2.2 Translational vs. Rotational

$$\frac{156}{420} m \quad \text{vs} \quad \frac{36\rho}{30L} I_{zz}$$

$$\frac{156}{420} \rho bhL \quad \frac{36\rho}{30L} \frac{bh^3}{12}$$

$$\frac{12}{60} (\rho bh) \frac{13L}{7} \quad \frac{12}{60} (\rho bh) \frac{3h^2}{4L}$$

Simplify by factoring the common coefficient. Then compare on the basis of a short beam ($L/h = 4$) and a long beam ($L/h = 12$).

$$\frac{13L}{7} \quad \text{vs} \quad \frac{3h^2}{4L} \quad \text{-----} \quad \frac{52}{21} \frac{L^2}{h^2} \quad \text{Short } 39.6 \text{ vs } 1. \quad \text{Long } 356.5 \text{ vs } 1.$$

Term 2,6 Translational vs Rotational

$$\frac{22L}{420} = (\rho b h L) \frac{22L}{420} \quad \text{vs} \quad \frac{3\rho}{30} I_{zz} = \frac{3\rho}{30} \frac{b h^3}{12}$$

$$\frac{11}{210} \frac{L^2}{b^2} \text{ vs } \frac{h^2}{120} \implies \frac{44}{7} \frac{L^2}{h^2} \text{ vs } 1. \quad \text{Short } 100.6 : 1. \quad \text{Long } 905.1 : 1.$$

Term 3,3 Translational vs Rotational

$$\frac{156}{420} = \frac{16}{35} \rho b h L \quad \text{vs} \quad \frac{36\rho}{30L} I_{yy} = \frac{36\rho}{30L} \frac{h b^3}{12} = \rho b h \frac{b^2}{10L}$$

$$\frac{26}{7} \frac{L^2}{b^2} \text{ vs } 1. \quad \text{Short } L/b = 12. \quad \text{Long } L/b = 36. \\ \text{Short } 534.8 : 1. \quad \text{Long } 4813.7 : 1.$$

Term 6,6 Translational vs Rotational

$$\frac{4L^2}{420} = \frac{L^2}{105} (\rho b h L) \quad \text{vs} \quad \frac{4\rho L}{30} I_{zz} = \frac{4\rho L}{30} \frac{b h^3}{12} = (\rho b h L) \frac{h^2}{90}$$

$$\frac{6}{7} \frac{L^2}{h^2} \text{ vs } 1. \quad \text{Short } 13.7 : 1. \quad \text{Long } 123.4 : 1.$$

The conclusions from these samplings is that for a typical beam cross-section, translational inertia coupling is 2 orders of magnitude more important than rotational inertia couplings for short beams, and for long beams is 3 orders of magnitude more important. I found these results amazing. I had pre-judged that when the distribution in one direction was markedly different from that in the other direction one would find the influence of the rotational coupling to be significant. One is comfortable with the idea that the sectional properties in the stiffness terms are limiting the non-dimensionalized deflections and thus are limiting the assumed translational accelerations. But the idea that the overhung moments of the translational masses should be the overriding influence vis-a-

vis the sum of all distributed inertias being accelerated in rotation by the beam slope leaves one uncomfortable. This result adds further commendation to the contribution of John Archer for providing us with so advanced a tool so early in the development of finite elements.

Experimental Results

Results of modeling for bending, axial, and torsion will be treated separately. Bending is discussed first. The most accurate method for simulating mass properties in bending modes is translational coupling. The rule for its use was stated by Archer in his original paper. One must employ one grid point more than the number of nodes for the mode associated with the highest frequency of interest. This is borne out by the data compiled from the NASTRAN runs for translational coupling modeled respectively with 2, 3, 4, and 11 points.

FREQUENCIES FOR FREE-FREE BENDING MODES MODELED WITH TRANSLATIONAL COUPLING CIRCULAR CROSS-SECTION

TIMOSHENKO	11 GRID POINTS	4 GRID POINTS	3 GRID POINTS	2 GRID POINTS
MODE FREQ	FREQ RATIO	FREQ RATIO	FREQ RATIO	FREQ RATIO
T2 874.92	874.97 1.00005	879.49 1.005	876.89 1.0023	1049.3 1.1993
T2 2411.68	2412.41 1.0003	2421.90 1.004	2744.40 1.1380	3584.2 1.3797
T2 4728.44	4732.45 1.00085	5465.33 1.156	.	.
T2 7815.6	7834.57 1.00242	.	.	.

*For a circular beam the modes in both transverse directions are the same, they are both being represented here by the notation T2 only.

RECTANGULAR CROSS-SECTION

TIMOSHENKO	11 GRID POINTS	4 GRID POINTS	3 GRID POINTS	2 GRID POINTS
MODE FREQ	FREQ RATIO	FREQ RATIO	FREQ RATIO	FREQ RATIO
T2 505.14	505.16 1.00005	507.77 1.005	506.27 1.0022	605.8 1.20
T2 1392.39	1392.80 1.00030	1398.28 1.004	1584.48 1.1379	2069.3 1.48
T3 1515.42	1515.49 1.00005	1523.32 1.005	1518.82 1.0022	1817.5 1.20
T2 2729.97	2732.28 1.00085	3155.40 1.156	3962.00 1.451	.
T3 4177.15	4178.40 1.00030	4194.85 1.004	4753.43 1.138	6207.9 1.486
T2 4512.35	4523.28 1.00240	5361.27 1.188	.	.

In the two point model of the beam of circular section, the frequency for the fundamental mode, which has 2 nodes, computes to only 20% of the correct value. In the three point model, the frequency of the fundamental is correct to 0.2%, but the 2nd bending mode, which has three nodes, computes to only 14% of the correct

value. In the four point model, the fundamental and 2nd bending modes are accurate to within 0.5%, but the 3rd bending mode, which has four nodes, computes to only 16% of the correct value. In the 11 point model, all frequencies for bending modes through the 9th are accurate to within 0.5%, but the tenth mode, which has eleven nodes is accurate to only 15%.

A similar pattern of accuracy evolves for the rectangular cross-section as for the circular beam for any one type of bending mode. Following the T2 modes to higher and higher harmonics shows that the 2 point model is not adequate, but as soon as one more point is added, the fundamental for the 3 point model gives 0.2% accuracy. That same pattern appears in following the T3 modes. Likewise the pattern of accuracy for the 4 point model follows the circular results taken one type of mode at a time.

Does this complete the discussion of modeling of mass for beams? It would if the only consideration were accuracy. The cost in manpower is in calculating the sectional properties and in preparing the PBAR cards and a PARAM COUPMASS card. Computer time would be considerable. Because the density of coupled mass matrices of a pure series BAR model is 4% per 102 rows compared to 1% per 102 rows for the oft-used diagonal matrix or to 0.5% per 102 rows for the scalar mass created by default from PBAR cards. If condensation is used to reduce the order of the analysis set, the density of matrices is further increased. Computer cost could decline due to smaller order, but it could increase from being condensed to higher density; what the net may become will depend on the connectivity of the model (assuming that the model is other than a pure series beam). A logical next question deals with the effect that condensing has on the accuracy of the model. If one made all the right decisions for the beams in his model and then was confronted with the necessity to condense to small order, will condensing degrade the model--or to put it another way, what things must be held sacred against omitting so as to preserve a model's functional integrity. A series of runs were made in which the 11 point model with translational coupling were condensed to 2, 3, & 4 grid points.

ORIGINAL PAGE IS
OF POOR QUALITY

CONDENSATION EFFECT ON CIRCULAR BAR MODELED WITH TRANSLATIONAL MASS COUPLING

TIMOSHENKO	11 GRID POINTS	11 TO 4 GP's	11 TO 3 GP's	11 TO 2 GP's
MODE FREQ	FREQ RATIO	FREQ RATIO	FREQ RATIO	FREQ RATIO
T2 874.92	874.97 1.00005	879.49 1.005	876.89 1.0023	1049.3 1.120
T2 2411.68	2412.41 1.0003	2421.90 1.004	2744.40 1.138	3584.2 1.38
T2 4728.44	4732.45 1.00085	5465.33 1.156	.	.
T2 7815.6	7834.57 1.00242			

CONDENSATION OF RECTANGULAR BAR MODELED WITH TRANSLATIONAL MASS COUPLING

TIMOSHENKO	11 GRID POINTS	11 TO 4 GP's	11 TO 3 GP's	11 TO 2 GP's
MODE FREQ	FREQ RATIO	FREQ RATIO	FREQ RATIO	FREQ RATIO
T2 505.14	505.16 1.00005	483.21 1.005	482.02 1.002	573.74 1.135
T2 1392.39	1392.80 1.00030	1253.79 1.004	1408.13 1.140	1780.03 1.278
T3 1515.42	1515.49 1.00005	1507.78 1.005	1503.41 1.002	1805.78 1.192
T2 2729.97	2732.28 1.00085	2559.19 1.156	3045.98 1.450	.
T3 4177.15	4178.40 1.00030	4070.93 1.004	4620.92 1.140	.
T2 4512.35	4523.28 1.00240	3886.84 1.188	4316.92 .	.

Note that so long as enough degrees of freedom are retained for a mode in the beam of circular section, the frequency degrades only by a few tenths of a percent with condensation. Note also that the accuracy of the frequency degrades markedly (jumps of 20%) when condensation leaves insufficient dof's in the model. Exactly the same kinds of observations can also be for the beam of rectangular cross-section, if one views bending in a given direction as a class. Now we can generalize by saying that translational coupling gives precisely the same results out to five places for all modes in a given class. More importantly, we observe that for any bending class for any prismatical beam, the accuracy of a coarse mesh is exactly the same as that for starting with a fine mesh and condensing to a mesh of like coarseness. A single table can summarize the results for mass modeled with translational coupling for all beams.

MODAL ACCURACY VS. MESH FOR BARS MODELED WITH TRANSLATIONAL MASS COUPLING

MODE	11 GP's	4 GP's	3 GP's	2 GP's
1ST	1.00005	1.005	1.0023	1.120
2ND	1.0003	1.004	1.138	1.380
3RD	1.00085	1.156		
4TH	1.00242			

Turn now from the ideal to the more traditional ways to model mass. The lazy approach is to invest no more time to model mass than to make an entry for density (RHO) on the material card. In so

doing the user depends on all of NASTRAN default conditions to take over. The mass matrix will have only scalar terms on the diagonal positions of translation dof's. If he does not condense and uses GIVENS method for eigenvalue extraction, he must provide an ASET1 card specifying dof's 1,2, & 3 for all Grid Points in order to remove the singularities from the rotational dof's of the mass matrix. In this case it becomes extremely important to have a fine mesh. A series of runs were made with increasingly fine mesh from 2, 3, 4, 5, 6, and 11. These models included these properties on the PBAR card: A, I1, & I2. J was omitted. No DMI nor CONM2 cards were used. A value was inserted for RHO on the MAT1 card and ASET1 was set to 123 for all Grid Points.

The results of these runs are shown in the following table.

FREQUENCIES FOR FREE-FREE BEND MODES MODELED WITH SCALAR MASS ONLY 3DOF/PT
CIRCULAR CROSS-SECTION

TIMOSHENKO	11 GP'S	6 GP'S	5 GP'S	4 GP'S	3 GP'S	2 GP'S
MODE FREQ	RATIO	RATIO	RATIO	RATIO	RATIO	RATIO
T2 874.92	0.97017	0.892	0.775	2.908	1.239	3.097
T2 2411.68	0.95086	0.838	0.745	.	.	.
T2 4728.44	0.93295	0.796
T2 7815.6	.	0.734	0.555	.	.	.

RECTANGULAR CROSS-SECTION

TIMOSHENKO	11 GRID POINTS	4 GRID POINTS	3 GRID POINTS	2 GRID POINTS
MODE FREQ	FREQ RATIO	FREQ RATIO	FREQ RATIO	FREQ RATIO
T2 505.14	490.07 0.9702	1468.93 2.908	625.72 1.239	1564.26 3.097
T2 1392.39	1248.10 0.8964	1534.08 1.102	.	.
T3 1515.42	1500.06 0.9898	4406.79 2.909	1877.11 1.239	.
T2 2729.97	2273.90 0.8329	.	.	.
T3 4177.15	4054.33 0.9706	.	.	.
T2 4512.35	3456.05 0.7659	.	.	.

For the models with only 2, 3, or 4 GP's the fundamental was not the lowest elastic mode. Some of the spurious modes had frequencies that one might expect in the range of the true modes; consequently one can be easily misled by coarse models with scalar mass. The frequencies of the true modes are off not by percentages but by factors as high as 3. But when the mesh is fine enough, frequencies accurate to within 5% are obtainable. Thus we do not sneer at this method. We say this can be quite useful for quick and dirty investigations of tentative designs especially in this day and age

ORIGINAL PAGE IS
OF POOR QUALITY

of CAD preprocessors for generating the models where it is simple to specify a fine mesh. Scalar mass modeling can be characterized by the girl with the curl in the nursery rhymes. "When she was good, she was very, very good; and when she was bad she was awful." The rule of thumb for avoiding awful results is to have from 6 to 10 more GP's than the number of nodes in the highest mode of interest.

But there is a remarkably good side to Scalar modeling, as well. This comes about from condensing. A series of runs were made in which the 11 point Scalar model was condensed to 2, 3, & 4 GP's. The one added feature however is that the ASET dof's were set to 5 instead of 3. Only torsion was omitted. In the Guyan reduction the stiffness matrix acts as a template for the condensation of mass. If the stiffness matrix has terms corresponding to rotational degrees of freedom, i.e. terms based on I1 and I2, it will cause coupling in the mass matrix such that terms in the rotational positions will also appear.

EFFECT OF CONDENSATION ON SCALAR MASS MODELS RETAINING 5 DOF/GP CIRCULAR CROSS-SECTIONS

TIMOSHENKO	11 GRID POINTS	11 - 4 POINTS	11 - 3 POINTS	11 - 2 POINTS
MODE FREQ	FREQ RATIO	FREQ RATIO	FREQ RATIO	FREQ RATIO
T2 874.92	848.83 0.97017	952.78 0.975	850.53 0.9721	1001.0 1.144
T2 2411.68	2293.17 0.95086	2301.19 0.954	2579.81 1.07	3192.9 1.324
T2 4728.44	4411.44 0.93295	5039.87 1.066	.	.
T2 7815.6

RECTANGULAR CROSS-SECTIONS

TIMOSHENKO	11 GRID POINTS	11 - 4 POINTS	11 - 3 POINTS	11 - 2 POINTS
MODE FREQ	FREQ RATIO	FREQ RATIO	FREQ RATIO	FREQ RATIO
T2 505.14	490.07 0.9702	492.35 0.975	491.05 0.972	577.93 1.144
T2 1392.39	1248.10 0.8964	1328.59 0.954	1489.45 1.07	1843.41 1.324
T3 1515.42	1500.06 0.9898	1477.05 0.975	1473.16 0.972	1733.79 1.144
T2 2729.97	2273.90 0.8329	2909.77 1.066	3368.46 1.234	.
T3 4177.15	4054.33 0.9706	3985.77 0.954	4468.36 1.07	.
T2 4512.35	3456.05 0.7659	4858.28 1.077	.	.

In condensing to two dof's the frequency for the fundamental is still not good, missing the correct value by 14%, but this is a distinct improvement over the single span ratio of 3. In fact it ranks with other single span models with initially more complete

mass inputs. Condensing to three points gives good results for the fundamental and a fair 10% ratio for the circular and a better 7% for the two rectangular 2nd bending modes. Condensing to four points give acceptable results out through the 4th bending mode.

A happy observation can be made here, to wit: if the initial modeling was made fine enough to give good results in a mode, that accuracy is maintained during condensation so long as the final mesh retains at least one grid point more than the number of nodes in the highest mode of interest.

The scheme that was considered to be sophisticated compared to scalar modeling before consistent mass was available for use was the lumping into 6x6 matrices at each point. The scheme is to take an arbitrary amount of mass surrounding the point and assign it and all of its distribution properties to just one point. For instance in a single span beam, one-half of the mass would be consigned to each end point and its center of gravity would be designated to be inboard from each end by one quarter of the length. It is incumbent on the user to supply 8 pieces of information about the mass for each grid point. Total mass, location of the center of gravity with respect to the parent grid point, and moments and products of inertia with respect to the center of gravity. With symmetrical beams such as the circular beam being run in these examples, this amounts to the three diagonal terms of moments of inertia, mass, and x-offset of the center of gravity. In our case the lumped mass matrix would be assembled internally in NASTRAN to look as follows.

$$\begin{array}{cccccc}
 m/2 & 0 & 0 & | & 0 & 0 & 0 \\
 0 & m/2 & 0 & | & 0 & 0 & \frac{m}{2} \bar{x} \\
 0 & 0 & m/2 & | & 0 & -\frac{m}{2} \bar{x} & 0 \\
 \hline
 0 & 0 & 0 & | & I_{xx} & 0 & 0 \\
 0 & 0 & -\frac{m}{2} \bar{x} & | & 0 & I_{yy} & 0 \\
 0 & \frac{m}{2} \bar{x} & 0 & | & 0 & 0 & I_{zz}
 \end{array}$$

Data is supplied on a CONN2 card and NASTRAN assembles it into the local matrix as shown above. A series of runs were made in which lumped matrices were supplied for a single span bar, double span, triple span, and ten-span bars. No mass was formed with PEAR's, but only with CONN2's. The results are in the following table.

FREQUENCIES FOR FREE-FREE MODES MODELED WITH LUMPED MASS
CIRCULAR CROSS-SECTION

TIMOSHENKO	11 GRID POINTS	4 GRID POINTS	3 GRID POINTS	2 GRID POINTS
MODE FREQ	FREQ RATIO	FREQ RATIO	FREQ RATIO	FREQ RATIO
T2 874.92	857.45 0.9800	787.50 0.900	764.14 0.8734	533.9 0.6102
T2 2411.68	2292.15 0.9504	1842.91 0.764	1510.17 0.6262	SPUR. .
T2 4728.44	4312.48 0.9120	2130.72 0.4506
T2 7815.6

RECTANGULAR CROSS-SECTION

TIMOSHENKO	11 GRID POINTS	4 GRID POINTS	3 GRID POINTS	2 GRID POINTS
MODE FREQ	FREQ RATIO	FREQ RATIO	FREQ RATIO	FREQ RATIO
T2 505.14	480.95 0.9521	442.67 0.876	431.03 0.853	299.66 0.593
T2 1392.39	1248.10 0.8964	1038.64 0.746	826.21 0.593	303.01 0.218
T3 1515.42	1500.06 0.9898	1376.55 0.908	1323.52 0.873	933.90 0.616
T2 2729.97	2273.90 0.8329	1686.38 0.618	1101.49 0.403	. .
T3 4177.15	4054.33 0.9706	3216.82 0.770	2634.75 0.631	. .
T2 4512.35	3456.05 0.766	1819.99 0.403	1113.13 0.247	. .

Note that even with an 11 point model the best accuracy that can be obtained is for the fundamental frequency and it varies from 1% for the stiffer rectangular to 2% for the circular and 5% for the softer rectangular. The 2nd bending frequency is accurate to 3% for the stiffer rectangular to 5% for the circular and only 10% for the softer rectangular. The 3rd bending frequency is within 9% for the circular but is off by 17% for the softer rectangular. The 4th bending is off by 14% and 23%. The 2 point models introduce spurious modes and miss the fundamental by 40%. The 3 point models give no spurious modes but are off the mark by 13% on the fundamental, by 38% on the frequency for 2nd bending and by 55% on that for 3rd bending. The 4 point models give only fair results for the fundamental frequency--within 10%-- and poor for the rest.

Now the question is, there are times when the nature of the structure is such that lumped mass is the only practical thing available to the analyst, so can the situation improve with condensation?

EFFECT OF CONDENSATION ON BARS MODELED WITH LUMPED MASS CIRCULAR CROSS-SECTION

TIMOSHENKO	11 GRID POINTS		11 TO 4 GP's		11 TO 3 GP's		11 TO 2 GP's	
MODE FREQ	FREQ	RATIO	FREQ	RATIO	FREQ	RATIO	FREQ	RATIO
T2 874.92	857.45	0.9800	861.76	0.985	859.36	0.982	1029.6	1.1769
T2 2411.68	2292.15	0.9504	2301.71	0.954	2604.86	1.080	3386.86	1.4044
T2 4728.44	4312.48	0.9120	4929.05	1.042	6192.49	1.296	.	.
T2 7815.6	.	.	7843.33	1.004	9071.65	1.161	.	.

RECTANGULAR CROSS-SECTION

TIMOSHENKO	11 GRID POINTS		11 TO 4 GP's		11 TO 3 GP's		11 TO 2 GP's	
MODE FREQ	FREQ	RATIO	FREQ	RATIO	FREQ	RATIO	FREQ	RATIO
T2 505.14	480.95	0.9521	483.21	0.956	482.02	0.954	573.74	1.135
T2 1392.39	1248.10	0.8964	1253.79	0.900	1408.13	1.011	1780.03	1.278
T3 1515.42	1500.06	0.9898	1507.78	0.995	1503.41	0.992	1905.78	1.192
T2 2729.97	2273.90	0.8329	2559.19	0.937	3045.98	1.116	.	.
T3 4177.15	4054.33	0.9706	4070.93	0.975	4620.92	1.106	6080.22	1.456
T2 4512.35	3456.05	0.766	3886.84	0.862	4316.93	0.957	.	.

Condensation improves the performance of lumped mass modeling by a fraction of a percent, so long as there are sufficient dof's for a nodal pattern. In the higher modes the overshooting of the frequency from too few dof's tends to have a beneficial effect to counteract the overconcentration of mass. For instance in the 11 to 4 point condensation the 3rd and 4th modes are within 4% and 0.4% respectively. The fundamental can be found to within 1% when sufficient dof's are retained. Once again the stiffer modes perform better than the softer ones. The three point model shows consistency in good behavior into harmonics higher than expected.

When I started this project, I thought that what I'm now about to present should be saved till last because it was supposed to be the climax. Well, it is more appropriate to characterize what I'm about to present as re-enforcing the adage "If it ain't broke, don't fix it." I knew that translational coupling was good, but I never looked closely at how it compared with theory. Consequently, when I discovered that when Archer applied the Maxwell Reciprocity to the beam, he omitted the rotational terms, I thought I could contribute to the effectiveness of the coupled mass approach. Here are the "complete" results. A series of runs were made in which the mass matrix was composed of the sum of contributions from translational coupling and rotational coupling. Timoshenko inferred that refinements would be beneficial to the higher modes when rotary inertia

was included, so it was in the higher modes that I had expected to see proof of this notion. The models were composed of 11, 4, 3, and 2 points. Results are tabulated below.

FREQUENCIES FOR FREE-FREE MODES MODELED WITH TRANS & ROTN COUPLING CIRCULAR CROSS-SECTION

TIMOSHENKO	11 GRID POINTS		4 GRID POINTS		3 GRID POINTS		2 GRID POINTS	
MODE FREQ	FREQ	RATIO	FREQ	RATIO	FREQ	RATIO	FREQ	RATIO
T2 874.92	861.74	0.9849	866.04	.990	863.59	.987	1030.2	1.177
T2 2411.68	2334.10	0.9678	2343.07	0.972	2649.22	1.098	3409.83	1.414
T2 4728.44	4477.47	0.9469	5144.51	1.088	6306.74	1.334	.	.
T2 7815.6	7216.31	0.9233	8494.81	1.088	9791.12	1.253	.	.
T 11675.78	10483.74	0.8970

RECTANGULAR CROSS-SECTION

TIMOSHENKO	11 GRID POINTS		4 GRID POINTS		3 GRID POINTS		2 GRID POINTS	
MODE FREQ	FREQ	RATIO	FREQ	RATIO	FREQ	RATIO	FREQ	RATIO
T2 505.14	483.20	0.9566	485.47	0.961	484.21	0.959	574.39	1.137
T2 1392.39	1268.73	0.9119	1273.50	0.915	1434.58	1.030	1805.32	1.297
T3 1515.42	1507.54	0.9948	1515.44	1.000	1511.03	0.997	1806.25	1.192
T2 2729.97	2350.22	0.861	2680.70	0.982	3186.08	1.398	.	.
T3 4177.15	4130.85	0.9898	4147.84	0.993	4696.57	1.124	.	.
T2 4512.35	3651.26	0.8092	4259.93	0.944	4791.08	1.062	.	.

Instead of producing an improvement, the added terms from rotational coupling depressed the frequencies such that none came closer than 2 orders of magnitude of those with only translational coupling. The higher modes, instead of being improved with order number got worse. The frequency of the fifth bending mode came no closer than 10%. The two point combination was 2% better than the two point translational coupling model. Neither was good. The excellent performance of the translational 3 and 4 point models of holding to within a fraction of a percent was violated by adding rotational coupling by several percentage points. A more appropriate test seemed to be one involving a beam of unequal moments of inertia such as a beam with a rectangular cross-section. Even here the translational alone matched within a few tenths of a percent while the combination with rotational coupling was off by 1% in the stiffer direction and by 4% in the limber direction. Condensing gave the same results as the coarser models. So it can be concluded that rotational coupling of mass is not only not helpful, it is harmful to the coupling method of modeling mass.

Axial Modes

There are only two methods available for modeling mass in the longitudinal axis of the beam. Lumping or coupling. Axial lumping puts all terms on the diagonal. Lumping by default to the PEAR card puts the center of gravity of the lumped mass at the Grid Point while lumping using CONM2 input allows the user to assign the center of gravity to a logical position. But it will be shown in the example runs later that shifting the center of gravity along the centroidal axis has no effect on axial modes. Only the fundamental axial frequency will be compared against the two methods of modeling. Runs were made with 11, 6, 5, 4, 3, and 2 points along the beam. Their results are shown below.

AXIAL MODES OF CIRCULAR BEAM. FUNDAMENTAL AXIAL MODE FREQUENCY FROM TIMOSHENKO 4914.57

	LUMPED		COUPLED	
# GP	FREQ	RATIO	FREQ	RATIO
11	4894.06	0.9959	4914.16	0.99998
6	4869.39	0.9908	4912.64	0.9996
5	4833.82	0.9836	4978.61	1.0131*
4	4546.16	0.925	4797.99	0.976
3	4424.39	0.9003	4846.67	0.9862
2	3128.52	0.6366	3831.63	0.7797

* This anomaly seems to have been caused by modeling 3 points close together in the middle, instead of spacing the points evenly.

One can reason that axial modes for prismatical beams should be independent of shape of the cross-section, so long as Poisson effects are not taken into account, thus it will suffice to study axial mass modeling with a circular section. Comparing the fine mesh models for scalar, lumping, or translational coupling indicates that just breaking the longitudinal mass into small pieces and distributing them amongst elastic elements has a beneficial effect. All three fine mesh models yield results within 0.5% of The fundamental frequency. So the question to be answered is "How fine is fine?" Starting at the extreme of a single span puts all the mass at the ends with all of the elastic material in between. The frequency comes to only 64% of correct. A coupled mass model of a single span puts 5 parts out of 12 parts of the mass at either end and puts 2 parts into the coupling between the ends. This improves the frequency calculation to 78% accuracy. A double span lumped model

(3 GP) puts half the mass in the middle and one quarter at either end. The frequency calculation improves to 90%. A coupled mass model of a two span beam puts 5 parts in 24 at either end and 10 parts in 24 at the middle while 4 parts in 24 do the coupling. This brings the frequency to 98.5% of actual. Going next to a 3 span lumped model, $\frac{1}{6}$ of the mass is put at either end while $\frac{1}{3}$ of the mass is put at the two middle points. The frequency for this 4 point model is 92.5% accurate. This is now compared with a 3 span coupled model wherein 5 parts out of 36 are put at the end points; 10 parts out of 36 are assigned to each of the middle points and the remaining 6 parts are assigned to coupling between points. Here we lose ground a little achieving only 97.6% accuracy.

If one wants to achieve the same accuracy of staying within 0.5% in axial modeling as with bending, where the rule for meshes is 1 greater than the modal nodes, one must supply 5 more Grid Points than nodes in an axial mode for the coupled option and 7 more Grid Points than nodes in an axial mode for the lumped option.

The next question to ask is whether, if one modeled with the ideal number, one can preserve the accuracy if he were to condense to a coarser mesh? Data was gathered by condensing the 11 point models for lumped and coupled options to meshes of 2, 3, and 4 points.

EFFECT OF CONDENSATION ON AXIAL MODES OF CIRCULAR BEAM.
FUNDAMENTAL AXIAL MODE FREQUENCY FROM TIMOSHENKO 4914.57

COND AMT.	LUMPED		COUPLED	
	FREQ	RATIO	FREQ	RATIO
11-2	5365.34	1.0917	5391.85	1.097
11-3	5365.34	1.0917	5391.85	1.097
11-4	5048.91	1.0273	5070.99	1.032

Condensing the lumped model to 2 points degrades the axial fundamental frequency to 9% high. Strange to say adding one more point does not improve the accuracy one bit. Similarly condensing the coupled model to 2 and 3 points degrades the frequency to 10% high. A fourth point does improve the accuracy for both models to just 3% high. Condensing has a more drastic effect on the axial

mode than on the bending modes. Modeling with coupling has the advantage over lumped modeling here in that one does not need to model a fine mesh first to achieve 3% accuracy.

Torsion

The field is much more narrow when it comes to modeling the torsional mass in beams. No coupling algorithm is available, so all modeling is done by lumping. All of the data gathered from the runs on torsion can be presented in one table.

FUNDAMENTAL TORSIONAL MODE OF BEAMS WITH AND WITHOUT CONDENSATION TIMOSHENKO CIRCULAR FN 3009.36 RECTANGULAR FN 1787.58

GP	UNCONDENSED		CONDENSED		UNCONDENSED		CONDENSED	
	FREQ	RATIO	FREQ	RATIO	FREQ	RATIO	FREQ	RATIO
11	3035.19	1.009	.	.	1705.11	0.967	.	.
4	2819.39	0.937	3327.46	1.38	1583.89	0.889	1759.06	0.987
3	2743.90	0.912	3327.46	1.38	1541.47	0.865	1869.31	1.049
2	1940.23	0.645	3327.46	1.38	1089.98	0.612	1869.31	1.049

A fine mesh model gives accuracy to within 1% for circular and 3% for rectangular and it degrades slowly with $\frac{1}{3}$ mesh to 94% and 90% with $\frac{1}{4}$ mesh to 91% and 87%, but a single span gives a poor 64% and 61%. Condensing from an eleven point model to a coarser one has a uniformly degrading effect of 38% for circular, but has a uniformly beneficial effect for rectangular. Introducing the stiffness matrix into the condensation for rectangular sections has a different effect than circular sections in torsion because it couples according to a stiffer pattern than that through which the mass actually acts.

Grid Point Weight Generator

It might be well to examine the relationship of the mass properties computed by the GPWG module versus the character of the matrices MCG. GPWG computes the total mass of a structure, then employs a user specified reference point to locate the center of gravity and for computing the moments of inertia of the distribution of scalar mass throughout the structure. GPWG completely ignores any moments of inertia that are supplied to the individual grid points

of the MGG matrix. Therefore GPWG will report moments of inertia for a model which has absolutely no rotational degrees of freedom. GPWG gives information about the mass in a structure when viewed as a rigid body, while MGG indicates how localized mass is modeled amongst the elastic elements of a model. It is a good idea in a study such as this one to include the GPWG in every run to ensure that the rigid body properties of every model is exactly alike to give assurance that the same structure is being treated in every run.

Summary of Beam Findings

If all we want to model is a beam or a beam-like structure we can form a few guide lines that can serve us well. It is when we get to complex structures in which beams make up only a part that the rules are less clear cut. Start with just beam-like structures. We will separate the decision making into three parts. Even before anything else, start with the back of an envelope and a reference like Den Hartog (4) or Timoshenko. Determine the frequency range of interest. Next decide what accuracy would be suitable for the task at hand. Estimate the average properties of the beam-like structure. Use those averages in the formulas, which Den Hartog has so logically published, to find out how many harmonics in bending, in torsion, and in longitudinal fall into the frequency range of interest. Decide on the level of detail that you want to invest and the degree of accuracy you want to achieve in your analysis. If a structure is in the early stage of design, many elements may be sketchy so that the approach may be to use a generous number of grid points in a model with primitive properties, then condense it. Then for modeling the mass one would use the rules for a scalar model. For bending, condense to a number of grid points equal to one more than the number of nodes in the highest harmonic. For axial modes condense to a grid point count equal to the number of nodes in the highest harmonic plus 7. For torsion, try to have as many grid points in the original model to represent the highest torsional mode without condensing, because they are liable to be degraded.

If the object is to certify a design, one generally has a

generous number of points in his model in order to recover stresses. In such cases, condensation will probably result in the retention of a mesh of points that will appear as a fine mesh to the vibrational modes. It is well however that the highest torsional mode and the highest axial mode be represented by a margin of about ten grid points.

One is advised to limit the use of CONM2 modeling of mass to those situations where there is not other alternative. For example, a non-prismatical beam, or mounted equipment, or a non-native portion of structure. If CONM2 elements are used with a well defined elastic model, it would be advisable to condense it by several factors to improve the mass modeling.

Summary for General Mass Modeling

One should still be guided by the expected harmonic nodal pattern as to the minimum number of grid points to assign to a model. For complicated structures this is not easy to estimate. As a start one could isolate individual pieces such as beams, plates, shells, or solids. Idealize each piece into classical closed form solution types such as free-free, pin-clamped, etc. Consult reliable sources for the modes and frequencies of these classical individuals, such as Den Hartog or Leissa (5). Determine the largest nodal pattern in the assembly, then try to extrapolate the mutual stiffening effect after these pieces are joined for the influence on the nodal pattern. You will probably have an adequate number based on the estimates from individual pieces. After the vibration analysis has been run, examine the nodal pattern of the highest harmonics of each class to see if you are close to a change in sign at every grid point. If so, you may have provided too coarse a mesh for harmonics that couldn't be found. If there are several grid points between nodes of the highest harmonics, you can be assured of having provided a good margin for that mode. Be especially careful in using lumped modeling to guard against too few grid points to avoid spurious modes.

Conclusion

The modeling of mass for BAR elements has been reviewed based on the accuracy to which various schemes predict the frequencies of modes with free-free boundary conditions only. The stiffness of BARS did not include the elasticity due to shear deformation. Findings confirmed that modeling by translational coupling will give almost perfect results for bending by following the guide line of one more grid point than nodes of the highest mode. Condensation has only a slight degrading effect on frequency prediction of bending modes when modeling mass with translational coupling. Condensation has an immensely beneficial effect on the bending modes when modeling mass with the scalar option or with CONM2 elements. Condensation can be tolerated for prediction of axial modes if the margin of retained grid points to nodes in the highest harmonic is generous. Condensation has a uniformly degrading effect on torsional modes. The ground work has been laid for extending the study of mass modeling from exclusively prismatical beams to non-prismatical beams. It was found that mass modeling by translational coupling cannot be improved upon by including rotary inertia coupling.

References:

1. John S. Archer, "CONSISTENT MASS MATRIX FOR DISTRIBUTED MASS SYSTEMS". Journal of the Structural Division, Proceedings of the American Society of Civil Engineers, Vol 89, No. ST4, August 1963, pp 161-178.
2. S. Timoshenko, "VIBRATION PROBLEMS IN ENGINEERING", D. Van Nostrand Company, Inc.
3. John B. Wilbur and Charles H. Norris, "ELEMENTARY STRUCTURAL ANALYSIS", McGraw-Hill Book Company, Inc.
4. J. P. Den Hartog, "MECHANICAL VIBRATIONS", McGraw-Hill Book Company, Inc.
5. Arthur W. Leissa, "VIBRATION OF PLATES", NASA SP-160.

THE USE OF NASTRAN
IN THE
DESIGN OF WIND TUNNEL RESEARCH AIRCRAFT

Michael Cooper
Dynamic Engineering, Inc.

SUMMARY

Trends toward more severe test environments and increased demand for test data have resulted in the need for more sophistication in the analysis of wind tunnel research aircraft. The relationship between NASTRAN and the wind tunnel model design process is discussed. Specific cases illustrating the use of NASTRAN for static, heat transfer, dynamic, and aeroelastic analyses are presented. Advantages and disadvantages of using NASTRAN are summarized.

INTRODUCTION

Dynamic Engineering, Inc. (DEI) is a world leader in the design and fabrication of wind tunnel research aircraft.

In past years, wind tunnel models were conservatively designed. This led to exceedingly strong and reliable models which were simple and inexpensive to analyze.

More recently, the design requirements for wind tunnel models have become increasingly complex. Models today must survive severe environments while gathering more data. Time schedules and program costs dictate that models yield more data at faster rates than ever before. Models are designed to have sophisticated electronics, instrumentation, and machinery built into a specified envelope.

For instance, the advent of high reynolds number wind tunnels, such as Langley Research Center's National Transonic Facility (NTF) require that some models survive cryogenic environments. High reynolds numbers can be obtained by decreasing viscous forces while keeping inertial forces constant. In order to reduce viscous forces, liquid nitrogen is injected into the tunnel air-stream. Consequently, the air temperature, and the research model temperature drops to minus 260 degrees fahrenheit.

Turboprop models are exceedingly elaborate propulsion model systems that are enjoying recent attention. What began as a set of propellers attached to a motor has evolved into a system of long counter-rotating shafts and sophisticated gear boxes. Often scale turboprop models must achieve rotor speeds in excess of 15000 rpm. Complicated shafting can lead to subcritical shaft modes that are difficult to damp. Whirl modes compound the problem. Mating these systems to wind tunnel supports can introduce other dynamic considerations.

Scaled helicopter systems offer the greatest challenge to the designer. DEI recently built a dynamically scaled model of the most sophisticated helicopter ever designed, the celebrated X-Wing helicopter. The research model had an intricate network of valves that open and close to allow air to pass into the rotating blades at the appropriate azimuth.

Dynamically scaled helicopter rotor blades are frequently fabricated from composite materials. Stiffness and mass distributions are carefully defined and must be closely matched. Natural frequencies and mode shapes of sample blades are measured to prove analysis and manufacture.

These stringent requirements place higher demands on the model design engineer than ever before. Designers must be well versed in the principles of elasticity, heat transfer, and dynamics. They must have access to state-of-the-art structural analysis tools.

DEI management recognized the need to upgrade analysis capability some years ago. After careful consideration and comparison with other analysis packages on the market, DEI obtained COSMIC NASTRAN in 1984. Moreover, DEI management authorized a training session for the design engineering staff in the use of NASTRAN. Well known NASTRAN expert, Tom Butler, was brought in to teach this training session.

NASTRAN is installed on the company's VAX 11/780 computer. The computer is also used to operate the UNIGRAPHICS CAD/CAM system by McAuto.

Part of the UNIGRAPHICS system is a finite element preprocessor module called GFEM. All design engineers are trained in the operation of UNIGRAPHICS. Finite element models are especially easy to generate when much of the geometry data already resides in the CAD system.

The purpose of this paper is to describe the analysis procedures at DEI used in the design of wind tunnel research aircraft.

STATIC ANALYSES

Most finite element analysis models generated at DEI use rigid format one, the static analysis. Load cases usually involve mechanical or aerodynamic pressures and forces, temperature loads, and gravity loads. Very few static analyses use optimization, differential stiffness, or buckling options.

FULL SCALE WING

Not all research models are scale models. DEI designed and built a full scale airplane wing. A new airfoil with a unique contour was to be tested as part of a joint project between NASA and an airplane manufacturer. It had a twenty three foot span and eight foot root chord.

To make a single flight-worthy wing would have been time consuming and costly. Tunnel safety requirements had to be met irregardless of weight. A model wing that maintained the appropriate geometry would be less expensive though heavy. Using estimates of the lift and drag for this new wing design, DEI engineers quickly generated a wing concept which included support tubes inside the wing, and a stressed skin. The wing would be tested in a near vertical position.

A large size means large loads. The full scale wing model must meet stringent safety requirements. Small scale research models can be built stronger with higher safety factors which would allow a more simplified analysis. This large wing would be unwieldy if it were over designed using handbook formulas. This project warranted a more sophisticated analysis.

NASTRAN was used to determine the relative load carrying ability of the skin and the inner support tubes. A detailed NASTRAN finite element model was generated using contour and geometry data that already existed in the CAD/CAM system. The GFEM preprocessor was used to generate the model. The generation of the finite element model took two weeks.

The finite element model consisted of 1722 bar and plate elements (See Figure 1). A pressure distribution that varied over the span and chord was applied to the finite element model. A computer program was written to automate the procedure of assigning pressures to elements, nonetheless, some pressures had to be adjusted manually. Forces and moments were applied to various locations along the trailing edge to represent the lift, drag, and bending effects of flaps and ailerons, which are physically connected at discrete locations for this analysis. The wing was considered to be a cantilever, fixed at the root.

The results showed the force distribution at the root section and the load path the aerodynamic forces took through the structure. In this way the design was verified.

NTF FLAT PLATE

Flow over a flat plate still fascinates people. DEI was given the task of designing a flat plate model to be tested in the NTF. It has an eight foot span and fifteen foot chord. The body is two inch honeycomb aluminum, and it has solid leading and trailing edges. The trailing edge is movable to adjust

the flow over the plate. The plate is supported by eight support struts that extend into the tunnel some 40 inches from the tunnel wall. The supports are airfoil shaped.

The test would be useless if the plate deformation was excessive. During the test, the pressure distribution is nearly uniform. But before testing, the airflow must be adjusted and there could be huge leading and trailing edge loads. Furthermore, there are thermal effects to consider.

Because of the non-uniform loading, and discrete support conditions it was decided to analyze the plate using NASTRAN. Due to the symmetry of the problem, only one half of the plate was modeled (See Figure 2). It had 793 grid points and 720 quad1 and quad2 elements. The model was quickly generated using the mesh portion of the GFEM preprocessor. A two dimensional interpolator was used to distribute the pressure load over the elements. The scan feature was used to search for the largest stresses. Centerline slopes were plotted externally from NASTRAN.

Contour plots of the stresses were requested, but the presence of the bar elements at right angles to the plate elements seemed to confuse NASTRAN. Spurious plate elements appeared as part of the plate outline.

HELICOPTER ROTOR FORCE TRANSDUCER

DEI designed and built a 600 Hp one half scale helicopter test rig and fuselage. It had a twenty foot diameter rotor section. We also designed the rotor force transducer and instrumentation.

The design of the five component rotor force transducer was quite complicated. The rotor shaft had to go through the force transducer without transferring loads. The force transducer had to have good sensitivity and still maintain good load carrying capability and have natural frequencies beyond the operating range.

A four bar cage concept was used in this model. Simple handbook formulas were used to get ballpark estimates. NASTRAN was used to get detailed distributions of the stress concentrations in each flexure. These were used to locate the position of the strain gauges. Finally, NASTRAN was used to ensure that the natural frequencies were sufficiently high (See Figure 3).

DYNAMIC ANALYSES

Most wind tunnel models are not dynamically scaled. For these models dynamics is not a consideration. But for helicopter models, turboprop models, and fixed wing flutter models, the structure must be designed to specific modes and frequencies.

Often, a customer will define stiffness and mass distributions for a model system. The job of the design engineer is to design a system that matches the customers flexibility requirements while maintaining model strength to keep within tunnel safety requirements.

TWO BODY STING

A researcher wanted to study the interference effects between bodies of revolution at high reynolds numbers. DEI engineers were charged with designing a research model that could withstand high dynamic pressures and low temperatures. The concept consisted of an upper body firmly attached to a sting, and a lower body designed to move in discrete intervals relative to the upper body. There were more than 100 distinct combinations of relative positions. A planform view is shown in Figure 4A, and an exploded view is shown in Figure 4B.

A dynamic analysis was requested to determine natural frequencies and mode shapes. It was considered impractical and unnecessary to analyze for all the combinations of position. Only four extreme configurations were considered which would bound all other modes of vibration.

Because of the complex nature of the geometry of the research model, handbook formulas for frequencies were considered to be too crude. It was decided that a more accurate representation of the geometry would be obtained using finite elements.

A single finite element model of the upper body and four separate models of the lower body were generated. These were done in such a way as to quickly swap grid and connection data for the lower body (See Figure 5A).

The upper and lower stings were modeled with bar elements. Special care was given to precisely model changes in geometry. Only structural parts of the connecting blade were modeled with plate elements. Non-structural parts, such as cover plates, were neglected. The bodies of revolution were included as point masses and inertias.

A modal analysis was requested using the inverse power method. To ensure that torsional modes were included properly, the coupled mass option was used. Modes shape data, in three views, was output using the plot capabilities in NASTRAN. Figure 5B shows a typical mode shape for one configuration.

COUNTER ROTATING TURBOPROP

There is much interest in turboprop models. An increase of 30 percent in operating efficiency can be obtained with new propeller technology and counter rotating turboprop systems.

**ORIGINAL PAGE IS
OF POOR QUALITY**

Scale turboprop models have interesting dynamics when mounted in a wind tunnel. Long cantilevered shafts are coupled through bearings. Hubs and shrouds are located at the forward most location, adding mass at the most dynamically effective position. High rotation speeds induce gyroscopic effects.

Ideally, the operating speed range should be free of vibration modes. There would be no dynamic problems if all vibration modes were above the operating range of interest. But this is hardly ever the case. The next best situation is to have low frequency modes that can be passed through quickly. However, this may cause static problems. Invariably, subcritical modes plague every design. The best that can be hoped for, then is to damp the subcritical modes so that they may be crossed safely.

Turboprop modal analysis presents a challenge to the model designer. A typical counter rotating turboprop is illustrated in Figure 6A. Turboprop design involves long shafts with changing diameters. Bearings and gears provide static coupling. Hubs, shrouds, and instrumentation are sources of point (or locally distributed) mass.

The dynamics of a typical turboprop system quickly becomes too complicated to analyze using classical techniques. Transfer matrix techniques are well suited to solve such problems. Finite elements, too, provide good estimates of the natural frequencies and mode shapes.

NASTRAN is used to determine the natural frequencies of the non-rotating shaft system. (See Figure 6B) Shafts are represented by bar elements, and bearings are modeled with spring elements. The mass effects of hubs and instrumentation are modeled as point masses and inertias. Mode shapes are conveniently output using the NASTRAN plot routines (See Figure 6C).

However, rotating shaft frequencies, such as whirl modes, are not determined (directly) from NASTRAN. Whirl modes depend on the system flexibility. NASTRAN is used to statically determine the flexibility coefficients at various locations. Then, whirl modes are determined external to NASTRAN using standard handbook formulas.

NASTRAN is used to evaluate the effect of damping. Varying magnitudes of viscous damping are input to the finite element model. A frequency response analysis is performed to determine if the damping is useful.

HELICOPTER ROTOR BLADES

Helicopter rotor blades are complicated structures with complicated dynamics. Most scale model blades are fabricated from fiberglass or graphite epoxy composites and have a balsa or foam core.

When a customer is interested in specific blade dynamics, it is the mass and stiffness distributions that are usually specified. The design engineer

must optimize the ply orientation of the composite materials to match stiffness and meet strength requirements. Lead or tungsten weights are inserted into the blade to meet mass and center of gravity requirements.

The bending dynamics of a rotating helicopter blade can be complex because strong centrifugal force couples axial with bending and torsion effects. Aeroelastic effects can be significant too. The manner in which the blade is connected to the hub can also affect bending dynamics.

NASTRAN is not used to determine rotor blade dynamics. When quick results are needed to evaluate a design concept, NASTRAN is too slow and cumbersome. When very accurate results are important, modeling time is better spent on dedicated blade analysis codes which are easier to use, include specific inputs (such as collective pitch angles and pitch control system stiffness) and have faster turn around.

For some blades, which are beamlike in nature and have relatively constant properties simple handbook calculations give good trends. Classical techniques are used to determine the non-rotating blade frequencies. Beam-column theory can be used to crudely estimate frequencies for rotating blades. Other blades, in which coupling effects, or aerodynamic effects are significant, specialized computer programs are used to determine blade dynamics.

COMPOSITE VERTICAL TAIL

One way to design a flutter model is to build a scale replica. The scaled model must have the correct scaled frequencies and the correct overall contour. This method of design is very expensive.

A particular flutter model built by DEI was fabricated from aluminum, balsa and fiberglass. The model's vertical tail was tested experimentally with our modal analysis equipment. The results showed that the first mode was in good agreement with the design mode, but higher modes were not close enough.

The decision was made to develop a NASTRAN model of the vertical tail to predict the effect of adding or subtracting plies. It is difficult to model composite material properties with NASTRAN. A computer program was developed to establish the in-plane and transverse stiffness of a laminate, given the number of plies, location and orientation, and material properties. Then equivalent orthotropic properties were calculated and the results were output in NASTRAN MAT3 format. Though the measured modes and frequencies were not predicted exactly, trends were useful.

HEAT TRANSFER

As was mentioned earlier, the National Transonic Facility (NTF) is a cryogenic wind tunnel. The temperature of the research models tested in this

tunnel drops about 350 degrees Fahrenheit from room temperature. Coupled with air speeds exceeding Mach one this becomes a very severe environment.

There are four distinct temperature phases that a research model must endure in the NTF. They are: 1) cool-down phase, 2) test phase, 3) warm-up phase, and 4) post model maintenance. The time span for each phase is well defined.

It is important to determine the magnitude of the thermal gradients that can exist in a research model. These gradients are caused by uneven cooling of the aircraft structure during the phases listed above. To determine the thermal gradients, a transient heat transfer analysis must be performed.

NASTRAN is not usually used for transient heat transfer analyses. The problem arises from the fact that heat transfer coefficients cannot be specified as functions of time. The heat transfer coefficient at high Reynolds numbers depend on temperature, Mach number, pressure, and density, all of which are, directly or indirectly, functions of time.

At DEI, we use an in-house developed finite difference code for transient heat transfer analyses. Conduction, convection, and radiation effects are included in this code. There is a user defined subroutine that allows for the time variation in heat transfer coefficient to be calculated from the quantities already mentioned. Temperature time histories, or gradient time histories can be directly plotted.

The disadvantage of the finite difference code is obvious when transferring temperatures to a different structural model. The heat transfer model is necessarily different from the structural model. The transfer process can be time consuming. Two or three dimensional interpolator routines are used to assign temperatures to grid points automatically. Nonetheless, some grid point temperatures must be adjusted manually.

AEROELASTIC ANALYSES

The stability of most aircraft model systems is usually governed by divergence--a static aeroelastic phenomenon. One of the parameters necessary to determine the dynamic pressure at which divergence will occur is the model system structural flexibility. This information is easily obtained from a finite element representation of the model system by applying unit loads individually at various locations and computing the resulting displacements and slopes. NASTRAN is often used to determine model system flexibility coefficients.

Sometimes, a flutter analysis is required for a research model. There exist some simplified analyses in the literature for determining the air speed at which flutter will occur. But these are really intended to illustrate the physical and mathematical nature of the flutter phenomenon - not to solve problems. Usually, the complex geometry and aerodynamic regime of the research

model violates assumptions on which the simplified analyses are based. NASTRAN is used to analyze all research models requiring a flutter analysis.

FAA FLUTTER CLEARANCE

DEI has on staff a designated engineering representative (DER) of the Federal Aviation Administration (FAA). This person can certify for the FAA that an aircraft is flight worthy regarding flutter. The aircraft certification process, may require a flutter analysis, a ground vibration test (GVT), or a flight flutter test.

A customer of DEI had a new aircraft design and requested that the aircraft be certified for flutter. NASTRAN was used to perform the flutter analysis.

An example of flutter analysis is briefly described here. The wing, wing flap, and fuselage of the aircraft were modeled with bar elements. Taking advantage of aircraft symmetry, one half of the airplane was modeled (See Figure 7). Symmetric and anti-symmetric vibration modes were computed. The doublet lattice method was used to represent the subsonic aerodynamics. With this relatively simple finite element model, a number of cases were considered. The customer was pleased with the results.

NTF MODEL FLUTTER

Every research model tested in the NTF must be checked for flutter. A customer asked DEI to perform a flutter analysis as part of the total model design. The flutter analysis had not yet been completed at the time this paper was written.

The research model consists of a fuselage, main wing, winglets, and four engine nacelles. There was no vertical or horizontal stabilizers. This was a sting mounted model and included a force transducer as part of the fuselage design.

Since the research model will be tested in various configurations (i.e. with and without winglets, with and without nacelles) the flutter speed of all test configurations must be determined. A detailed finite element model of the wing and winglet was developed using plate elements (See Figure 8). The wing and winglet thickness distributions were computed from contour data already in the CAD system. A two dimensional interpolation routine was used to automatically assign thicknesses to element properties. The mass and inertia effects of the engine nacelles were included. The sting and fuselage were modeled using bar elements. Only one half of the aircraft was modeled taking advantage of the aircraft symmetry. Both symmetric and anti-symmetric vibration modes were computed.

As of this writing, the subsonic aerodynamics was being modeled using double lattice theory.

CONCLUSION

DEI uses NASTRAN for a wide variety of structural analyses.

The advantages of using NASTRAN in the analysis of wind tunnel research models are many. NASTRAN offers a number of analytical capabilities that are needed such as static, dynamic, heat transfer, and aeroelastic analyses.

For many model designs, geometry and contour data is already programmed into the CAD system. This greatly facilitates the generation of finite element models when using the GFEM pre-processor. Finite element data is automatically output in NASTRAN format.

The chief disadvantages of using NASTRAN are summarized below.

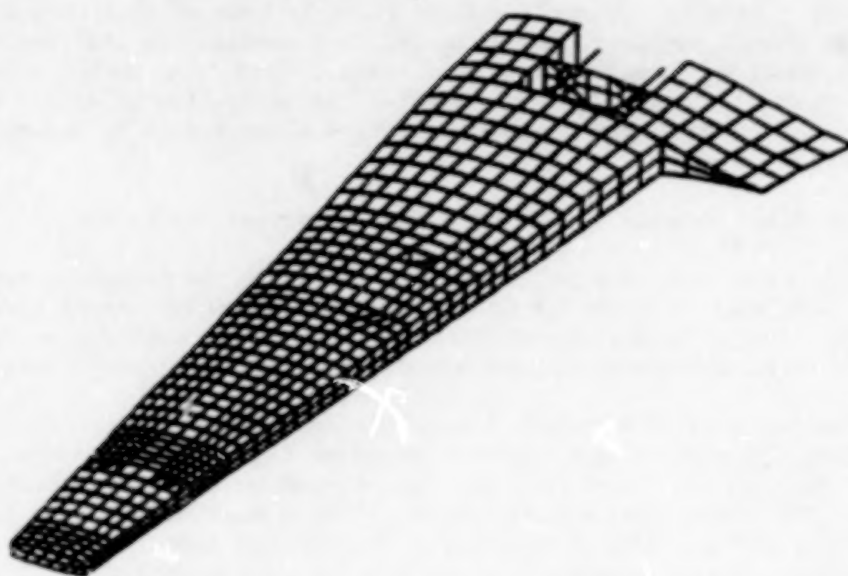
NASTRAN is often too slow and cumbersome to use in the design process. It becomes too difficult or time consuming to alter geometry design parameters with NASTRAN. For this reason, NASTRAN is most often used for a detailed analysis of a final design rather than to evaluate different design concepts.

Heat transfer coefficients are impossible to describe as a function of time in NASTRAN. Transient heat transfer problems regarding wind tunnel models involve well defined time histories of air temperature, pressure, density and Mach number. The heat transfer coefficient at high Mach numbers is a function of all these parameters, thus indirectly a function of time. This limitation makes the NASTRAN thermal analyzer undesirable for such problems.

NASTRAN is unsuited for the modal analysis of dynamically scaled helicopter rotor blades. Difficulties involved with modeling composite material properties and blade/hub attachments make other dedicated programs more desirable to use.

NASTRAN does not include gyroscopic effects (such as whirl modes) in the dynamic analysis of rotating shafts.

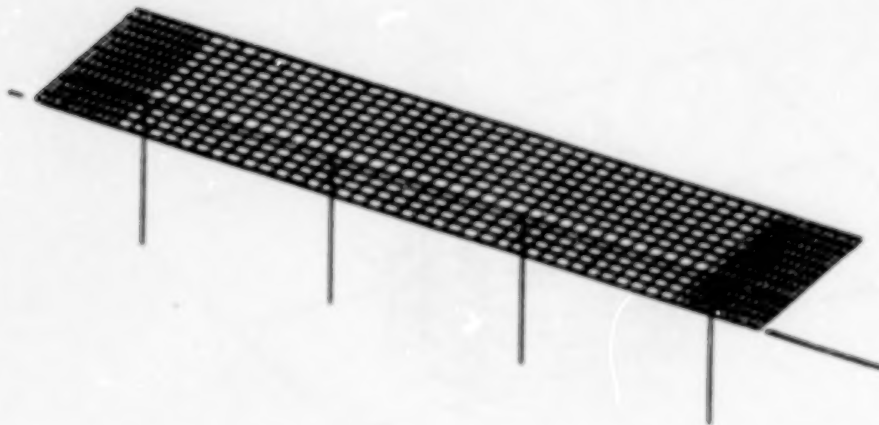
FIGURE 1



FULL SCALE WING FINITE ELEMENT MODEL
HIDDEN LINE PLOT

- O 23 FOOT SPAN, 8 FOOT CHORD
- O FLAPS AND AILERONS WERE NOT MODELED
- O NON-STRUCTURAL COVERPLATE REMOVED FROM UPPER SURFACE
REVEALS ONE OF 18 RIBS AND 2 OF 3 INNER SUPPORT TUBES
- O 1722 BAR AND PLATE ELEMENTS

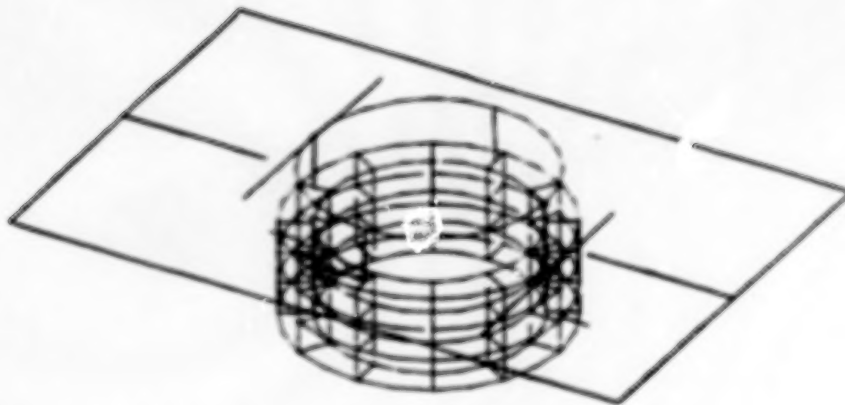
FIGURE 2



NTF FLAT PLATE FINITE ELEMENT MODEL
SYMMETRIC MODEL

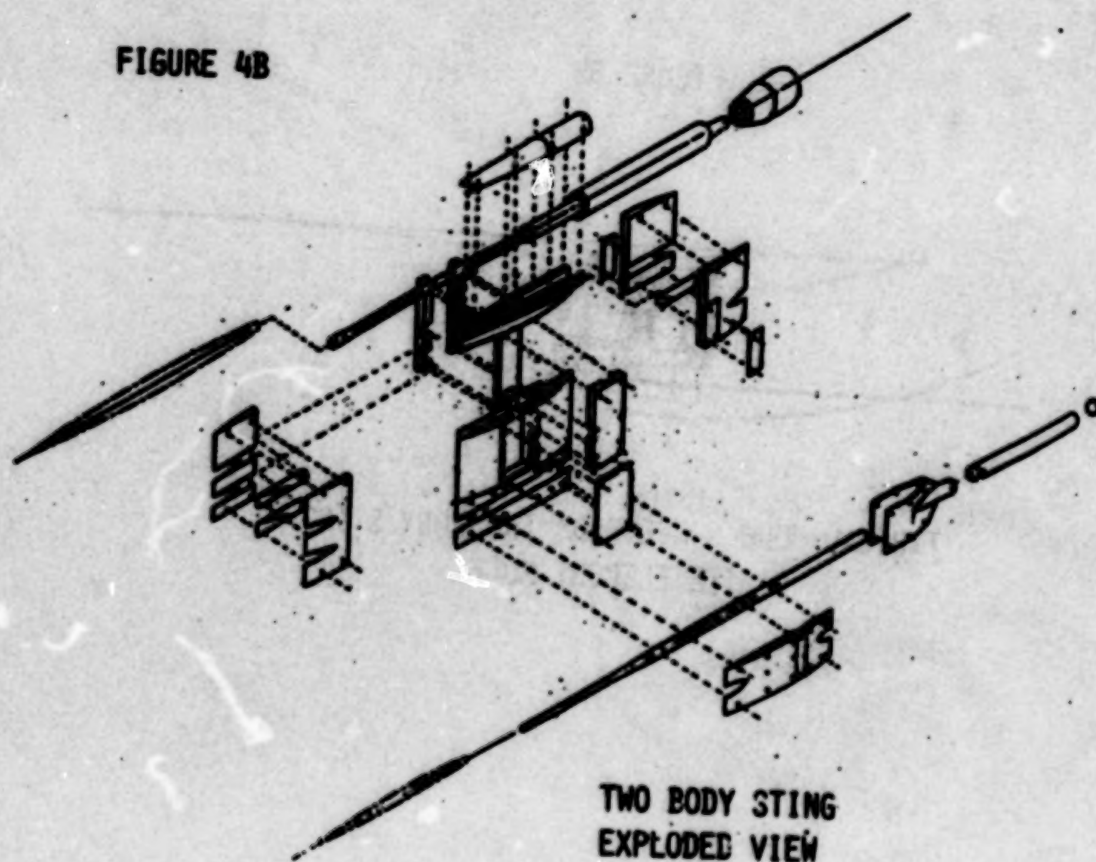
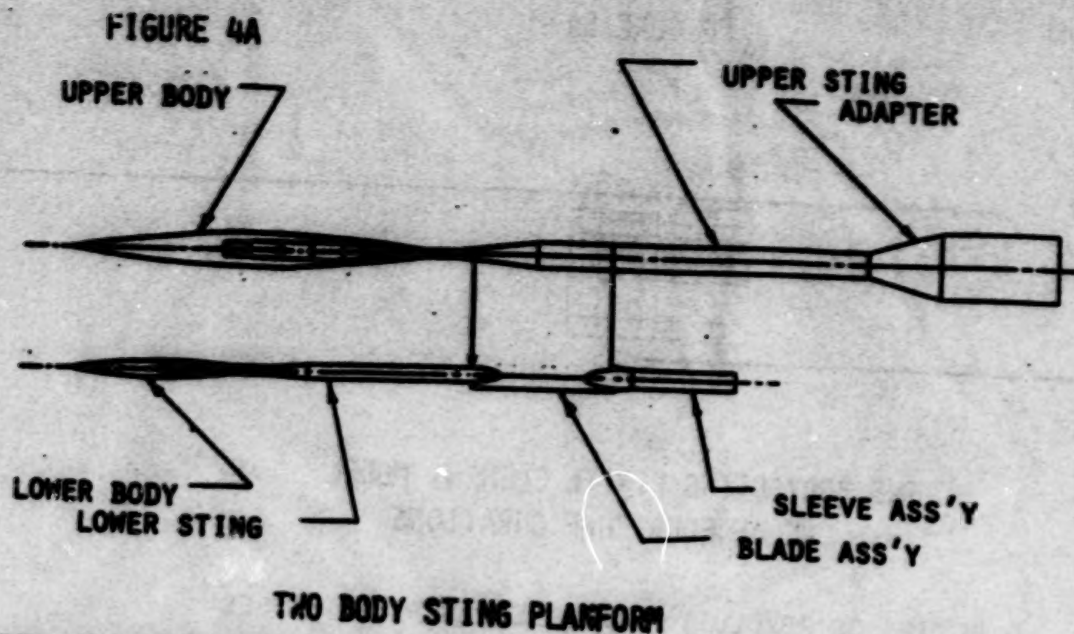
- O 8 FOOT SPAN, 15 FOOT CHORD
- O PRESSURE AND TEMPERATURE LOADS
- O 793 GRID POINTS, 720 PLATE ELEMENTS
- O SOLID ALUMINUM LEADING AND TRAILING EDGES,
HONEYCOMB ALUMINUM BODY

FIGURE 3



FORCE TRANSDUCER FINITE ELEMENT MODEL

- 0 FIVE LOAD CONDITIONS REPRESENT THRUST, DRAG, SIDE FORCE, PITCHING MOMENT, AND ROLLING MOMENT
- 0 FOUR TAPERED FLEXURES ARE REPRESENTED BY BAR ELEMENTS. THEY CONNECT THE THIN UPPER RING MODELED WITH BAR ELEMENTS, TO THE THICK LOWER RING MODELED WITH SOLID ELEMENTS.



C-3

FIGURE 5A



**TWO BODY STING FINITE ELEMENT MODEL
ONE OF FOUR CONFIGURATIONS**

- O BODIES OF REVOLUTION INCLUDED AS POINT MASSES**
- O UPPER AND LOWER STINGS CONNECTED BY RIGID ELEMENTS**

FIGURE 5B



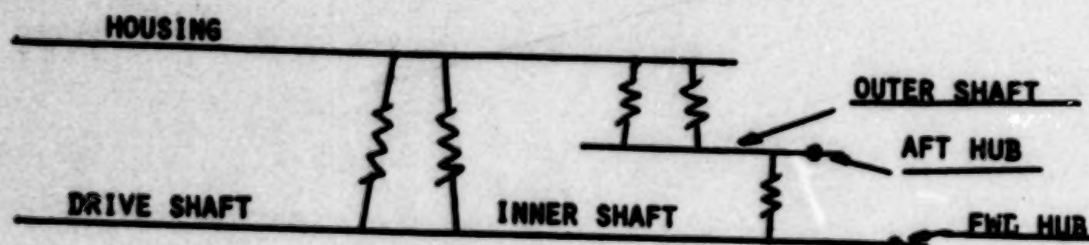
**TYPICAL MODE SHAPE FROM TWO BODY STING
FINITE ELEMENT MODEL**

FIGURE 6A



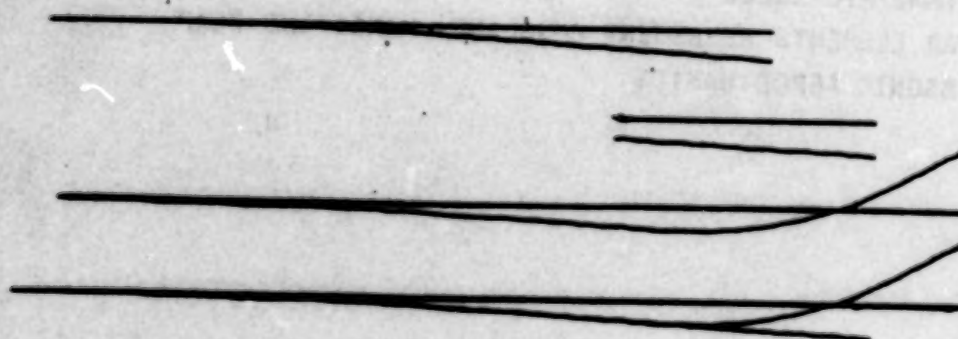
COUNTER ROTATING TURBOPROP CONCEPT

FIGURE 6B



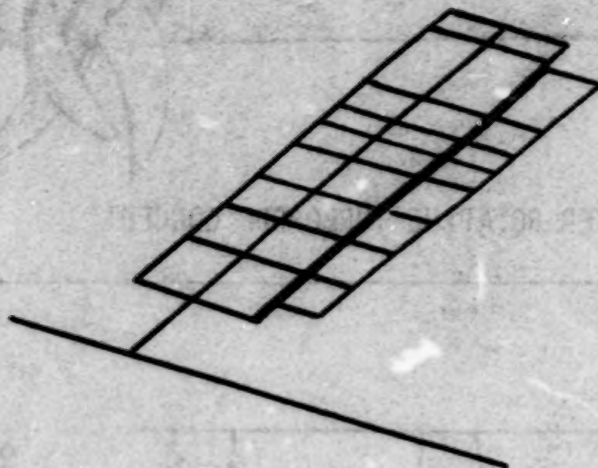
SCHEMATIC REPRESENTATION OF TURBOPROP

FIGURE 6C



TYPICAL REPRESENTATION OF TURBOPROP MODE SHAPE

FIGURE 7



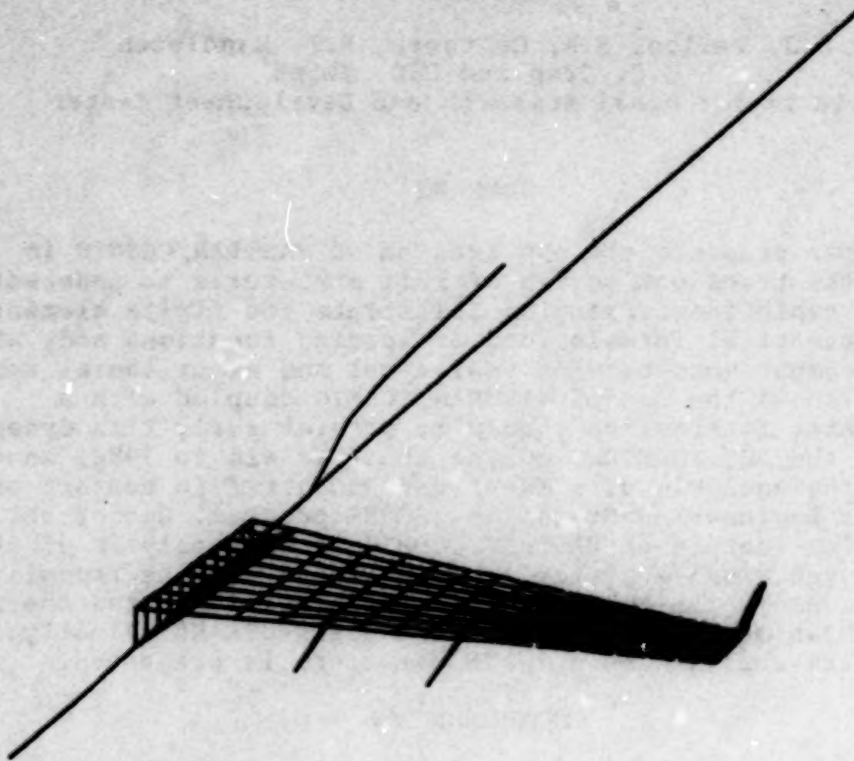
FINITE ELEMENT MODEL FOR FAA FLUTTER CERTIFICATION

O SYMMETRIC MODEL

O BAR ELEMENTS REPRESENT FUSELAGE, WING, AND FLAP

O SUBSONIC AERODYNAMICS

FIGURE 8



FINITE ELEMENT MODEL FOR FLUTTER ANALYSIS

- O SYMMETRIC MODEL**
- O BAR ELEMENTS REPRESENT FUSELAGE AND STING**
- O PLATE ELEMENTS REPRESENT WING AND WINGLET**
- O NACELLES REPRESENTED BY POINT MASSES AND INERTIAS**
- O SUBSONIC AERODYNAMICS**

**Application of NASTRAN/COSMIC
in the
Analysis of Ship Structures to Underwater Explosion Shock**

D.J. Fallon, F.A. Costanzo, R.T. Handleton
G.C. Camp and D.C. Smith
David Taylor Naval Research and Development Center

SUMMARY

This paper presents the application of NASTRAN/COSMIC in predicting the transient motion of ship structures to underwater non-contact explosions. Examples illustrate the finite element models, mathematical formulations of loading functions and, where available, comparisons between analytical and experimental results. One example shows the use of NASTRAN/COSMIC coupled with a structure/water interaction theory to predict early time dynamic response of the USS YORKTOWN during shock trials in 1984. Another example is the analysis of a MK-45 gun conducted in support of the Ship Systems Engineering Standards (SSES) program. Use of the substructuring feature of NASTRAN/COSMIC in the analysis of the Vertical Launch Missile System is illustrated for the recently constructed USS MOBILE BAY. Another example illustrates the analyses of two mast structures on the USS KAUFMANN. Finally, an example of the analysis of a SWATH structure is presented.

INTRODUCTION

The evaluation of dynamic responses of surface ships and submarines to a shock environment is a very important problem in naval research. The fundamental characteristic of the shock experienced aboard naval vessels is the sudden increase in the velocity of the structural member. Equipment supported by these structural members may be adversely affected by this sudden increase in motion. There are two basic types of damage to equipment which concerns the naval designer: mechanical damage and mal-operation.

Surface ship shock loading may result from three sources: 1. underwater non-contact explosions, 2. contact explosions and 3. air blast from aerial bombs or from the vessel's own armament. Of particular importance to the United States Navy is the response of ship structure to underwater non-contact explosions. The Underwater Explosions Research Division (UERD) of the David Taylor Naval Research and Development Center (DTNSRDC) uses both analytical and experimental techniques in research efforts aimed at finding solutions to this complex problem. One of the primary analytical tools used at UERD is NASTRAN/COSMIC.

ANALYSIS OF USS YORKTOWN

The USS YORKTOWN (CG-48) is the second ship constructed in the

USS TICONDEROGA CLASS of guided-missile cruisers. The USS YORKTOWN has an approximate displacement of 9,100 tons. This ship is a revised version of the USS SPRUANCE class destroyer using the same hull and propulsion system but incorporating the AEGIS weapon system(1). The USS YORKTOWN was shock tested in September of 1984. The purpose of this section is to illustrate the use of NASTRAN/COSMIC coupled with a structure/water interaction theory to predict the early time vertical response of the entire ship during these trials.

The simplest representation of the structure/water interaction is with an impulse equal to the momentum of the displaced water in the free field. This impulse is applied from below to a beam model of the ship. At the termination of the impulse load atmospheric and gravitational forces are applied to the model from above (Refer to Figure 1). This approach is reasonable because the ship displaces its mass in the water and buoyant forces are lost due to cavitation around the ship during the impulse loading phase of the ship motion. This approach emphasizes the structural response while de-emphasizing the complex fluid-structure interaction; thereby, considerably simplifying the analytical calculations of the dynamic response.

Previous UERD research efforts have shown that the total momentum of a structural node on a surface ship can be approximated by the use of the "spar buoy" model. The fundamental assumption of the "spar buoy" model is that a given structural node is "kicked off" with the same average velocity as a column of water with the same depth as the draft of the ship at the corresponding location in the free field. The derivations of the equation to compute the total momentum can be found in Reference 2.

A finite element model consisting of forty flexural beam elements was utilized to evaluate the dynamic response of the ship. The element's sectional properties (i.e., moment of inertia and cross sectional area) and mass distribution were obtained from design calculations performed by the Naval Sea Systems Command (NAVSEA). Previous analytical and experimental work (3) has demonstrated that the higher frequencies of vibration are significantly effected by the exclusion of shear deformation. Shock loadings tend to excite the higher modes of vibration; therefore, to ensure more accurate results the contribution due to shear energy via an effective shear area was included in the analysis. Due to the spherical nature of the shockwave, proper consideration was given the the arrival of the shockwave at each structural node. Gravity and atmospheric pressure were accounted for by use of a loading function applied at the time of cut-off of the impulse load. The analysis was performed on a CDC 176 mainframe.

Figure 2 illustrates a comparison of the normalized experimental and analytical results for a location on the ship's keel near the stern. This figure illustrates excellent correlation between the experimental and analytical curves with respect to shape and peak value for the first thirty milliseconds. A similar comparison is illustrated in Figure 3 for the velocity at the

amidships location. Finally, a comparison of the velocity at a location near the bow of the ship is depicted in Figure 4. As in the case of the other two locations, excellent correlation was obtained for the first thirty milliseconds.

ANALYSIS OF A MK 45 GUN MODEL

Modular weapons installation is a very important concept to naval ship and weapons designers. The modular weapons design concept offers the United States Navy several advantages over the classical methodology of designing ships. The first major advantage is the flexibility of upgrading weapons as the technology of weapon design changes in the future. Another important advantage is the ability to interchange weapons systems in the fleet. This allows the Navy to essentially change the mission of any given ship as may be required by the ever changing world situation.

DTNSRDC/UERD was tasked to participate in the analysis and development of design standards for modular weapons via the Ship Systems Engineering Standards (SSES) program. The first part of this task was to perform a detailed analysis of the MK 45-54 caliber 5 inch gun module. To accomplish this task a NASTRAN/COSMIC finite element model (see Figure 5) was prepared for the forward ship zone between structural bulkheads of the DDG-51 at the location of the gun module. A NASTRAN/MSC model (see Figure 6) of the gun module developed by FMC/MOD was converted to a NASTRAN/COSMIC model and then interfaced with the ship model. The combined model was accelerated at the hull with a prescribed motion history to simulate the expected motions of the ship during a full scale shock test in the vertical and athwartship directions.

The basic assumption in the computation of the transient motion of the MK 45 gun module is that the hull of any section of the ship between transverse bulkheads moves as a rigid body in the vertical and athwartship directions. To compute this rigid body motion in the vertical direction, the method outlined in the previous section was utilized. Specifically, a NASTRAN/COSMIC beam finite element representation of the entire ship was analyzed in the time domain. The ship loading was via the "spar buoy" assumption. The output from this analysis was then used as input for the analysis of the gun module.

The translational motion in the athwartship direction is an adaptation of a technique for computing submarine rigid body motion. Figure 7 illustrates the structural model used to compute the rigid body motion of the hull in the athwartship direction. This model assumes the hull is 1) a rigid body, 2) the loading function is an exponential decaying function calculated by the explosive charge similitude equation, 3) the loads are applied to the structural nodes on the shot side of the hull and 4) the resistance of the water on the side away from the shot is proportional to the velocity (i.e., viscous damping). Writing the equations of motion and numerically integrating through the time domain yields a prescribed displacement for the motion of the hull. Figure 8 illustrates a normalized comparison of the analytical and

experimental values for a typical cross section of the USS YORKTOWN. As illustrated, the early time history of the ship is predicted quite accurately.

The finite element model of the ship structure consisted of CQUAD1, CTRIA1 and CBAR elements. Orthotropic plate theory was assumed in modeling the plate and stiffener combination of the ship bulkheads. A coarse finite element mesh was assumed since interest was in the computation of displacements and not stresses in the ship structure. The computation of the response of structures due to impulsive loadings, the computations were performed on the coupled equations of motion through the time domain. To achieve the prescribed acceleration at the boundary nodes, a force of a magnitude equal to the acceleration times 10 was applied at the boundary node having a mass of 10 .

ANALYSIS OF THE VERTICAL LAUNCH SYSTEM

The MK41 Vertical Launch System (VLS) as shown in Figure 9 is an important addition to the United States Navy weapons arsenal. The MK41 system provides offensive and defensive capabilities in a single launcher and was designed as an alternative to single and dual-rail launching systems. The weapon system meets the Navy's needs for reliability, increased firepower, flexibility and reduced manning at manageable costs.

DTNSRDC/UERD was tasked by NAVSEA to participate in the predicting the shock response of the VLS in the recently constructed USS MOBILE BAY (CG-53) during full scale ship shock trials scheduled for the later part of May 1987. The specific objective of the UERD task was to predict the transient response between the VLS foundation and the USS MOBILE BAY ship structure. To accomplish this goal, NASTRAN/COSMIC finite element models were prepared for sections of the ship structure at the forward and aft launcher locations. A reduced mathematical representation (stiffness and mass matrices) of the VLS generated by the prime contractor, Martin Marietta, using NASTRAN/NSC on an IBM 370 computer was substructured into the ship structure models. The combined model was accelerated at the hull with a prescribed acceleration to simulate the expected motion of the ship during a full scale shock test in the vertical and athwartship directions in exactly the same technique described earlier for the MK-45 gun module. The results of these analyses were provided to Martin Marietta for use in detailed stress calculations through the time domain.

Figure 10 and Figure 11 illustrate the completed finite element models for the forward and aft launcher locations, respectively. In developing these models, substructuring capabilities of NASTRAN/COSMIC were extensively utilized to expedite model generation and to aid in combining the mathematical models of the VLS to the ship structure model. Figure 12 illustrates the use of the substructuring commands to generate the completed model of the forward launcher location. First a finite element model of one half of the ship structure as illustrated in

Figure 12a was created as a basic structure in a Phase One run. The centerline bulkhead structure illustrated in Figure 12b was also created as a basic structure. In addition, the mathematical representation of the VLS structure as illustrated in Figure 12c was used to define a basic structure via use of the INPUT2 DMAP module. Finally, a Phase Two run was completed which created a symmetrical image of the basic structure in Figure 12a (illustrated in Figure 12d) and combined all the basic structure at interfacing grid points to form the complete ship structure. An additional Phase Two transient (Rigid Format 9) run was performed on the complete structure to obtain the motion at the foundation interface between the VLS and the ship structure. The results of this analysis was recovered via a Phase Three run and provided to Martin Marietta for the analysis of their superelement representation of the VLS through the time domain.

As previously mentioned, the USS MOBILE BAY will be shock tested in May 1987. The results of this analysis will be used to make comparisons with the experimental data obtained. The VLS will be heavily monitored during the test; hence, there will be an excellent data base to compare experimental and predicted results.

ANALYSIS OF MAST STRUCTURES ON USS KAUFMANN (FFG-59)

The dynamic response of mast structures under shock loading is of great concern to the ship shock community. Although the structural model of a mast type structure is rather simple, the complexity in the analysis comes from the assumed boundary conditions and the loading in terms of motion histories at these boundaries. DTNSRDC/NERD has been tasked by NAVSEA in support of the future shock trials of the USS KAUFMANN to develop a methodology to estimate the dynamic response of the masts and equipment supported by the masts.

The USS KAUFMANN supports two primary masts: Foremast/SPS-49 Support Tower and the Main Mast. The primary function of the foremast is to carry the SPS-49 Air Search Radar. This radar is an important element in the ship's C3I (Command, Control, Communications, and Intelligence) capabilities. The main mast supports the great majority of the remainder of the ship's C3I equipment. This equipment aids the ship in communications, navigation and readiness for combat.

Figure 13 and Figure 14 illustrate the finite element models of the main mast and the foremast, respectively. The structural tubing and platform stiffeners were modeled using CBAR elements. Platforms on both masts were modeled using CQUAD2 and CTRIA2 plate elements. Equipment was modeled as concentrated masses via the CONM2 bulk data card.

As previously mentioned the complexity of the analysis of mast structures lies in the evaluation of the kinematic description of the boundary conditions. At the writing of this paper, studies are being conducted to develop a technique to determine the most valid set of boundary conditions to employ. The use of the "spar buoy"

model and the athwartship model discussed in preceding sections appears promising. Studies are being made to determine a mathematical model which accounts for the attenuation of the keel response (which the "spar buoy" model approximates) through the ship structure to the base of the mast structure at the weather deck level.

ANALYSIS OF SMATH STRUCTURE

The Small Waterplane Area Twin-Hulled (SMATH) ship is a unique United States Navy hull form. Figure 15 presents a cross sectional view of a SMATH ship finite element model. This half bay, half cross section finite element model was generated by the Ship Structures Division of DTNSRDC. The model was designed to analyze stresses generated in the haunched region by a pseudo-static wave loading on the strut. DTNSRDC/NERD was tasked to analyze the SMATH hull form to a shock loading from an underwater explosion.

The finite element model, provided by the Ship Structures Division, consists of membrane, plate, rod, and bar elements. The model employs 1500+ elements and 10000+ degrees of freedom. To conduct a dynamic analysis, several modifications were made to the model. The primary change involved increasing the mass of the model to equal the displaced mass of a comparable section of the ship under construction. The Nodal Weight Generator of NASTRAN/COSMIC reduced the effort of this modification.

A force-time history impulsive type loading was applied at the strut end cap to simulate the underwater shock loading. This type of loading was simple to calculate and to apply to the structure. An impulsive type loading could be applied to this structure because of the area of concern is the haunched region. Excessive stresses in the strut due to localization of the loading were ignored.

The shock loading from an underwater explosion to the SMATH hull form loads both struts and submerged hulls. The shock loading is not symmetrical (Figure 16). The near hull loading differs from the far hull loading in magnitude, direction, and phasing. To account for the unsymmetrical loading it was necessary to utilize a full cross section model of the SMATH. Due to the detail of the model and time requirements, substructuring was chosen to create an equivalent structure and combine the two substructures into one composite structure. Substructuring allowed for varying the magnitude and the direction of loadings to each substructure. Utilizing the DELAYS card, the phasing delay of the shock loading was easily implemented.

CONCLUDING REMARKS

This paper has presented the analyses using NASTRAN/COSMIC of several different types of naval structures subjected to a non-contact underwater explosive loading that the Underwater Explosions Research Division has conducted. Predicting the response of ships to withstand underwater shock loads is as much (if not

more) an art as it is a science. Hence the development of reliable analytical techniques to evaluate the response of ships to this type of shock loading provides a very fertile area for research. Using experimental and analytical methods, DTMB/USND is committed to assisting the Naval community in achieving this goal. The NASTRAM/COSMIC is an important tool in this task.

REFERENCES

1. Palmer, Norman, The Ships and Aircraft of the U. S. Fleet, Naval Institute Press, Annapolis, Md, Copyright, 1981.
2. Fallon, Dennis J., "The Dynamic Response of Naval Structures to the Application of a Loading Function to Predict Underwater Explosions," Old Dominion University Research Report, March, 1985.
3. Mathewson, Alice W., "Calculation of the Normal Vertical Flexural Modes of Vibration by the Digital Process," TMB Report 706, February, 1950.

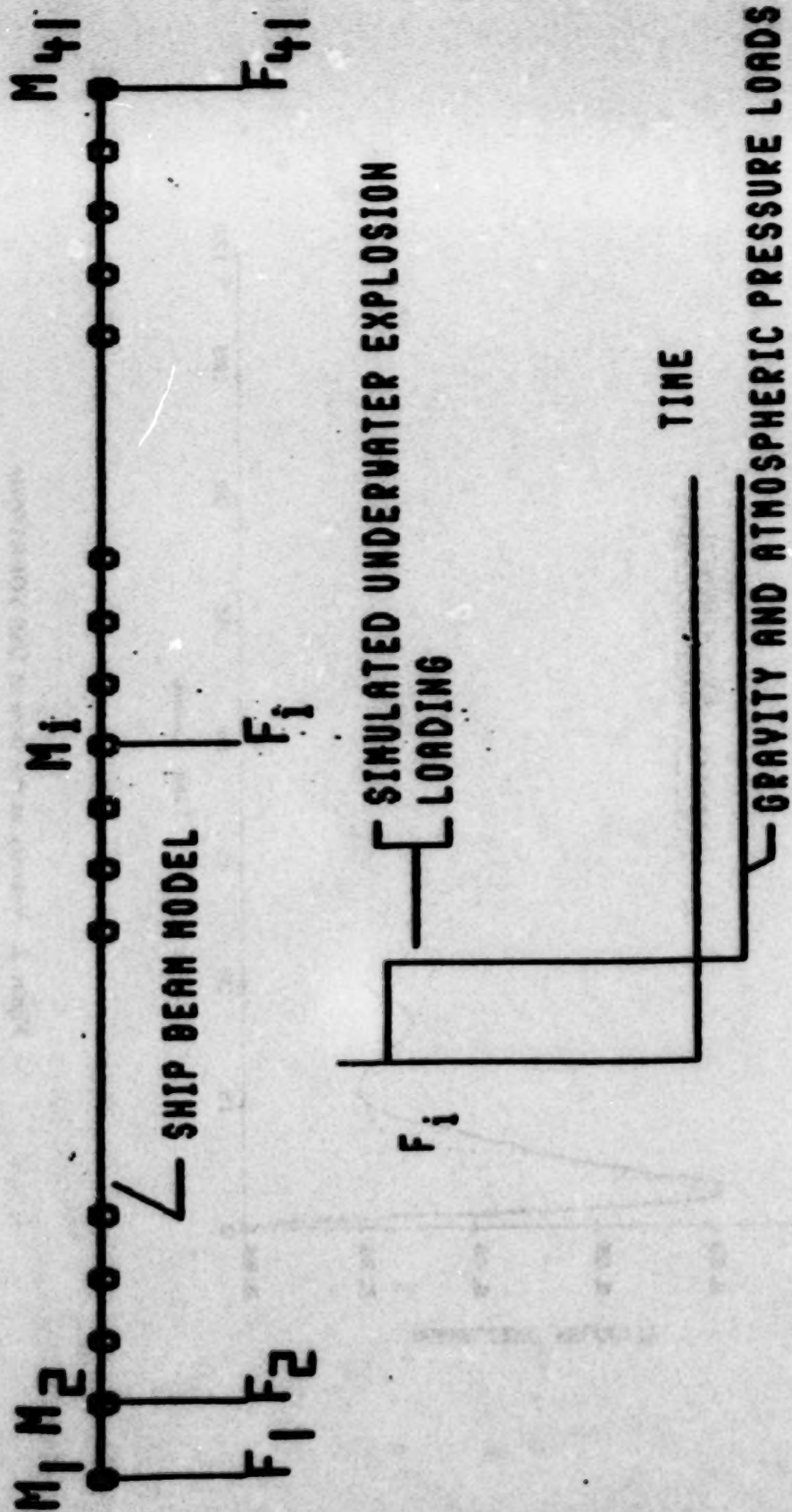


Figure 1: Ship beam model and loading function

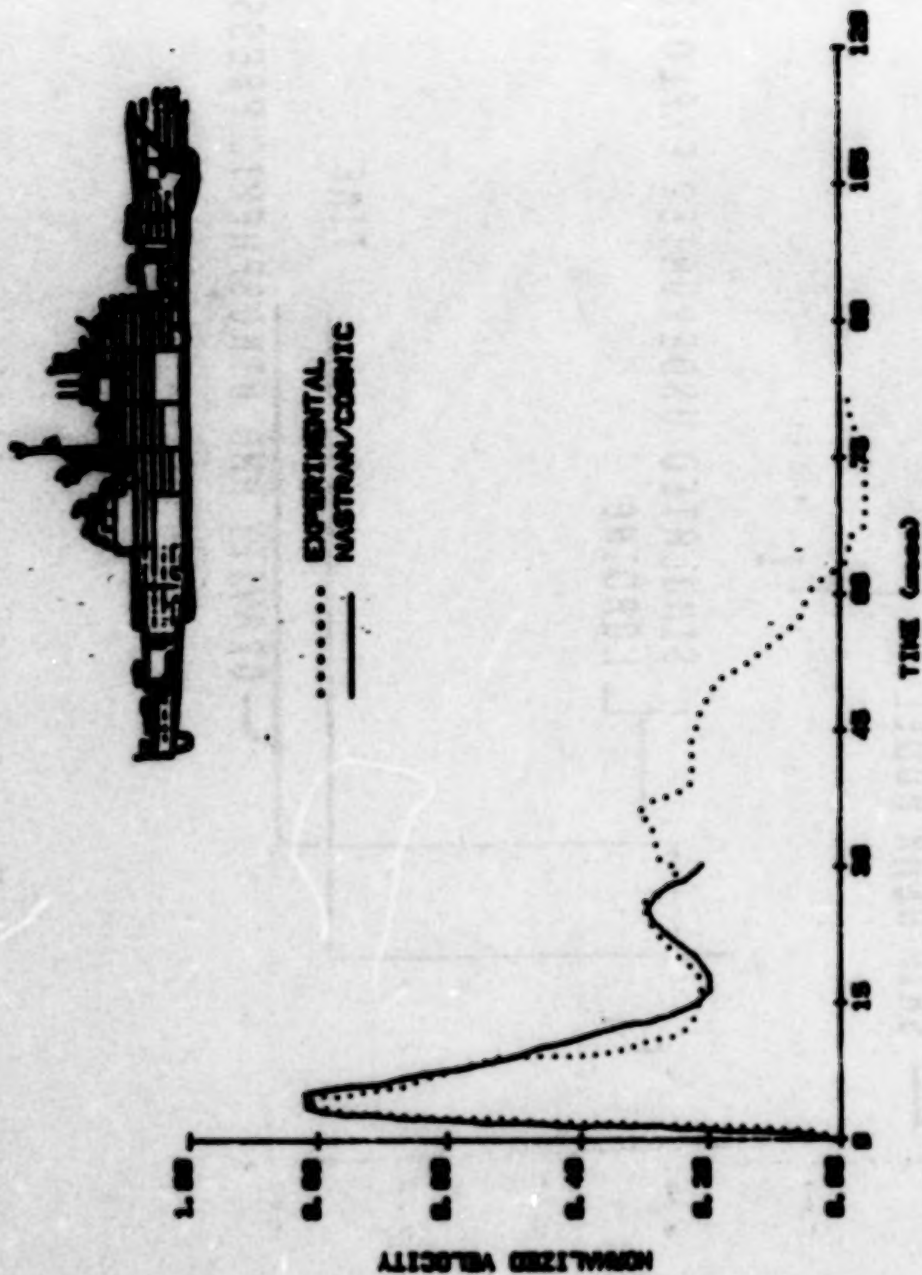


Figure 2: Velocity at the stern of USS YORKTOWN

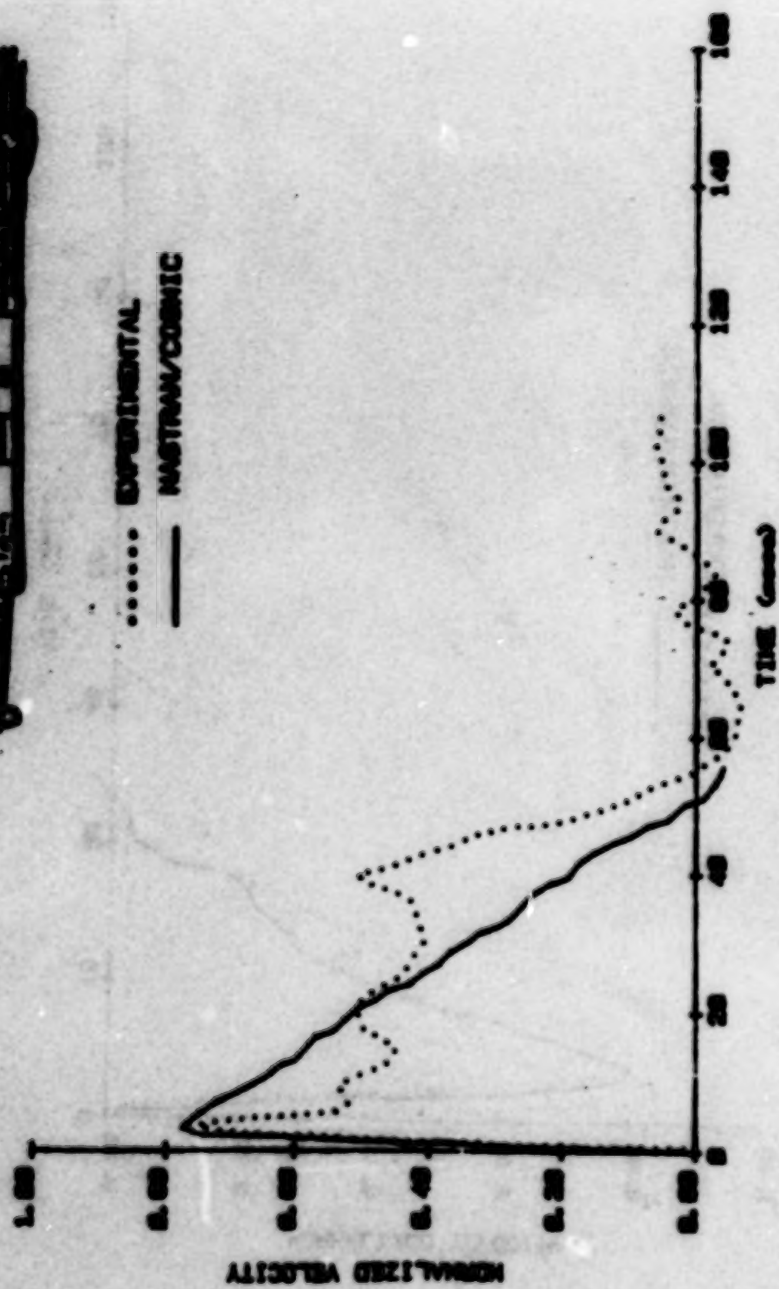


Figure 3: Velocity at midships of USS YORKTOWN

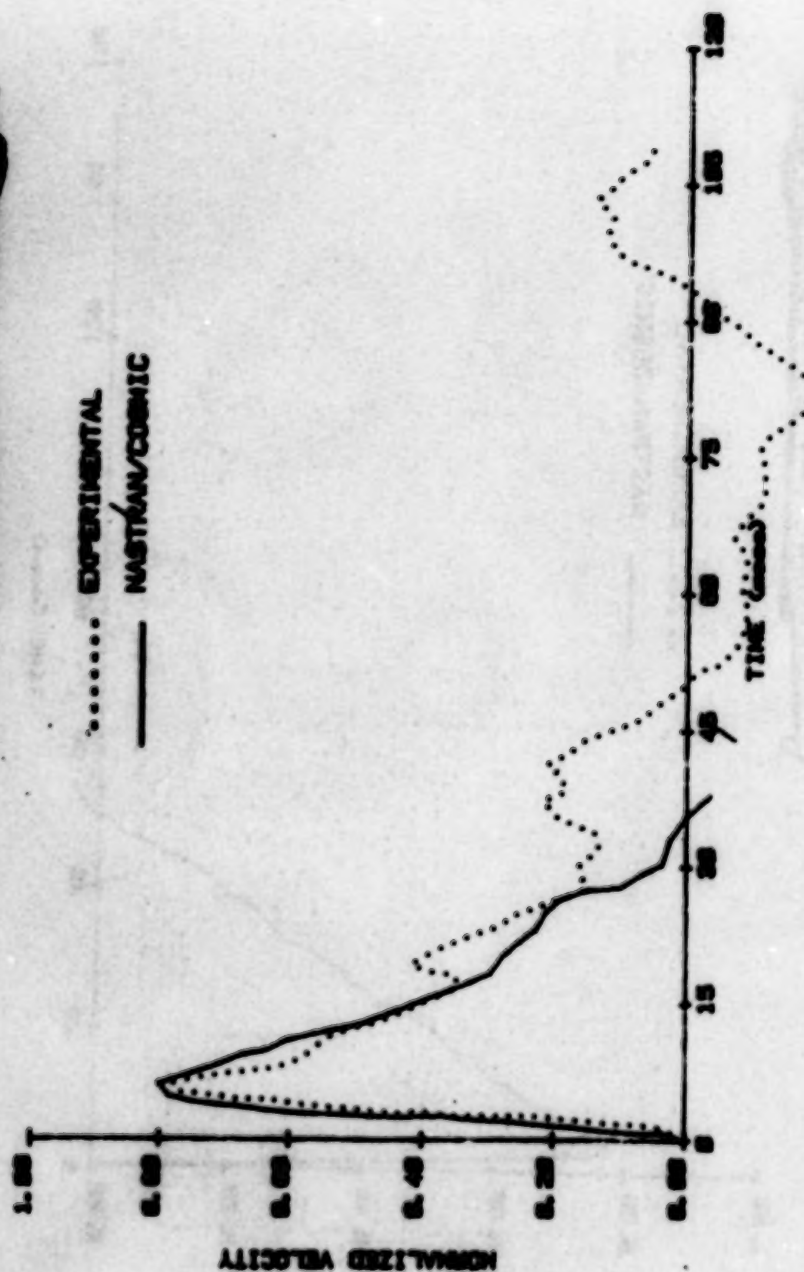
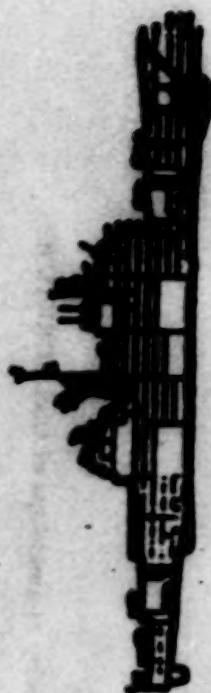


Figure 4: Velocity at bow of USS YORKTOWN

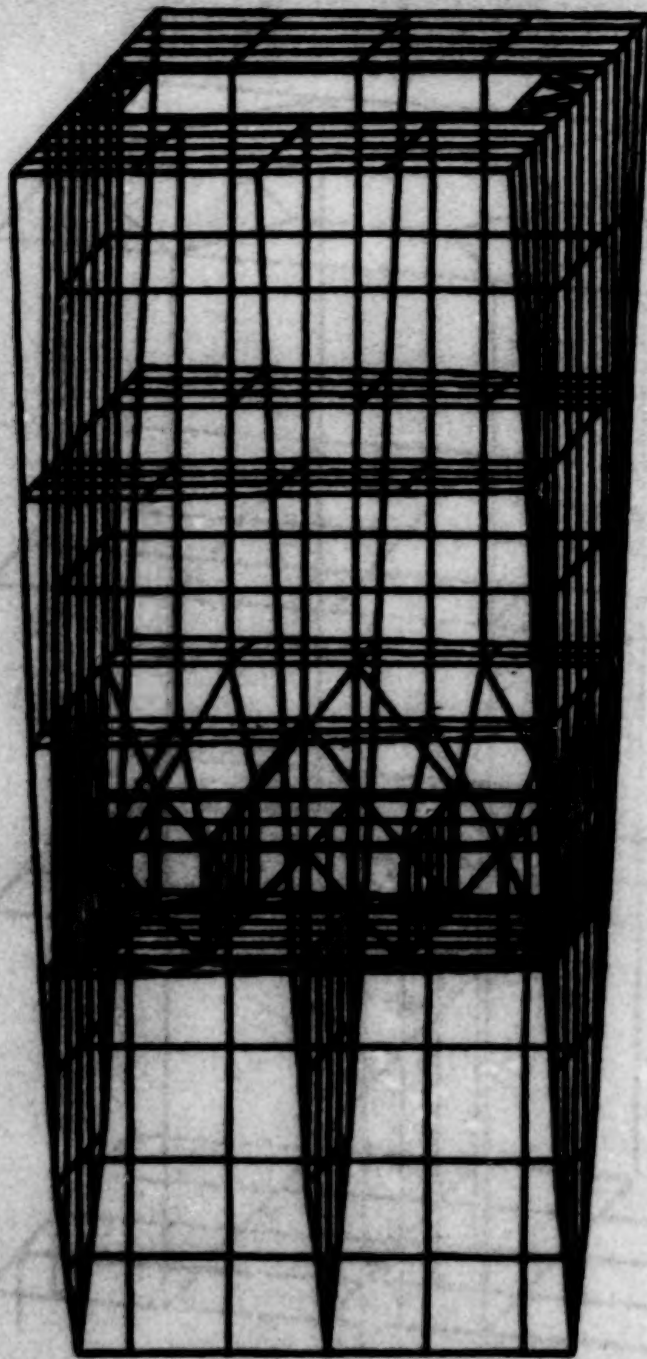


Figure 3: Finite element model DDG - 51 gun location

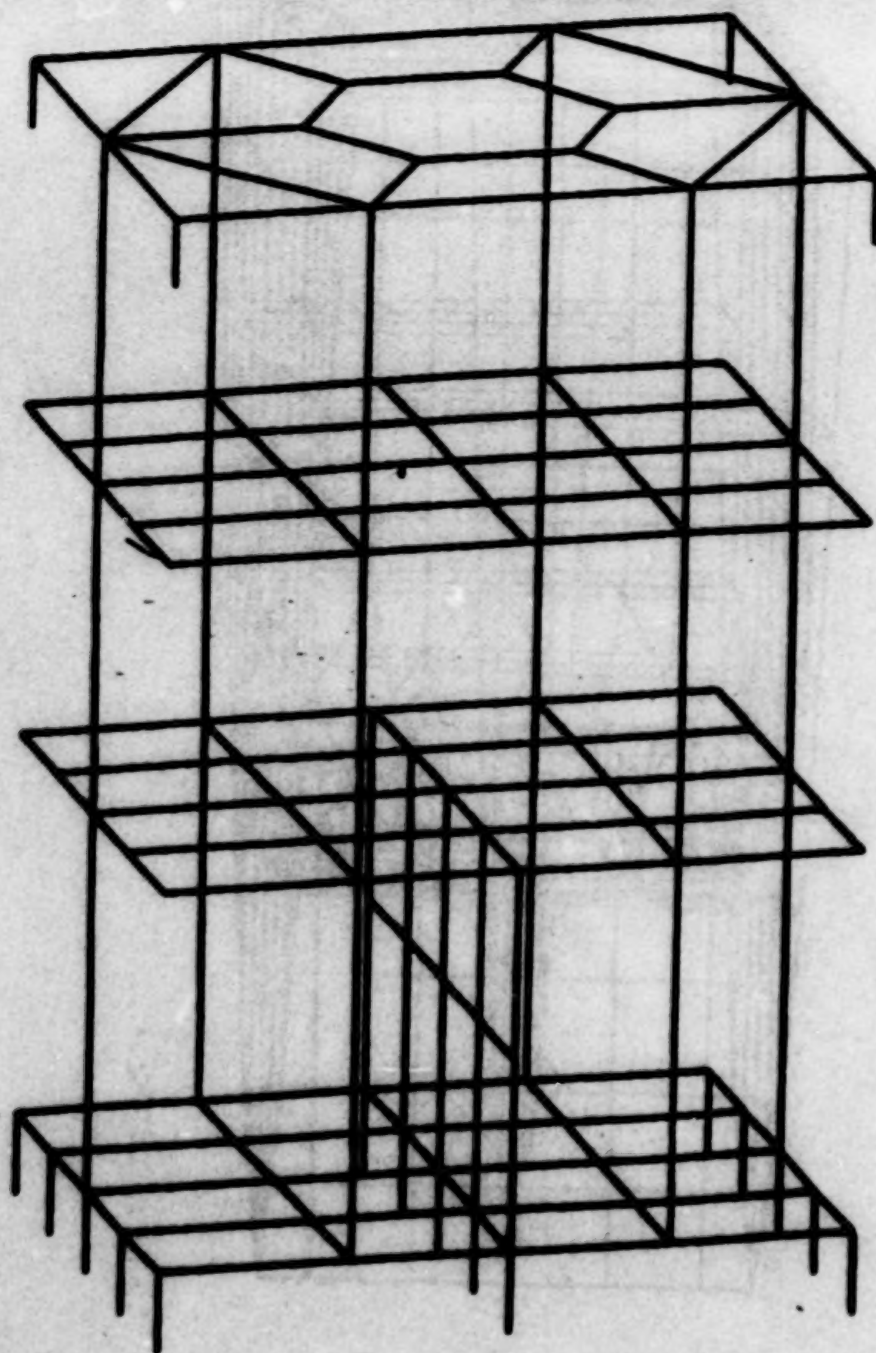


Figure 6: Finite element model MK45 gun module



Figure 7: Adversity mathematical model

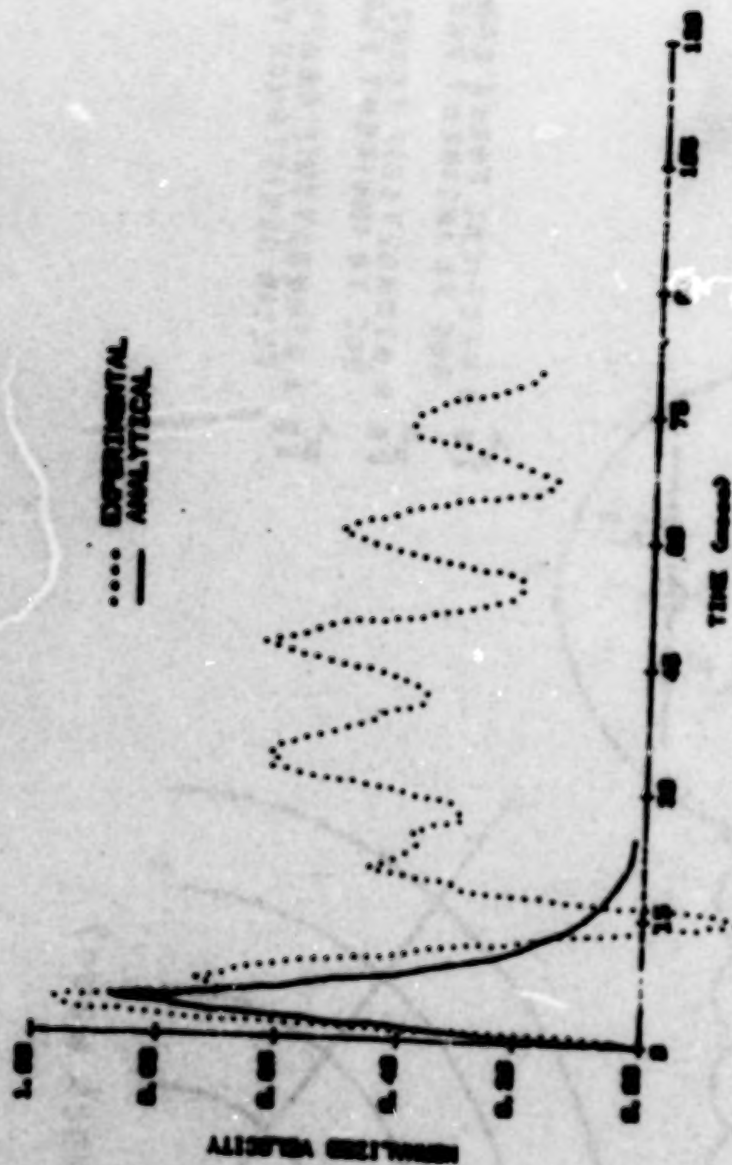


Figure 8: Comparison experimental and analytical shipboard motion USS YORKTOWN

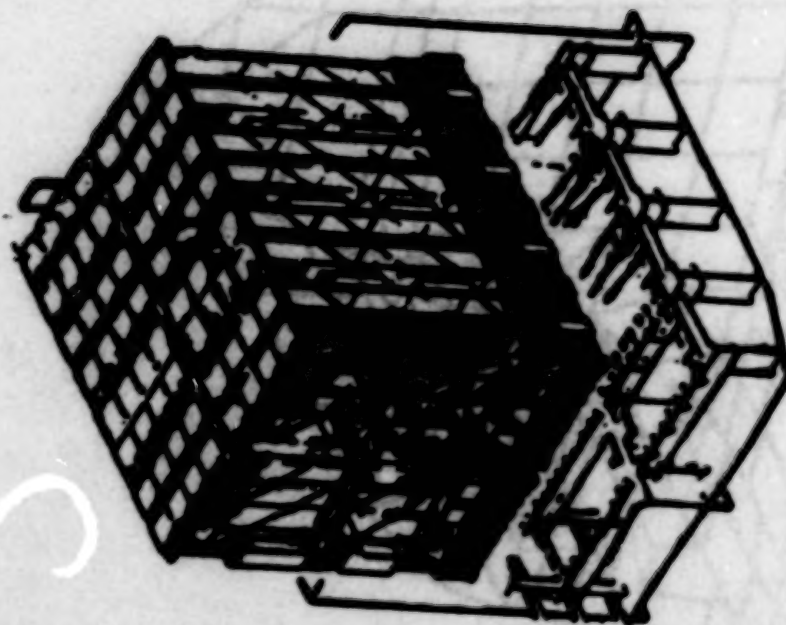


Figure 9: Vertical Launch Missile System

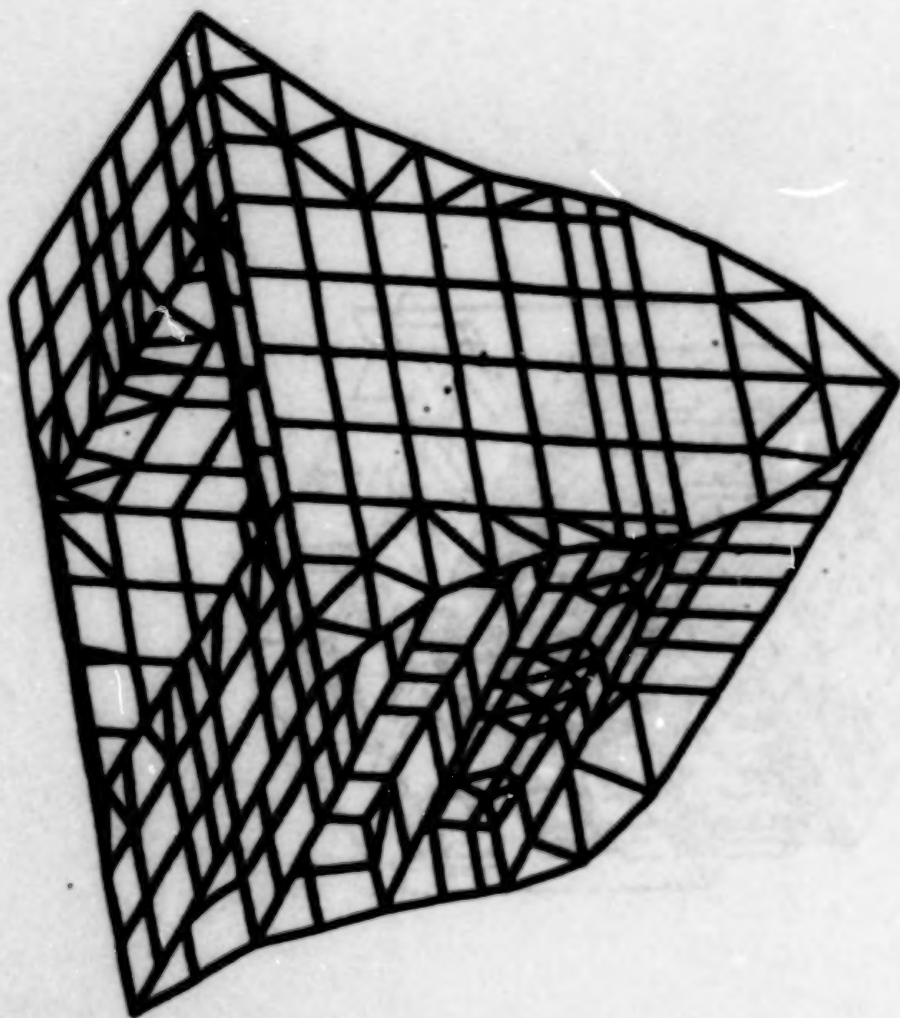


Figure 10: Finite element model forward launcher

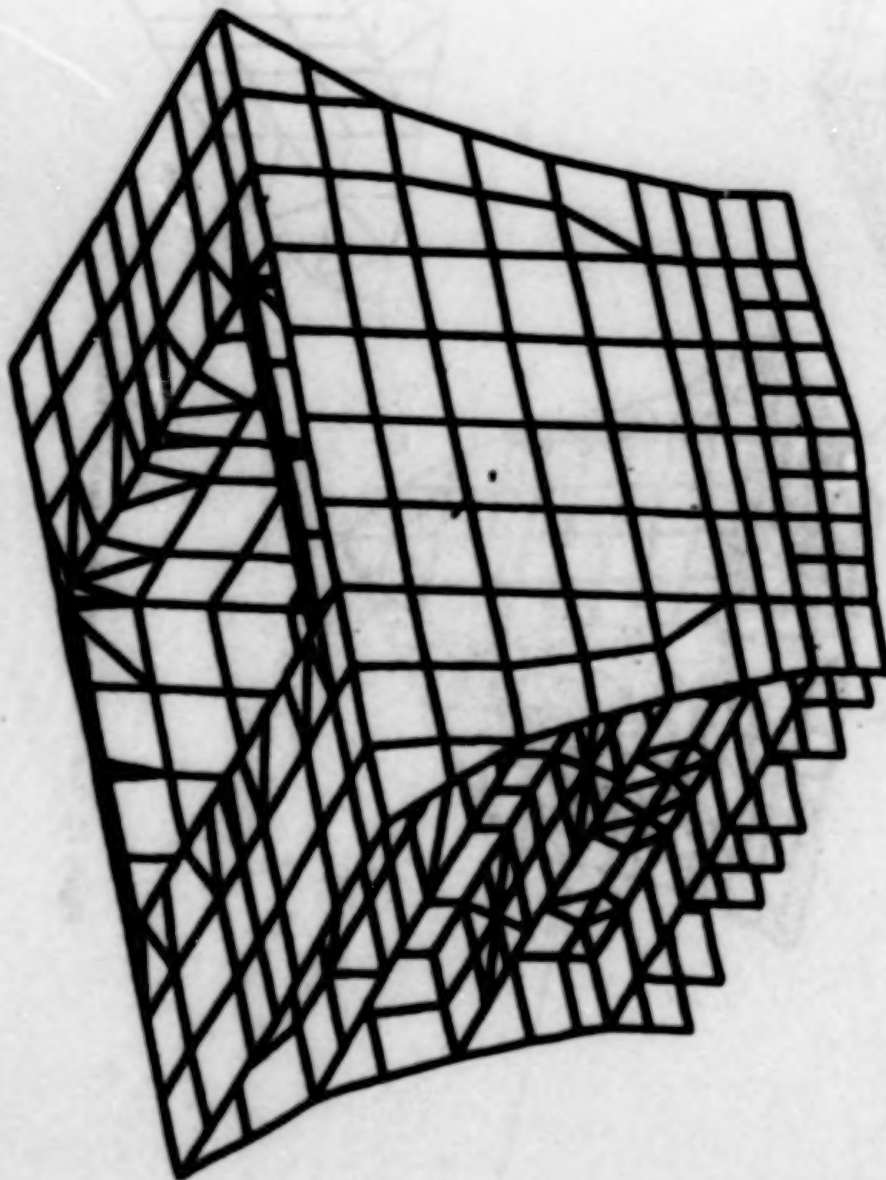


Figure 11: Finite element model aft launcher

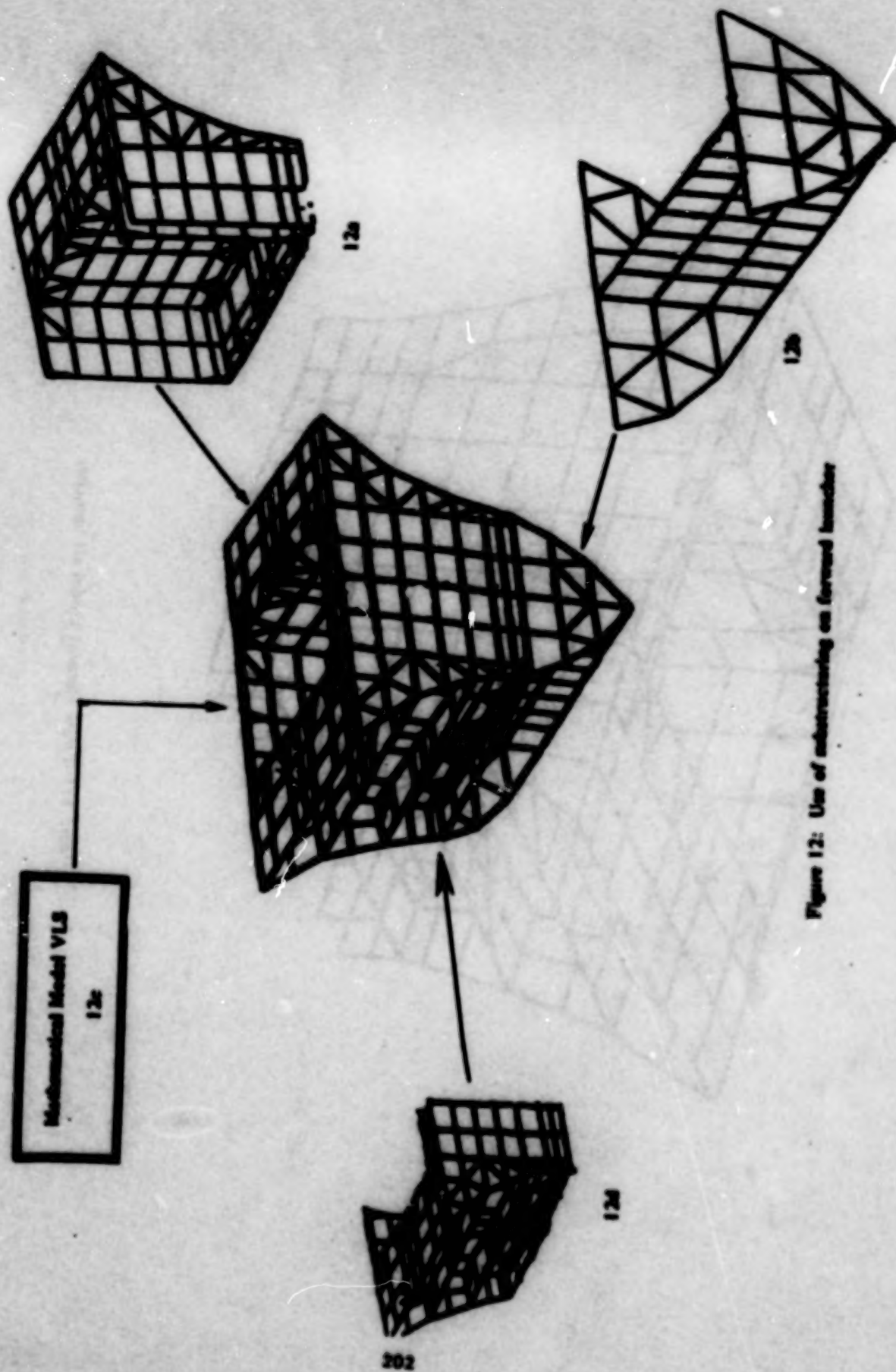


Figure 12: Use of substructuring on forward launchers

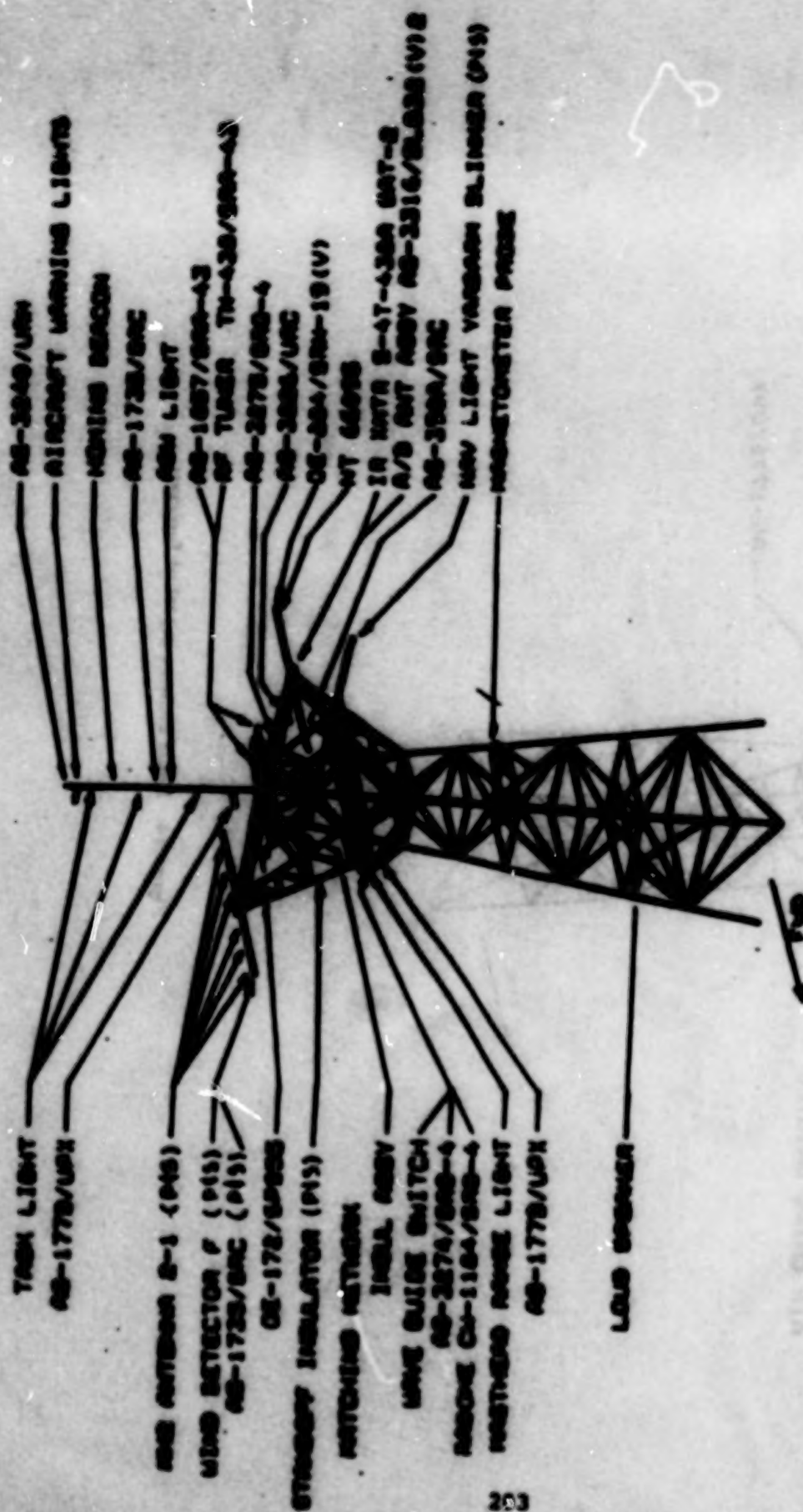


Figure 13: Finite element model of main mast

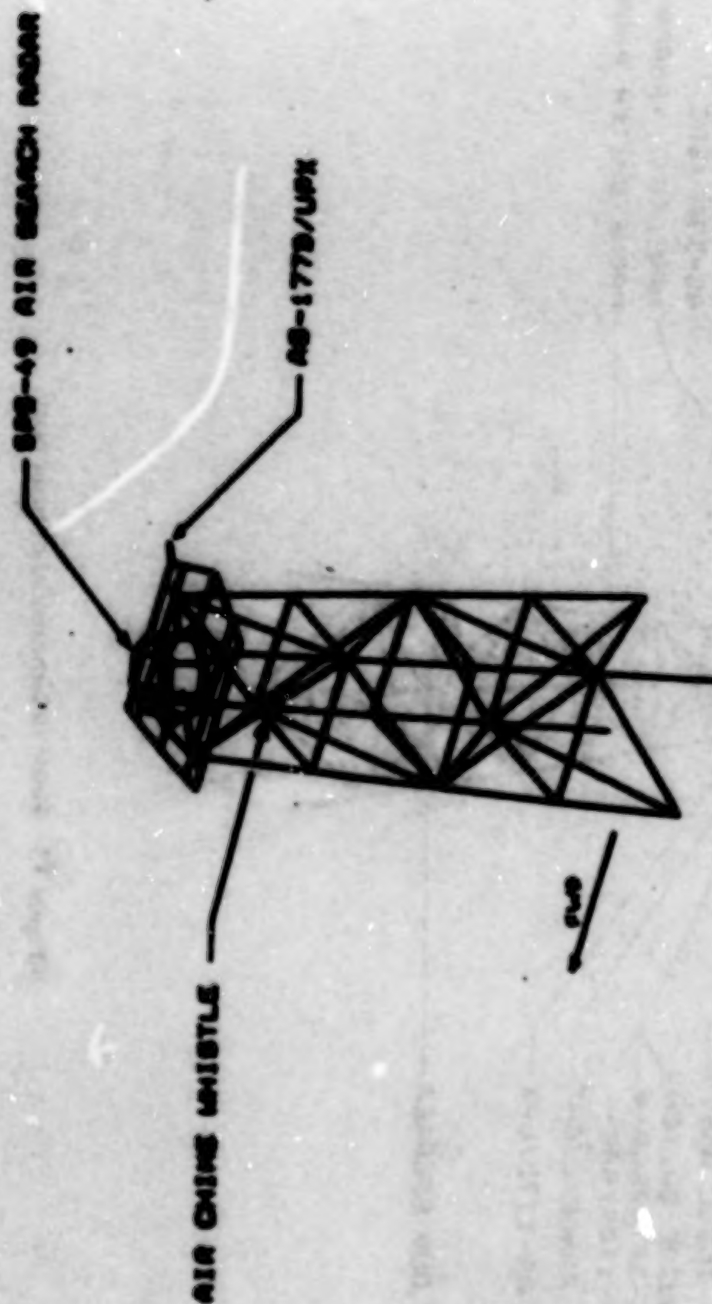


Figure 14: Finite element model of tower

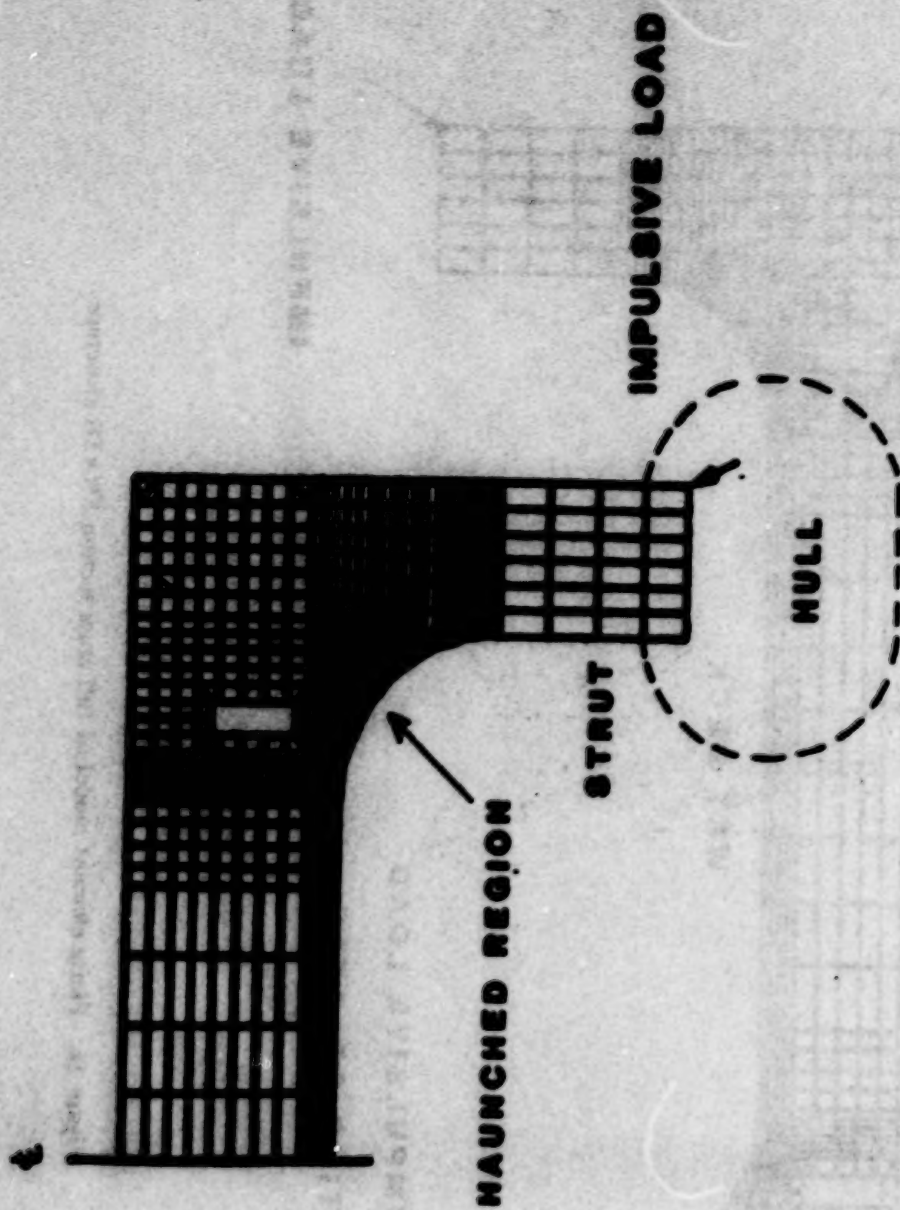


Figure 15: Finite element model of half cross section SWATH structure

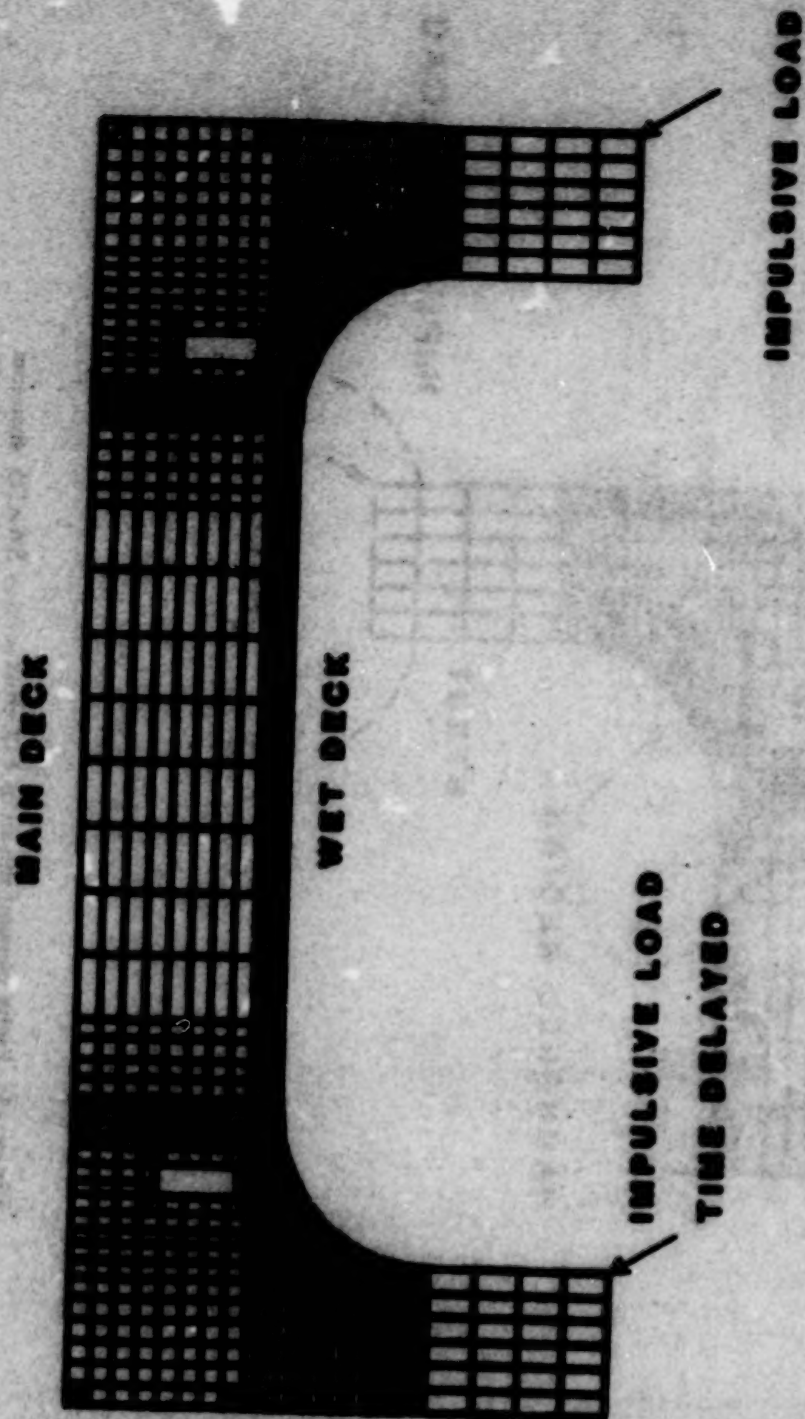


Figure 16: Finite element model of full cross section SWATH structure

CALCULATION OF FORCES ON MAGNETIZED BODIES USING COSMIC NASTRAN

JOHN SHEERER

TEXAS INSTRUMENTS DATA SYSTEMS GROUP

INTRODUCTION:

The analogy between the equations of Heat Transfer and Magnetostatics has been used by several researchers to calculate magnetic fields in a variety of applications and shown to give correct results in theoretically verifiable cases. The resultant fields and fluxes have been used to find forces upon moving charged particles in the design of particle accelerators (1) and upon electrical conductors in the design of electrical machinery (2). Magnetostatic forces, due to the action of magnetic fields on magnetically permeable bodies, are a less tractable problem. Analytical methods (3,4,5) generally applied to obtaining an net force on a body of iron in air have produced apparently conflicting expressions for forces based upon the virtual work method, calculation of Maxwell stresses, and use of a free magnetic pole model. Carpenter has reconciled the apparent discrepancies (5) but the expressions obtained are not entirely suitable for finite element analysis, as they are shown by Carpenter to be mathematical devices to produce an equivalent force on a body rather than a true representation of a force distribution. While in many cases an equivalent force is all that is required, such an approach is not appropriate to problems involving structural deformation.

MAGNETOSTATIC EQUATIONS

The equations of Magnetostatics are based upon forces between field sources. In the S.I. system of units, the Ampere is the current required to produce unit force between two long parallel conductors separated by unit distance. In the older c.g.s. e.m.u. system, unit force was produced between unit magnetic poles in vacuo at unit distance. The imaginary but convenient concept of a magnetic pole is difficult to express in the modern system of units. It is convenient to describe the properties of a magnetic material in terms of the applied magnetic field, H , and the volume magnetization, M , where the flux density, B , is given by:

$$\underline{B} = \mu_0 \underline{H} + \underline{M} \quad (1)$$

where μ_0 is the permeability of free space. This is the Kennelly SI system. In the Sommerfield S.I. system the magnetization is dimensionally the same as the field strength and is also operated on by the permeability constant to obtain B :

$$\underline{B} = \mu_0 (\underline{H} + \underline{M}) \quad (2)$$

In order to use the NASTRAN heat transfer solver the equation must be recast in the form :

$$\underline{B} = \mu \underline{H} \quad (3)$$

where μ is the permeability of the material. This formulation is analogous to the heat transfer equation but in no way represents the physical relationship between B and H . At the boundary between materials of different permeability the total magnetic flux, Φ , is conserved. The normal component of magnetic flux, B_n , and the tangential component of the magnetic field, H_n , are also continuous across the interface. These conditions are essential to all the subsequent force derivations.

MAGNETOMECHANICAL DEVICES

A magnetic field has associated with it an energy given by the equation

$$U = \int \underline{H} \cdot d\underline{B} \quad (4)$$

Given that in equation (3) the value of permeability in a ferromagnetic material is several thousands, it is apparent that the energy required to support a given flux density in an air gap greatly exceeds that required if the same volume contains a ferromagnetic material. Two categories of device utilize this mechanically: devices employing electromagnets generate a mechanical force to reduce the volume of an airgap, thereby minimizing magnetic field energy, when a magnetizing force is generated by a coil, while in stored energy devices a permanent field is generated by a permanent magnet, producing a force that is eliminated by the action of an opposing electromagnet when it is required to remove the mechanical force. The magnetic field energy may be converted to kinetic energy or strain energy.

THE VIRTUAL WORK METHOD

The virtual work method is the most widely known means of force calculation. It is generally applied by calculation of the working gap energy, which is subsequently differentiated with respect to a direction of motion to obtain a force in the direction under consideration. In air, the usual working gap,

$$\underline{B} = \mu_0 \underline{H} \quad (5)$$

Thus, by substitution in equation (4), an expression for air gap energy from which forces may be derived is obtainable in certain

geometries. Between two large parallel plates the force per unit area is:

$$F = \frac{1}{2} \mu_0 H^2 \quad (6)$$

This formula neglects the energy changes within the magnetic material, and applies to a highly idealised orientation. Further, the result is a global force rather than a distributed force. Physically, the assumptions are that the magnetic material is of infinite permeability and that the source of magnetomotive force (MMF), is infinitely stiff. If the field energy of the magnetic material filling the gap is considered equation (6) becomes

$$F = \frac{1}{2} \mu_0 \left(1 - \frac{\mu_0^2}{\mu^2}\right) H^2 \quad (7)$$

ADAPTION FOR FINITE ELEMENT METHOD

The finite element method can be applied to the virtual work model to obtain a higher degree of accuracy. Since the NASTRAN heat transfer solver calculates both B and H it is possible to obtain the energy associated with each element for an initial configuration and geometrical perturbations thereof. If the permeability across the element is constant, as it must be, equation (4) becomes simply,

$$U = \frac{1}{2} B \cdot H \quad (8)$$

If a rigid body is being analysed, perturbation in the six degrees of freedom, with the system energy summed in each case, should in theory provide complete data about the forces acting upon the body. The advantages of the finite element approach over analytical and boundary element methods are:

- (I): Account is taken of field energy inside the magnetic materials
- (II): The technique comprehends non-uniform fields, leakage flux etc. in the circuit

Since only an equivalent force is derived the approach is inapplicable to problems where deformation occurs and a distributed force is required. It is particularly suited, however, to applications where the displacement or deformation is constrained to a single degree of freedom. Applications such as linear and rotary solenoid/actuators or rotating armature printheads may be modelled using this technique.

THE MAXWELL STRESS METHOD

Equation (8) may be rewritten:

$$U = \frac{1}{2} \mu H^2 \quad (9)$$

For a spatially varying field, the equation has the more general form

$$U = \frac{1}{2} \iiint \mu H^2 dx dy dz \quad (10)$$

giving x, y and z force components of the form

$$F_x = \frac{1}{2} \iiint \frac{\partial \mu}{\partial x} H^2 dx dy dz \quad (11)$$

If the permeability is constant then equation (11) has a value of zero. Consequently, traction forces are only exerted at the boundaries between regions of different permeability, or where the permeability varies continuously. A spatially varying field will not of itself produce traction forces. If a closed surface is constructed around a magnetized part then, from equation (11) a stress through the surface and a pressure tangential to it are obtained,

$$F_s = \frac{1}{2} \mu H^2 \cdot \hat{n} \quad (12)$$

$$F_p = \frac{1}{2} \mu H^2 \times \hat{n} \quad (13)$$

The expressions reduce to zero if no discontinuities in H are enclosed. They may be resolved into components normal and tangential to the surface:

$$F_n = \frac{1}{2} \mu (H_n^2 - H_t^2) \quad (14)$$

$$F_t = \mu H_n H_t \quad (15)$$

If the surface is constructed outside of a magnetic part (in free space) then $H_t = 0$. Alternatively a surface may be constructed within the part. In this latter case no field sources are enclosed, since all field sources lie at the interface between the part and free space, and a zero resultant force is obtained.

ADAPTION TO THE FINITE ELEMENT METHOD

Equations (14) and (15) may be applied by construction of a surface enclosing a part, located arbitrarily close to the boundary between the part and free space. This force acts thru a closed surface on enclosed field sources, and are not necessarily a physical representation of the true surface force distribution. The case will now be considered where a pill-box is constructed normal to the boundary, of vanishingly small thickness, and extending to both sides of the boundary. By this construction the sources of field are localized within the box and forces may be obtained in direction both out of and into the magnetic body:

$$\mu_o H_o_n = \mu_o H_i_n + M \quad (16)$$

$$H_o_t = H_i_t$$

where the suffices o and i denote inside and outside values of the field and permeability. If μ_r is defined as the ratio of internal to external permeability then

$$F_n = \frac{1}{2} \mu_o \left(1 - \frac{1}{\mu_r}\right) H_o_n^2 \quad (17)$$

$$F_t = \mu_o \left(1 + \frac{1}{\mu_r^2}\right) H_o_n H_o_t \quad (18)$$

This appears to be a local force, and reduces to equation (7) for the case where the field is normal to the interface. The model, however, does not impart physical insight into the phenomena, and there are implied assumptions in the neglect of the sides of the pill box surface.

THE FREE POLE METHOD

The magnetization process consists of realignment of magnetic domains in a ferromagnetic material so as to orient them with the external magnetic field. Within the material, macroscopically, each North pole produced will be cancelled by a South pole, and there will be no discontinuities in H within the material. At the boundaries of the material, however, the alignment (polarization) of the domains produces free magnetic poles. The magnetization, M , is equal to the free pole density. The free poles are acted upon by the field H with a force in proportion to both H and M ,

$$F = H \cdot M \quad (19)$$

The normal component of the force acting on M free poles is obtained by considering the force which must be applied to an increment dM , in order to move it to the interface from an arbitrary noncoincident point. Since the free poles themselves affect the relationship between internal and external values of H , an integration is required to obtain the normal force:

$$F_{i_n} = \int_0^M H_{i_n} dM = \frac{1}{2} \mu_o (H_o_n^2 - H_i_n^2) \quad (20)$$

In considering the field from the poles alone, it is physically apparent that it must be normal to the surface on which the poles lie. Therefore, the tangential force is simply:

$$F_t = \mu_o H_o_t M \quad (21)$$

These equations may be reformulated to be comparable with the results of the other methods discussed:

$$F_n = \frac{1}{2} \mu_0 \left(1 - \frac{1}{\mu_r}\right) H_n^2 \quad (21)$$

$$F_t = \mu_0 \left(1 - \frac{1}{\mu_r}\right) H_n H_t \quad (22)$$

MASTRAN CALCULATIONS

For the theoretically verifiable case of an air gap between two large parallel plates, forces on the plates have been calculated from MASTRAN heat transfer output by the methods described above. Since the methods reduce to the same theoretical base equation in this geometry, it is not surprising that the results are in agreement with theory and with each other. The problem of finding a non-trivial yet theoretically verifiable test problem remains.

COMPARISON OF DERIVATIONS

Equations for a net magnetic traction force have been obtained by virtual work and Maxwell stress methods. Distributed forces have been obtained by the free pole method and a variation of the Maxwell Stress method. All methods are equivalent for cases where the magnetic field at an interface between the magnetic medium and air is normal to the surface. The equations governing the angle of field on either side of the medium are:

$$H_i \cos \alpha_i = H_o \cos \alpha_o - (N/\mu_0) \cos \alpha_i$$

$$H_i \sin \alpha_i = H_o \sin \alpha_o$$

where α_i is the incident angle of the internal field H_i and α_o is the incident angle of the external field H_o . Thus,

$$\tan \alpha_i = H_o \sin \alpha_o / (H_o \cos \alpha_o - (N/\mu_0) \cos \alpha_i) \quad (24)$$

For reasonable values of N , $\alpha_i \neq 0$. Thus in all but extremely saturated magnetic materials the normal force will be orders of magnitude larger than the tangential forces, and the latter can be ignored for all practical purposes.

Although not admired by theoreticians, the polar model of magnetism is mathematically valid and there is no reason to doubt the results obtained above. The polarization model is based on an analogy between electrostatic and magnetostatic phenomena which is not entirely valid, but which provides the same results in terms of force and energy as for the more correct domain model of ferromagnetism. The use of analogy has been compared unfavourably with the mathematical purity of Maxwell's equations, since it is little known that these were derived using a tortuous mechanical analog of electrostatics and magnetostatics. The Maxwell stress method described above is one of three stress systems presented by Maxwell, one of which is in total contradiction and has been described by Carpenter (5) as completely useless. The discrepancy between the Maxwell and free poles methods is likely due to the neglect of the side surfaces of the pill-box structure described above, and in any case is of negligible magnitude.

CONCLUSIONS

The methods described may be used with a high degree of confidence for calculations of magnetic traction forces normal to a surface. In this circumstance all models agree, and test cases have resulted in the theoretically correct result. It is shown above that the tangential forces are in practice negligible. The surface pole method is preferable to the virtual work method because of the necessity for more than one NASTRAN run in the latter case, and because distributed forces are obtained. The derivation of local forces from the Maxwell stress method involves an undesirable degree of manipulation of the problem and produces a result in contradiction of the surface pole method.

REFERENCES

- [1]: J. Sinkin and C.W. Troubridge, IEE Proc., Vol. 127, 368-374 (1980)
- [2]: J. L. Brauer, Research and Development, 71-73, (Dec. 1984)
- [3]: Maxwell, Electricity and Magnetism, Clarendon Press (1891)
- [4]: Lehman, Trans A.I.E.E., 45, 383, (1926)
- [5]: Carpenter, Proc. IEE, 107C, 19, (1959)

**BUCKLING ANALYSIS OF THE QUADRIPOD
STRUCTURE FOR THE NASA 70-METER ANTENNA**

CHIAN T. CHIAN

Jet Propulsion Laboratory, Pasadena, CA

SUMMARY

The diameter extension of the three NASA DSN (Deep Space Network) large Earth-based antennas from the existing 64 meters to 70 meters will provide a needed increase in space communication capability for the Voyager 2 - Neptune encounter in August 1989.

As part of the upgrade effort, a slim-profiled quadripod structure was designed to support the 7.7-m-diameter subreflector for the 70m antenna. The new quadripod design, which particularly emphasizes reduced radio-frequency (RF) blockage, is achieved by means of a narrow cross-sectional profile of the legs.

Buckling analysis, using NASTRAN, was conducted in this study to verify the safety margin for the quadripod structural stability.

INTRODUCTION

The upgrade of the three NASA/JPL 64m diameter antennas will provide a needed increase in Earth-based space communication capability at all three Deep Space Communications Complexes: Goldstone, California (DSS-14); Canberra, Australia (DSS-43); and Madrid, Spain (DSS-63). In addition to the increase of the antenna aperture area from 64m to 70m, a number of significant improvements in the quadripod, surface panels, subreflector positioner, and microwave aspects are included in the design. The upgrade objective is to increase the radio-frequency (RF) gain/noise temperature (G/T) by about 1.9 dB at X-band (8.45 GHz).

As part of the upgrade effort, a new, high-precision 7.7-m (25.4 ft) diameter subreflector and positioning mechanism are needed. Consequently, an entirely new quadripod structure is required to support the subreflector. The new quadripod design particularly emphasizes reduced RF blockage, which is achieved by means of a narrow cross-sectional profile of the legs. The profile adopted provides about 0.32 dB of gain improvement in comparison with the existing 64 meter design (Ref. 1). This report addresses the stability analyses performed on the new quadripod design to ensure that it has an adequate safety margin for buckling and that the minimum natural frequency is compatible

with control system requirements.

QUADRIPED DESIGN

The quadripod assembly is a tubular space frame steel structure with four trapezoidally shaped legs connected to another large space frame at the apex, as shown in Fig. 1 and 2. The four legs are supported at the corner points of the rectangular truss system of the main reflector structure as shown in Fig. 2. The final slim profile leg cross-section envelope selected is shown in Fig. 3. Also, the quadripod will be used occasionally for hoisting the cassegrain feed cones, the subreflector, or other heavy equipment which may be removed and reinstalled.

The finite element model of the 70m quadripod truss structure is a pin-jointed frame (3 translational degrees of freedom per node) comprising 156 nodes, 445 axial bars, and 28 membrane plates. The JPL/IDEAS (Iterative Design of Antenna Structures) computer program was used for analysis and design (Ref. 2). The program employs the optimality criterion to minimize the structural weight (objective function) with a constraint placed on the lowest natural frequency. A subsequent analysis of the 70m model, accounting for bending and torsional stiffness at the joints (6 degrees of freedom per node) using NASTRAN (Ref. 3), showed only a small increase in the torsional natural frequency (Ref. 1). Outrigger braces (Fig. 2) were added thereafter to increase the lowest natural frequency.

Due to the slinness of the quadripod legs, the following requirements had to be considered:

Static buckling stability: The occasional use of the quadripod as a derrick required a check on the possibility of buckling instability. A factor of safety of at least 1.5 was recommended. The smallest eigenvalue found from a structural buckling analysis is equivalent to this factor of safety. Since the IDEAS program that was used for design and natural frequency analyses does not perform buckling analysis, the new quadripod design was optimized for the frequency requirement using IDEAS and then analyzed for buckling using NASTRAN (NASA Structural Analysis Program). NASTRAN was used to determine the buckling loads of the natural frequency-constrained quadripod design. Two versions of the NASTRAN program were used because of possible different finite element formulations: the NASTRAN-COSMIC (NASA's Computer Software Management and Information Center) (Ref. 4) and the proprietary NASTRAN-HSC version (MacNeal-Schwendler Corporation) (Ref. 3). The two versions were used both for the buckling and natural frequency analyses, and the results obtained were compared.

RESULTS OF BUCKLING ANALYSIS

The Rigid Format No. 5 of the NASTRAN program was used to perform the buckling analysis. The results of the buckling analysis for the quadripod pin-joined model are presented in Table 1. Both the COSMIC and MSC versions of the NASTRAN program were used and compared. Four antenna configurations, each subject to the maximum loads anticipated to be hoisted when employing the quadripod as a derrick, in addition to the quadripod weight, were considered in the quadripod buckling analysis:

- (1) Zenith look with outriggers.
- (2) Zenith look without outriggers.
- (3) Horizon look with outriggers.
- (4) Horizon look without outriggers.

Table 1 shows that the outriggers tend to at least double the buckling load capability.

FINITE ELEMENT PLATE STIFFNESS REPRESENTATION

Comparisons of the COSMIC-NASTRAN and MSC-NASTRAN results on the quadripod model in Table 1 show that the plate element CQDNEM2 in the COSMIC version gives a different stiffness matrix representation compared with the CQUAD4 plate element in the MSC version, or with the IDEAS plate element CQDNEM.

A parametric study was conducted to readjust the moduli of elasticity of the COSMIC CQDNEM2 plate elements to produce results similar to those of the MSC elements. Comparison of the results of the stiffness parameterization study is shown in Table 2 for the quadripod buckling analysis. The plate element used in the NASTRAN-COSMIC employs the constant stress formulation, while the elements used in the NASTRAN-MSC or IDEAS permit a stress variation. As a result, the COSMIC element generates a stiffer structure than the other elements.

CONCLUSIONS

A structural stability study was conducted for the 70m antenna quadripod. The quadripod was found to be stable in buckling when the outrigger braces were included. One computer program used in the investigation was found to give an over-estimate of the stiffness. In order to correct the excessive stiffness, a parametric study was conducted to derive empirical coefficients to adjust the plate stiffness for future use of this program.

REFERENCES

1. Cuccchiassi, J. J., "A New 70-Meter Antenna Quadripod With Reduced RF Blockage," TDA Progress Report 42-82, pp. 24-30, Jet Propulsion Laboratory, Pasadena, CA, Aug. 15, 1985.
2. Levy, R., and Chai, K., "Implementation of Natural Frequency Analysis and Optimality Criterion Design," Computers and Structures, Vol. 10, pp. 277-282, Pergamon Press Ltd., Great Britain, 1979.
3. McCormick, C. W., Editor, MSC/NASTRAN User's Manual, MSR 39, The MacNeal-Schwendler Corporation, 1983.
4. The NASTRAN Theoretical Manual (level 15.5), NASA SP-221 (06), Scientific and Technical Information Office, NASA, Wash. DC, Jan. 1981.

ACKNOWLEDGEMENT

The author acknowledges the assistance given by his JPL colleagues, Dr. R. Levy and J. Cuccchiassi, during the various execution steps of this work.

Table 1 The quadruped buckling analysis results

Case	Antenna configuration	NASTRAN COSMIC version	NASTRAN MSC version
1	Zenith lock, with outriggers	22.81	12.27
2	Zenith lock, without outriggers	9.23	(not run)
3	Horizon lock, with outriggers	12.87	3.77
4	Horizon lock, without outriggers	4.12	1.66

Table 2 Comparison of the plate element stiffness and the smallest eigenvalues for the quadruped buckling analysis

Program	Plate element	Young's modulus, N/m^2 (psi)	Shear modulus, N/m^2 (psi)	λ_{min}
(a) Zenith Lock Antenna Configuration, with Outrigger Braces:				
NASTRAN-MSC	CQUAD4	20.0×10^{10} (29.0×10^6)	8.3×10^{10} (12.0×10^6)	12.27
NASTRAN-COSMIC	CQDMEM2	10.7×10^{10} (15.5×10^6)	4.4×10^{10} (6.4×10^6)	12.30
(b) Horizon Lock Antenna Configuration, with Outrigger Braces:				
NASTRAN-MSC	CQUAD4	20.0×10^{10} (29.0×10^6)	8.3×10^{10} (12.0×10^6)	3.77
NASTRAN-COSMIC	CQDMEM2	5.3×10^{10} (7.5×10^6)	2.2×10^{10} (3.2×10^6)	3.97

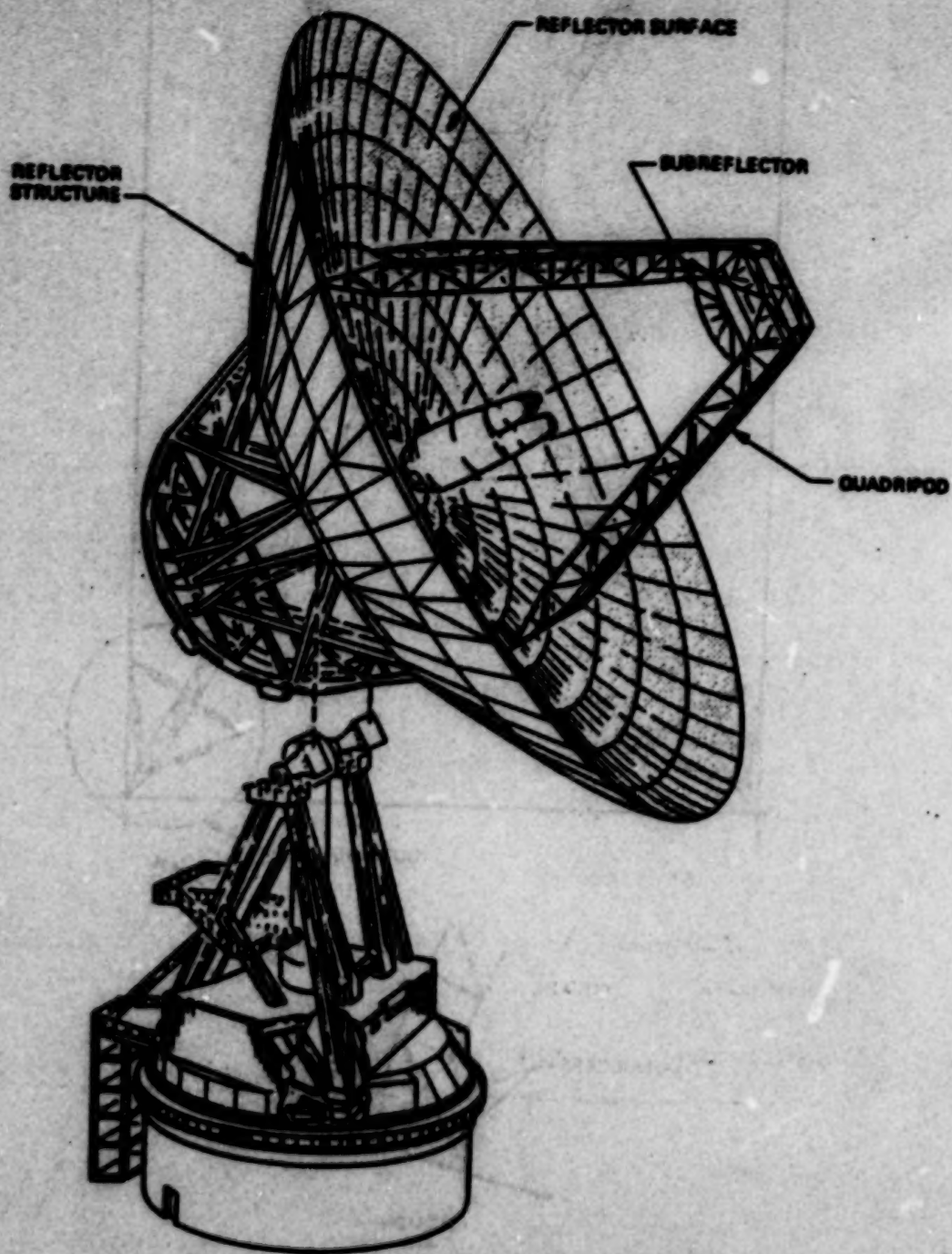


Fig. 1. Antenna quadripod and reflector system

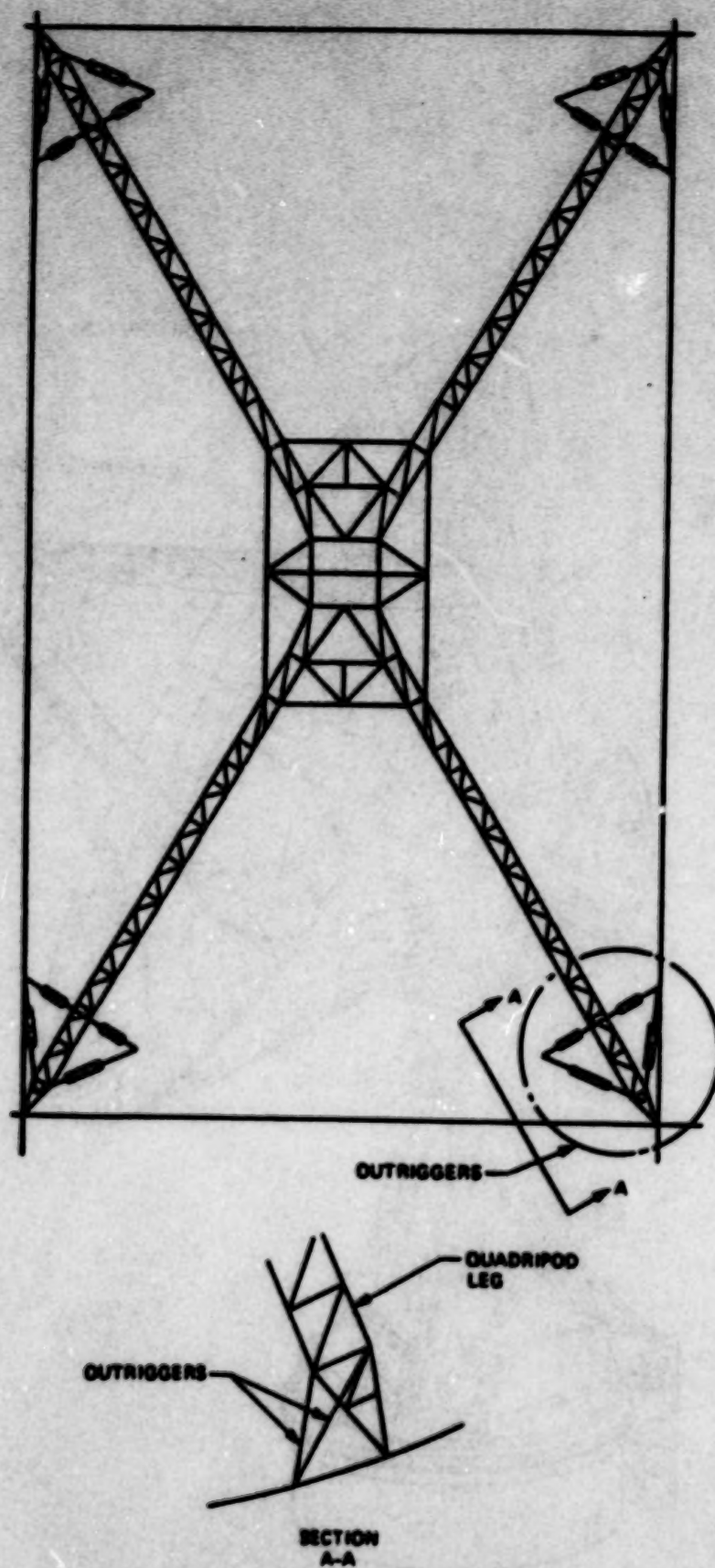


Fig. 2. Plan view of 70-m quadripod with outriggers

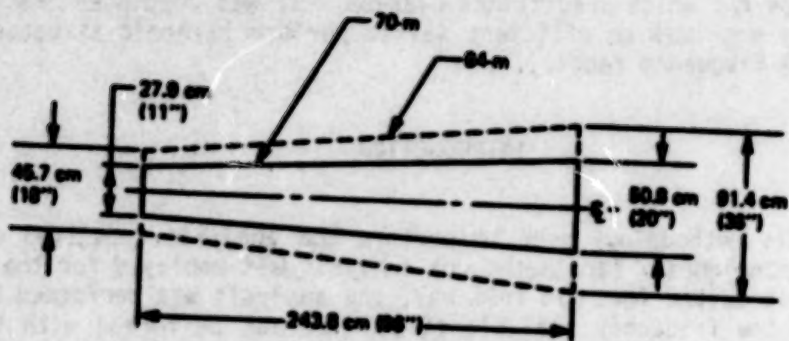


Fig. 2. Quadrilateral cross-sectional profile

THEORETICAL ANALYSIS OF HVAC DUCT HANGER SYSTEMS

R.B. Miller
MEF Engineering, Inc.

SUMMARY

The transmission of vibration from heating, ventilation, and air conditioning (HVAC) systems through a structure can be a potential source of unwanted noise in a ship or building. In order to effectively reduce the transfer of vibration from HVAC ducting to the supporting structure, the ducting may be supported with resilient hangers. This paper addresses methods which together can be used to analyze the harmonic response of an HVAC duct hanger system over an extensive frequency range. The finite element, component mode synthesis, and statistical energy analysis methods are demonstrated. Results for the duct hanger analysis are presented including vibratory response and power flow calculations. The methods are shown to yield reasonably close predictions for the frequency ranges for which predictions overlap. It was concluded that the overall methodology provides an efficient way to perform harmonic structural analysis over a wide frequency range.

INTRODUCTION

The overall methodology used to perform the analysis consisted of several mathematical techniques. Each method of analysis was employed for the frequency range it is best suited for. In this way, the analysis was performed very efficiently. The low frequency analysis (0-300 Hz) was performed with the finite element method (FEM) using NASTRAN. Standard finite element modeling of the system was performed in this frequency range. The mid-range (300-1,000 Hz) was analyzed using Component Mode Synthesis (CMS) with NASTRAN. For this analysis, the duct (a cylinder in this case) was modeled with generalized coordinates as a modal component. A pre-processor was developed to provide NASTRAN with the required generalized coordinate properties and modal expansions for the duct. The high frequency range (800-5,000 Hz) analysis was conducted with Statistical Energy Analysis (SEA) coupled with a closed-form harmonic beam analysis program. These techniques cover overlapping frequency ranges, therefore providing independent checks on each analysis. Following a brief discussion of each method of analysis, results for a typical duct hanger configuration are presented.

TECHNICAL APPROACH

The four methods used in predicting the harmonic response of a section of an HVAC ducting system with duct hangers are presented in the following paragraphs. The reason for using several techniques is to minimize cost and maximize accuracy and efficiency of the analysis. The CMS method plays a crucial role in that it economically bridges the gap between the FEM and SEA solutions.

Finite Element Analysis

The finite element method (FEM) is an excellent method for analyzing the harmonic response of a duct hanger system at low frequency. The code NASTRAN was selected for conducting the analysis (Reference 1). NASTRAN has a large amount of flexibility and is able to account for a high level of detail in structural modeling. With this method it is possible to model each component of the system with sufficient detail to accurately represent the modes in the low frequency range of analysis. Typically, at least 6 to 10 grids per wavelength are required for accurate solutions.

A typical NASTRAN model of a duct hanger system is shown in Figure 1. Due to symmetry it was only necessary to model half of the system.

Selected mode shapes of the first 10 modes are given in Figure 2. The number of axial half-waves and circumferential waves are identified for each mode.

The FEM becomes costly when a large number of modes of a cylinder are to be considered. This is because each wave across the cylinder in both longitudinal and circumferential directions must be modeled. As the number of degrees of freedom is increased, the cost also increases. Harmonic analysis involves the inversion of the complex matrix shown in Equation (1).

$$[-\omega^2 M + i\omega C + K]u = F \quad (1)$$

This matrix must be inverted for each frequency analyzed. For example, if one desired to compute a response every 10 Hz from 1-500 Hz, this would require 50 inversions of the complex matrix in Equation (1).

The FEM is used at low frequency (0-300 Hz) due to the high reliability and accuracy of the method. The analysis was performed at 10 Hz intervals over the frequency range. Greater accuracy in the neighborhood of resonances may be obtained by using a finer frequency increment. The results of this harmonic analysis provides a basis of comparison for other more cost effective methods discussed subsequently.

Component Mode Synthesis

In order to improve accuracy and efficiency of the FEM, it is possible to provide a model description for a component when the associated natural frequencies and mode shapes are known. Component mode synthesis (CMS) is a method which allows the cylinder to be described in terms of modes and the duct hanger assembly to be modeled with finite elements. Since the majority of the degrees of freedom of the finite element model are associated with the cylindrical duct, it is desirable to replace the finite element model of the duct by a modal representation. Fortunately, the natural frequencies and modes of a cylinder are well known (Reference 2). Donnell shell theory was selected on the basis of accuracy, especially for the mid-frequency range of this analysis.

The duct of the HVAC test section consists of a steel duct with end flanges. Typical values for properties used in analyzing the duct are given in table I.

For short cylinders ($L/R < 8$, L = length of cylinder, R = radius), there are three mode classifications: torsional, bending and coupled radial-axial modes. The modal pattern for selected radial-axial modes is depicted in Figure 3.

In addition to the linear elastic thin shell assumptions, it is assumed that the ends of the cylinder have shear diaphragm boundary conditions. This boundary condition is equivalent to that of a simply supported beam and is reasonable in the present analysis since the sections selected terminate with flanges on each end.

Small Shell Theory yields the following solution for natural frequencies of axial-radial modes as Equation (2) (Reference 2):

$$\omega_m = \frac{1}{2\pi R} \left[\frac{E}{\rho_0 (1 - \nu)^2} \right]^{1/2} \quad (2)$$

$$\lambda_m = \frac{\left\{ (1 - \nu)^2 \left(\frac{E}{\rho_0} \right)^4 + \left(\frac{E^2}{\rho_0^2} \right) \left[n^2 + \left(\frac{E}{\rho_0} \right)^2 \right]^4 \right\}^{1/2}}{\left(\frac{E}{\rho_0} \right)^2 + n^2} \quad (3)$$

Combining (2) and (3) obtain the form of Equation (4)

$$\omega_m = \left[\frac{E^2}{4\pi^2 (1 - \nu)^2 \rho_0} \left(\left(\frac{L}{R} \right)^2 + \left(\frac{R}{L} \right)^2 \right)^2 + \frac{E^4}{4\pi^2 \rho_0 L^4} \left(\left(\frac{L}{R} \right)^2 + \left(\frac{R}{L} \right)^2 \right)^{-2} \right]^{1/2} \quad (4)$$

The first term under the radical of Equation (4) may be identified as the natural frequency of a flat plate. Thus, it is observed that the natural frequency of the cylinder is based on the sum of the bending term of a flat plate and a membrane term for the cylinder which acts to increase the frequency above that of a flat plate.

Mode shapes used in DNS analysis include tangential and radial components of Reference 2, shown in Equations (5) and (6), respectively:

$$v = B \sin n\theta \sin \frac{m\pi x}{L} \quad (5)$$

$$u = C \cos n\theta \sin \frac{m\pi x}{L} \quad (6)$$

The generalized masses for beam bending modes and cylinder modes are given by Equations (7) and (8), respectively.

$$M_{bm} = \frac{H}{2} \quad m = 1, 2, 3 \dots n = 1 \quad (7)$$

$$M_{cm} = \frac{H}{4} \quad m = 1, 2, 3 \dots n = 0, 2, 3, 4 \quad (8)$$

Given the eigenvalue of Equation (2) and the generalized mass of Equations (7) and (8) the determination of the generalized stiffness and damping terms are straightforward.

Since mode shape magnitudes are arbitrary, C was set equal to 1 and B/C was computed based on Equations (9) through (11).

$$\frac{B}{C} = \frac{a_{33} a_{21} - a_{31} a_{23}}{a_{22} a_{31} - a_{32} a_{21}} \quad (9)$$

where

$$\begin{aligned} a_{11} &= -\xi^2 - \frac{(1-\nu)}{2} n^2 + \lambda^2 & a_{12} &= \frac{(1+\nu)}{2} \xi n \\ a_{22} &= -\frac{(1-\nu)}{2} \xi^2 + \lambda^2 - n^2 & a_{23} &= -n \\ a_{13} &= \nu \xi & a_{31} &= -\nu \xi \\ a_{21} &= a_{12} & a_{32} &= n \\ & & a_{33} &= 1 + k (\xi^2 + n^2)^2 - \lambda^2 \end{aligned} \quad (10)$$

and

$$\begin{aligned} \lambda^2 &= \frac{\rho_s (1-\nu^2) R^2 \omega^2}{\xi} \\ k &= \frac{h^2}{12R^2} \\ \xi &= \frac{mR}{L} \end{aligned} \quad (11)$$

The procedure for coupling the modal representation of a component with the finite element model of any arbitrary structure is found in Section 14 of the NASTRAN Theoretical Manual (Reference 3). Briefly, the finite element model of any grid points not associated with the duct are not affected. The degrees of freedom (DOF) associated with the duct are removed by multipoint constraints which replace the DOF of the grid by a summation of modal coordinates. The response of these modal coordinates is governed by the scalar spring-mass-damper system consisting of the generalized mass, stiffness and damping associated with each mode. In other words, the duct response at each desired point of the duct

has been replaced by an eigenvector expansion. In this way, the size of the matrix required for the duct is limited to the number of modes kept in the analysis. For the duct configuration of Figure 1, 30 modes are required for 20-1000 Hz analysis.

This method has a much greater efficiency than the finite element method, allowing computation from (20-1000 Hz) in the same CPU time required for 0-300 Hz by the FEM. The analysis was performed at 10 Hz increments over the frequency range of 20 to 1,000 Hz. Greater accuracy in the neighborhood of resonances may be obtained by using a finer frequency increment.

Statistical Energy Analysis

The basic assumption used in SEA analysis is that within each band the modes are receiving energy equally. It is further assumed that the ratio of energy transmitted to modes in adjoining sections is the same for all modes within a band. Additional background regarding the SEA technique is found in References 4 and 5.

Analysis is performed by solving for the steady state energy conservation of the sections of the duct. In view of the influence of flanges on duct vibration, an appropriate procedure is to segregate duct resonances into modal groups by duct sections between flanges. For this purpose the duct test model was divided into 2 sections as shown in Figure 4.

A schematic of the mechanical energy transmission within the duct is shown in Figure 5.

Energy levels into section 1 (P_F) may be computed as follows. The desired source parameter is the net time averaged mechanical power transmitted to the set of duct structural modes. In complex notation this input power is given by:

$$P_F = 1/2 \text{ Real } [F v^*] \quad (12)$$

where: "Real" signifies taking the real part of the bracketed complex product and

F = magnitude of applied force to the duct

v^* = complex conjugate of resulting duct velocity

The relation between force and velocity was provided by the impedance of an infinite elastic cylindrical shell (Reference 6).

Of this energy some is lost due to damping in the duct (P_1^D), a certain amount is transferred to adjoining sections (P_{1j}) and the remainder is retained as vibration energy.

Applying the principle of conservation of energy establishes the relationship for the 1th model system as:

$$\text{Net input power } P_1^I = P_1^D + P_1^H + \sum_j P_{1j} \quad (13)$$

The power dissipated in the i th system can be expressed as:

$$P_i^D = \omega \eta_i^D E_i \quad (14)$$

where η_i^D is the dissipation loss factor. The power transferred to the hanger is represented in similar fashion, i.e.,

$$P_i^H = \omega \eta_i^H E_i \quad (15)$$

where η_i^H is the loss factor of the hanger system.

The power transferred to and from adjacent systems is given by:

$$P_{ij} = \omega \eta_{ij} - \omega \eta_{ji} E_i \quad (16)$$

The set of above equations as applied to each of the three identical mode sets is conveniently represented in matrix form as:

$$\omega[\eta][E] = [P] \quad (17)$$

where: $[E]$ is a column matrix of subsystem total energies

$[P]$ is a column matrix of subsystem input power and

$[\eta]$ is a square matrix of dissipation, and coupling loss factors

The coupling loss factors were taken from Reference 4 and the damping loss factor used was that given in Reference 7.

For each 1/3 octave band frequency, the power into the forced section of the duct is given by Equation (12). The corresponding matrix equation can then be solved for the modal energies of each system for each 1/3 octave band; e.g.,

$$[E] = \frac{1}{\omega} [\eta]^{-1} [P] \quad (18)$$

Structural Response

The average velocity associated with each duct section may be obtained from the energy of that section as follows:

$$\bar{v} = \frac{\sqrt{2E}}{m} \quad (19)$$

where m is the mass of the cylinder.

In order to perform accurate statistical energy analysis (SEA), it is necessary to consider the number of modes for each component of the system in the frequency range of interest (10-5000 Hz). For example, consider the typical duct configuration of Figure 1. This system has four components; the cylinder, mount, hanger and foundation. The geometric and material properties of the duct, mount, and hanger are provided in tables I through III. The foundation impedance was taken to be a 0.5-inch infinite steel plate. Shell theory of Donnell predicts 300 modes of the duct section in the frequency range of interest. There are four modes per 1/3 octave band beginning at 800 Hz. The

number of modes in all other components is limited to one or no modes per 1/3 octave band.

In view of the number of modes for each component given above, consider the SEA method. Based on the number of modes per 1/3 octave band for the cylinder, the SEA method is applicable at and above 800 Hz. Due to the low mode count for the remaining components, it would be inappropriate to attempt to represent the mount, hanger, or foundation as a modal subsystem. However, the effect of the hanger assembly on the cylinder may be included through the use of a coupling loss factor. The computation of a loss factor to represent power flow from the cylinder to the hanger assembly was obtained from an analysis of the hanger assembly shown in Figure 6. The method used to obtain the loss factor was that of the Dynamic Direct Stiffness Method (DDSN). This method also provides transfer functions between the response of the cylinder at the attachment point and the response of points along the hanger assembly and foundation. Following SEA analysis of the cylinder, these transfer functions were used to relate the cylinder response to the desired responses of the duct hanger and foundation.

Dynamic Direct Stiffness Method

In order to effectively analyze hanger designs over a large range of frequencies, the DDSN (Direct Dynamic Stiffness Method) was used. A detailed derivation of the method is found in Reference 8. Basically, the method involves a matrix representation of a beam (or network of beams) which is frequency dependent and is an exact solution to the fourth order flexural beam equation for harmonic excitation. A computer program has been developed by NKF to create and solve the system of equations for the DDSN. The computer program has been enhanced to include models for isolators, and attached impedances of infinite beams, plates and cylinders.

RESULTS OF ANALYSIS

In order to demonstrate the methodology just described, the duct section shown in Figure 1 was analyzed. The hanger system consists of a pipe modeled with beams, and an isolator modeled as a beam. The cylinder was modeled with CQUAD elements in the case of the FEM and with Donnell shell eigensolutions for the ONS and SEA methods. The system was harmonically excited by a unit concentrated radial force located 11 inches in from the end of the duct.

The results computed include the velocities on the cylinder and hanger system and the power flow from the excitation through an impedance representing a foundation attachment. The impedance of the foundation in this case was taken to be that of an infinite 1/2-inch steel plate.

The results for the velocity on the duct are presented in Figures 7 and 8. It is observed that the FEM and ONS solutions show reasonable agreement. The main reason for discrepancy is that the ONS method is based on Donnell shell theory which tends to give a low frequency estimate for the first few cylinder modes. Donnell shell theory frequency estimates improve rapidly with wave number. Since the modal mass is fixed per Equations (7) and (8), a low estimate of frequency results in a low stiffness and consequently an estimate of velocity which is slightly conservative. The SEA results are the average velocities over

the cylinder and are only expected to be accurate when there are at least four modes in a band (above 800 Hz). When comparing the OIS and SEA velocities in the 800-1000 Hz range, it is observed that the velocity of the drive point is greater for OIS than for SEA, as expected. In the case of the velocity at the duct below the mount shown in Figure 8, there appears to be only one predominant mode out of several modes in the 800-1000 Hz band. For this reason the OIS prediction is higher than that given by SEA. It is expected that as the analysis of OIS is extended beyond 1000 Hz, the OIS method would approach the SEA solution.

The velocities for the duct hanger system are shown in Figures 9 and 10. The velocity directly above the mount, shown in Figure 9, shows reasonable correlation between all three methods. Again, the appropriate range of comparison between methods is relatively narrow, 0-300 Hz for FEA versus OIS and 800-1000 Hz for OIS versus SEA.

The results for the termination point are shown in Figure 11. The velocities in this case are associated with the axial velocity of the duct hanger at the attachment point to the foundation. It is observed in Figure 11 that there are few modes participating, even in the 800 Hz band. For this reason, the OIS and SEA analyses have not converged. It is anticipated that as the analysis is extended above 1000 Hz, that the OIS analysis would approach the SEA solution.

The power flow results for the axial power flow through the duct hanger into the foundation per unit force of input to the duct are given in Figure 12. The SEA force power magnitudes are low by as much as 10 dB in agreement with the axial termination velocities. The same comments made for Figure 11 apply in this case as well.

The moment power flow results through the duct hanger system to the foundation are shown in Figure 13. In this case the SEA results match closely with the OIS and FEA results.

The analysis presented here involved the following computation times on a VAX 11/780:

- FEA - 8 hours, 0-500 Hz
- OIS - 4 hours, 0-1000 Hz
- SEA - 1 hour, 0-5000 Hz

The relative efficiency and accuracy of each method is now apparent. For a very accurate analysis of the low frequency range, the FEA method is affordable while the OIS method is reasonably accurate for the mid-range and the SEA method is appropriate at the high end of the spectrum.

CONCLUSIONS

In this paper several methods have been presented which, together, may be used in the analysis of duct hanger systems over a wide range of frequencies. The FEA and OIS methods are used for low- to mid-frequency range computations and have been shown to yield reasonably close results. The SEA method yields

predictions which agree with the CNS results for the 800-1000 Hz range provided that a sufficient number of modes participate. The CNS approach has been shown to yield valuable insight into the mid-frequency range of the analysis. It has been demonstrated that it is possible to conduct an analysis of a duct/hanger system in a cost-effective manner for a wide frequency range, using several methods which overlap for several frequency bands. Using several methods in this way gives a high degree of confidence in the results.

REFERENCES

1. McCormick, C.W., "The NASTRAN User's Manual (Level 17.5)."
2. Blevins, R., "Formulas for Natural Frequency and Mode Shape," Van Nostrand Reinhold Co., New York, 1979.
3. MacNeal, R.H., "The NASTRAN Theoretical Manual (Level 17.5)."
4. Lyon, R., "Statistical Energy Analysis of Dynamical Systems: Theory and Applications," The MIT Press, 1975.
5. Miller, R.D. and Kasper, P.K., "Underwater Radiated Noise of a Stiffened Shell: Analytical Methodology Using a Combined Formulation," 57th Shock and Vibration Symposium, 15 October 1986.
6. Hackle, M., "Vibrations of Point-Driven Cylindrical Shells," J. Acoust. Soc. Am. 34, 1553-1557, 1962.
7. Cramer, L., M. Hackle, and E. Ungar, "Structureborne Sound," Springer-Verlag, 1973.
8. Clough and Penzien, "Dynamics of Structures," McGraw-Hill, New York, 1975.

TABLE 1.- DUCT PROPERTIES

Property	Value
Shell Thickness	$h = 0.05 \text{ in.}$
Section Length (x2 Sections)	$L = 40 \text{ in.}$
Section Radius	$R = 4 \text{ in.}$
<u>End Flanges</u>	
Cross-Sectional Area	0.05 in^2
Second Moment of Area	0.00417 in^4

TABLE II.- MONIT PROPERTIES

Property	Value
Young's Modulus	$E = 555 \text{ lb/in}^2$
Shear Modulus	$G = 189.7 \text{ lb/in}^2$
Weight Density	$\gamma = 0.0420 \text{ lb/in}^3$
Cross-Sectional Area	$A = 0.800 \text{ in}^2$
Second Moment of Area	$I = 0.0420 \text{ in}^4$

TABLE III.- DUCT HANGER PROPERTIES

Property	Value
Young's Modulus	$E = 30.0 \text{ E}+6 \text{ lb/in}^2$
Shear Modulus	$G = 11.5 \text{ E}+6 \text{ lb/in}^2$
Weight Density	$\gamma = 0.283 \text{ lb/in}^3$
Cross-Sectional Area	$A = 0.785 \text{ in}^2$
Second Moment of Area	$I = 0.0491 \text{ in}^4$

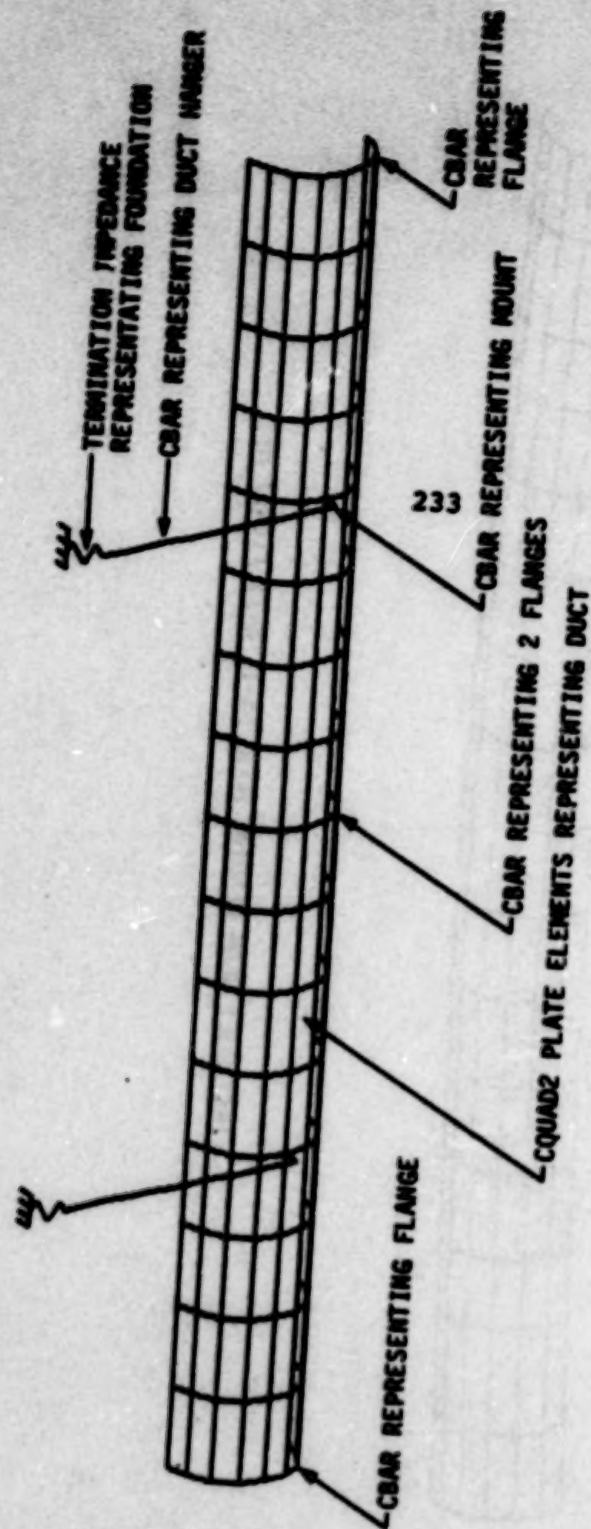


FIGURE 1.- TYPICAL NASTRAN MODEL OF A DUCT HANGER TEST CONFIGURATION



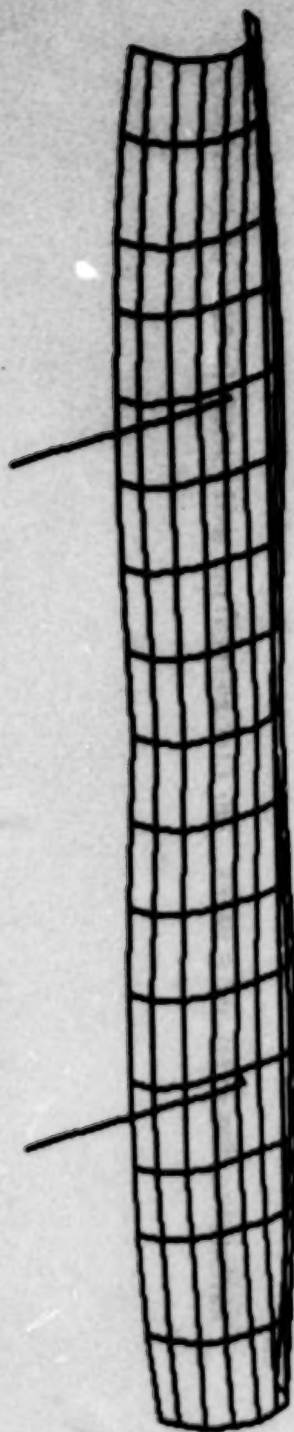
FIRST DUCT BEAM BENDING MODE ($m=1$, $n=1$) (144.7 Hz)

FIGURE 2.- TYPICAL DUCT HANGER SYSTEM MODAL ANALYSIS (SHEET 1 OF 5)



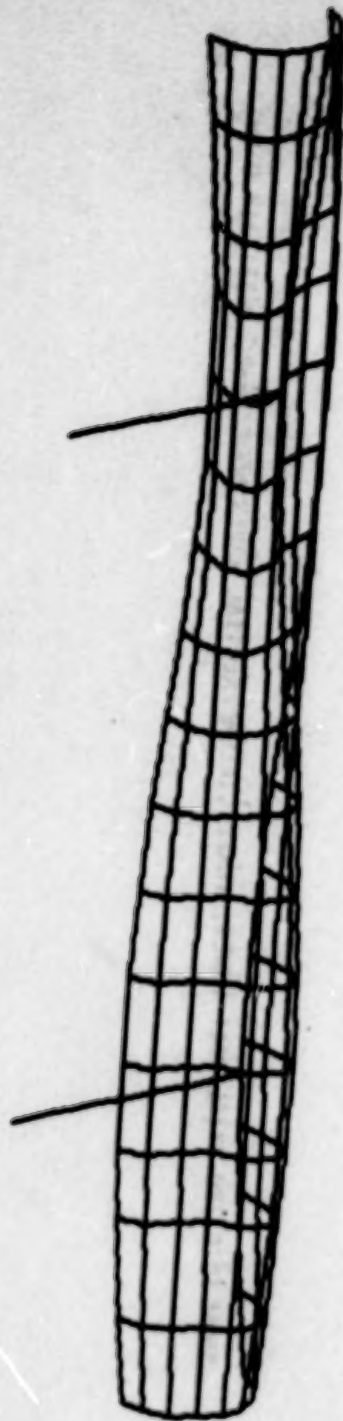
ASYMMETRIC TWO-AXIAL HALF WAVES, TWO CIRCUMFERENTIAL WAVES MODE ($m=2$, $n=2$) (241.3 Hz)

FIGURE 2.- TYPICAL DUCT NUMBER SYSTEM MODAL ANALYSIS (SHEET 2 OF 5)



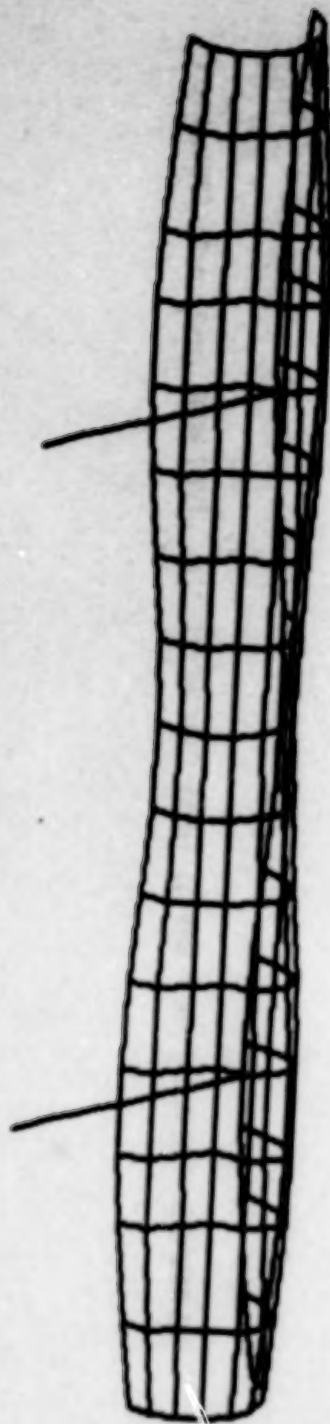
SYMMETRIC TWO-AXIAL HALF WAVES, TWO CIRCUMFERENTIAL WAVES MODE ($m=1$, $n=1$) (200.4 Hz)

FIGURE 2.- TYPICAL DUCT HANGER SYSTEM MODAL ANALYSIS (SHEET 3 OF 5)



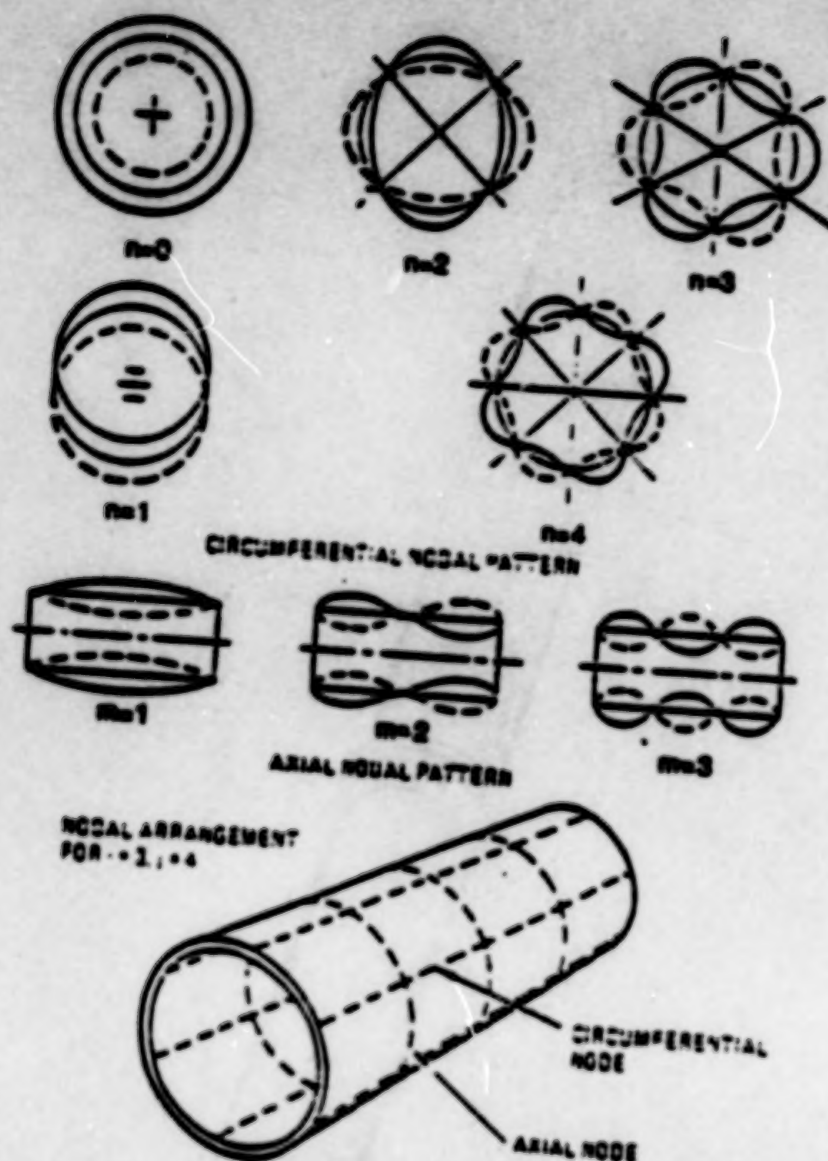
ASYMMETRIC TWO-AXIAL HALF WAVES, THREE CIRCUMFERENTIAL WAVES MODE ($m=2$, $n=3$) (201.3 Hz)

FIGURE 2.- TYPICAL DUCT HANGER SYSTEM MODAL ANALYSIS (SHEET 4 OF 5)



SYMMETRIC TWO-AXIAL HALF WAVES, THREE CIRCUMFERENTIAL WAVES MODE ($m=2$, $n=3$) (318.0 Hz)

FIGURE 2.- TYPICAL DUCT HANGER SYSTEM MODAL ANALYSIS (SHEET 6 OF 6)



n = Number of Axial Half-Waves
 m = Number of Circumferential Waves

FIGURE 3.- NODAL PATTERNS FOR A SIMPLY SUPPORTED CYLINDER WITHOUT AXIAL CONSTRAINTS (REFERENCE 2)

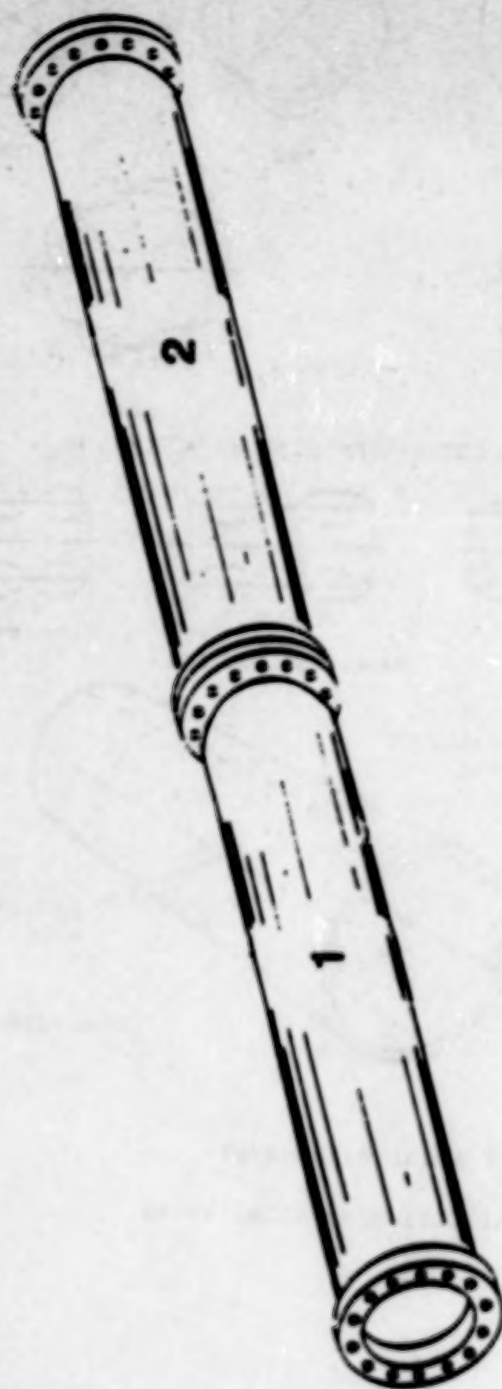


FIGURE 4.- TYPICAL DUCT SECTIONS

P_1^D = POWER DISSIPATED BY DUCT DAMPING

P_1^H = POWER TRANSFERRED TO DUCT HANGER

P_{12} = POWER TRANSFERRED BETWEEN SECTION 1 AND 2

P_F = VIBRATION POWER TRANSMITTED BY POINT FORCE

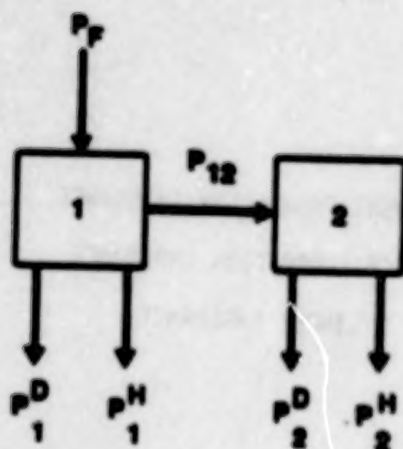
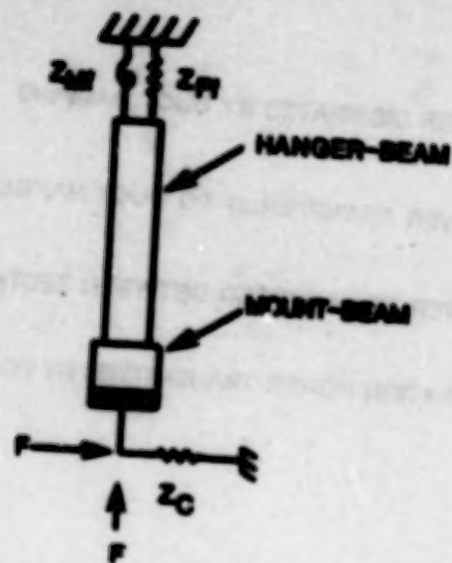


FIGURE 5.- SCHEMATIC REPRESENTATION OF SEA MODEL OF A DUCT HANGER SYSTEM BY NODAL SUBSYSTEMS



- Z_M = POINT MOMENT FOUNDATION IMPEDANCE
 Z_{FF} = POINT FORCE FOUNDATION IMPEDANCE
 Z_C = INFINITE CYLINDER IMPEDANCE

FIGURE 6.- DUCT HANGER ASSEMBLY/FOUNDATION MODEL

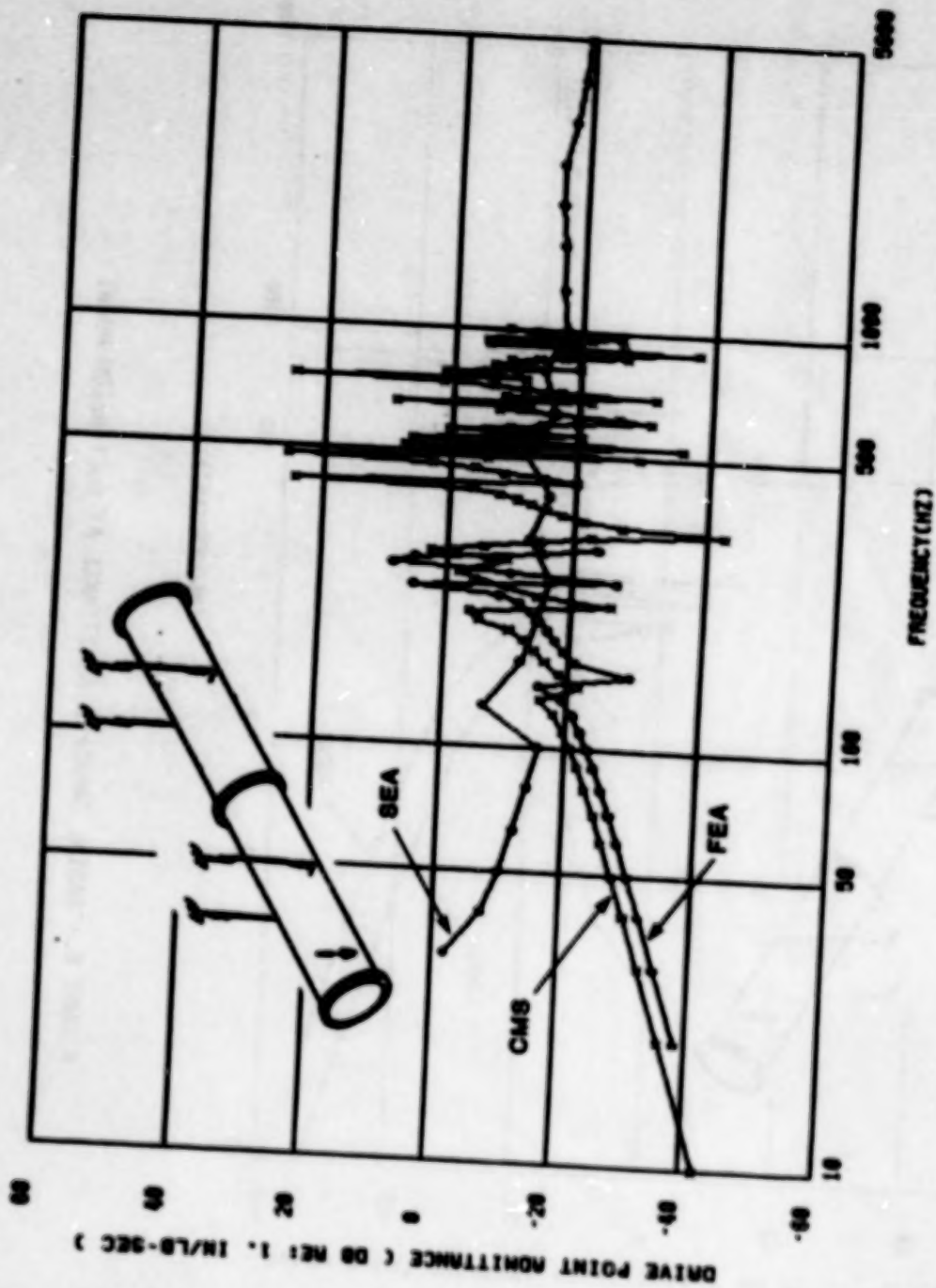


FIGURE 7.- FEA AND CMS DRIVE POINT ADMITTANCE VS. SEA AVERAGE DUCT VELOCITY

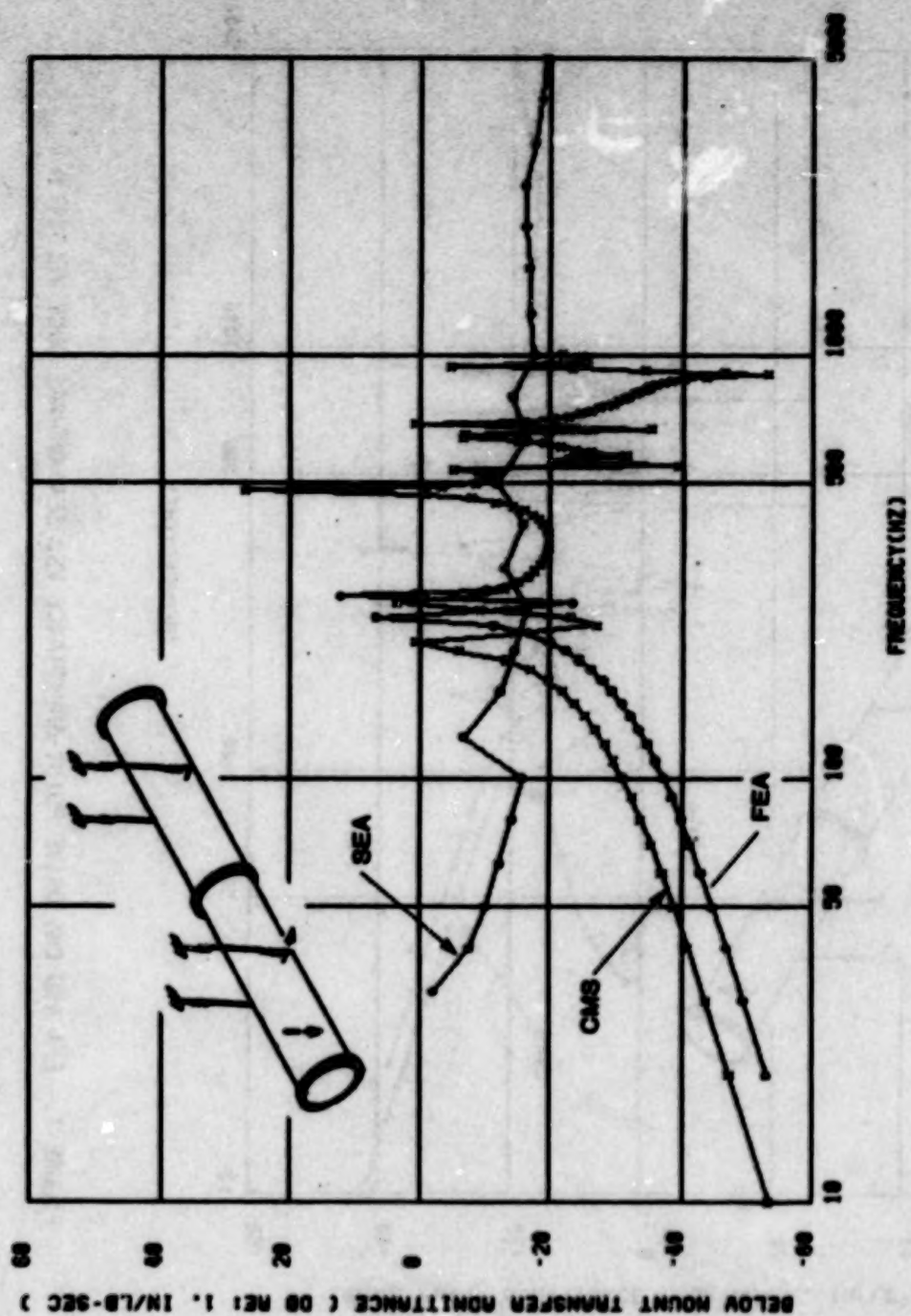


FIGURE 8.- RADIAL TRANSFER ADMITTANCE AT DUCT BELOW MOUNT.

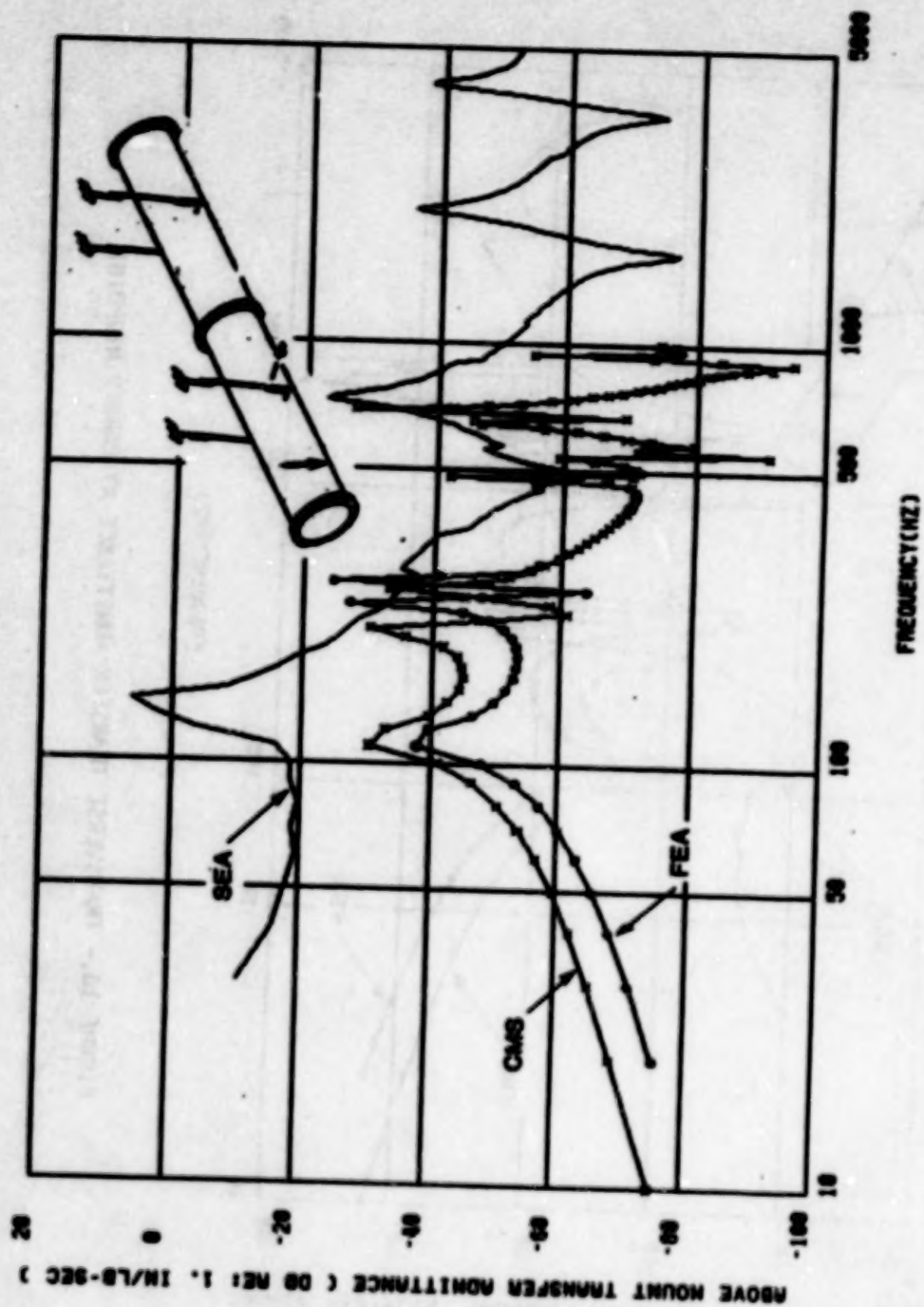


FIGURE 9.- TRANSVERSE TRANSFER ADMITTANCE AT HANGER ABOVE MOUNT

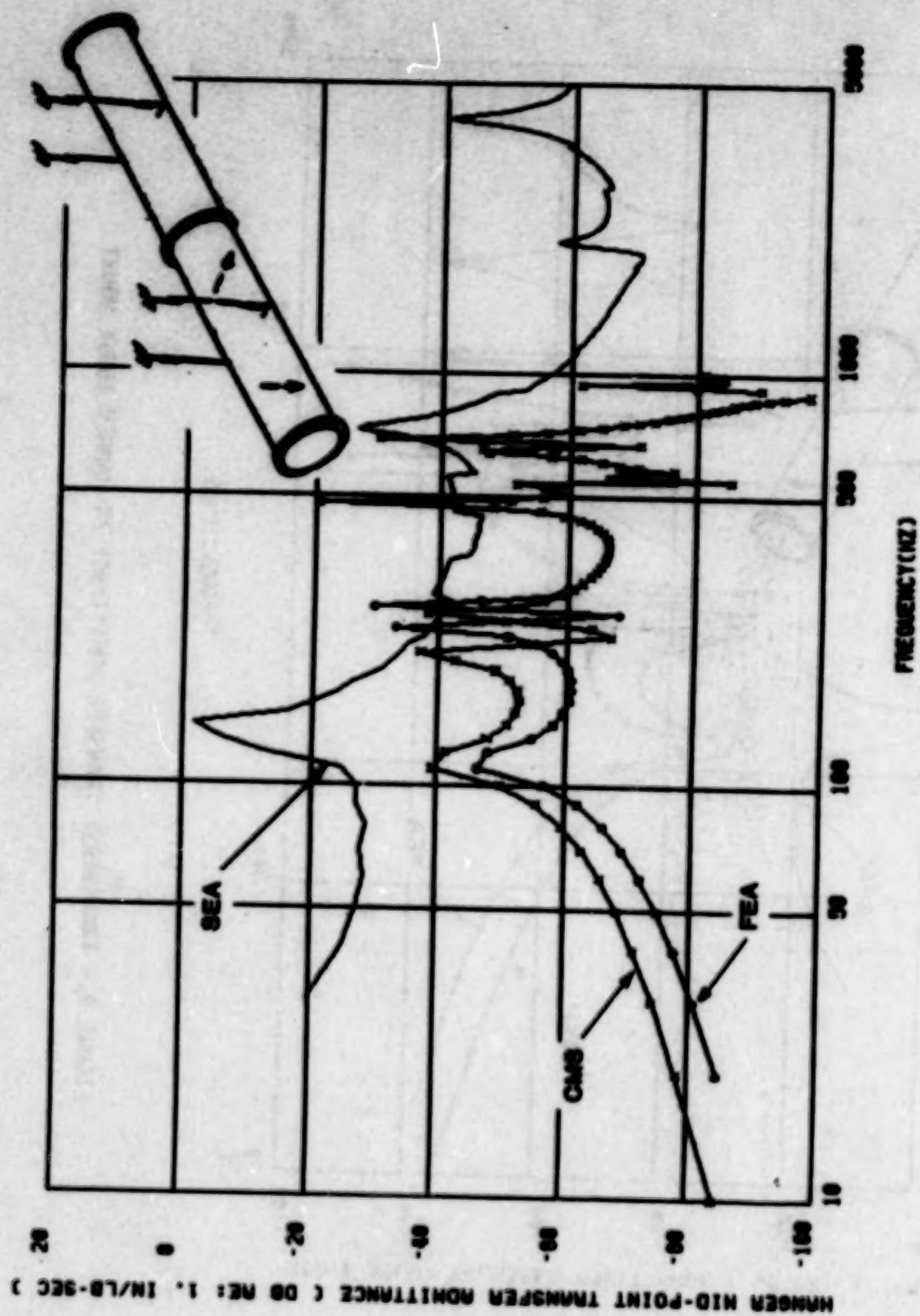


FIGURE 10.- TRANSVERSE TRANSFER ADMITTANCE AT HANGER MIDPOINT

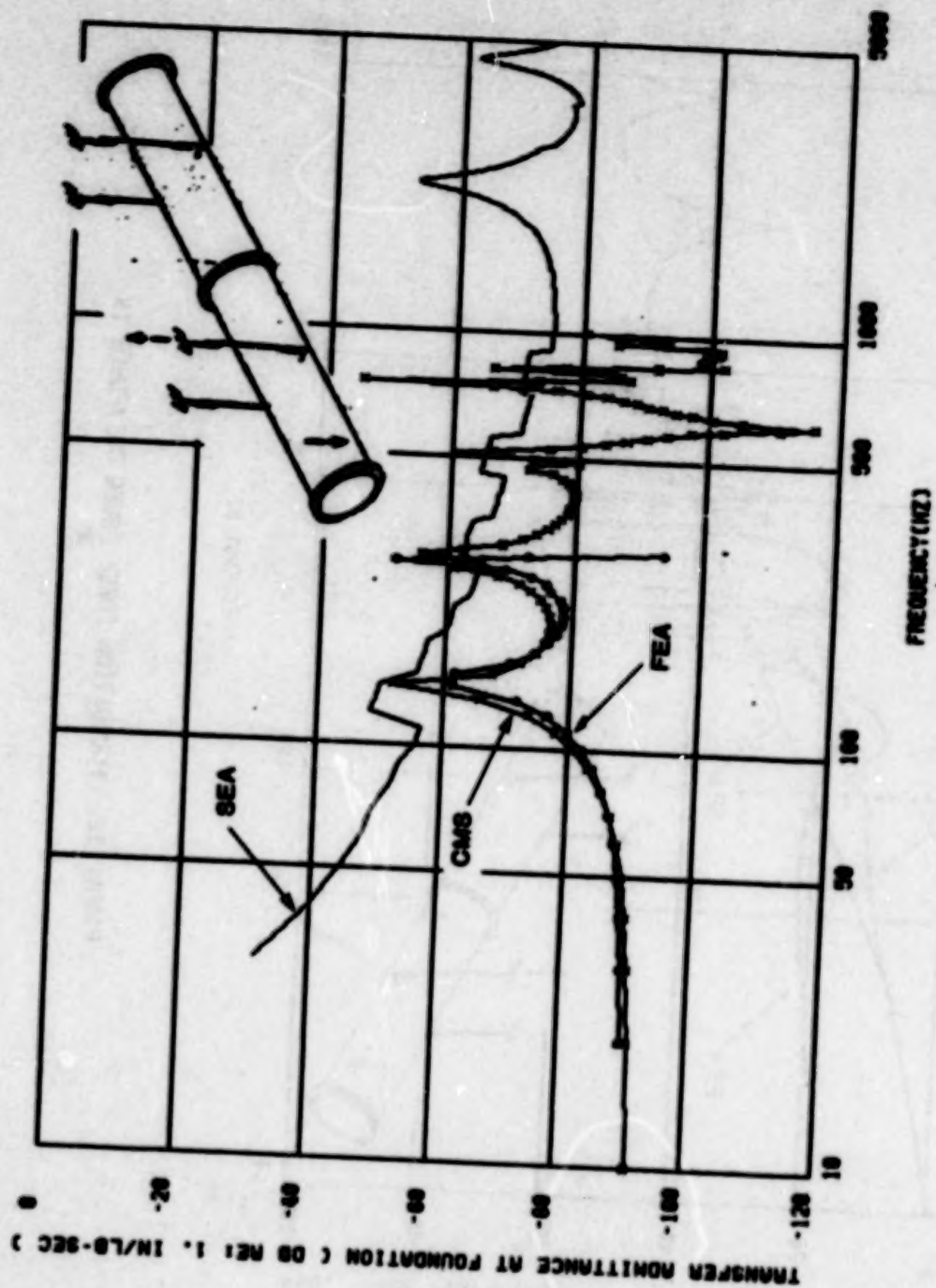


FIGURE 11.- VERTICAL TRANSFER ADMITTANCE AT FOUNDATION

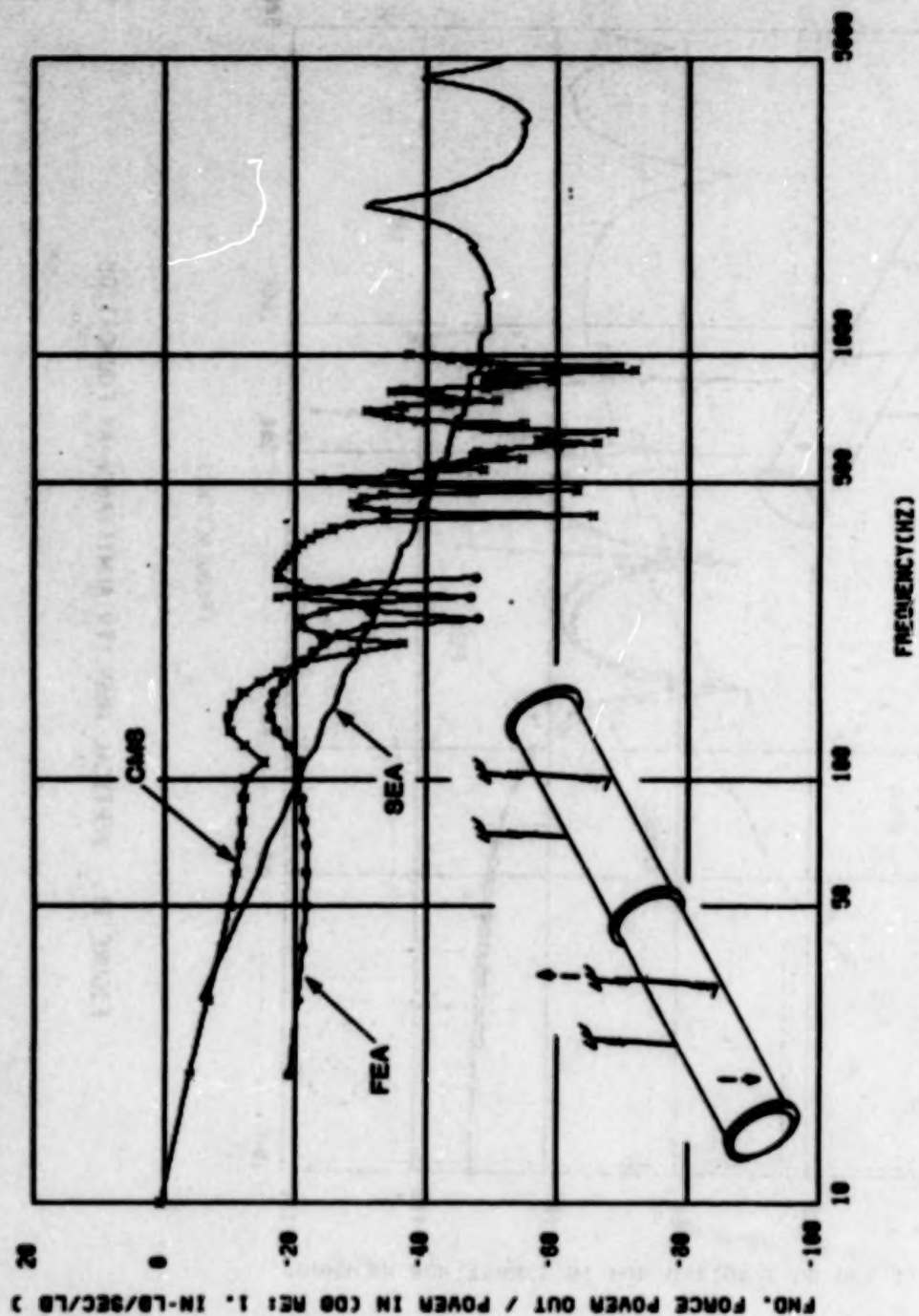


FIGURE 12.- FOUNDATION FORCE POWER OUT/POWER IN

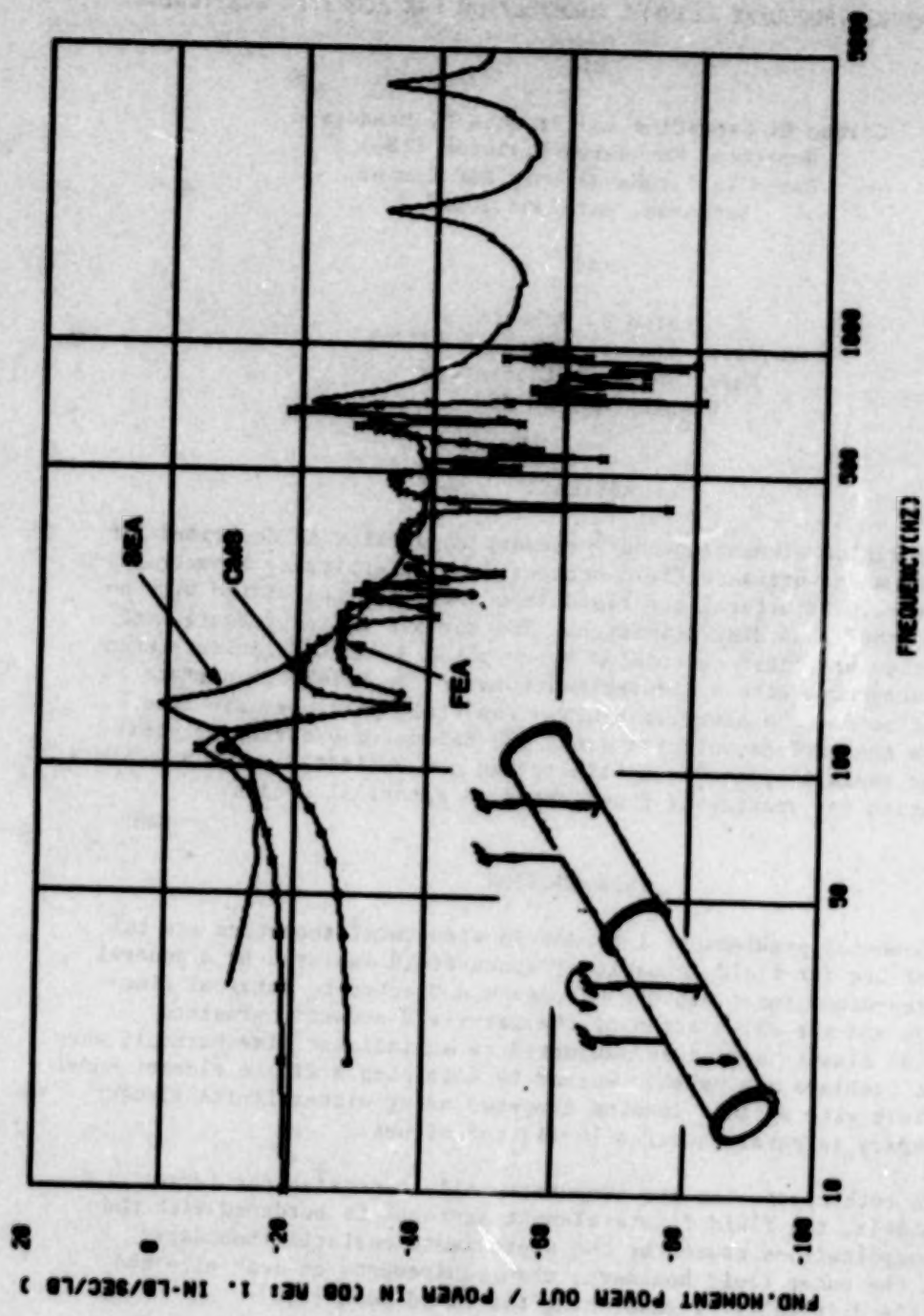


FIGURE 13.- FOUNDATION MOMENT POWER OUT/POWER IN

COUPLED NASTRAN/BOUNDARY ELEMENT FORMULATION FOR ACOUSTIC SCATTERING

by

Gordon C. Everstine and Francis M. Henderson
Numerical Mechanics Division (184)
David Taylor Naval Ship R&D Center
Bethesda, Maryland 20084

and

Luise S. Schuets
Physical Acoustics Branch (5130)
Naval Research Laboratory
Washington, DC 20375

ABSTRACT

A coupled finite element/boundary element capability is described for calculating the sound pressure field scattered by an arbitrary submerged 3-D elastic structure. Structural and fluid impedances are calculated with no approximation other than discretization. The surface fluid pressures and normal velocities are first calculated by coupling a NASTRAN finite element model of the structure with a discretized form of the Helmholtz surface integral equation for the exterior fluid. Far-field pressures are then evaluated from the surface solution using the Helmholtz exterior integral equation. The overall approach is illustrated and validated using a known analytic solution for scattering from submerged spherical shells.

INTRODUCTION

Two fundamental problems of interest in structural acoustics are the calculation of the far-field acoustic pressure field radiated by a general submerged three-dimensional elastic structure subjected to internal time-harmonic loads and the calculation of the far-field acoustic pressure scattered by an elastic structure subjected to an incident time-harmonic wave train. These problems are usually solved by combining a finite element model of the structure with a fluid loading computed using either finite element [1-3] or boundary integral equation [4-11] techniques.

Although both approaches are computationally expensive for large structural models, the fluid finite element approach is burdened with the additional complications caused by the approximate radiation boundary condition at the outer fluid boundary, the requirements on mesh size and extent, and the difficulty of generating the fluid mesh [1,3].

In contrast, the boundary integral equation (BIE) approach for generating the fluid loading is mathematically exact (except for surface discretization error) and requires little or no additional modeling effort to convert an existing model of a dry structure for use in submerged analyses. The saving in engineering time, however, is partially offset by the somewhat greater computing costs associated with the BIE approach.

Several general BIE acoustic radiation capabilities have been developed previously [4, 7, 11]. One, called NASHUA [11], couples a NASTRAN finite element model of a dry structure with a fluid loading calculated by a discretized form of the Helmholtz surface integral equation. NASHUA is the only capability developed for a widely-used, public domain, general purpose structural analysis code. Here we present an extension to NASHUA to handle also the problem of acoustic scattering from general three-dimensional elastic structures.

The primary purposes of this paper are to summarize the theoretical basis for NASHUA and to demonstrate its validity for scattering by showing results of calculations for the elementary problem of plane-wave scattering from a thin spherical shell.

THEORETICAL APPROACH

Consider an arbitrary submerged 3-D elastic structure subjected to either internal time-harmonic loads or an external time-harmonic incident pressure wave train. The matrix equation of motion for the structural degrees of freedom (DOF) can be written as

$$Zv = F - GAP \quad (1)$$

- where Z = structural impedance matrix (dimension $s \times s$),
 v = complex amplitude of the velocity vector for all structural DOF (wet or dry) in terms of the coordinate systems selected by the user ($s \times r$),
 F = complex amplitude of the vector of mechanical forces applied to the structure ($s \times r$),
 G = rectangular transformation matrix of direction cosines to transform a vector of outward normal forces at the wet points to a vector of forces at all points in the coordinate systems selected by the user ($s \times f$),
 A = diagonal area matrix for the wet surface ($f \times f$), and
 p = complex amplitude of total pressures (incident + scattered) applied at the wet grid points ($f \times r$).

In this equation, the time dependence $\exp(i\omega t)$ has been suppressed. In the above dimensions, s denotes the total number of structural DOF (wet or dry), f denotes the number of fluid DOF (the number of wet points), and r denotes the number of load cases. In general, surface areas in NASHUA are obtained

from the NASTRAN calculation of the load vector resulting from an outwardly directed static unit pressure load on the structure's wet surface.

In Equation (1), the structural impedance matrix Z (the ratio of force to velocity) is given by

$$Z = (-\omega^2 M + i\omega B + K)/i\omega \quad (2)$$

where M , B , and K are the structural mass, viscous damping, and stiffness matrices, respectively, and ω is the circular frequency of excitation. For structures with material damping or a nonzero loss factor, K is complex.

The total fluid pressure p satisfies the reduced wave equation

$$\nabla^2 p + k^2 p = 0 \quad (3)$$

where $k = \omega/c$ is the acoustic wave number, and c is the speed of sound in the fluid. Equivalently, p is the solution of the Helmholtz integral equation [7,12]

$$\int_S p(\underline{x})(\partial D(r)/\partial n) dS - \int_S q(\underline{x}) D(r) dS = \begin{cases} p(\underline{x}')/2 - p_I, & \underline{x}' \text{ on } S \\ p(\underline{x}') - p_I, & \underline{x}' \text{ in } E \end{cases} \quad (4)$$

where S and E denote surface and exterior fluid points, respectively, p_I is the incident free-field pressure, r is the distance from \underline{x} to \underline{x}' (Figure 1),

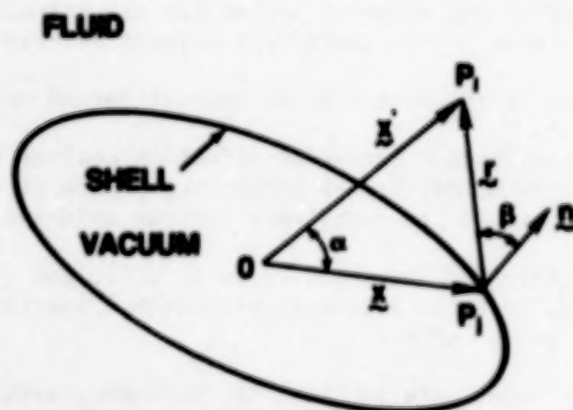


Figure 1 - Notation for Helmholtz Integral Equations

D is the Green's function

$$D(r) = e^{-ikr}/4\pi r \quad (5)$$

and

$$q = \partial p / \partial n = -i\rho p v_n \quad (6)$$

where ρ is the density of the fluid, and v_n is the outward normal component of velocity on S . As shown in Figure 1, \underline{x} in Equation (4) is the position vector for a typical point P_j on the surface S , \underline{x}' is the position vector for the point P_i which may be either on the surface or in the exterior field E , the vector $\underline{r} = \underline{x}' - \underline{x}$, and \underline{n} is the unit outward normal at P_j . We denote the lengths of the vectors \underline{x} , \underline{x}' , and \underline{r} by x , x' , and r , respectively. The normal derivative of the Green's function D appearing in Equation (4) can be evaluated as

$$\partial D(r) / \partial n = (e^{-ikr}/4\pi r) (ik + 1/r) \cos \beta \quad (7)$$

where β is defined as the angle between the normal \underline{n} and the vector \underline{r} , as shown in Figure 1.

The substitution of Equations (6) and (7) into the surface equation (4) yields

$$\begin{aligned} p(\underline{x}')/2 - \int_S p(\underline{x}) (e^{-ikr}/4\pi r) (ik + 1/r) \cos \beta \, dS \\ = i\rho \int_S v_n(\underline{x}) (e^{-ikr}/4\pi r) dS + p_I \end{aligned} \quad (8)$$

where \underline{x}' is on S . This equation is an integral equation relating the total pressure p and normal velocity v_n on S . If the integrals in Equation (8) are discretized for numerical computation (the details of which were presented previously [11]), we obtain the matrix equation

$$E p = C v_n + p_I \quad (9)$$

on S , where p is the vector of complex amplitudes of the total pressure on the structure's surface, E and C are fully-populated, complex, non-symmetric, frequency-dependent matrices, and p_I is the complex amplitude of the incident pressure vector (if any). The number of unknowns in this system is f , the number of wet points on the fluid-structure interface.

The normal velocities v_n in Equation (9) are related to the total velocities v by the same transformation matrix G :

$$v_n = G^T v \quad (10)$$

where T denotes the matrix transpose. If velocities v and v_n are eliminated from Equations (1), (9), and (10), the resulting equation for the coupled fluid-structure system is

$$H p = Q + P_I \quad (11)$$

where

$$H = E + C G^T Z^{-1} G A \quad (12)$$

and

$$Q = C G^T Z^{-1} F \quad (13)$$

Since H and Q depend on geometry, material properties, and frequency, Equation (11) may be solved to yield the total surface pressures p . The vector v of velocities at all structural DOF may be recovered by solving Equation (1) for v :

$$v = Z^{-1} F - Z^{-1} G A p \quad (14)$$

Surface normal velocities v_n may then be recovered by substituting this solution for v into Equation (10). The triangular factors of Z are saved when first generated in Equation (12) and reused in Equations (13) and (14).

The free-field incident pressure for planar or spherical waves is calculated in the following way. Consider an arbitrary surface S subjected to a time-harmonic incident wave train of speed c and circular frequency ω as shown in Figure 2. The complex amplitude p_I of the incident pressure at a typical point i is given by

$$p_I = \begin{cases} p_0 \exp(i\theta_i), & \text{plane wave} \\ p_0 \exp(i\theta_i) s/(s - \delta_i), & \text{spherical wave} \end{cases} \quad (15)$$

where p_0 is the pressure amplitude at the coordinate origin (where the phase angle is arbitrarily set to zero), s is the length of the vector \underline{s} (the vector from the origin to the source), δ_i is the distance (positive or negative)

from the origin to the wavefront through point 1, and θ_1 is the phase angle for point 1. These last two quantities can be computed using

$$\theta_1 = k \delta_1 \quad (16)$$

and

$$\delta_1 = \begin{cases} \underline{x}_1 \cdot \underline{s}/c, & \text{plane wave} \\ s - |\underline{x}_1 - \underline{s}|, & \text{spherical wave} \end{cases} \quad (17)$$

where \underline{x}_1 is the position vector for point 1. For plane waves, only the direction cosines of \underline{s} are used. Positive values of θ_1 and δ_1 for a point 1 correspond to that point's being closer to the source than the origin is.

To summarize, the NASHUA solution procedure uses NASTRAN to generate K, M, B, and F and to generate sufficient geometry information so that E, C, G, A, and p_1 can be computed by a separate program (SURF). Then, given all matrices on the right-hand sides of Equations (12) and (13), NASTRAN DMAP is used to compute H and Q. Equation (11) is then solved for the surface pressures p using a new block solver (OCSOLVE) written especially for this problem by E.A. Schroeder of the David Taylor Naval Ship R&D Center. Next, NASTRAN DMAP is used to recover the surface normal velocities v_n and the vector v of velocities at all structural DOF. This completes the surface solution. In general, this approach combines in a highly automated fashion a finite element model of the structure with a Helmholtz boundary integral equation model of the fluid.

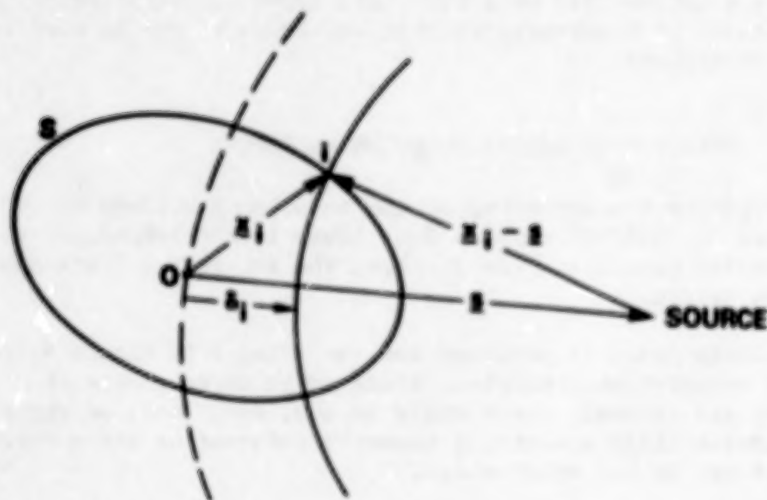


Figure 2 - Geometry for Calculating Incident Pressure

The Far-Field Solution

Given the solution for the total pressures and velocities on the surface, the exterior Helmholtz integral equation, Equation (4), can be integrated to obtain the radiated (or scattered) pressure at any desired location \underline{x}' in the field. We first substitute Equations (6) and (7) into Equation (4) to obtain a form suitable for numerical integration:

$$p(\underline{x}') = \int_S [i\rho v_n(\underline{x}) + (ik + 1/r)p(\underline{x}) \cos \beta] (e^{-ikr}/4\pi r) dS \quad (18)$$

where all symbols have the same definitions as were used previously, and \underline{x}' is in the exterior field. Thus, given the total pressure p and normal velocity v_n on the surface S , the radiated or scattered pressure at \underline{x}' can be determined by numerical quadrature using Equation (18).

In applications, however, the field pressures generally of interest are in the far-field, so we use instead an asymptotic (far-field) form [11] of Equation (18):

$$p(\underline{x}') = (ike^{-ikx'}/4\pi x') \int_S [\rho c v_n(\underline{x}) + p(\underline{x}) \cos \beta] e^{i\sqrt{x} \cos \alpha} dS \quad (19)$$

where α is the angle between the vectors \underline{x} and \underline{x}' (Figure 1), and, for far-field points, $\cos \beta$ is computed using

$$\cos \beta = \underline{n} \cdot \underline{x}'/x' \quad (20)$$

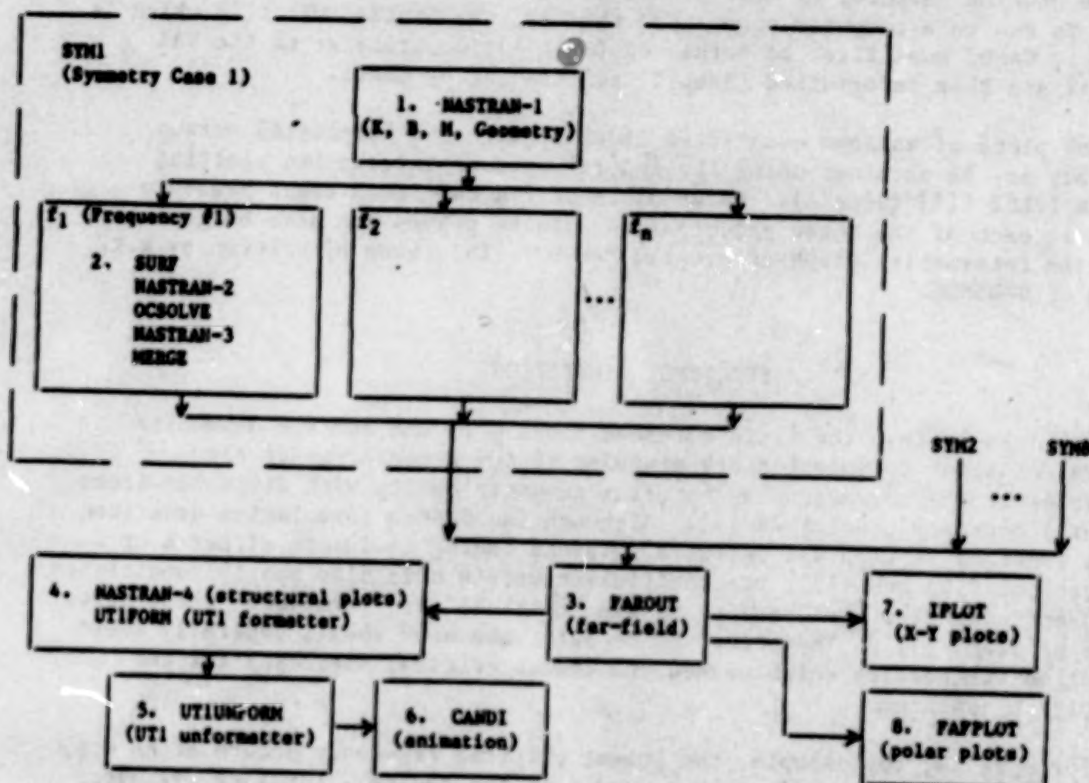
We note that, since Equation (19) is a far-field formula, the pressure varies inversely with distance x' everywhere so that any range x' may be used in its evaluation (e.g., 36 inches).

OVERVIEW OF NASHUA SOLUTION PROCEDURE

The overall organization and setup of the solution procedure is summarized in Figure 3. NASTRAN appears four times in the procedure; to distinguish one NASTRAN execution from another, the integers 1-4 are appended to "NASTRAN" in the figure.

A separate NASTRAN model is prepared and run (Step 1 in Figure 3) for each unique set of symmetry constraints. Since up to three planes of reflective symmetry are allowed, there would be one, two, four, or eight such runs. Step 1 generates files containing geometry information and a checkpoint file for subsequent use in the other steps.

For each symmetry case and drive frequency, the Step 2 sequence is run in a single job. The SURF program reads the geometry file generated by NASTRAN in Step 1 and, using the Helmholtz surface integral equation, generates the fluid matrices E and C for the exterior fluid, the area matrix A, the structure-fluid transformation matrix G, the free-field incident pressure vector p_i , and a geometry file to be used later by FAROUT (Step 3) for the field calculation. SURF is followed by a NASTRAN job which takes the matrices K, M, B, and F from Step 1 and the matrices E, C, A, and G from SURF and calculates H and Q according to Equations (12) and (13). Equation (11) is then solved for the surface pressure vector p by program OCSOLVE written by E.A. Schroeder of DTNSRDC. OCSOLVE is a general block solver for full, complex, nonsymmetric systems of linear, algebraic equations. The program was designed to be particularly effective on such systems and executes about 20 times faster than NASTRAN's equation solver, which was not designed for efficient solution of such systems of equations. NASTRAN is then re-entered in Step 2 with p so that the velocities v and v_n can be recovered using DMAP operations according to Equations (14) and (10), respectively.



NOTE: Each solid block is a separate job submission.

Figure 3 - Summary of NASHUA Solution Procedure

The surface pressures, normal velocities, and full g-set displacements are then reformatted and merged into a single file (for each symmetry case) using program MERGE.

Steps 1 and 2 are repeated for each symmetry case. After all symmetry cases have been completed and merged, program FAROUT (Step 3) is run to combine the symmetry cases and to integrate over the surface. FAROUT uses as input the geometry file generated by SURF (Step 2) and the surface solutions from the one, two, four, or eight symmetry cases generated by MERGE. The far-field pressure solution is obtained by integrating the surface pressures and velocities using the far-field form of the exterior Helmholtz integral equation, Equation (19). Output from FAROUT consists of both tables and files suitable for various types of plotting.

The remaining steps in the NASHUA procedure are for graphical display. Deformed structural plots of the frequency response may be obtained by restarting NASTRAN (Step 4) with the checkpoint file from Step 1 and a results file from FAROUT. In addition, animated plots can be generated on the Evans & Sutherland PS-330 graphics terminal using the CANDI program (Step 6) written for the DEC/VAX computer by R.R. Lipman of DTNSRDC [13]. If the rest of NASHUA is run on a computer other than the VAX, the NASTRAN Utl file which is passed to CANDI must first be formatted (Step 4) for transfer to the VAX computer and then unformatted (Step 5) for reading by CANDI.

X-Y plots of various quantities (both surface and far-field) versus frequency may be obtained using the general purpose interactive plotting program IPLOT [14] (Step 7). Polar plots of the far-field sound pressure levels in each of the three principal coordinate planes can also be generated using the interactive graphics program FAPLOT [15] (Step 8) written by R.R. Lipman of DTNSRDC.

FREQUENCY LIMITATIONS

It is known that the fluid matrices E and C in the surface Helmholtz integral equation formulation are singular at the frequencies of the resonances of the corresponding interior acoustic cavity with Dirichlet (zero pressure) boundary conditions [5]. Although the NASHUA formulation described in the previous section was designed to avoid having to invert either E or C in Equations (12) and (13), the coefficient matrix H is also poorly conditioned at these frequencies (referred to as the "critical" or "forbidden" frequencies of the problem) [11]. Therefore, to be safe, the user should generally avoid excitation frequencies which exceed the lowest critical frequency for the geometry in question.

For spheres, for example, the lowest critical frequency occurs at $ka = \pi$, where k is the acoustic wave number, and a is the radius. For long cylinders with flat ends, the lowest critical frequency occurs at $ka = 2.4$, where a is the radius. For short cylinders with flat ends, the lowest critical frequency is slightly higher than for long cylinders.

RESTRICTIONS ON MODEL

Although the NASHUA solution procedure was designed to be general enough so that arbitrary three-dimensional structures could be analyzed, a few restrictions remain. In our view, however, none is a burden, since a NASTRAN deck for a dry structure modeled with low-order finite elements can usually be adapted for use with NASHUA in a few hours. The following general restrictions apply:

1. All translational degrees of freedom (DOF) for wet points must be in NASTRAN's "analysis set" (a-set), since all symmetry cases must have the same wet DOF, and the fluid matrices E and C involve all wet points. This restriction also affects constraints. Thus, constraints on translational DOF of wet points may not be imposed with single point constraint (SPC) cards, but must instead be imposed using large springs connected between the DOF to be constrained and ground. Generally, this restriction affects only those DOF which are constrained due to symmetry conditions.
2. The wet face of each finite element in contact with the exterior fluid must be defined by either three or four grid points, since the numerical discretization of the Helmholtz surface integral equation assumes the use of low order elements. In particular, NASTRAN elements with midside nodes (e.g., TRIM6, IS2D8, or INEX2) may not be in contact with the exterior fluid.
3. Symmetry planes must be coordinate planes of the basic Cartesian coordinate system.
4. No scalar points or extra points are allowed, since program SURF assumes that each point is a grid point.
5. For cylindrical shells, the axis of the cylinder should coincide with one of the three basic Cartesian axes; for spherical shells, the center of the sphere should coincide with the basic origin. These restrictions facilitate the treatment of symmetry planes and the calculation of curvatures in program SURF.
6. At least one degree of freedom in the model should be constrained with an SPC, MPC, or ONIT card so that the NASTRAN data block PL is generated.
7. Thin structures with fluid on both sides should be avoided, since the formulations for the fluid matrices are singular if two wet points are coincident. A precise restriction is not known.

TIME ESTIMATION

On CDC computers, most of the computer time required to execute the entire NASHUA procedure is associated with the forward/backward solve (FBS) operation in Step 2, Equation (12), in which the matrix $Z^{-1}GA$ is computed given the triangular factors of Z and the matrix GA. Z is a complex, symmetric, banded matrix of dimension $s \times s$, where s is the number of structural DOF in the problem, and GA is a real, sparsely-populated,

rectangular matrix of dimension $s \times f$, where f is the number of fluid DOF (the number of wet points on the surface). This FBS time is proportional to the product of s , f , and W_{avg} (the average wavefront for the stiffness matrix K), and, for large jobs, accounts for a substantial part (perhaps two-thirds) of the total time to make a single pass through the NASHUA Step 2 procedure.

For example, consider a problem with the following characteristics:

$s = 2973$ (number of structural DOF)
 $f = 496$ (number of fluid DOF)
 $W_{avg} = 129$ (average wavefront of stiffness matrix)

On the CDC Cyber 176 computer at DTNSRDC, the computer time ("wall-clock" time) required to solve this problem in a dedicated computer environment for a single symmetry case and one drive frequency was about 30 minutes, of which 19 minutes were spent in the FBS operation.

PROGRAM VALIDATION

For radiation problems, NASHUA has been validated previously [11] for submerged spherical shells driven internally by both uniform and non-uniform (sector) pressure loads. Here we demonstrate NASHUA's ability to solve scattering problems by solving the problem of the submerged thin spherical shell subjected to an incident time-harmonic planar wave train, as shown in Figure 4. The solution of this problem exhibits rotational symmetry about the spherical axis parallel to the direction of wave propagation. The benchmark solution to which the NASHUA results will be compared is a series solution published in the Junger and Feit book [16].

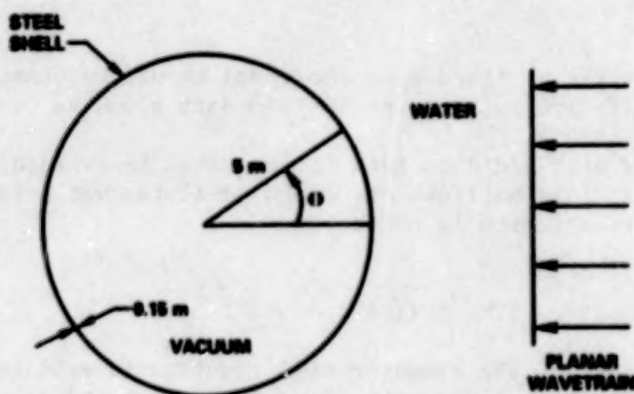


Figure 4 - Plane Wave Scattering from an Elastic Spherical Shell

The problem to be solved has the following characteristics [17]:

$a = 5 \text{ m}$	(shell radius)
$h = 0.15 \text{ m}$	(shell thickness)
$E = 2.07 \times 10^{11} \text{ Pa}$	(Young's modulus)
$\nu = 0.3$	(Poisson's ratio)
$\rho_s = 7669 \text{ kg/m}^3$	(shell density)
$\eta = 0$	(shell loss factor)
$\rho = 1000 \text{ kg/m}^3$	(fluid density)
$c = 1524 \text{ m/s}$	(fluid speed of sound)

One octant of the shell was modeled with NASTRAN's CTRIA2 membrane/bending elements as shown in Figure 5. With 20 elements along each edge of the domain, the model has 231 wet points and 1263 structural DOF. Since the incident loading does not exhibit three planes of symmetry, the NASHUA solution of this problem requires decomposing the solution into both symmetric and antisymmetric parts of the problem, thus providing a good check on NASHUA's ability to combine symmetry cases for scattering problems.

The NASHUA model was run for 15 different drive frequencies in the nondimensional frequency range $ka = 0.5$ to $ka = 5.0$, where a is the shell radius. Two of the excitation frequencies are near a critical frequency. (The first 13 critical frequencies are located at $ka = \pi, 4.49, 5.76, 2\pi, 6.99, 7.73, 8.18, 9.10, 9.36, 3\pi, 10.4, 10.5$, and 10.9 [18].) Figure 6 shows a comparison between the NASHUA calculations and the series solution for the far-field scattered pressure in the forward direction ($\theta = 180$ degrees).

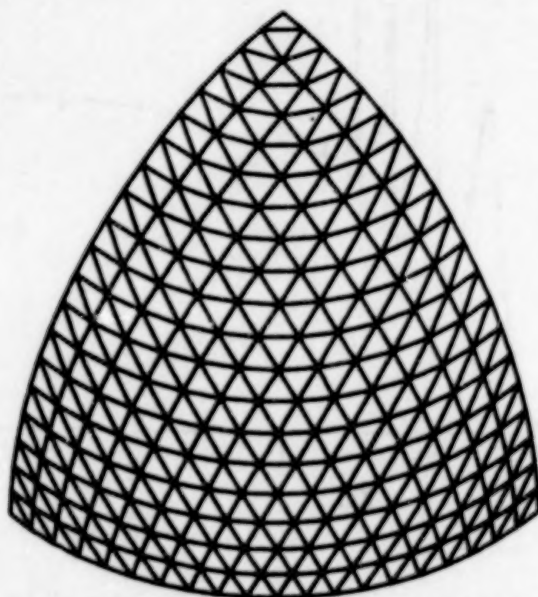


Figure 5 - Finite Element Model of One Octant of Spherical Shell

The ordinate of this figure is the normalized pressure $|p_r r / p_0 a|$, where p_r is the far-field scattered pressure at distance r from the origin, and p_0 is the magnitude of the incident pressure. Clearly, the NASHUA solution agrees very well with the exact (i.e., converged series) solution. We note that the NASHUA calculation at $ka = 4.5$ is adversely affected by the forbidden frequency at $ka = 4.49$. (Often, the effect of a forbidden frequency is very severe [11].) For several of the excitation frequencies, we also tabulate on the next page the far-field scattered pressure patterns. Again the agreement between the NASHUA calculations and the series solution is excellent, even at $ka = 1.6$, which is near a resonant peak. At the sharper resonant peaks, the results would be much more sensitive to small changes in frequency.

DISCUSSION

A very general capability has been described for predicting the acoustic sound pressure field scattered by arbitrary three-dimensional elastic structures subjected to time-harmonic incident loads. Sufficient automation is provided so that, for many structures of practical interest, an existing

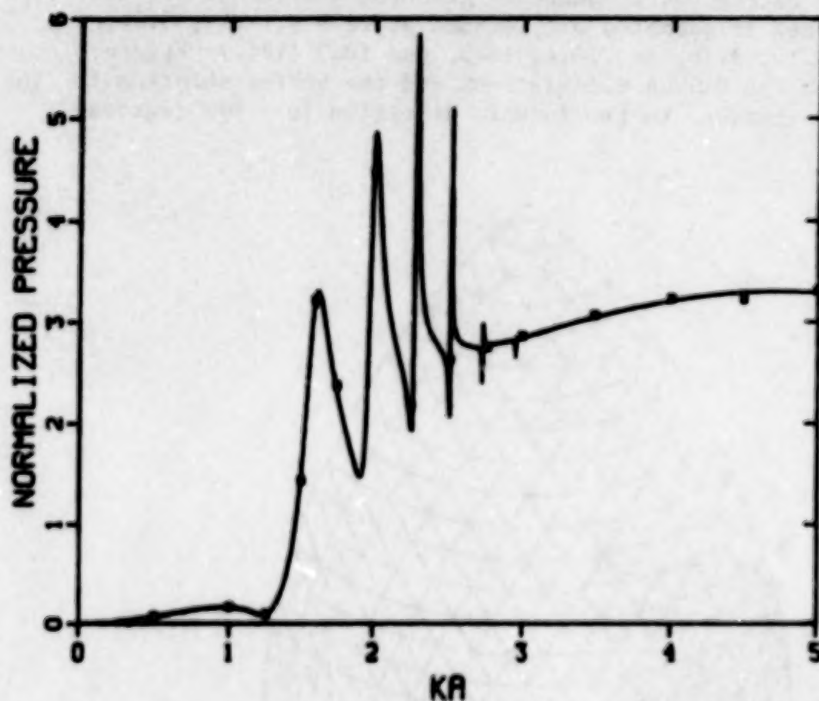


Figure 6 - Normalized Far-Field Pressure $|p_r r / p_0 a|$ Scattered in the Forward Direction ($\theta = 180$ degrees) by a Spherical Shell; Solid Curve is Converged Series Solution [16], and Square Boxes are NASHUA Solution.

Table - Comparison of NASHUA Solution with Converged Series Solution for Scattering from Spherical Shell

ka	Angle θ (degrees)	Normalized Far-Field Pressure, P_r/P_{∞}		% Error
		NASHUA	Exact	
0.5	0*	0.0083	0.0081	2.5
	30	0.0144	0.0143	0.7
	60	0.0299	0.0299	0.0
	90	0.0481	0.0481	0.0
	120	0.0626	0.0626	0.0
	150	0.0708	0.0708	0.0
	180	0.0734	0.0733	0.1
1.0	0*	0.0892	0.0903	1.2
	30	0.0382	0.0389	1.8
	60	0.0886	0.0886	0.0
	90	0.1926	0.1930	0.2
	120	0.2208	0.2210	0.1
	150	0.1893	0.1887	0.3
	180	0.1662	0.1652	0.6
1.6	0*	3.146	3.149	0.1
	30	1.993	1.995	0.1
	60	0.325	0.320	1.6
	90	1.515	1.498	1.1
	120	0.561	0.540	3.9
	150	2.058	2.092	1.6
	180	3.213	3.245	1.0
4.0	0*	0.166	0.160	3.8
	30	0.105	0.101	4.0
	60	0.068	0.069	1.4
	90	0.274	0.269	1.9
	120	0.562	0.554	1.4
	150	1.769	1.757	0.7
	180	3.228	3.205	0.7
* $\theta = 0$ corresponds to the back-scattered direction.				

NASTRAN structural model can be adapted for NASHUA acoustic analysis within a few hours.

One of the major benefits of having NASHUA linked with NASTRAN is the ability to integrate the acoustic analysis of a structure with other dynamic analyses. Thus the same finite element model can be used for modal analysis, frequency response analysis, linear shock analysis, and underwater acoustic

analysis. In addition, many of the pre- and postprocessors developed for use with NASTRAN become available for NASHUA as well.

The principal area in which NASHUA could be improved would be to remove the frequency limitation caused by the presence of the critical frequencies inherent in the Helmholtz integral equation formulation. With the limitation, cylindrical shells, for example, can be safely analyzed by NASHUA only for $ka < 2.4$, where a is the radius. Since for some problems, it would be of interest to treat higher frequencies, the limitation should be removed. A conversion to a different formulation (e.g., Burton and Miller [8] or Mathews [10]) is being considered.

REFERENCES

1. Everstine, G.C., "A Symmetric Potential Formulation for Fluid-Structure Interaction," J. Sound and Vibration, vol. 79, no. 1, pp. 157-160 (1981).
2. Everstine, G.C., "Structural-Acoustic Finite Element Analysis, with Application to Scattering," Proc. 6th Invitational Symposium on the Unification of Finite Elements, Finite Differences, and Calculus of Variations, ed. by H. Kardestuncer, Univ. of Connecticut, pp. 101-122 (1982).
3. Kalinowski, A.J., and C.W. Nebelung, "Media-Structure Interaction Method," The Shock and Vibration Bulletin, vol. 51, part 1, pp. 173-193 (1981).
4. Chen, L.H., and D.G. Schweikert, "Sound Radiation from an Arbitrary Body," J. Acoust. Soc. Amer., vol. 35, no. 10, pp. 1626-1632 (1963).
5. Schenck, H.A., "Improved Integral Formulation for Acoustic Radiation Problems," J. Acoust. Soc. Amer., vol. 44, no. 1, pp. 41-58 (1968).
6. Henderson, F.M., "A Structure-Fluid Interaction Capability for the NASA Structural Analysis (NASTRAN) Computer Program," Report 3962, David Taylor Naval Ship R&D Center, Bethesda, Maryland (1972).
7. Wilton, D.T., "Acoustic Radiation and Scattering From Elastic Structures," Int. J. Num. Meth. in Engrg., vol. 13, pp. 123-138 (1978).
8. Burton, A.J., and G.F. Miller, "The Application of Integral Equation Methods to the Numerical Solution of Some Exterior Boundary-Value Problems," Proc. Roy. Soc. Lond. A, vol. 323, pp. 201-210 (1971).
9. Baron, M.L., and J.M. McCormick, "Sound Radiation from Submerged Cylindrical Shells of Finite Length," ASME Trans. Ser. B, vol. 87, pp. 393-405 (1965).

- 84378-784
10. Mathews, I.C., "A Symmetric Boundary Integral-Finite Element Approach for 3-D Fluid Structure Interaction," in Advances in Fluid-Structure Interaction - 1984, PVP-Vol. 78 and AMD-Vol. 64, ed. by G.C. Everstine and M.K. Au-Yang, American Society of Mechanical Engineers, New York, pp. 39-48 (1984).
 11. Everstine, G.C., F.M. Henderson, E.A. Schroeder, and R.R. Lipman, "A General Low Frequency Acoustic Radiation Capability for NASTRAN," Fourteenth NASTRAN Users' Colloquium, NASA CP-2419, National Aeronautics and Space Administration, Washington, DC, pp. 293-310 (1986).
 12. Lamb, H., Hydrodynamics, sixth edition, Dover Publications, New York (1945).
 13. Lipman, R.R., "Computer Animation of Modal and Transient Vibrations," NASTRAN Users' Colloquium, National Aeronautics and Space Administration, Washington, DC (1987). (this volume)
 14. Everstine, G.C., "A Portable Interactive Plotter for Digital X-Y Data," Report CMLD-86-45, David Taylor Naval Ship R&D Center, Bethesda, Maryland (1986).
 15. Lipman, R.R., "Calculating Far-Field Radiated Sound Pressure Levels from NASTRAN Output," Fourteenth NASTRAN Users' Colloquium, NASA CP-2419, National Aeronautics and Space Administration, Washington, DC, pp. 282-292 (1986).
 16. Junger, M.C., and D. Feit, Sound, Structures, and Their Interaction, second edition, The MIT Press, Cambridge, Massachusetts (1986).
 17. Huang, H., and Y.F. Wang, "Asymptotic Fluid-Structure Interaction Theories for Acoustic Radiation Prediction," J. Acoust. Soc. Amer., vol. 77, no. 4, pp. 1389-1394 (1985).
 18. Huang, H., "Helmholtz Integral Equations for Fluid-Structure Interaction," Advances in Fluid-Structure Interaction - 1984, AMD-Vol. 64, ed. by G.C. Everstine and M.K. Au-Yang, American Society of Mechanical Engineers, New York (1984).

NASTRAN APPLICATION FOR THE PREDICTION OF AIRCRAFT INTERIOR NOISE

Francesco Marulo
University of Naples
NASA Langley Research Center
Hampton, VA 23665-5225

and

Todd B. Beyer
NASA Langley Research Center
Hampton, VA 23665-5225

Abstract

The application of a structural-acoustic analogy within the NASTRAN finite element program for the prediction of aircraft interior noise is presented. The reliability of the procedure is assessed through an analysis of the principle components involved in the fluid-structure coupling, and is compared to simple structures with known theoretical results. Some refinements of the method, which reduce the amount of computation required for large, complex structures, are then discussed. Finally, further improvements are proposed and preliminary comparisons with structural and acoustic modal data obtained for a large composite cylinder, are presented.

Introduction

The prediction and reduction of aircraft interior noise are important considerations for conventional propeller aircraft now entering the commercial market as well as for aircraft currently being developed, such as the advanced turboprop. Consequently, the interior noise problem is receiving attention even during the first stages of the aircraft design process.^{1,2} Also, the need for laboratory tests on full scale models to validate new theoretical prediction methods has been recognized.^{3,4} The theoretical approach has progressed through several stages, beginning with very simple models of the aircraft fuselage⁵ and proceeding to very detailed methods and computer programs which discretize the structure and the interior acoustic volume and define the coupling characteristics therein. Among the several analytical methods available, the finite element method has been chosen for this study for several reasons. It is fully documented, available worldwide, and can be used to model complex structural and acoustic geometries. The theory which defines the finite element solution for fluid-structure interaction problems is available in the literature,⁷⁻¹² as is the practical application using the NASTRAN code.¹³⁻¹⁷ Only recently has this approach been applied to aircraft structures.^{18,19} An analysis of the fluid-structure interaction problem based on the finite element method and NASTRAN is presented in this paper and compared with studies in the literature. The initial results are very promising, however, some refinement of the numerical techniques may be necessary (especially for large structures with many degrees of freedom) in order to reduce computational costs and provide a cost-effective tool for use during the final definition phase of aircraft design. This paper also presents preliminary numerical predictions using both the structural and acoustic finite element models to describe an actual aircraft fuselage model

available in the laboratory of the Acoustics Division of the NASA Langley Research Center. These predictions are in good agreement with experimentally obtained results. Finally, refinements of the NASTRAN model and plans for future work are discussed.

Symbols

[A]	area matrix for fluid-structure coupling (equation 13)
[B]	material definition matrix (equation 5)
c	speed of sound
E	Young's modulus
$e^{i\omega t}$	time dependence of the harmonic forcing function
F_0	amplitude of the harmonic forcing function
$\{F_s\}$	external forcing vector
G	tangential elasticity modulus
i	imaginary unit = -1
[K]	stiffness matrix
[M]	mass matrix
n	normal vector (positive outward)
p	pressure variation from equilibrium pressure value
t	time variable
u_x	displacement in the x-direction
∇^2	Laplacian operator. In cartesian coordinates $\frac{\partial^2}{\partial x^2} + \frac{\partial^2}{\partial y^2} + \frac{\partial^2}{\partial z^2}$
$\frac{\partial}{\partial x}, \frac{\partial}{\partial y}, \frac{\partial}{\partial z}, \frac{\partial}{\partial n}$	partial derivative with respect to x, y, z, or n
$\frac{\partial^2}{\partial x^2}, \frac{\partial^2}{\partial y^2}, \frac{\partial^2}{\partial z^2}$	second partial derivative with respect to x^2 , y^2 , or z^2
$\{\epsilon\}$	strain vector
λ, μ	Lamé's constants
ν	Poisson's ratio

ρ	mass density
$\{\sigma\}$	stress vector
σ_{xx}	axial stress in the x-direction
$\tau_{xy}, \tau_{yz}, \tau_{xz}$	shear stress in the x-y, y-z, or x-z plane
ω	angular frequency of harmonic forcing function
$[]^T$	transpose matrix
$\ddot{}$	double dot. Second time derivative

Subscripts

a	acoustic
n	normal direction
s	structure

Structural-Acoustic Analogy

It is possible to solve acoustic problems using structural code which already exists in the Finite Element Method. The technique is based on a structural-acoustic analogy which relates structural displacement to acoustic pressure. Specific problems have been solved using this approach,⁷⁻¹⁹ and the theoretical development has been well documented. In this paper the fundamental steps are included for the sake of clarity.

Theory

The scalar acoustic wave equation in terms of the variation of pressure from the equilibrium pressure is

$$\nabla^2 p = \frac{1}{c^2} \frac{\partial^2 p}{\partial t^2} \quad (1)$$

which, in Cartesian coordinates is

$$\frac{\partial^2 p}{\partial x^2} + \frac{\partial^2 p}{\partial y^2} + \frac{\partial^2 p}{\partial z^2} = \frac{1}{c^2} \frac{\partial^2 p}{\partial t^2} \quad (2)$$

The equation governing the equilibrium of stresses in a material in a particular direction (x, for example) is

$$\frac{\partial \sigma_{xx}}{\partial x} + \frac{\partial \tau_{xy}}{\partial y} + \frac{\partial \tau_{xz}}{\partial z} = \rho_s \frac{\partial^2 u_x}{\partial t^2} \quad (3)$$

Equations (2) and (3) are mathematically similar, and an "analogy" can be obtained if

$$\sigma_{xx} = \frac{\partial p}{\partial x}; \tau_{xy} = \frac{\partial p}{\partial y}; \tau_{xz} = \frac{\partial p}{\partial z}; \rho_s = \frac{1}{c^2}; u_x = p \quad (4)$$

Thus, it is possible to solve acoustic problems using existing structural analysis codes based on the displacement formulation of the Finite Element Method, in particular NASTRAN.^{20, 21}

In order to complete the analogy and give practical ideas as to its NASTRAN application, consider the general stress-strain relationship,

$$\{\sigma\} = [B] \{\epsilon\} \quad (5)$$

If we consider the displacement in the x-direction only ($u_y = u_z = 0$), equation (5) can be written in terms of the relations (4) as

$$\begin{pmatrix} \sigma_{xx} \\ \sigma_{yy} \\ \sigma_{zz} \\ \tau_{xy} \\ \tau_{yz} \\ \tau_{xz} \end{pmatrix} = \begin{bmatrix} 1 & B_{12} & B_{13} & 0 & B_{15} & 0 \\ & B_{22} & B_{23} & 0 & B_{25} & 0 \\ & & B_{33} & 0 & B_{35} & 0 \\ & & & 1 & B_{45} & 0 \\ \text{SYMM.} & & & & B_{55} & 0 \\ & & & & & 1 \end{bmatrix} \begin{pmatrix} \partial u_x / \partial x \\ 0 \\ 0 \\ \partial u_x / \partial y \\ 0 \\ \partial u_x / \partial z \end{pmatrix} \quad (6)$$

where the terms B_{ij} are arbitrary. However, it is often convenient to choose B_{ij} so that the matrix $[B]$ is isotropic and therefore invariant for any coordinate system. This can be achieved in NASTRAN by using the card which defines a linear, temperature-independent, isotropic material (MAT1 card), and substituting the proper values for the material constants. For example, the material definition matrix, $[B]$, for the three-dimensional problem²⁰ is

$$[B] = \begin{bmatrix} \lambda+2\mu & \lambda & \lambda & 0 & 0 & 0 \\ & \lambda+2\mu & \lambda & 0 & 0 & 0 \\ & & \lambda+2\mu & 0 & 0 & 0 \\ & & & \mu & 0 & 0 \\ & \text{SYM} & & & \mu & 0 \\ & & & & & \mu \end{bmatrix} \quad (7)$$

where $\lambda + 2\mu = 1$ and $\mu = 1$ in order to obtain the general matrix given by equation (6). Since the Lamé constants λ and μ are

$$\lambda = \frac{Ev}{(1+\nu)(1-2\nu)} \quad ; \quad \mu = G = \frac{E}{2(1+\nu)} \quad (8)$$

the following values input with the MAT1 card

$$E = 1 \times 10^{20} \quad ; \quad G = 1 \quad ; \quad \nu = .5 \times 10^{20} \quad ; \quad \rho = \frac{1}{c^2} \quad (9)$$

define the acoustic analogy. Similarly, the [B] matrix for the two-dimensional case is

$$[B] = \frac{E}{1-\nu^2} \begin{bmatrix} 1 & \nu & 0 \\ \nu & 1 & 0 \\ 0 & 0 & \frac{(1-\nu)}{2} \end{bmatrix} \quad (10)$$

and the corresponding material properties are input as

$$E = 2 \times 10^{-6} \quad ; \quad G = 1 \quad ; \quad \nu = -.999999 \quad ; \quad \rho = \frac{1}{c^2} \quad (11)$$

Using this approach, equation (1) can be solved for many cases, and proves especially useful when the geometry of the enclosure is irregular and cannot be studied adequately using known results for simple geometries.

Finite Element Formulation and Validation Examples

The equation of motion of an acoustic enclosure with rigid walls and no forcing function can be written in terms of the Finite Element notation as

$$[M_a]\{\ddot{p}\} + [K_a]\{p\} = \{0\} \quad (12)$$

where $[M_a]$ is the acoustic 'mass' matrix, $[K_a]$ is the acoustic 'stiffness' matrix and $\{p\}$ is the vector of pressure values at the grid points. If the pressure is harmonic, equation (12) becomes a classical eigenvalue problem that can be solved using standard NASTRAN methods and the acoustic resonance

frequencies and acoustic mode shapes for any geometry can easily be extracted. The validity of this formulation has been studied for cavities with simple geometries which have straightforward theoretical solutions. For the present paper two particular geometries have been studied, one having a rectangular cross section and one with a circular cross section. A comparison of the acoustic mode shapes and resonance frequencies for the 2-dimensional cross section and the 3-dimensional volume derived theoretically and predicted using the present NASTRAN formulation is tabulated in Table I. These data are in general good agreement, with some small differences at higher modes where a finer mesh may be necessary. For the NASTRAN formulation the QUAD2 membrane element was used to model the cross-sectional area for the 2-dimensional case and the HEXA2 solid element was used to model the 3-dimensional acoustic volume. Figure 1 shows some of the acoustic mode shapes predicted using the NASTRAN formulation and plotted using PATRAN-G post-processing capabilities.

Fluid-Structure Interaction

Theory

A complete description of the fluid-structure interaction problem, in terms of finite element models of the structure and the enclosed acoustic volume, is given by the following coupled equation of motion

$$\begin{bmatrix} M_s & 0 \\ -(\rho c)^2 A^T & M_a \end{bmatrix} \begin{Bmatrix} \ddot{u} \\ \ddot{p} \end{Bmatrix} + \begin{bmatrix} K_s & A \\ 0 & K_a \end{bmatrix} \begin{Bmatrix} u \\ p \end{Bmatrix} = \begin{Bmatrix} F_s \\ 0 \end{Bmatrix} \quad (13)$$

where the matrix, $[A]$, ensures the proper coupling between structural and acoustic models. At a fluid-structure interface the boundary condition is

$$\frac{\partial p}{\partial n} = -\rho \ddot{u}_n \quad (14)$$

where n is the normal, positive outward, unit vector at the interface and ρ is the mass density of the fluid. For the present finite element application, the force exerted by the structure on the fluid is $(\rho c)^2 A \ddot{u}_n$ at each grid point located along the fluid-structure interface. Here, A is the surface area associated with the grid point and u_n is the normal component of the fluid particle acceleration. The force of the fluid acting on the structure is expressed as a surface pressure force equal to $-pA$ applied to each interface structural grid point.

The general equation of motion, therefore, can be written as

$$[M_s] \{\ddot{u}\} + [K_s] \{u\} = \{F_s\} - [A] \{p\} \quad (15)$$

for the structural model and

$$[M_a] \{\ddot{p}\} + [K_a] \{p\} = (\rho c)^2 [A]^T \{\ddot{u}\} \quad (16)$$

for the acoustic model. The matrix $[A]$ must be entered by the user since it is not included in the standard, rigid format of COSMIC/NASTRAN. It is a sparse $(n \times n)$ matrix whose non-zero elements correspond to the fluid-structure interface locations. The non-zero elements are the lumped areas at the designated interface grid points and can be extracted from the OLOAD output which results from the application of a unit pressure level to the structure surface.¹² These values are entered in the appropriate locations of the complete mass and stiffness matrices using the DMIG (Direct Matrix Input at Grid points) card available in NASTRAN.

For the current procedure, only the coupling terms for the stiffness matrix need to be input using the DMIG cards. The coupling terms for the mass matrix are computed by the simple alteration sequence (ALTER) shown in figure 2, which transposes the $[A]$ matrix and multiplies it by $-(\rho c)^2$.

The solution to the fluid-structure interaction problem can be obtained using a direct or a modal approach. The direct approach solves equation (13) directly with NASTRAN^{20,21} for the frequencies or grid points selected by the user. This solution can be retained for comparison with other more approximate solutions which modify the basic equations in order to reduce the computation time.

The modal approach to the fluid-structure interaction problem can also be used within the NASTRAN framework.¹¹ First, the eigenvalues and eigenvectors of equation 13 are computed while ignoring the coupling terms. Then the modal content of the coupling matrices is extracted and combined with the previously obtained modal mass and stiffness matrices. These new matrices then describe the entire problem. In order to reduce the computation time required to solve these matrix equations it is necessary to reduce the size of the matrices. This can be accomplished by considering only the significant modes in a specified frequency range and disregarding those modes which do not appreciably influence the solution. However, these modes must be selected carefully to avoid unacceptable errors, such as those shown in reference 19.

Another approach which reduces the computational effort,¹⁹ untested in the present study, is based on the assumption that the effects of the acoustic medium on the structure are negligible. If this is true equation 13 can be split into equations 15 and 16 which can then be decoupled, since the pressure forcing term, $[A]\{p\}$, on the right hand side of equation 15 is negligible with respect to the structural forcing terms, $\{F_a\}$. In this way the accelerations can be computed from equation 15 and input to equation 16 to obtain the corresponding pressure values. These uncoupled equations can be solved with NASTRAN based on a direct, modal, or mixed approach, depending on the computational evidence.

Examples

In order to more completely understand the fluid-structure interaction problem, as defined according to the NASTRAN formulation above, some simple models have been developed and compared with studies existing in the literature.^{18,19}

The basic acoustic model is the same as described previously — a cylinder with a circular cross section. The structural model was designed to fit with the acoustic model. The cylinder's dimensions are 914.4 mm (radius) by 25.4 mm (length) with a skin thickness of 0.8128 mm. These dimensions are needed to compute the BAR element used to model a structural strip. A point force of the form $F = F_0 e^{i\omega t}$ ($F_0 = .4534$ kgf) was applied to the structure. The frequency response resulting from this forcing function is shown in Figures 3 and 4. Figure 3 shows the frequency response of the structure at the point where the force is applied, and compares predictions using both the direct and modal approach. Figure 4 shows the frequency response at three points in the acoustic volume, A, B, and C: the interface point where the force is applied, a point at one-half the radius, and a point on the cylinder axis (zero radius). Again, predictions based on the direct and modal approach are compared. In order to depict the three-dimensional response, the post-processing program PATRAN-G, available at NASA Langley Research Center, has been used. Figure 5 shows some of the cylinder's responses for certain specific frequencies. These results are in good agreement with those found in the literature with some minor discrepancies due to differences in the corresponding mesh size and damping characteristics.

The three-dimensional fluid-structure interaction problem has not been completed because the amount of computation time was considered too large and costly for the immediate needs of this preliminary study. Table II lists the number of degrees of freedom and corresponding CPU time (using the CDC CYBER 855 computer at NASA LaRC) for the models in the present study. Obviously, the large increase in CPU time required to go from the basic acoustic problem to the fluid-structure interaction problem is not only caused by the increased complexity of the solution but is also related to the increase in number of degrees of freedom required to describe the problem.

Experimental Application

In order to further validate the finite element model presented in the previous paragraphs, a real structure was modeled and predictions were compared to measured data. The test structure is a cylindrical fuselage model under study in the laboratory of the Acoustics Division at NASA Langley Research Center. It is a stiffened, filament wound composite cylinder 838.2 mm in diameter and 3657.6 mm in length with a skin thickness of 1.7 mm. Additional details of the cylinder's geometric properties are available in reference 4. Figure 6 shows some of the mode shapes predicted from the structural and acoustic finite element models for the two- and three-dimensional cases. An experimental modal analysis of the test cylinder's structure and enclosed volume has been performed. Table III lists the mode shapes and frequencies predicted by the finite element model and measured on the test cylinder. These results indicate that the lowest structural modes are dominated by the frame vibration and the individual panels behave like simple lumped masses. Thus the two-dimensional structural model agrees quite well with the experimental results and no significant improvements are obtained from the three-dimensional, one bay model. The acoustic behavior is different. The first few acoustic modes are dominated by the largest dimension, the cylinder length, so the three-dimensional finite element model yields better agreement with the experimental results than the two dimensional model.

Also included in Table III are predictions of the structural and acoustic modal frequencies obtained from the Propeller Aircraft Interior Noise (PAIN) model.²³ The PAIN program was developed to predict aircraft interior noise based on assumed functions for the structural modes and a finite difference formulation for the modes of the enclosed acoustic volume. Comparisons of data from the different prediction models indicate that the two-dimensional model may be sufficient for studying trends but the three-dimensional finite element acoustic model is required for practical applications. As stated previously, the computer time must be reduced to allow cost effective studies of different geometric configurations. One possibility would be to couple the two-dimensional structural model to the three dimensional acoustic model, especially in the region of low structural modal density. Another technique to reduce the computer time is to use the uncoupled solution presented in reference 19, that has been briefly described above.

Concluding Remarks

A NASTRAN finite element application has been presented which can predict the interior noise of an aircraft fuselage. The principal theoretical steps have been presented and comparisons between the numerical predictions and exact theoretical results for simple structures have shown the method's practicality, especially in the low modal density region. The coupled fluid-structure interaction problem, implemented with NASTRAN, was then described and preliminary results show good agreement with the available literature. Finally, validation of the finite element structural and acoustic models has been obtained through comparison with experimental data obtained on a laboratory cylinder. Ongoing analysis of the finite element model will indicate the feasibility of the uncoupled solution for large structures, and will study the effects of various parameters on the interior noise level, such as cabin pressurization, damping, structural modifications,²⁴ etc. These are important aspects which can be studied easily due to the great flexibility of the finite element model.

References

1. Carbone, A.; Paonessa, A.; Lecce, L.; and Marulo, F.: Cabin Noise Reduction for a New Development Turboprop Commuter Aircraft. AGARD CP-366 on "Aerodynamics and Acoustics of Propellers," Toronto, Canada, October 1-4, 1984.
2. Carbone, A.; Paonessa, A.; Lecce, L.; and Marulo, F.: Control of Interior Noise in Advanced Turbopropeller Aircraft. Proceedings of 15th ICAS Congress, London, England, September 7-12, 1986, vol. 2, pp. 1171-1185.
3. Carbone, A.; Paonessa, A.; Lecce, L.; and Marulo, F.: Theoretical and Experimental Modal Analysis of a Turboprop Aircraft Fuselage. L'Aerotecnica-Missili e Spazio, vol. 64, no. 1, March 1985, pp. 5-11.
4. Grosveld, F. W.; and Beyer, T. B.: Modal Characteristics of a Stiffened Composite Cylinder with Open and Closed End Conditions. AIAA 10th Aeroacoustics Conference, July 9-11, 1986, Seattle, Washington, AIAA-86-1908.

5. Lecce, L.; Marulo, F.; Carbone, A.; and Mandarini, S.: Sul Problema Della Riduzione Del Rumore a Basse-Medie Frequenze All'interno di Fusoliera, Mediante Modificazione dei Parametri Strutturali. L' Aerotecnica-Missili e Spazio, vol. 61, no. 4, December 1982 (in Italian).
6. Lecce, L.; Marulo, F.; Carbone, A.; and Paonessa, A.: Risultati Teorici e Sperimentali Relativi Alla Risposta Dinamica di Strutture Tipiche di Fusoliera Eccitate Acusticamente. L' Aerotecnica-Missili e Spazio, vol. 62, no. 4, December 1983 (in Italian).
7. Everstine, G. C.: Structural Analogies for Scalar Field Problems. Int. Journal of Numerical Methods in Engineering, vol. 17, no. 3, March 1981, pp. 471-476.
8. Everstine, G. C.: A Symmetric Potential Formulation for Fluid-Structure Interaction. Journal of Sound and Vibration, vol. 79, no. 3, 1981, pp. 157-160.
9. Petyt, M.; Lim, S. P.: Finite Element Analysis of the Noise Inside a Mechanically Excited Cylinder. Int. Journal for Numerical Methods in Engineering, vol. 13, 1978, pp. 109-122.
10. Craggs, A.: An Acoustic Finite Element Approach for Studying Boundary Flexibility and Sound Transmission Between Irregular Enclosures. Journal of Sound and Vibration, vol. 30, no. 3, 1973, pp. 343-357.
11. Wolf, J. A.: Modal Synthesis for Combined Structural-Acoustic Systems. AIAA Journal, vol. 15, no. 5, May 1977, pp. 743-745.
12. Jerrard, A. J. (editor): MSC/NASTRAN, Application Manual. The MacNeal-Schwendler Corporation, Los Angeles, CA, 1981.
13. Wolf, J. A.; Nefske, D. J.: NASTRAN Modeling and Analysis of Rigid and Flexible Walled Acoustic Cavities. NASA TM X-3278, 1975, pp. 615-631.
14. Everstine, G. C.; Schroeder, E. A.; Marcus, M. S.: The Dynamic Analysis of Submerged Structures. NASA TM X-3278, 1975, pp. 419-429.
15. Nefske, D. J.; Wolf, J. A.; Howell, L. J.: Structural-Acoustic Finite Element Analysis of the Automobile Passenger Compartment: A Review of Current Practice. Journal of Sound and Vibration, vol. 80, no. 2, 1982, pp. 247-266.
16. Suna, S. H.; and Nefske, D. J.: A Coupled Structural-Acoustic Finite Element Model for Vehicle Interior Noise Analysis. Journal of Vibration, Acoustics, Stress, and Reliability in Design, vol. 106, no. 2, April 1986, pp. 314-318.
17. Everstine, G. C.: A NASTRAN Implementation of the Doubly Asymptotic Approximation for Underwater Shock Response. NASA TM X-3428, 1976, pp. 207-228.
18. Mera, A.; Yantis, T. F.; Sen Gupta, G.; and Landmann, A. E.: MSC/NASTRAN Implementation of Coupled Structural-Acoustic Responses for Aircraft Cabin Noise Prediction. Proceedings of MSC/NASTRAN Users' Conference, Los Angeles, CA, March 1986.

19. Sen Gupta, G.; Landmann, A. E.; Mera, A., and Yantis, T. F.: Prediction of Structure-Borne Noise, Based on the Finite Element Method. AIAA Paper 86-1861, AIAA 10th Aeroacoustics Conference, July 9-11, 1986, Seattle, WA.
20. MacNeal, R. H. (editor): The NASTRAN Theoretical Manual. NASA SP 221(06), NASA, Washington, DC, 1981.
21. McCormick, C. W. (editor): The NASTRAN Users' Manual. NASA SP 222(06), NASA, Washington, DC, 1981.
22. Anonymous: PATRAN-G User's Guide. Software Products Division, PDA Engineering, Santa Ana, CA, March 1984.
23. Pope, L. D.; Wilby, E. G.; and Wilby J. F.: Propeller Aircraft Interior Noise Model. NASA CR 3813, July 1984.
24. Marulo, F.; Lecce, L.; Buono, G.; Carbone, A.; and Cianciaruso, M.: Theoretical Studies on Frame Applied Dynamic Absorbers to Reduce Cabin Vibration and Noise of Turboprop Aircraft. AIAA 8th National Congress, September 23-27, 1985, Torino, ITALY, pp. 1087-1103.

TABLE 1. ACOUSTIC NATURAL FREQUENCIES FOR TWO- AND THREE-DIMENSIONAL ENCLOSURES. COMPARISON BETWEEN THEORY AND NASTRAN RESULTS.

2-D					
Square Enclosure (1000 mm x 1000 mm)			Circular Enclosure (R = 914.4 mm)		
	Frequency (Hz)			Frequency (Hz)	
Mode	Theory	NASTRAN	Mode	Theory (Ref. 19)	NASTRAN
0,0	0.00	0.00	0,0	0.00	0.00
0,1	170.10	169.40	1,0	109.05	108.39
1,0	170.10	169.40	2,0	180.83	178.64
1,1	240.56	239.57	0,1	226.86	224.77
2,0	340.21	334.64	3,0	248.74	237.19
0,2	340.21	334.64	4,0	314.82	289.52
2,1	380.36	375.07	1,1	315.64	313.11
1,2	380.36	375.07			
2,2	481.12	473.25			

3-D					
Rectangular Enclosure (1000 mm x 1000 mm x 10000 mm)			Cylindrical Enclosure (R = 914.4 mm, L = 4064 mm)		
	Frequency (Hz)			Frequency (Hz)	
Mode	Theory	NASTRAN	Mode	Theory (Ref. 19)	NASTRAN
0,0,0	0.00	0.00	1,0,0	41.85	41.77
0,0,1	17.01	16.92	1,1,0	116.77	116.20
0,0,2	31.02	33.33	3,0,0	125.55	123.20
0,0,3	51.03	48.73	3,1,0	166.27	164.90
0,0,4	68.04	62.65	1,2,0	185.61	183.42
.	.	.	5,0,0	209.25	198.46
.	.	.			
.	.	.			
1,0,0	170.10	165.77			
0,1,0	170.10	165.77			
1,0,1	170.95	166.58			
0,1,1	170.95	166.58			

TABLE II. NUMBER OF DEGREES OF FREEDOM (DOF) AND CPU TIME (CDC CYBER 855) FOR SOME SIMPLE AND COMPLEX NASTRAN FINITE ELEMENT MODELS.

TYPE OF COMPUTATION	NASTRAN FINITE ELEMENT MODEL	DEGREES OF FREEDOM	CPU TIME (SEC.)
Normal Mode Analysis (Acoustic part only)	2-D rectangular cross section	121	40
	3-D rectangular volume	250	120
	2-D circular cross section	89	18
	3-D cylindrical volume	546	300
Fluid-Structure Coupling (Direct Approach)	2-D circular cross section	228	360
	3-D cylinder	991	— (unavailable)

TABLE III. NATURAL FREQUENCIES OF COMPOSITE CYLINDERS. COMPARISON OF MEASURED DATA TO NASTRAN AND PAIN PREDICTIONS FOR THE STRUCTURAL AND ACOUSTIC MODELS.

Structure

Mode Shape (l, c)	Frequency (Hz)		
	NASTRAN 2-D Model	NASTRAN 3-D Model (one bay)	Experiment
0,2 A	29.34	31.58	—
0,2 S	48.50	54.53	46
0,3 A	89.40	96.07	84
0,4 S	131.38	134.34	121
0,4 A	149.07	156.67	—
1,4 S	148.16	162.40	—
0,5 A	232.81	250.67	—

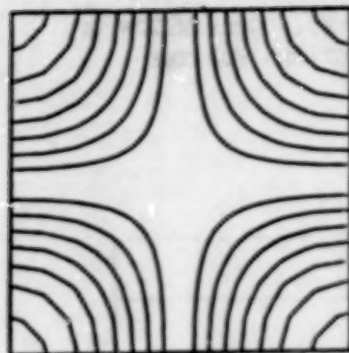
A — antisymmetric
l — longitudinal

S — symmetric
c — circumferential

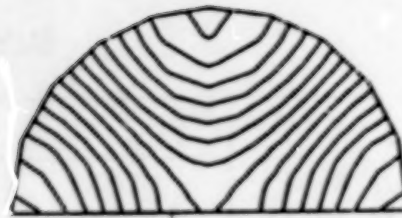
Acoustic Volume

Mode Shape (l, h, v)*	Frequency (Hz)			
	NASTRAN 2-D Model	NASTRAN 3-D Model (full length)	Experiment	PAIN Program
1,0,0	—	49	47	48
2,0,0	—	97	94	96
1,1,0	109	121	121	125
3,0,0	—	142	143	143
2,1,0	—	148	150	150
0,0,1	154	161	171	160
3,1,0	—	183	183	184
4,0,0	—	—	191	191
3,0,1	—	218	216	215
1,2,0	197	232	230	228
5,0,0	—	233	239	239

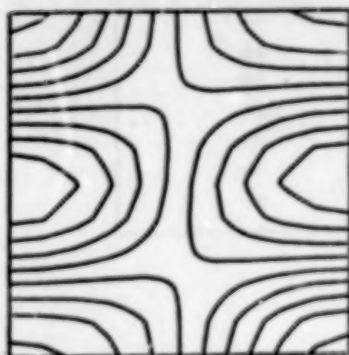
* l — longitudinal, h — horizontal, v — vertical



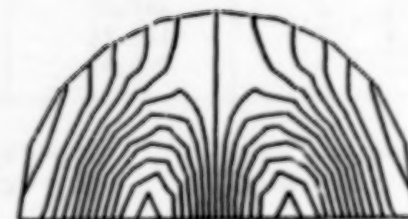
(1, 1) 239.57 Hz



(2, 0) 178.64 Hz



(2, 1) 375.07 Hz



(1, 1) 313.11 Hz



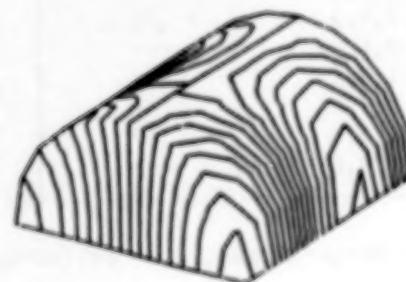
(0, 0, 3) 48.73 Hz



(1, 1, 0) 116.20 Hz



(1, 0, 1) 166.58 Hz



(3, 1, 0) 164.90 Hz

Figure 1. Examples of acoustic mode shapes for some simple geometries predicted with NASTRAN using a structural-acoustic analogy.

```

ID FIR,ACO
TIME 100
APP DISP
SOL 8,0
ALTER 100,100 $
MTRXIN CASEXX,MATPOOL,EQDYN,,TFPOOL/K2DPP,,B2PP/LUSETD/S,N,
      NOK2DPP/S,N,NOB2PP $
ALTER 100 $
LABEL LBLSAV $
TRNSP K2DPP/XMP $
ADD XMP,/M2DPP/C,Y,ALPHA=(-1.81-15,0.0)/C,Y,BETA=(0.0,0.0) $
PARAM //C,N,NOP/V,N,NOM2DPP=1 $
ENDALTER
CEND

```

```

ID FIR,ACO
TIME 100
APP DISP
SOL 11,0
ALTER 91,91 $
MTRXIN CASEXX,MATPOOL,EQDYN,,TFPOOL/K2PP,,B2PP/LUSETD/S,N,
      NOK2PP/S,N,NOB2PP $
ALTER 91 $
LABEL LBLSAV $
TRNSP K2PP/XMP $
ADD XMP,/M2PP/C,Y,ALPHA=(-1.81-15,0.0)/C,Y,BETA=(0.0,0.0) $
PARAM //C,N,NOP/V,N,NOM2PP=1 $
ENDALTER
CEND

```

Figure 2. ALTER sequence for solution of fluid-structure interaction.
 Direct approach - COSMIC/NASTRAN solution 8. Modal approach -
 COSMIC/NASTRAN solution 11.

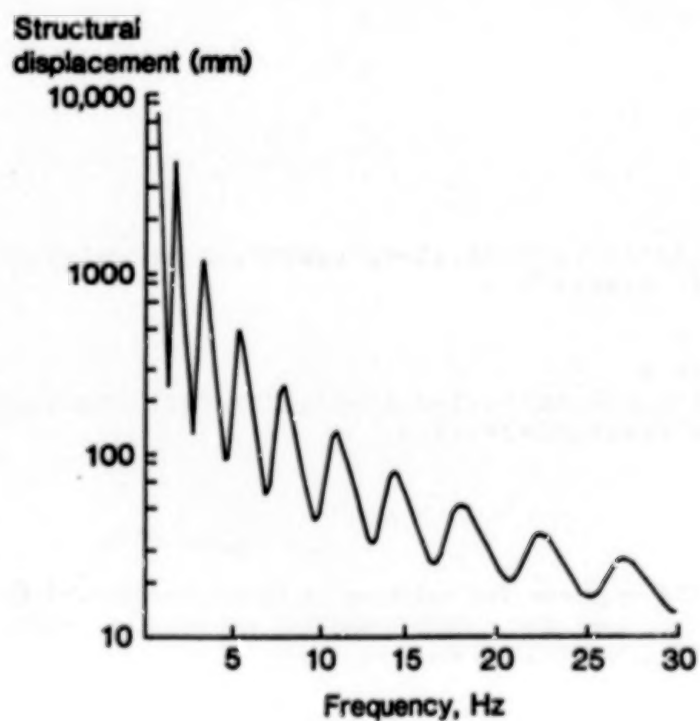
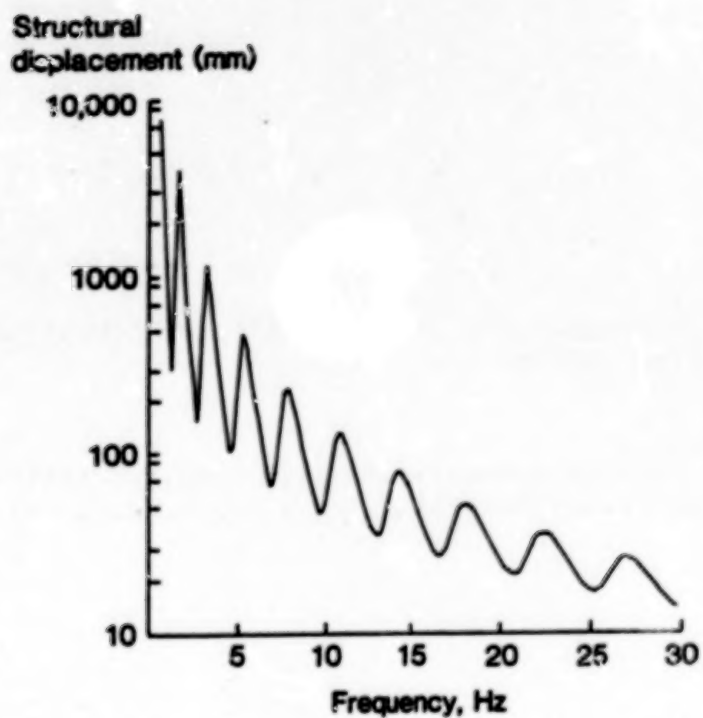


Figure 3. Frequency response function of structural point located directly under load. (a) NASTRAN direct approach, (b) NASTRAN modal approach.

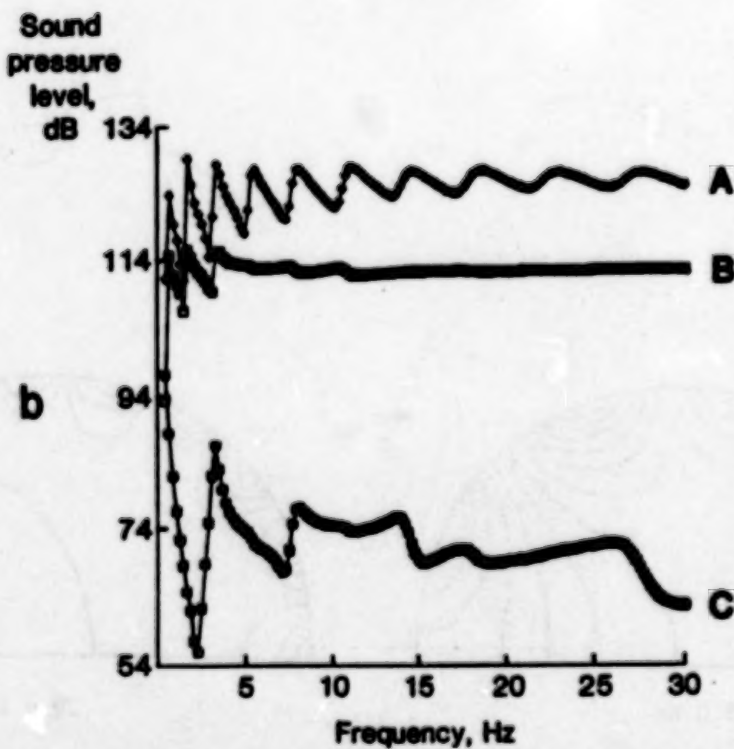
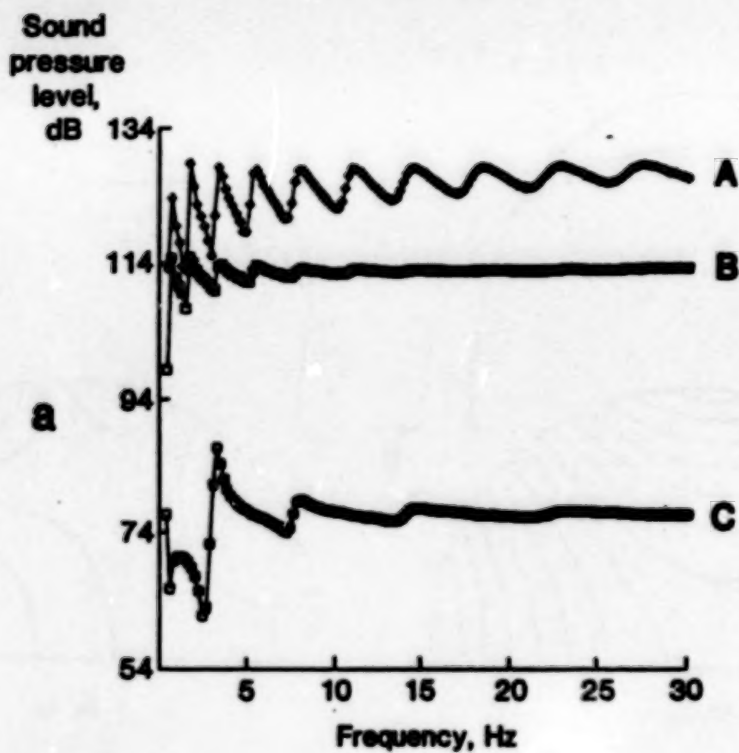


Figure 4. Acoustic frequency response: A = acoustic - structure interface, B = half-radius, C = center, (a) NASTRAN direct approach, (b) NASTRAN modal approach

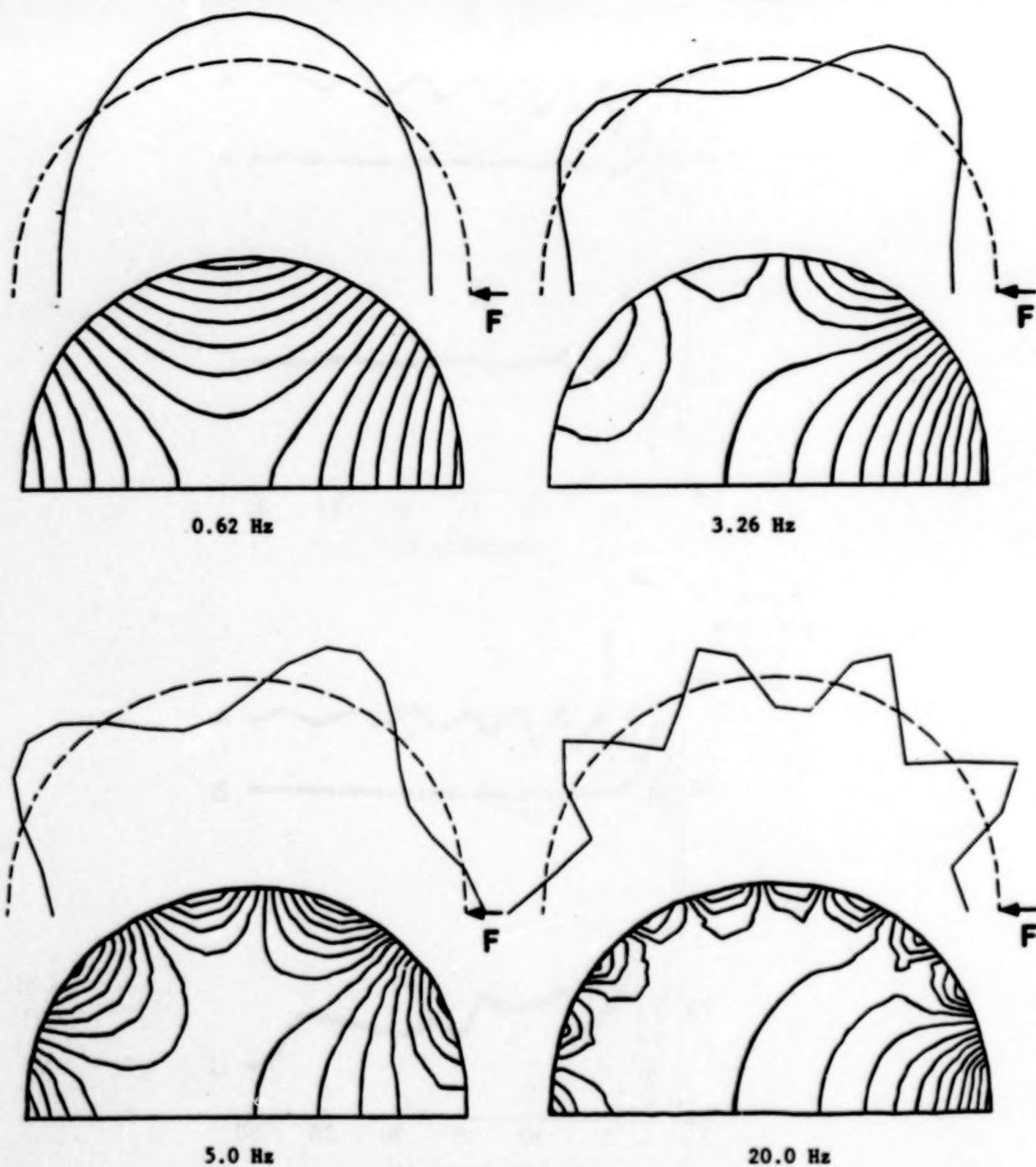
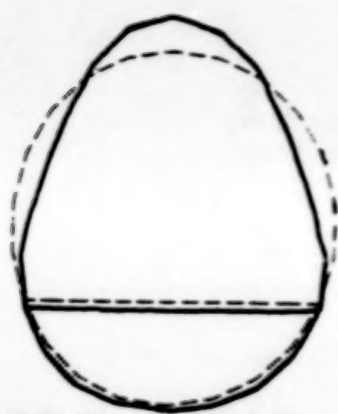


Figure 5. Dynamic shapes of structure and acoustic space predicted with NASTRAN using 2D model and fluid-structure interaction equations. Frequency indicated is for structure.

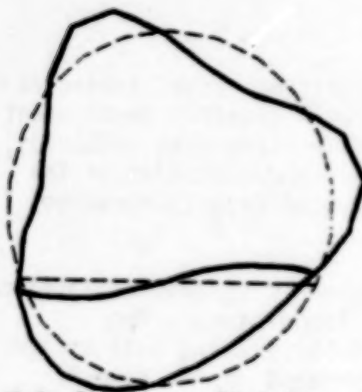
04975-787



Mode 2S 48.5 Hz



Mode 2S 54.53 Hz



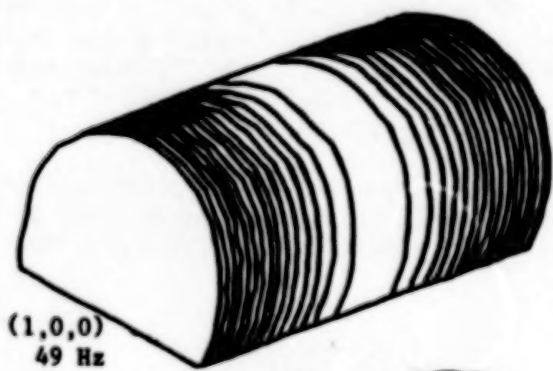
Mode 3A 89.4 Hz



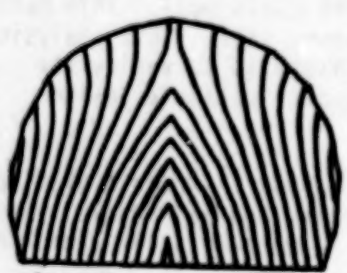
Mode 3A 96.07 Hz



(0, 1) 154 Hz



(1, 0, 0) 49 Hz



(2, 0) 197 Hz



(1, 1, 0) 121 Hz

Figure 6. NASTRAN predictions of structural and acoustic mode shapes of composite cylinder based on two- and three-dimensional models.

A STRUCTURAL ANALYSIS OF AN OCEAN GOING
PATROL BOAT SUBJECTED TO PLANING LOADS

by: James H. Clark
Robert Lafreniere
Robert Stoodt
John Wiedenheft
Code 44
Naval Underwater Systems Center
New London, CT 06320

SUMMARY

A static structural analysis of an ocean going patrol vessel subjected to hydrodynamic planing loads is discussed. The analysis required development of a detailed model that included all hull plating, five structural bulkheads, longitudinal and transverse stiffeners, and a coarse representation of the superstructure. The finite element model was developed from fabrication drawings using the Navy CAD system.

The wetted hull surface is subjected to a pressure distribution developed in accordance with the Heller-Jasper planing load formulation. The Heller-Jasper formulation is a recognized standard for planing hull design. This equivalent quasi-static load represents the product of the dynamic planing load and a corresponding dynamic load factor. This pressure distribution varies with percent of hull length from the bow and transverse offset. Some machinery loads, tankage loads, and the weight of the superstructure are included. Symmetry conditions and buoyancy springs have been employed to address the longitudinal symmetry of the ship and the hull displacements respectively.

Various stress and displacement contours are shown for the entire hull. Because several critical areas appeared to be overstressed these areas were remeshed for detail and are presented for completeness.

INTRODUCTION

The U.S. Coast Guard Research & Development Center tasked NUSC Code 44 to perform a static structural analysis of the 110 ft WPB class hull. This hull may experience large hydrodynamic planing loads in heavy seas. This analysis is intended to provide supporting documentation and analysis to verify the structural integrity or to provide information to support possible design modifications to this hull design.

The finite element analysis was divided into two phases. Phase I utilized a coarse mesh model of the entire hull, major bulkheads, and main deck. Phase II consisted of selecting two highly stressed areas from Phase I and remeshing to develop a more detailed stress field in these areas.

In each case, planing loads were applied over the entire wetted hull area in accordance with the Heller Jasper formulation detailed in reference (1). The analysis incorporated some of the significant machinery loads, as well as a coarse estimate of the total superstructure loading on the deck and bulkhead areas.

The analysis was completed using Nastran and was executed on a VAX 11/785 at NUSC. Run times were typically on the order of eight hours.

The results of the analysis consisted of stress contours and displacement contours over the entire modeled areas. Since hull plating is the primary structural area of interest in this analysis - stresses and displacements in the deck and bulkheads are not addressed here.

MODEL DEVELOPMENT

The finite element model of the 110' WPB hull was created from offsets provided by the U.S. Coast Guard. These offsets detailed the hull form via bulkhead locations, longitudinal and transverse stiffeners, and the main deck. These offsets were utilized by the NUSC CAD/CAM system in developing the finite element model used in this analysis.

The steps in this process are shown graphically in figures 1, 2, and 3. Figure 1 represents the offset data provided as a starting point. Figure 2 represents the results of the B spline curve fitting process used to link points into lines. Figure 3 depicts the results of a B spline surface routine which links lines into surfaces representing the hull. Figure 4 represents the final configuration of the hull and superstructure before discretization.

Figures 5 and 6 depict the totally discretized finite element model of the hull, bulkheads, and main deck. This model includes all transverse and longitudinal stiffeners detailed in the original table of offsets. Because the structure is symmetric about a longitudinal plane only one half of the structure requires modelling.

The finite element model utilizes bending plate elements (CQUAD & CTRIA elements) for the hull plate and beam elements (CBARS) in all stiffeners. The bulkheads are corrugated plate structures. An equivalent stiffness smearing approach has been utilized to enable modelling of the bulkheads as a plate structure, this is consistent with the assumptions regarding hull plating as the focus of the analysis.

Upon assembly, the model consists of 2625 quadrilateral plate elements, 590 triangular plate elements, and 2813 beam elements defined by 3094 nodes. Plate thickness were provided by USCG R&D Center and range from 4 pound plate up to 20 pound plate. Longitudinal and transverse member geometries were obtained from blueprints provided by USCG R&D Center and are available from the author.

The results of the analysis of the coarse mesh model indicated that the areas between bulkheads 13 and 17 in the vicinity of the keel warranted closer examination. These areas have been remeshed and are shown in figure 6A.

LOAD GENERATION

Machinery and superstructure loads were specified by the sponsor. Since these loads were not originally part of the load specification, the actual foundations were not modelled, in the interest of completeness these loads were smeared along the appropriate longitudinal and transverse frames. When appropriate, tankage loads were specified.

The primary loading of the hull consisted of a pressure distribution developed in accordance with the Heller Jasper formulation developed in reference (1). This equivalent static load represents the product of the dynamic load and corresponding dynamic load factor. The formulation consists of a pressure distribution that varies with both percent of hull length from the bow and transverse offset. This formulation utilizes an analytical expression for the transverse pressure distribution of the form

$$P = \left[\frac{P_0}{2} \left(1 + \cos 2 \left(\frac{Z}{G} - \frac{B}{2} \right) \right) \right]$$

where

P is the pressure to be applied at each structural node

P₀ varies longitudinally in accordance with the hull impact factor specified in figure 7, given two initial values of
P₀ = 25 PSI and P₀ = 15 PSI

z, G, and B are based on hull geometry and in accordance with figure 8

A Fortran program utilizing this formulation and generating the appropriate Nastran loading cards (PLOAD2) is available from the author. The gravity loads resulting from all the hull structure has been incorporated in the model as well. Figure 8A shows an overall schematic representation of the loads utilized in this analysis.

BOUNDARY CONDITIONS

The boundary conditions utilized in the problem invoke symmetry along the longitudinal plane by only allowing in plane displacements and rotations. Other than buoyancy, no other boundary conditions required specification.

The buoyancy at each wetted node is accounted for by means of scalar spring elements (CELAS2). These elements are attached to each wetted node and are given a spring constant derived from the ships weight/displacement characteristics. These springs were configured to react in the z direction.

DISCUSSION AND RESULTS

The stress and displacement data has been post-processed using PATRAN in an effort to simplify the graphic representation of a moderate quantity of output data. The data presented here is for the coarse mesh analysis at two values of P_o (25 PSI and 15 PSI) In that this analysis is linear elastic, the 15 PSI values are correctly obtained by scaling the 25 PSI results.

In an effort to facilitate design questions, the stress output is presented in a Von Mises format. Practical considerations encourage utilizing this yield criteria since comparison to tensile stress versus strain performance of the materials used can then be made directly. This failure criteria presumes that yield is the dominant failure mode.

Figure 9 depicts the Von Mises stress contours throughout the hull plating. The highest stress areas are near frames 13 and 17, therein the justification for the fine mesh model. Von Mises stresses in the 25,000 PSI to 45,000 PSI range are clearly visible.

Figure 10 represents minimum principal stresses and figure 11 the maximum principal stresses. These values are used in developing the Von Mises stress contours and are included for completeness.

Figures 12 and 13 depict the displacements in the Y and Z directions respectively. These displacements are shown for P_o values of 25 PSI and 15 PSI.

Collectively, the stress data and displacement data justify the remeshing of the area along the keel between frames 13 and 17. As mentioned previously, this area has been remeshed as shown in figure 6A. This finer mesh analysis will result in a more detailed definition of the stress field. It should be noted, however, that overall trends will not change significantly as a result of the finer mesh analysis. Results from this last phase of the analysis will be shown in figures 14, 15, and 16.

CONCLUSIONS

The analysis reported herein indicates that for a material with a Young's Modulus of 30,000,000 PSI and a Poisson's ratio $\nu = .33$, the maximum Von Mises stresses are 45,000 PSI.

This analysis has not addressed possible fatigue failure modes or corrosion related issues. While fatigue and corrosion are very important NUSC was not tasked to examine these issues.

REFERENCES

1. "On the Structural Design of Planing Craft," by S. R. Heller, N. H. Jasper, Quarterly Transaction RINA, July 1960.

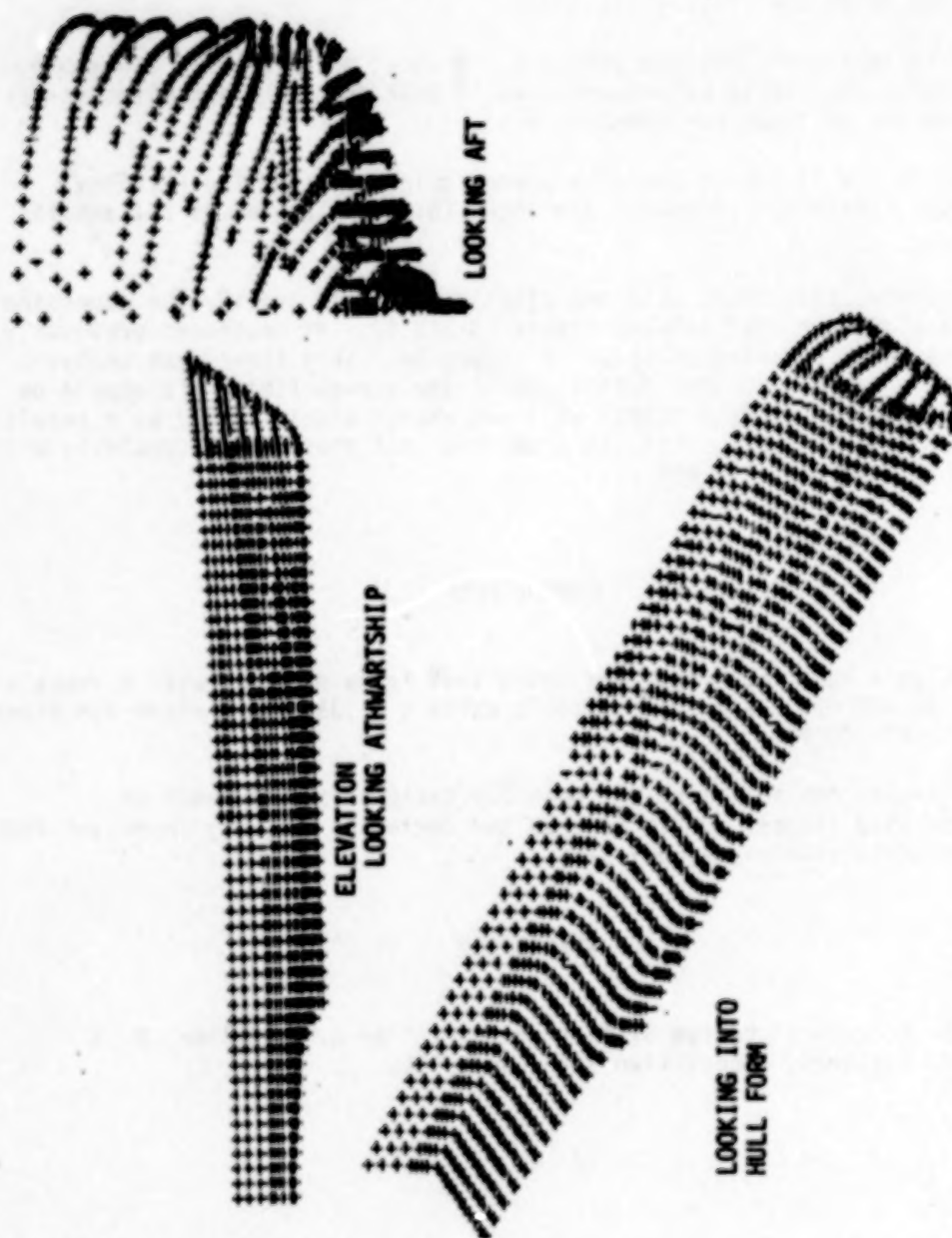


Figure 1

Spatial Representation of Offsets Used to Define 110 ft WPB Hull and Associated Stiffeners

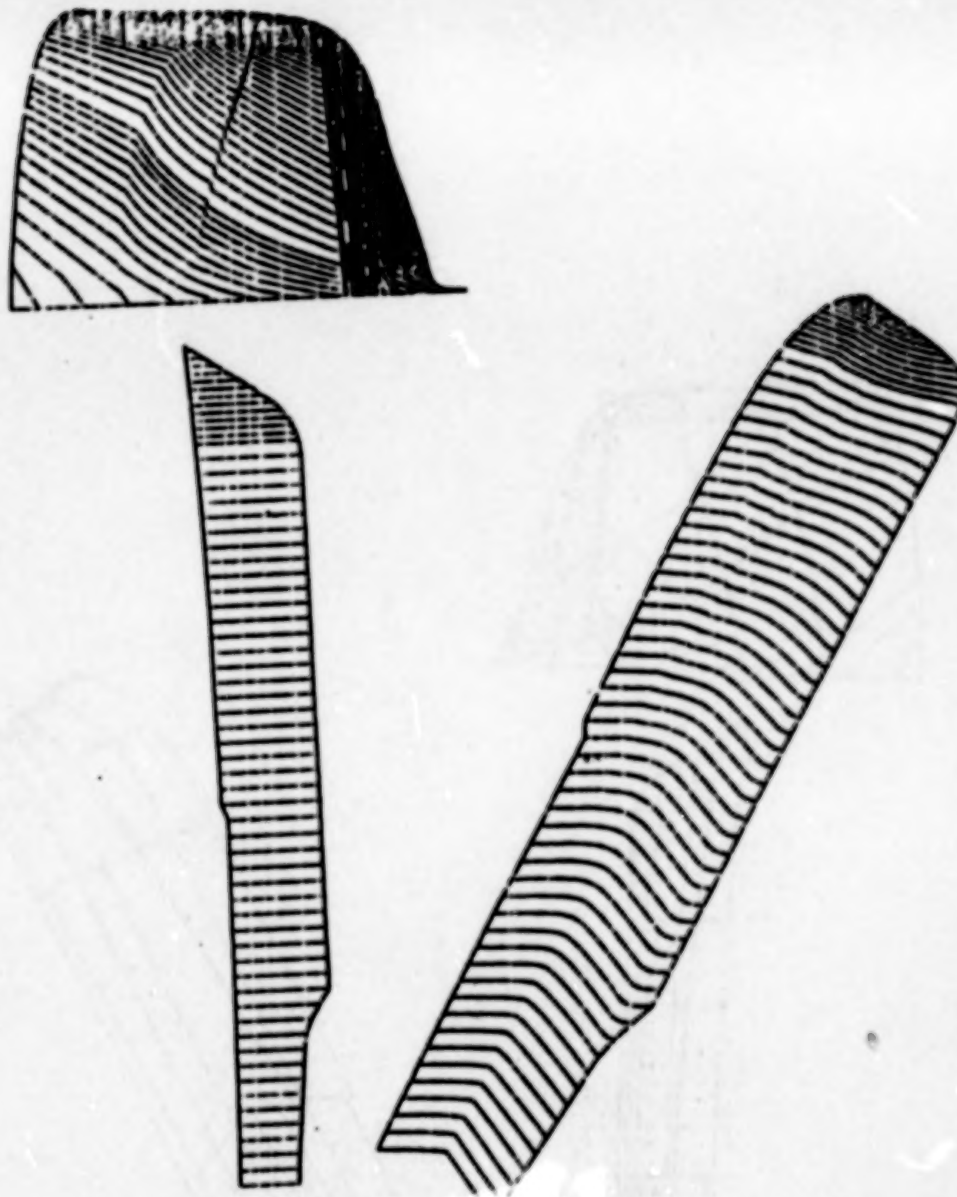


Figure 2
(B-Spline) Fit of Offsets Forming Lines Defining Hull Sections
These Lines Correspond to Frame Locations

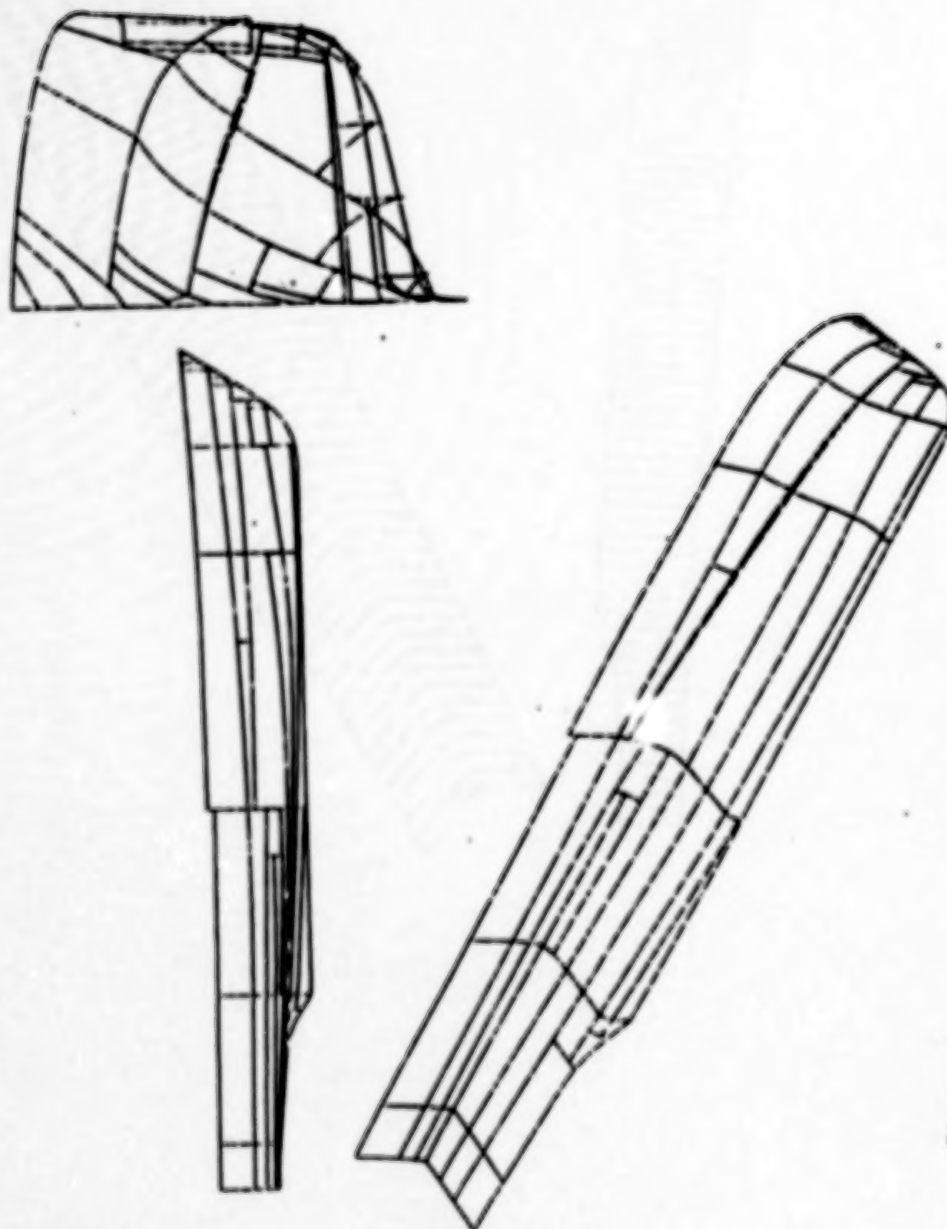


Figure 3
B-Spline Fit of Lines Forming Surfaces That Define Hull Form

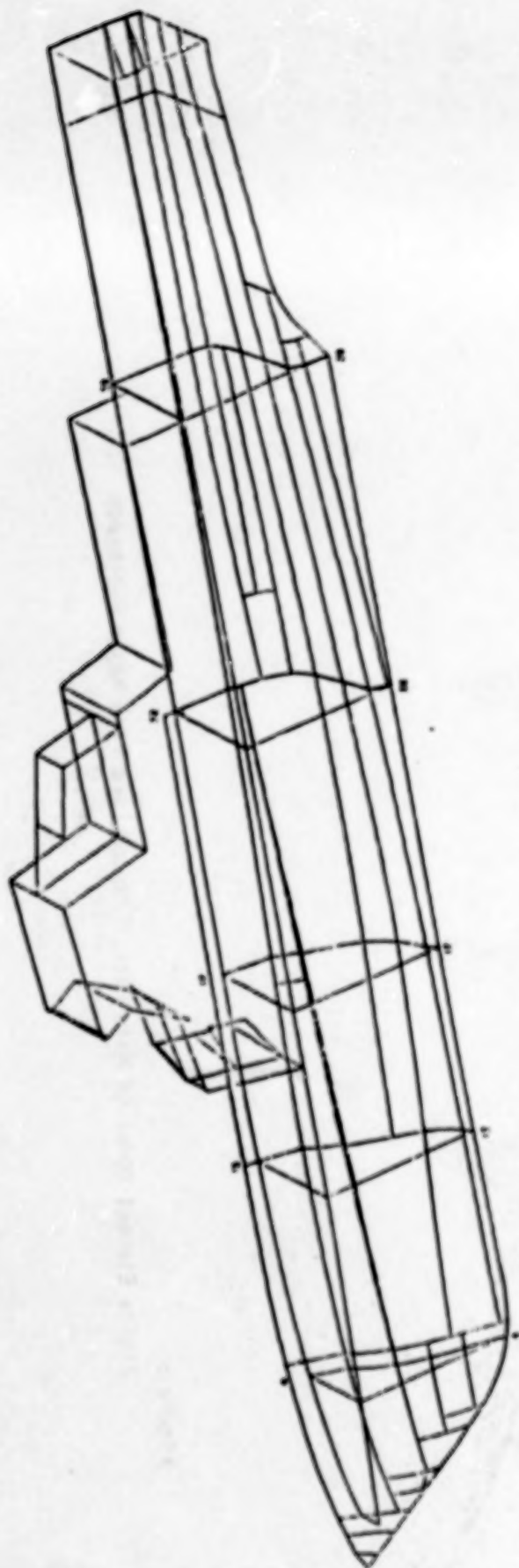


Figure 4
Final Configuration of Hull Surfaces and Superstructure Before Meshing.
Major Bulkheads at Frames 8, 13, 17, 22, and 28 are shown.

ORIGINAL PAGE IS
OF POOR QUALITY

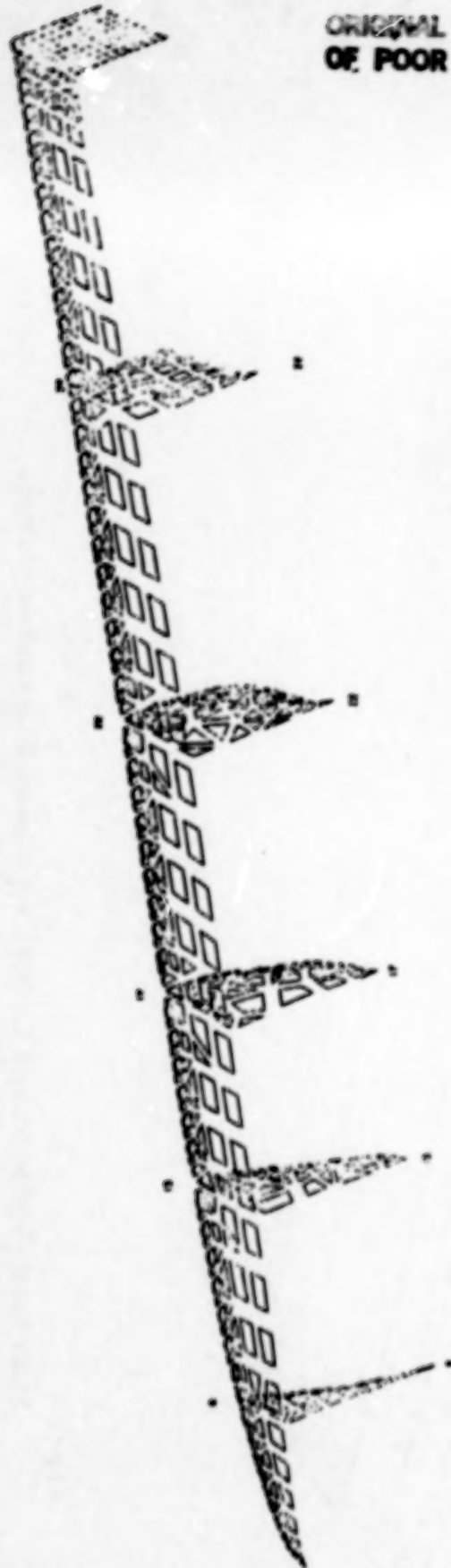


Figure 5

Finite Element Model of Main Deck, Transom, and Five Major Bulkheads

ORIGINAL PAGE IS
OF POOR QUALITY

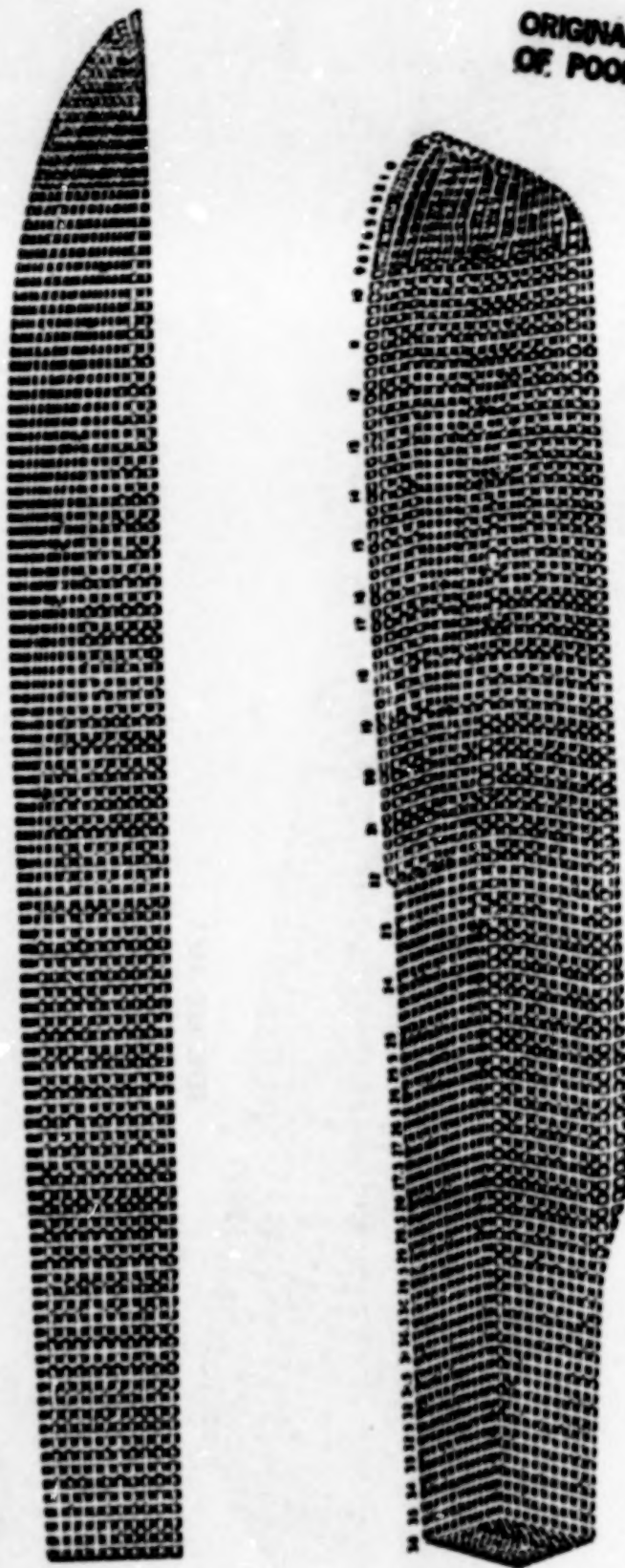


Figure 6
Finite Element Model of All Hull Platings Including Transom

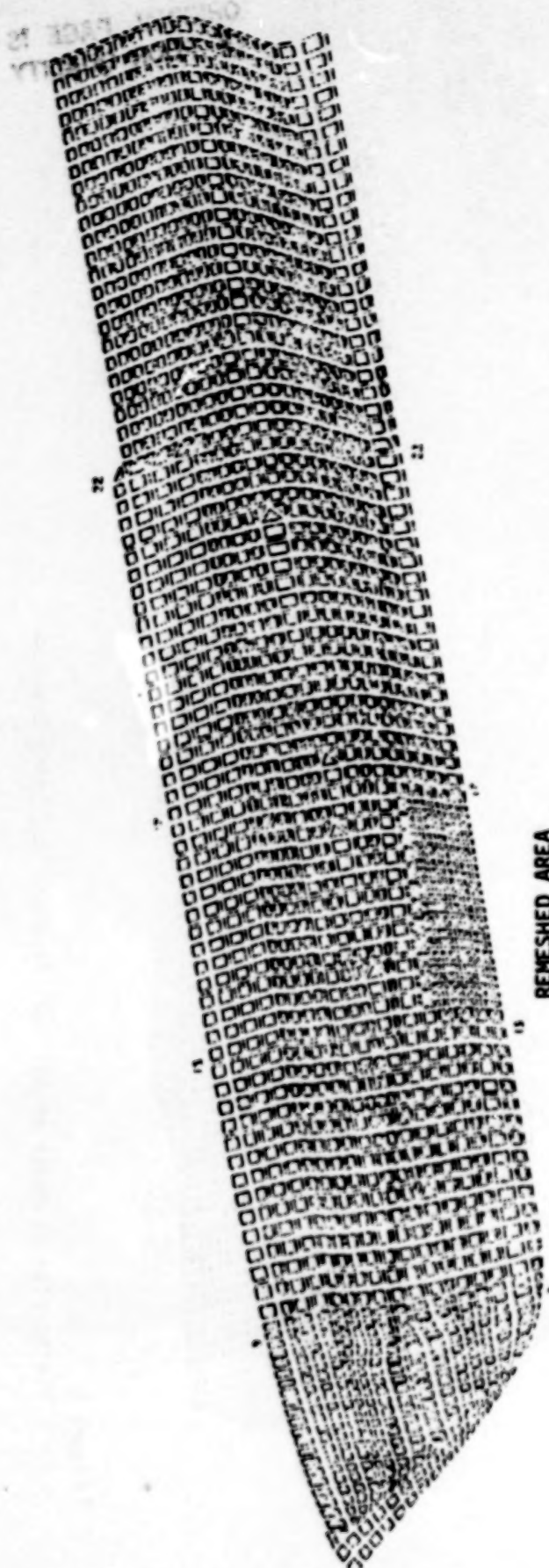


Figure 6A
Finite Element Model of Hull Plating with Remedied Area Between Frames 13 and 17

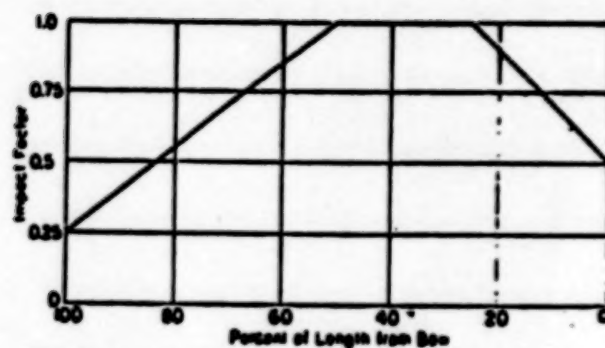


FIG. 7.—IMPACT FACTOR AS A FUNCTION OF DISTANCE FROM BOW

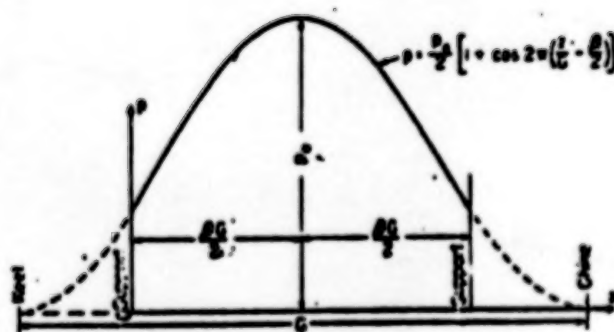


FIG. 8.—GEOMETRY AND NOTATION OF TRANSVERSE LOAD DISTRIBUTION

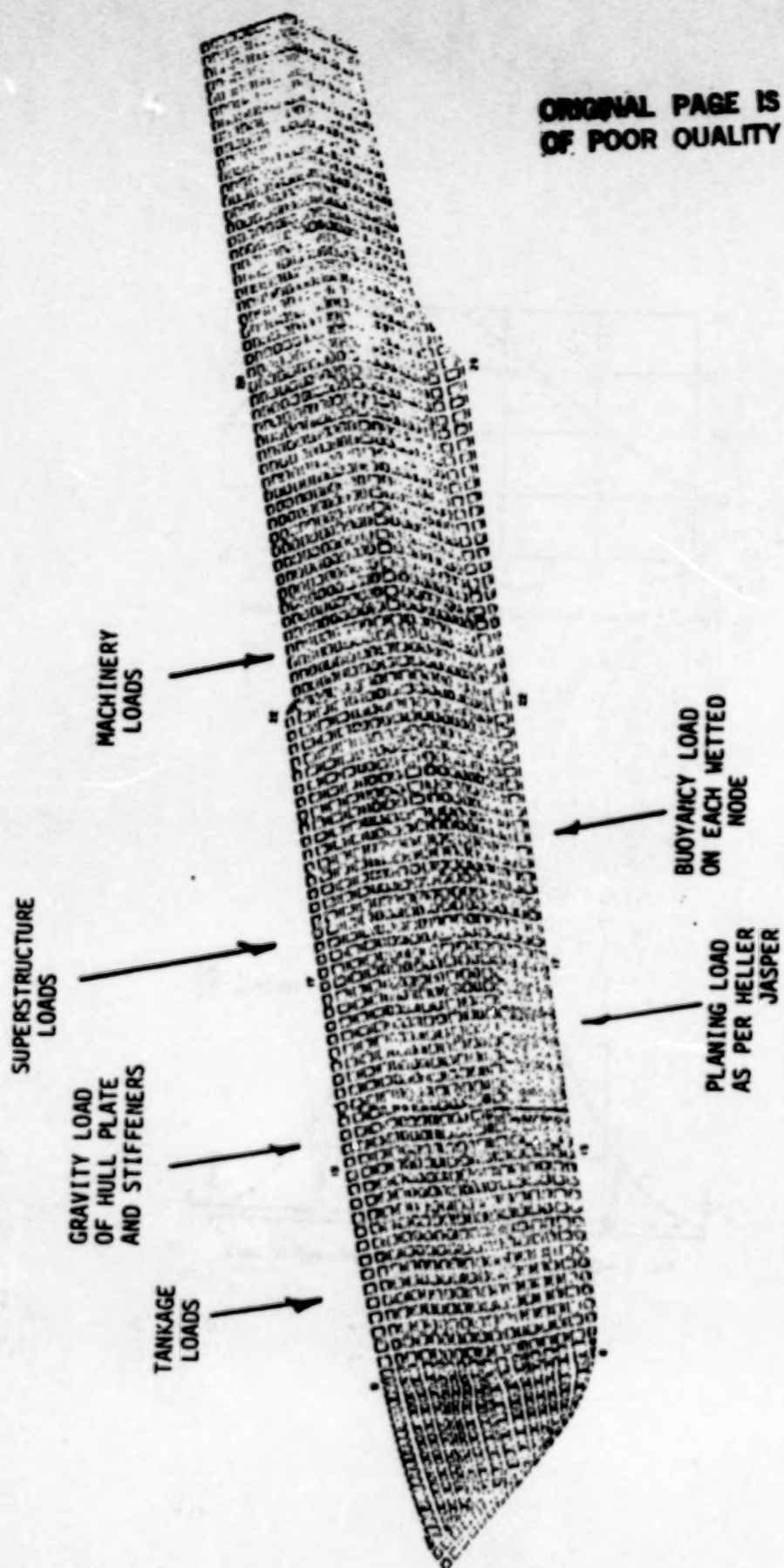


Figure 8A

Schematic Representation of Loads Applied to WPB Hull

ORIGINAL PAGE IS
OF POOR QUALITY

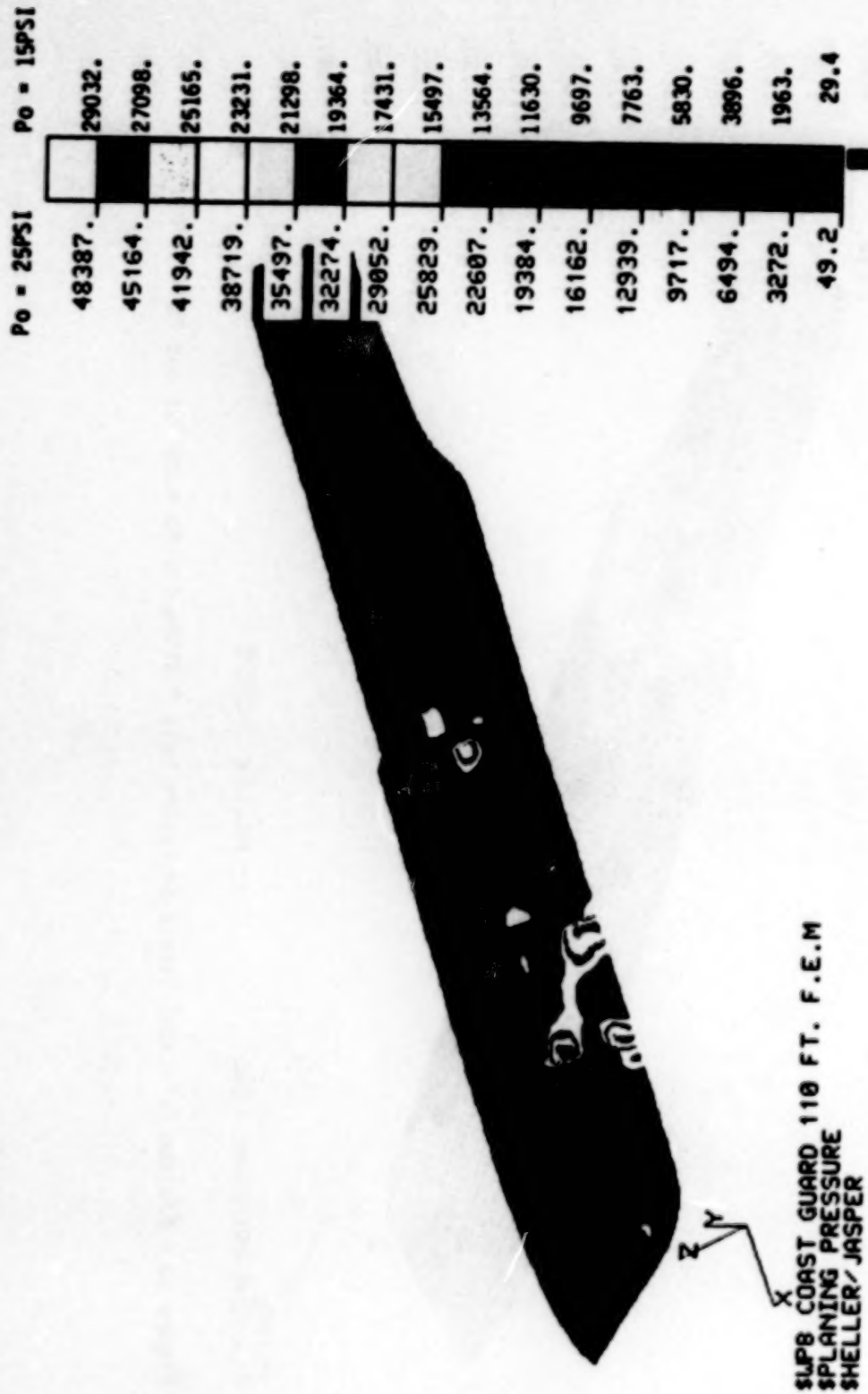


Figure 9
Von Mises Stress Distribution on Entire Hull Plating
For Po = 25PSI and Po = 15PSI

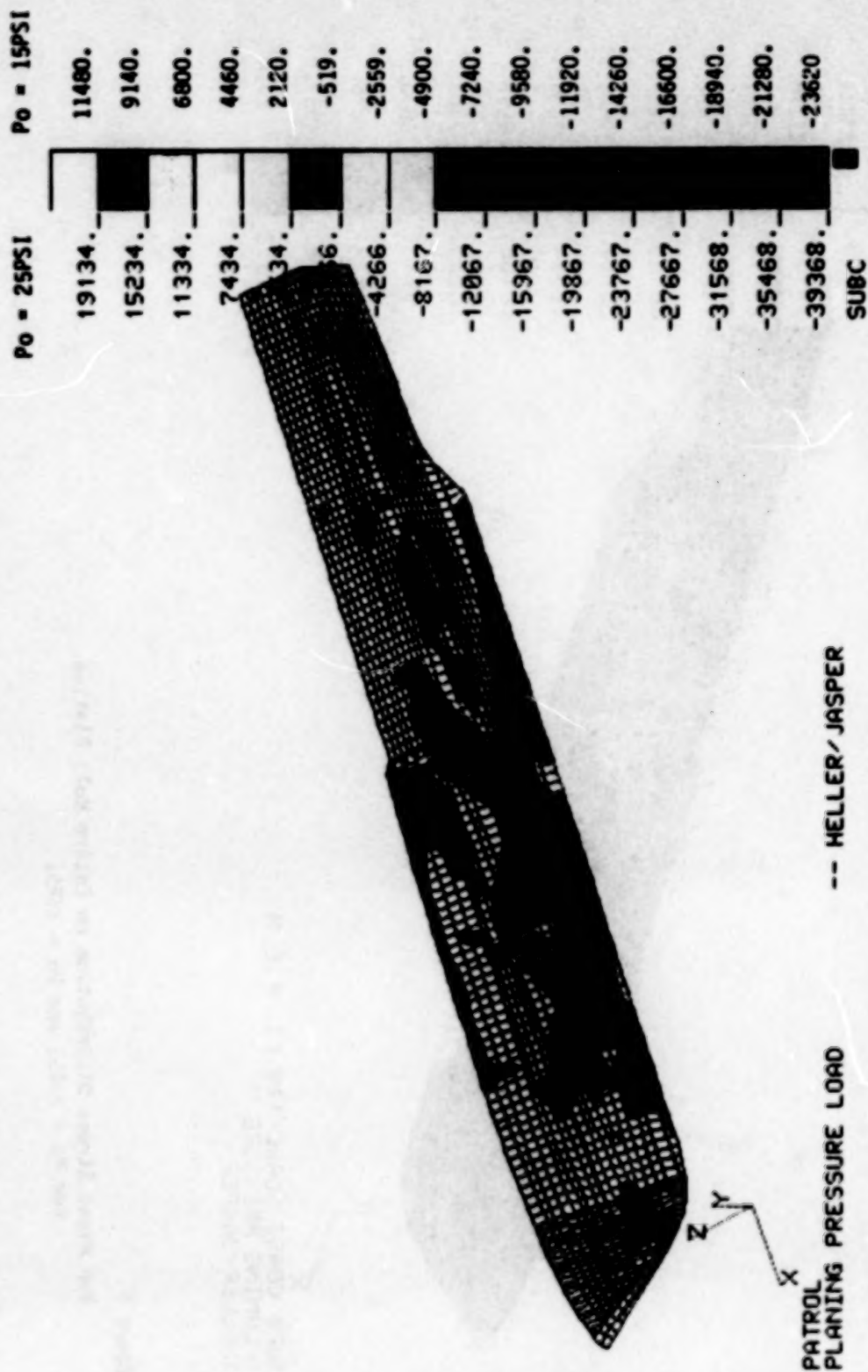


Figure 10 - Minimum Principal Stress on Entire Hull Plating For $P_o = 25$ PSI and $P_o = 15$ PSI

ORIGINAL PAGE IS
OF POOR QUALITY

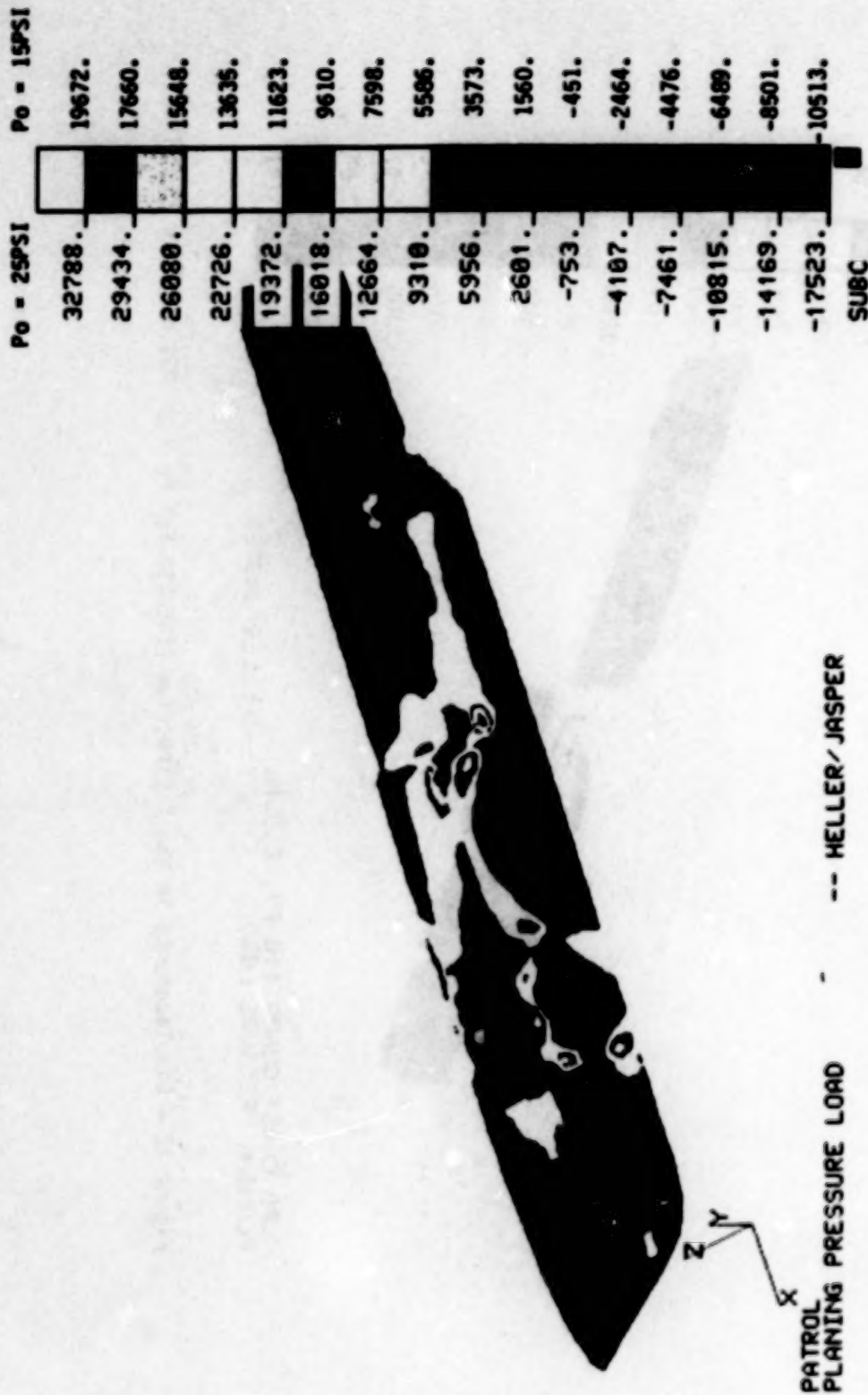


Figure 11 - Maximum Principal Stress on Entire Hull For Po = 25 PSI and Po = 15 PSI

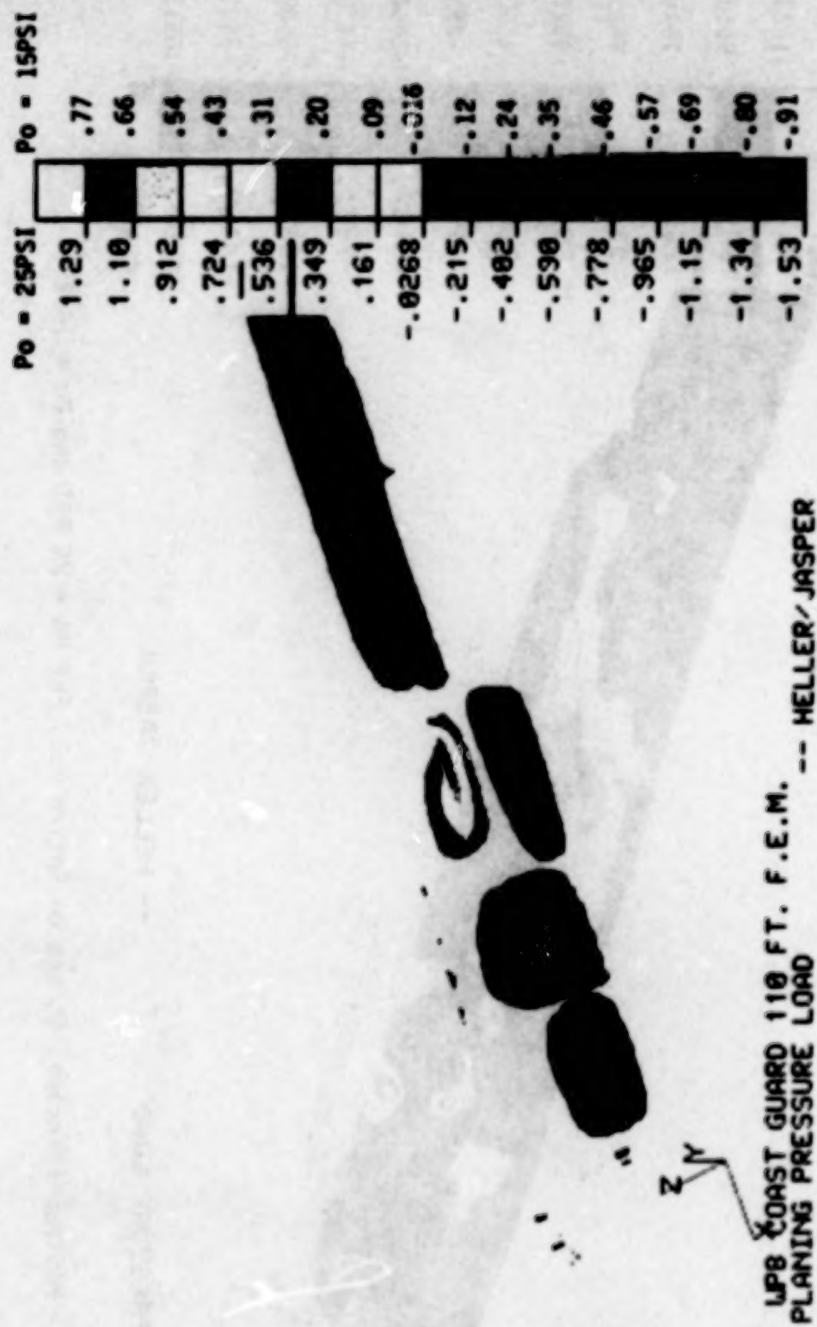


Figure 12 - Displacements in the Y Direction (INCHES) For Po = 25 PSI and Po = 15 PSI

ORIGINAL PAGE IS
OF POOR QUALITY



Figure 13 - Displacements in the Z Direction (INCHES) For Po = 25 PSI and Po = 15 PSI

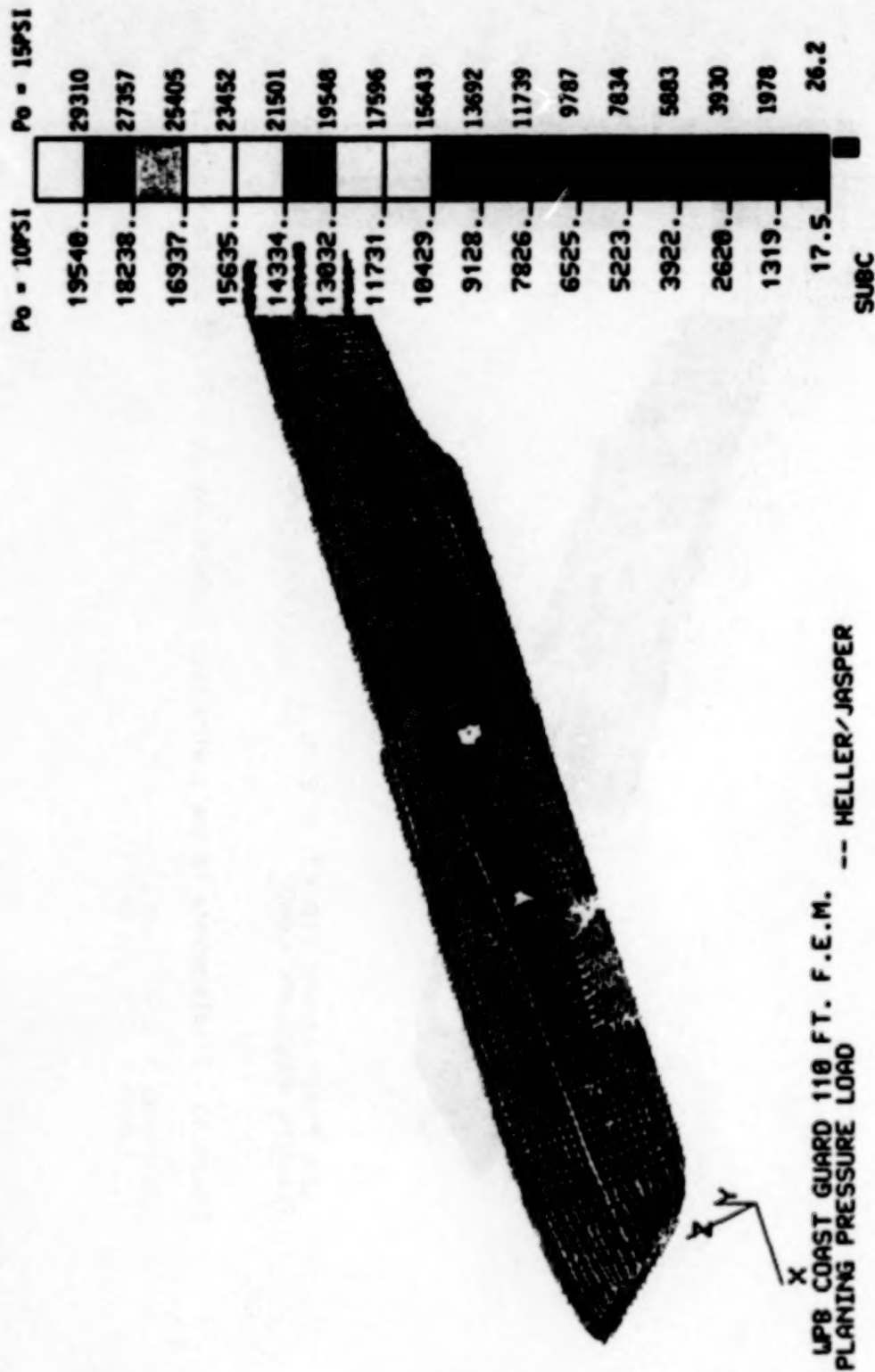


Figure 14 Von Mises Stress Distribution on Entire Hull Plating
For Po = 15PSI and Po = 10PSI

ORIGINAL PAGE IS
OF POOR QUALITY



LP8 COAST GUARD 110 FT. F.E.M. -- HELLER/JASPER
PLANING PRESSURE LOAD

Figure 15
Displacements In the Y Direction (INCHES)
For Po = 15PSI and Po = 10 PSI



LP8 COAST GUARD 110 FT. F.E.M. -- HELLER/JASPER
PLANING PRESSURE LOAD

Figure 16
Displacements in the Z Direction (INCHES)
For Po = 15PSI and Po = 10PSI

END

DATE

FILMED

OCT 26 1987